UNIVERSITAT DE BARCELONA

Desenvolupament de sensors i llengües electròniques voltamperomètriques per a la determinació d'ions metàl·lics en mostres d'interès ambiental

Clara Pérez Ràfols

UNIVERSITAT DE BARCELONA

FACULTAT DE QUÍMICA
DEPARTAMENT D'ENGINYERIA QUÍMICA I QUÍMICA ANALÍTICA

Programa de doctorat:
Química Analítica i Medi Ambient

Desenvolupament de sensors i llengües electròniques voltamperomètriques per a la determinació d'ions metàl·lics en mostres d'interès ambientals

Memòria presentada per
Clara Pérez Ràfols
per optar al grau de doctor per la Universitat de Barcelona

Sota la direcció de
Dr. José Manuel Díaz Cruz
Dra. Núria Serrano Plana
del Departament d'Enginyeria Química i Química Analítica

El Dr. José Manuel Díaz Cruz, professor catedràtic del Departament d'Enginyeria Química i Química Analítica de la Universitat de Barcelona, i la Dra. Núria Serrano Plana, professora agregada del mateix Departament,

CERTIFIQUEN

Que la present memòria de tesi doctoral, que porta per títol *"Desenvolupament de sensors i llengües electròniques voltamperomètriques per a la determinació d'ions metàl·lics en mostres d'interès ambiental"* ha estat realitzada per la Sra. Clara Pérez Ràfols sota la nostra direcció al Departament d'Enginyeria Química i Química Analítica i que tots els resultats presentats són fruït de la recerca realitzada per l'esmentada doctoranda.

Barcelona, setembre de 2019

Dr. José Manuel Díaz Cruz

Dra. Núria Serrano Plana

Dona'm la mà
i així podrem creure altre cop que
tot el que hem volgut
només espera un gest
com si fos el vent
que amb el nostre esforç tenaç desfermarem

Miquel Martí i Pol, fragment de dóna'm la mà

Agraïments

Ara fa quatre anys començava el doctorat pensant que tenia tot el temps per endavant. I és que quan comences quatre anys semblen tota una vida. Però aquí estem, no te n'adones que ja estàs acabant d'escriure la tesi. Una altra etapa que s'acaba per donar pas a altres de noves...

I com a qualsevol final d'etapa, sempre és bo parar-se i mirar enrere, reflexionar sobre tot el que ha passat i recordar els bons moments i aquelles persones amb qui els has compartit, aquelles persones que t'han ajudat a arribar fins aquí. Així, també és bon moment ara per donar les gràcies.

En primer lloc als meus directors de tesi, la Dra. Núria Serrano i el Dr. José Manuel Díaz, sense els quals aquesta tesi no hauria estat possible. Gràcies Núria i José Manuel per estar sempre allà, per tots els consells donats, pel vostre recolzament i per tot el que he pogut aprendre amb vosaltres des que vaig entrar al grup d'Electroanàlisi.

Als altres membres del grup d'Electroanàlisi, al Dr. Miquel Esteban que va ser el primer en parlar-me dels sensors electroquímics i els elèctrodes serigrafiats i a la Dra. Cristina Ariño, per presentar-me el grup d'Electroanàlisi i donar-me l'oportunitat d'entrar a formar-hi part durant el meu últim any de grau.

A tots aquells que han anat passant pel grup d'Electroanàlisi i, especialment, aquells amb qui he treballat més de prop: el Pedro, el Jaume i el Miguel.

Al Juanfra i a l'Alejandro, amb els que des de l'inici hem compartit múltiples cafès i a tots aquells que s'hi han anat afegint ja sigui per quedar-s'hi com l'Ane, el Guillem i la Noemí o només de passada com el Camilo, l'Alex i l'Alessandra. Gràcies per tots els moments compartits, dins i fora de la facultat.

Al Dr. Julio Bastos que m'ha introduït al món nano i ha fet possible les col·laboracions amb els grups de la UPC i la UdG, sense les quals tota la part d'aquesta tesi referent a nanopartícules no hauria estat possible.

Al Grupo de Electroanálisis y (Bio)Sensores Electroquímicos de la Universidad Complutense de Madrid, y en especial a la Dra. Paloma Yañez-Sedeño y a Sara Guerrero, por permitirme realizar una breve estancia en su laboratorio y aprender de su experiencia en la modificación química por electrografting.

A la Dra. Beatriz Prieto per l'estada realitzada al Monash Institute of Pharmacy and Pharmaceutical Sciences. Gràcies Bea per oferir-me la possibilitat de realitzar una estada a Austràlia, per fer-me sentir com a casa i per tot el que vaig aprendre amb tu durant aquells quatre mesos. Aquí vull agrair també a totes aquelles persones que van contribuir a que aquesta estada fos molt positiva a nivell personal i professional. Gràcies Xavi per tots els teus consells sobre el dia a dia a Austràlia i per ajudar-me a gestionar tots aquells aspectes que sempre fan més respecte quan marxes tan lluny. Thank you Keying for all those pSi samples prepared, even after I came back to Barcelona. Hedieh, Mei, Tommy, Tong, Bo, Roshan, Kathy, Arianna, Pau, Parham, Zyckry, Ishdeep… to all those who welcomed me into your group, thanks for the good moments, for the lunches together, for Fridays Happy Hour and social dinners and for all those ping-pong and tennis matches. Special thanks to Hedieh, Mei, Rezza and Amir for all the weekends spend in Melbourne and visiting around Australia, my stay there wouldn't have been the same without you.

A la família, als meus pares i als meus germans, gràcies per la vostra estima i suport. Jo he tingut la sort de no ser la primera en emprendre aquest camí i poder aprendre també de la vostra experiència.

Finalment, agrair també el suport econòmic atorgat pel Ministerio de Educación, Cultura y Deporte a través de la beca FPU que m'ha permès realitzar aquest doctorat.

A tots i totes, gràcies!!

Resum

La problemàtica mediambiental associada a la contaminació per ions metàl·lics és mundialment coneguda. En les últimes dècades hi ha hagut un enduriment de la legislació associada a aquests contaminants que ha permès disminuir les seves emissions al medi ambient però, degut a la seva elevada persistència i al seu caràcter no biodegradable, les concentracions dels ions metàl·lics en mostres mediambientals són encara preocupants.

Actualment, tot i que existeixen diverses tècniques analítiques per a la determinació d'ions metàl·lics, encara és necessari el desenvolupament de noves metodologies analítiques que permetin la determinació d'aquests contaminants *on-site* i a nivell traça. En aquest sentit, les tècniques voltamperomètriques de redissolució són una bona opció ja que són tècniques sensibles i reproduïbles que proporcionen anàlisis ràpides i no requereixen d'instrumentació voluminosa o excessivament costosa. A més, el caràcter portàtil d'aquestes tècniques s'ha vist afavorit amb la introducció en els últims anys dels elèctrodes serigrafiats, que són dispositius compactes (inclouen els tres elèctrodes que configuren la cel·la electroquímica en una mateixa unitat), miniaturitzats, versàtils i que es poden produir en massa.

Un dels avantatges que proporcionen els elèctrodes serigrafiats és la possibilitat de modificar el seu elèctrode de treball per tal de millorar la seva sensibilitat i selectivitat o permetre treballar a diferents condicions experimentals. En aquest sentit, una primera part d'aquesta tesi doctoral s'ha centrat en el desenvolupament de nous elèctrodes serigrafiats voltamperomètrics per a la determinació d'ions metàl·lics a nivell traça en mostres mediambientals. Concretament, s'han estudiat diferents estratègies de modificació com la modificació química, la formació de pel·lícules metàl·liques i l'ús de diversos nanomaterials (nanopartícules metàl·liques, nanoal·lòtrops de carboni i silici porós). Per a cadascuna d'aquestes estratègies s'han estudiat diferents aspectes del procés de modificació del sensor i s'ha avaluat l'aplicabilitat del sensor que proporciona millors resultats en mostres reals.

Sovint però, en l'anàlisi de mostres reals trobem mescles complexes on els ions metàl·lics s'interfereixen entre si o donen lloc a pics solapats. En aquests casos l'ús d'un sol sensor voltamperomètric no permet determinar correctament la concentració dels diferents ions i cal recórrer a altres estratègies d'anàlisi més sofisticades. Aquest és el cas de les llengües voltamperomètriques, on es combinen diversos sensors no específics amb un tractament de dades multivariant per resoldre el sistema. Així, la segona part d'aquesta tesi doctoral s'ha centrat en el desenvolupament de llengües voltamperomètriques per a l'anàlisi de mostres complexes d'ions metàl·lics. Concretament s'han estudiat el sistema Tl(I) i In(III) i el sistema Cd(II), Pb(II), Tl(I) i Bi(III) en presència de Zn(II) i In(III), que es caracteritzen, respectivament, per la presència de dos metalls que donen lloc a senyals fortament solapats i per la presència d'un elevat nombre de metalls. Concretament, s'ha estudiat la selecció dels sensors que componen la llengua voltamperomètrica, la seva disposició i el disseny experimental.

Un altre aspecte que és crucial en el desenvolupament de les llengües voltamperomètriques és el tractament de dades. Així, en la segona part d'aquesta tesi doctoral també s'ha fet èmfasi en aquest tema, on s'han estudiat diversos pretractaments i s'han construït diversos models quimiomètrics basats en la regressió per mínims quadrats parcials (PLS). A més, s'han estudiat també dos sistemes de calibratge multivariant, el calibratge multivariant extern i l'addició estàndard multivariant, per a la qual s'ha desenvolupat una nova estratègia basada en l'ús de PLS i la simulació del blanc de la mostra a partir de

de l'etapa de preconcentració de la mesura voltamperomètrica. Aquest segon mètode de calibratge proporciona prediccions més acurades en el cas de mostres amb un fort efecte matriu.

Els resultats obtinguts a partir dels estudis realitzats al llarg d'aquesta tesi doctoral han donat lloc a 12 articles, 9 d'ells referents a la part de desenvolupament de sensors voltamperomètrics i 3 referents al desenvolupament de llengües voltamperomètriques.

Abstract

The environmental problems associated to metal ion contamination have been known for years. During the last decades the legislation concerning these contaminants has become stricter, achieving a decrease in metal emissions to the environment. However, due to their persistence and their non-biodegradable character, metal ion concentrations in the environment are still concerning.

Currently, although there are several analytical techniques for the determination of metal ions, it is still necessary to develop new analytical methodologies for their *on-site* determination at trace levels. In this sense, stripping voltammetric techniques are a good option due to their high sensitivity and reproducibility and the fact that they provide fast analysis with relatively low cost and portable equipment. These last features are further enhanced by the coupling of stripping voltammetric measurements with screen-printed electrodes, which are compact (they contain the working, auxiliary and reference electrode onto the same strip), miniaturized and versatile devices that can be mass-produced in a reproducible manner.

One of the advantages related to the use of screen-printed electrodes is the possibility to modify their working electrode surface, which can provide improvements in sensitivity and selectivity or allow them to work in different experimental conditions. In this sense, a first part of this PhD thesis has focused on the development of new screen-printed voltammetric sensors for the determination of metal ions at trace levels in environmental samples. In particular, several modification strategies, including chemical modification, deposition of metal films and the modification with several nanomaterials (metal nanoparticles, carbon nanoallotropes and porous silicon), have been studied. For all of these strategies, some aspects of the sensor modification process were evaluated and their applicability to real samples was tested for the sensor that provided better results.

Frequently though, the analysis of real samples involves complex mixtures where metal ions interact with each other or give rise to highly overlapped peaks. In these scenarios, the use of just one voltammetric sensor does not allow their proper determination and it is necessary to resort to more sophisticated analytical strategies. This is the case of voltammetric tongues, where several non-specific sensors are combined with data treatment in order to resolve these complex systems. Thus, the second part of this PhD thesis has focused on the development of voltammetric tongues for the analysis of complex mixtures of metal ions. In particular, two systems have been studied: Tl(I) and In(III), which is characterized by two metals that give rise to highly overlapped peaks, and Cd(II), Pb(II), Tl(I) and Bi(III) in the presence of Zn(II) and In(III), which is characterized by the presence of a high number of metals. In both cases, several studies involving the selection of sensors, their arrangement and the experimental design were carried out.

Another aspect that is crucial to the development of voltammetric tongues is data treatment. Thus, the second part of this PhD thesis has also focused on this topic, studying several data pretreatments and building different chemometric models based on partial least squares (PLS). Furthermore, two multivariate calibration systems were studied, multivariate external calibration and multivariate standard addition, for which a new strategy based on PLS and the simulation of a blank signal by skipping the deposition step of stripping

voltammetry was developed. This second calibration method provides more accurate predictions in the case of real samples with strong matrix effect.

The results achieved in the studies carried out throughout this PhD thesis have resulted in 12 articles, 9 related to the development of voltammetric sensors and 3 related to the development of voltammetric tongues.

Abreviatures

AAS	Espectrometria d'absorció atòmica *Atomic absorption spectroscopy*
ABA	Àcid aminobenzoic *Aminobenzoic acid*
(ABA)Cys-SPCNFE	Elèctrode serigrafiat de nanofibres de carboni modificat amb cisteïna i enllaçat pel grup amino *Cysteine modified screen-printed carbon nanofibers electrode, coupled through the amino group*
AdSV	Voltamperometria de redissolució per adsorció *Adsorptive stripping voltammetry*
AE	Elèctrode auxiliar *Auxiliary electrode*
AEM	Agència Europea de Medicaments *European Medicines Agency*

AEMA	Agència Europea del Medi Ambient *European Environment Agency*
Ag-nanoprisms-SPCNFE	Elèctrode serigrafiat de nanofibres de carboni modificat amb nanopartícules de plata prismàtiques *Screen-printed carbon nanofiber electrode modified with prismatic silver nanoparticles*
Ag-nanoseeds-SPCNFE	Elèctrode serigrafiat de nanofibres de carboni modificat amb nanopartícules de plata esfèriques *Screen-printed carbon nanofiber electrode modified with spherical silver nanoparticles*
ANN	Xarxes neuronals artificials *Artificial neural networks*
ASV	Voltamperometria de redissolució anòdica *Anodic stripping voltammetry*
ATR-FTIR	Espectroscòpia infraroja per transformada de Fourier amb reflectància total atenuada *Attenuated total reflectance Fourier transform infrared*
Bi_{sp}SPE	Elèctrode serigrafiat de bismut modificat pel mètode *sputtering* *Sputtered bismuth screen-printed electrode*
CC	Catecol *Catechol*
CLS	Calibratge per mínims quadrats *Least-square calibration*
CMA	Concentració màxima admissible *Maximum allowable concentration*
CNF	Nanofibres de carboni *Carbon nanofibers*

CNT	Nanotubs de carboni *Carbon nanotubes*
Crown-6-SPCNFE	Elèctrode serigrafiat de nanofibres de carboni modificat amb 4-carboxibenzo-18-corona-6 *4-carboxybenzo-18-crown-6 modified screen-printed carbon nanofibers electrode*
CV	Voltamperometria cíclica *Cyclic voltammetry*
Cys	Cisteïna *Cysteine*
Cyst	Cistina *Cystine*
Cyst-SPCNFE	Elèctrode serigrafiat de nanofibres de carboni modificat amb cistina *Cystine modified screen-printed carbon nanofibers electrode*
DMF	Dimetilformamida *Dimethylformamide*
DMG	Dimetilglioxima *Dimethylglyoxime*
DPV	Voltamperometria d'impulsos diferencials *Differential pulse voltammetry*
DWT	Transformada d'ona discreta *Discrete wavelet transform*
E_a	Potencial del pic anòdic *Anodic peak potential*
E_{acc}	Potencial d'acumulació *Accumulation potential*

$\mathbf{E_c}$	Potencial del pic catòdic *Cathodic peak potential*
$\mathbf{E_d}$	Potencial de deposició *Deposition potential*
$\mathbf{E_{int}}$	Interval de potencial *Interval potential*
$\mathbf{E_p}$	Potencial d'impuls *Pulse potential*
EDC	Hidroclorur de N-(3-dimetilaminopropil)-N'-etilcarbodiimida *N-(3-dimethyla-minopropyl)-N'-ethylcarbodiimide hydrochloride*
ELISA	Assaig d'inmunoabsorció lligat a enzims *Enzime-linked immunosorbent assay*
***Ex-situ*-BiSPCE**	Elèctrode serigrafiat de carboni modificat *ex-situ* amb bismut *Ex-situ bismuth modified screen-printed carbon electrode*
***Ex-situ*-BiSPE**	Elèctrode serigrafiat modificat *ex-situ* amb bismut *Ex-situ bismuth modified screen-printed electrode*
***Ex-situ*-SbSPCE**	Elèctrode serigrafiat de carboni modificat *ex-situ* amb antimoni *Ex-situ antimony modified screen-printed carbon electrode*
***Ex-situ*-SbSPE**	Elèctrode serigrafiat modificat *ex-situ* amb antimoni *Ex-situ antimony modified screen-printed electrode*
FET	Transistor d'efecte de camp *Field-effect transistor*

FFT	Transformada ràpida de Fourier *Fast Fourier transform*
Green-AgNPs-SPCNFE	Elèctrode serigrafiat de nanofibres de carboni modificat amb nanopartícules de plata sintetitzades per una ruta verda *Screen-printed carbon nanofiber electrode modified with silver nanoparticles synthesized through a green route*
GSH	Glutatió *Glutathione*
GSH-SPCE	Elèctrode serigrafiat de carboni modificat amb glutatió *Glutathione modified screen-printed carbon electrode*
GSH-SPCNFE	Elèctrode serigrafiat de nanofibres de carboni modificat amb glutatió *Glutathione modified screen-printed carbon nanofibers electrode*
GSMA	Mètode d'addició estàndard generalitzat *Generalized standard addition method*
HDME	Elèctrode de gota penjant de mercuri *Hanging drop mercury electrode*
HEPES	Àcid 4-(2-hidroxietil)-1-piperazinetansulfònic *4-(2-hydroxyethyl)-1-piperazineethanesulfonic acid*
HQ	Hidroquinona *Hydroquinone*
I_a	Intensitat del pic anòdic *Anodic peak current*
I_c	Intensitat del pic catòdic *Cathodic peak current*

ICP	Plasma acoblat inductivament *Inductively coupled plasma*
ICP-MS	Plasma acoblat inductivament amb espectrometria de masses *Inductively coupled plasma mass spectrometry*
ICP-OES	Plasma acoblat inductivament amb espectrometria d'emissió òptica *Inductively coupled plasma optical emission spectroscopy*
***In-situ*-SbSPCE**	Elèctrode serigrafiat de carboni modificat *in-situ* amb antimoni *In-situ antimony modified screen-printed carbon electrode*
***In-situ*-SbSPCNFE**	Elèctrode serigrafiat de nanofibres de carboni modificat *in-situ* amb antimoni *In-situ antimony modified screen-printed carbon nanofibers electrode*
***In-situ*-SbSPCNTE**	Elèctrode serigrafiat de nanotubs de carboni modificat *in-situ* amb antimoni *In-situ antimony modified screen-printed carbon nanotubes electrode*
***In-situ*-SbSPE**	Elèctrode serigrafiat modificat *in-situ* amb antimoni *In-situ antimony modified screen-printed electrode*
***In-situ*-SbSPGPHE**	Elèctrode serigrafiat de grafè modificat *in-situ* amb antimoni *In-situ antimony modified screen-printed graphene electrode*
IRMM	Institut de Materials i Mesures de Referència *Institute for Reference Materials and Measurements*

ISE	Elèctrode selectiu d'ions *Ion-selective electrode*
IUPAC	Unió Internacional de Química Pura i Aplicada *International Union of Pure and Applied Chemistry*
JCR	Centre Comú d'Investigació *Joint Research Centre*
LDA	Anàlisi discriminant lineal *Linear discriminant analysis*
LOD	Límit de detecció *Limit of detection*
LOQ	Límit de quantificació *Limit of quantification*
LV	Variable latent *Latent variable*
MES	Àcid 2-(N-morfolin-etansulfònic) *2-(N-morpholino)ethanesulfonic acid*
MWCNT	Nanotubs de carboni de paret múltiple *Multi-walled carbon nanotubes*
NP	Nanopartícula *Nanoparticle*
OSC	Correcció ortogonal del senyal *Orthogonal signal correction*
PCA	Anàlisi de components principals *Principal component analysis*
PCR	Regressió de components principals *Principal component regression*

PIPES	Àcid piperazin-N,N'-bis(2-etansulfònic) *Piperazine-N,N'-bis(2-ethanesulfonic acid)*
PLS	Mínims quadrats parcials *Partial least squares*
PLS-DA	Mínims quadrats parcials amb anàlisi discriminant *Partial least squares - discriminant analysis*
PNA	4-Nitroanilina *4-Nitroaniline*
(PNA)Cys-SPCNFE	Elèctrode serigrafiat de nanofibres de carboni modificat amb cisteïna i enllaçat pel grup carboxílic *Cysteine modified screen-printed carbon nanofibers electrode, coupled through the carboxylic group*
pSi	Silici porós *Porous silicon*
PSSS	Sulfonat sòdic de poliestirè *Poly(sodium styrenesulphonate)*
RC	Resorcinol *Resorcinol*
RE	Elèctrode de referència *Reference electrode*
RMSE	Arrel de l'error quadràtic mitjà *Root mean square error*
RSD	Desviació estàndard relativa *Relative standard deviation*
SAM	Monocapa autoensamblada *Self-assembled monolayer*
SeCyst	Selenocistina *Selenocystine*

SeCyst-SPCNFE	Elèctrode serigrafiat de nanofibres de carboni modificat amb selenocistina *Selenocystine modified screen-printed carbon nanofibers electrode*
SEM	Microscòpia electrònica de rastreig *Scanning electron microscopy*
SOM	Mapa autoorganitzat *Self-organizing map*
SPCE	Elèctrode serigrafiat de carboni *Screen-printed carbon electrode*
SPCNFE	Elèctrode serigrafiat de nanofibres de carboni *Screen-printed carbon nanofibers electrode*
SPCNTE	Elèctrode serigrafiat de nanotubs de carboni *Screen-printed carbon nanotubes electrode*
SPE	Elèctrode serigrafiat *Screen-printed electrode*
SPGPHE	Elèctrode serigrafiat de grafè *Screen-printed graphene electrode*
$\mathbf{s_{rate}}$	Velocitat d'escombratge *Scan rate*
Sulfo-NHS	N-hidroxisulfosuccinimida *N-hydroxysulfosuccinimide*
SVM	Màquina de vector de suport *Support vector machine*
SWCNT	Nanotubs de carboni de paret simple *Single-walled carbon nanotubes*
SWV	Voltamperometria d'ona quadrada *Square wave voltammetry*

TCpSi	Silici porós tèrmicament carbonitzat *Thermally carbonized porous silicon*
$\mathbf{t_{acc}}$	Temps d'acumulació *Accumulation time*
$\mathbf{t_d}$	Temps de deposició *Deposition time*
TEM	Microscòpia electrònica de transmissió *Transmission electron microscopy*
THCpSi	Silici porós tèrmicament hidrocarbonitzat *Thermally hydrocarbonized porous silicon*
$\mathbf{t_{int}}$	Interval de temps *Interval time*
$\mathbf{t_p}$	Temps d'impuls *Pulse time*
WE	Elèctrode de treball *Working electrode*

Índex

Objectius

L'objectiu principal d'aquesta tesi doctoral se centra en el desenvolupament de sensors voltamperomètrics basats en elèctrodes serigrafiats i de llengües electròniques voltamperomètriques per a la determinació d'ions metàl·lics a nivell traça en mostres mediambientals.

Per tal d'assolir aquest objectiu general s'han plantejat diversos objectius específics que s'exposen a continuació:

- Desenvolupar nous sensors voltamperomètrics basats en la modificació d'elèctrodes serigrafiats seguint diferents estratègies: modificació química, formació de pel·lícules metàl·liques i modificació amb diversos nanomaterials (nanopartícules metàl·liques, nanoal·lòtrops de carboni i silici porós).

- Caracteritzar microscòpica i electroquímicament les diferents etapes de modificació dels sensors desenvolupats.

- Avaluar el comportament analític dels diferents sensors per a la determinació d'ions metàl·lics a nivell traça.

- Aplicar els sensors òptims a la determinació d'ions metàl·lics en mostres reals d'interès ambiental.

- Estudiar la resposta creuada dels diferents sensors desenvolupats per tal de seleccionar-ne aquells que permetin formar una llengua voltamperomètrica per a la resolució de mostres complexes d'ions metàl·lics.

- Determinar voltamperomètricament els ions metàl·lics considerats en mostres sintètiques i reals mitjançant els sensors seleccionats i d'acord al disseny experimental, i posteriorment processar les dades dels senyals obtinguts mitjançant tècniques d'anàlisi multivariant per tal de quantificar aquests ions metàl·lics en mostres complexes.

- Desenvolupar una nova estratègia d'addició estàndard multivariant basada en l'ús de la regressió per mínims quadrats parcials i la simulació del blanc de la mostra a partir de l'omissió de l'etapa de preconcentració de la mesura voltamperomètrica per tal de minimitzar l'efecte matriu en mostres reals complexes.

Contingut i estructura de la memòria

Aquesta memòria de tesi doctoral està estructurada en sis parts que s'exposen a continuació.

La primera part de la memòria consisteix en una **Introducció** general, dividida en tres capítols, on es contextualitza la temàtica objecte d'estudi. El **Capítol 1** és una breu introducció als metalls pesants on s'incideix sobre la seva terminologia, la problemàtica mediambiental que suposen, la seva toxicitat, la legislació vigent i les principals tècniques analítiques emprades per a la seva determinació. Al **Capítol 2** s'exposa l'evolució que han patit els sensors voltamperomètrics en els últims anys i es fa especial èmfasi en els elèctrodes serigrafiats i en les diferents estratègies de modificació amb què s'ha treballat al llarg d'aquesta tesi doctoral (modificació química, formació de pel·lícules metàl·liques i modificació amb diversos nanomaterials com les nanopartícules metàl·liques, els nanoal·lòtrops de carboni o el silici porós). En el **Capítol 3** s'introdueixen les llengües electròniques, incidint sobre la seva definició i algunes consideracions experimentals referides a la selecció i disposició dels

sensors que formen la llengua, així com els models de calibratge i validació més emprats en funció de si es tracta d'una anàlisi qualitativa o quantitativa.

La segona part d'aquesta memòria presenta la **Metodologia analítica** emprada al llarg d'aquesta tesi doctoral. Així, al **Capítol 4** s'explica el fonament de les tècniques instrumentals utilitzades, on s'inclouen tècniques voltamperomètriques i tècniques de microscòpia electrònica, i al **Capítol 5** es detallen els diferents tractaments de dades, amb un primer apartat referent als preprocessats i un segon apartat relacionat amb els sistemes de calibratge.

La tercera part d'aquesta memòria recull l'**Experimental** realitzat al llarg d'aquesta tesi doctoral. En el **Capítol 6** es llisten la instrumentació i els reactius emprats en els diferents treballs i el **Capítol 7** detalla els diferents procediments experimentals, que fan referència a la modificació d'elèctrodes serigrafiats, a la fabricació d'elèctrodes de silici porós, a la caracterització dels diferents sensors emprats, a les mesures voltamperomètriques i als calibratges multivariants.

La quarta part d'aquesta memòria correspon als **Resultats i discussió.** Aquesta tesi doctoral es presenta com a compendi de publicacions i els resultats s'han dividit en dos capítols. En el **Capítol 8** es recullen i discuteixen tots els resultats associats al desenvolupament de sensors voltamperomètrics, que corresponen a les 9 primeres publicacions. Aquesta discussió engloba tant la caracterització dels sensors com la seva aplicació analítica i s'ha dividit en quatre apartats corresponents als quatre tipus de sensors voltamperomètrics: sensors modificats químicament, sensors basats en pel·lícules metàl·liques, sensors modificats amb nanopartícules metàl·liques i elèctrodes de silici porós. En aquest punt cal mencionar que aquest últim apartat referit als elèctrodes de silici porós correspon als resultats obtinguts durant una estada de pràcticament 4 mesos realitzada al Monash Institute of Pharmaceutical Sciences (Melbourne, Austràlia) sota la supervisió de la Dra. Beatriz Prieto-Simón per la qual s'opta a la Menció Internacional de Doctorat.

En el **Capítol 9** es recullen i discuteixen els resultats relacionats amb el desenvolupament de llengües voltamperomètriques, que corresponen a les 3 últimes publicacions. En aquest capítol la discussió està dividida en tres apartats que fan referència a la selecció i disposició dels sensors, al disseny experimental i al tractament quimiomètric de les dades.

Finalment, a les últimes dues parts d'aquesta memòria es presenten les **Conclusions** generals d'aquesta tesi doctoral i les **Referències** bibliogràfiques consultades.

Els treballs presentats en aquesta memòria de tesi doctoral són:

(1) *Glutathione modified screen-printed carbon nanofiber electrode for the voltammetric determination of metal ions in natural samples*
Clara Pérez-Ràfols, Núria Serrano, José Manuel Díaz-Cruz, Cristina Ariño, Miquel Esteban
Talanta 155 (2016) 8-13
https://doi.org/10.1016/j.talanta.2016.04.011

(2) *A chemically-bound glutathione sensor bioinspired by the defense of organisms against heavy metal contamination: Optimization of the immobilization conditions*
Clara Pérez-Ràfols, Núria Serrano, José Manuel Díaz-Cruz, Cristina Ariño, Miquel Esteban
Chemosensors 5 (2017) 12-19 ***(Open Access)***
https://doi.org/10.3390/chemosensors5020012

(3) *Selenocystine modified screen-printed electrode as an alternative sensor for the voltammetric determination of metal ions*
Jaume Puy-Llovera, Clara Pérez-Ràfols, Núria Serrano, José Manuel Díaz-Cruz, Cristina Ariño, Miquel Esteban
Talanta 175 (2017) 501-506
https://doi.org/10.1016/j.talanta.2017.07.089

(4) *Expanding the possibilities of electrografting modification of voltammetric sensors through two complementary strategies*
Clara Pérez-Ràfols, Miguel Rosal, Núria Serrano, Cristina Ariño, Miquel Esteban, José Manuel Díaz-Cruz
Electrochimica Acta 319 (2019) 878-884
https://doi.org/10.1016/j.electacta.2019.07.034

(5) *New approaches to antimony film screen-printed electrodes using carbon-based nanomaterials substrates*
Clara Pérez-Ràfols, Núria Serrano, José Manuel Díaz-Cruz, Cristina Ariño, Miquel Esteban
Analytica Chimica Acta 916 (2016) 17-23
https://doi.org/10.1016/j.aca.2016.03.003

(6) *Determination of Pd(II) using an antimony film coated on a screen-printed electrode by adsorptive stripping voltammetry*
Clara Pérez-Ràfols, Pedro Trechera, Núria Serrano, José Manuel Díaz-Cruz, Cristina Ariño, Miquel Esteban
Talanta 167 (2017) 1-7
https://doi.org/10.1016/j.talanta.2017.01.084

(7) *Ag nanoparticles drop-casting modification of screen-printed electrodes for the simultaneous voltammetric determination of Cu(II) and Pb(II)*
Clara Pérez-Ràfols, Julio Bastos-Arrieta, Núria Serrano, José Manuel Díaz-Cruz, Cristina Ariño, Juan de Pablo, Miquel Esteban
Sensors 17 (2017) 1458-1469 ***(Open Access)***
https://doi.org/10.3390/s17061458

(8) *Green synthesis of Ag nanoparticles using grape stalk waste extract for the modification of screen-printed elèctrodes*
Julio Bastos-Arrieta, Antonio Florido, Clara Pérez-Ràfols, Núria Serrano, Núria Fiol, Jordi Poch, Isabel Villaescusa
Nanomaterials 8 (2018) 946-959 ***(Open Access)***
https://doi.org/10.3390/nano8110946

(9) *Carbon-stabilized porous silicon as novel voltammetric sensor platforms*
Clara Pérez-Ràfols, Keying Guo, Nicolas H. Voelcker, Beatriz Prieto-Simon
Manuscrit en fase de revisió

(10) *Simultaneous determination of Tl(I) and In(III) using a voltammetric sensor array*
Clara Pérez-Ràfols, Núria Serrano, José Manuel Díaz-Cruz, Cristina Ariño, Miquel Esteban
Sensors and Actuators B 245 (2017) 18-24
https://doi.org/10.1016/j.snb.2017.01.089

(11) *A screen-printed voltammetric electronic tongue for the analysis of complex mixtures of metal ions*
Clara Pérez-Ràfols, Núria Serrano, José Manuel Díaz-Cruz, Cristina Ariño, Miquel Esteban
Sensors and Actuators B 250 (2017) 393-401
https://doi.org/10.1016/j.snb.2017.04.165

(12) *A new multivariate standard addition strategy for stripping voltammetric electronic tongues: Application to the determination of Tl(I) and In(III) in samples with complex matrices*
Clara Pérez-Ràfols, Jaume Puy-Llovera, Núria Serrano, Cristina Ariño, Miquel Esteban, José Manuel Díaz-Cruz
Talanta 192 (2019) 147-153
https://doi.org/10.1016/j.talanta.2018.09.035

PART I
INTRODUCCIÓ

1

Els metalls pesants

El terme metall pesant va ser proposat per primera vegada el 1936 per N. Bjerrum [1], que el va definir com a qualsevol metall amb una densitat superior a 7 g cm^{-3}. Des de llavors diversos autors han modificat aquesta definició emprant altres valors de llindar de densitat, que fluctuen entre el 3,5 i el 7, o altres paràmetres com la massa atòmica, el nombre atòmic, la toxicitat o altres propietats químiques més específiques [2]. Aquest fet ha generat un debat a la comunitat científica sobre si és apropiat o no emprar aquest terme. Així, alguns autors defensen l'abolició del terme metall pesant argumentant que es tracta d'un terme imprecís, que sovint fa referència tant als elements com als compostos que contenen aquests metalls, i que engloba un conjunt de metalls diferents en funció de la definició que es prengui com a referència, arribant fins i tot en alguns casos a englobar semi-metalls com l'arsènic o l'antimoni [2–6]. Aquest grup d'autors proposa doncs, dues alternatives: (i) emprar altres classificacions de metalls ja existents [2,5] o nous termes més precisos [7] o (ii) llistar els metalls estudiats o, en cas que el nombre de metalls sigui molt nombrós, referir-se a ells simplement com a ions metàl·lics o metalls tòxics o a nivell traça [3–6]. Per contra, hi ha un segon grup d'autors que defensa que el terme metall pesant és un terme útil i ben establert que, per tant, no s'hauria

d'eliminar [8–10]. Així, aquests darrers proposen acordar una definició o, en el seu defecte, un llistat tancat de metalls per tal d'uniformar l'ús d'aquest terme. Tenint en compte aquesta controvèrsia, al llarg d'aquesta tesi doctoral s'ha procurat limitar l'ús del terme metall pesant i optar, en la majoria dels casos, per llistar els diferents metalls o referir-se a aquests com a ions metàl·lics.

1.1 Problemàtica mediambiental

Els metalls són components naturals de l'escorça terrestre que poden ser fàcilment alliberats al medi ambient. Els fluxos entre els diferents compartiments del medi ambient (litosfera, hidrosfera, atmosfera i biosfera) estan controlats per processos naturals, sent el desgast, l'erosió, l'activitat volcànica, els focs forestals i les fonts biogèniques els processos amb major contribució (figura 1.1) [11,12]. No obstant, al llarg del temps aquests fluxos s'han vist greument afectats per fonts antropogèniques de metalls que, a més de generar un gran increment en les quantitats de metall alliberades, també provoquen alteracions en la seva especiació, fet que afecta el comportament geoquímic (mobilitat, reactivitat) i biològic (biodisponibilitat, toxicitat) dels metalls [13].

Aquestes alteracions dels cicles biogeoquímics naturals dels metalls es remunten a temps prehistòrics amb el descobriment de la mineria i les diferents tècniques per treballar els metalls. Les primeres societats mediterrànies van desequilibrar encara més aquests cicles ja que requerien grans quantitats de metalls per a mantenir el seu elevat nivell de vida, però no va ser fins la revolució industrial, i més particularment, fins a principis del segle XX que les emissions de metalls van començar a créixer exponencialment. Aquest increment en la quantitat de metalls alliberada va anar acompanyat també d'un augment en la diversitat dels metalls alliberats, fet que sol atribuir-se a les demandes generades pels camps de l'electrònica, la indústria espacial i les aplicacions militars [14,15].

La preocupació pels efectes d'aquest augment en la quantitat i la diversitat dels metalls alliberats ha portat a establir un control sobre les emissions dels metalls. L'any 1989 es va publicar el primer inventari a escala mundial que recollia les emissions de 13 metalls a l'atmosfera, el sòl i l'aigua, evidenciant que les fonts

naturals de metalls eren pràcticament menyspreables davant les fonts antropogèniques [16].

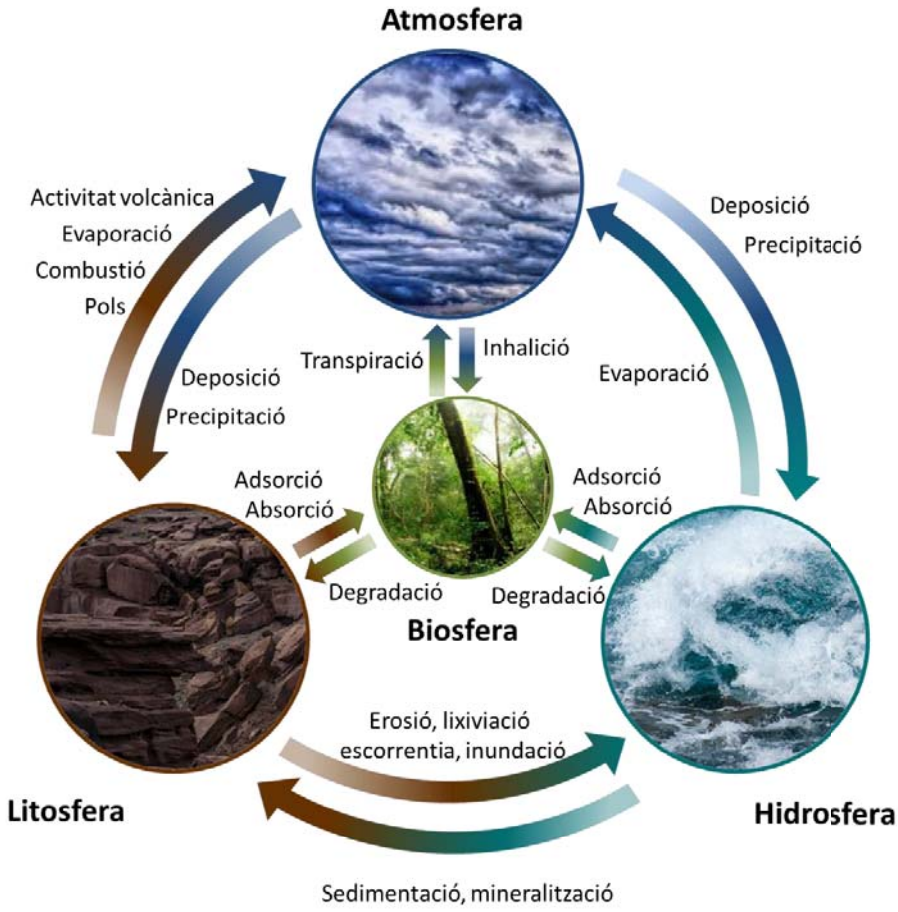

Figura 1.1. Cicle biogeoquímic dels metalls.

A nivell europeu, des de l'any 2006 el reglament 166/2006 sobre l'establiment d'un registre europeu de les emissions i transferències de contaminants obliga a reportar emissions d'arsènic, cadmi, crom, coure, plom, mercuri, níquel i zinc superiors a les quantitats que es mostren a la taula 1.1, que es fan públiques a través de l'Agència Europea del Medi Ambient (AEMA). Tal com es pot observar a la figura 1.2, que mostra l'evolució de les emissions d'aquests vuit metalls a Europa en el període 2007-2016, les emissions de zinc representen més de la meitat de les emissions d'aquests metalls i, d'entre els quatre metall més tòxics

(cadmi, plom, mercuri i arsènic) el plom és el que té uns nivells d'emissions més elevats. D'altra banda, també es pot observar una disminució de les emissions totals al llarg dels anys. Aquesta tendència es pot explicar en alguns casos per la disminució de la fosa o demanda del metall i, en altres casos, per l'aparició de regulacions estrictes sobre l'ús del metall. Alguns exemples d'aquest últim cas serien la prohibició de la benzina amb plom o la regulació europea sobre el mercuri [12].

Taula 1.1. Llindar a partir del qual cal reportar les emissions de metalls segons el reglament europeu 166/2006.

	Llindar d'emissions (kg any^{-1})[a]		
	Atmosfera	**Aigua**	**Sòl**
Arsènic i compostos	20	5	5
Cadmi i compostos	10	5	5
Crom i compostos	100	50	50
Coure i compostos	100	50	50
Mercuri i compostos	10	1	1
Níquel i compostos	50	20	20
Plom i compostos	200	20	20
Zinc i compostos	200	100	100

[a]Tot i considerar tant metalls com compostos de metalls, en tots els casos els llindars d'emissions s'expressen com a kg de metall.

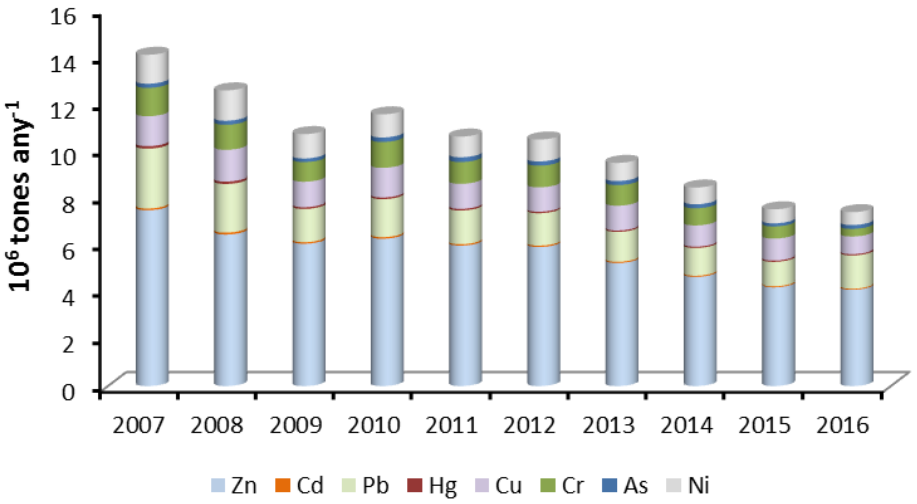

Figura 1.2. Evolució de les emissions de metalls a Europa en els anys 2007-2016.

Aquestes mateixes dades també permeten veure quines són les principals fonts antropogèniques de metalls segons si es tenen en compte les emissions a l'aigua i al sòl o a l'atmosfera (figura 1.3). Tot i que el patró és diferent per a cada metall, en general s'observa que les fonts que més impacte tenen en les emissions de metalls a l'aigua i al sòl són la gestió de residus i aigües residuals, el sector energètic i la indústria química, mentre que les emissions a l'atmosfera estan dominades per la producció i transformació de metalls i el sector energètic.

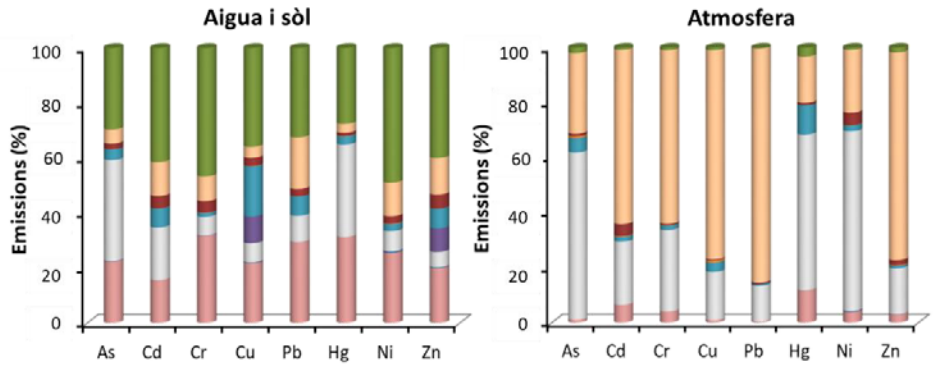

Figura 1.3. Principals fonts antropogèniques de les emissions de metalls a l'aigua i al sòl i a l'atmosfera. (●) Gestió de residus i aigües residuals, (●) Fabricació i transformació del paper i la fusta, (●) Mineria, (●) Sector energètic, (●) Indústria química, (●) Producció i transformació de metalls, (●) Ramaderia intensiva i aqüicultura, (●) Productes d'origen animal i vegetal de la indústria alimentària i de begudes i (●) Altres activitats.

L'emissió antropogènica de metalls és especialment preocupant ja que, a diferència d'altres contaminants, els metalls no són biodegradables i persisteixen en el medi ambient. Això suposa un gran repte per a la seva remediació ja que, tot i que existeixen diferents mètodes (excavació i recobriment, tractaments tèrmics, bioremediació...), tots ells són processos costosos, lents o destructius per al medi ambient. A més, la no biodegradació dels metalls potencia la seva tendència a bioacumular-se, és a dir, a augmentar la seva concentració en organismes biològics al llarg del temps, arribant a assolir nivells molts superiors als que trobem al seu entorn. Aquesta bioacumulació és conseqüència de dos processos diferents, la bioconcentració i la biomagnificació. En el primer cas, els metalls s'absorbeixen directament del

medi a través de la pell o els pulmons mentre que en el segon cas l'absorció del metall té lloc a través de la dieta [17].

1.2 Toxicitat dels metalls

A nivell de toxicitat, podem dividir els metalls en dos grans grups: els micronutrients essencials i els metalls traça no essencials. Els micronutrients essencials són aquells metalls que són necessaris en petites concentracions per al correcte desenvolupament de diversos processos vitals en plantes i animals com el metabolisme, el creixement o la integritat de les membranes entre d'altres. Dins d'aquest grup trobem el cobalt, el coure, el ferro, el manganès, el molibdè, el níquel i el zinc. D'altra banda, els metalls traça no essencials són metalls que no tenen cap funció biològica coneguda com, per exemple, el plom, el cadmi i el mercuri. Aquest grup de metalls també poden tenir alguns efectes positius temporalment quan es troben a concentracions molt baixes generant, per exemple, un accelerament del creixement de les plantes, un increment dels nivells de respiració o una estimulació de l'activitat fotosintètica [18].

No obstant, tot i què en baixes concentracions tots dos grups de metalls poden arribar a tenir efectes positius en plantes i animals, a concentracions més elevades tots els metalls acaben sent tòxics. La toxicitat dels metalls però, no depèn únicament de la seva concentració total sinó que es pot veure afectada per diversos factors ambientals com la capacitat d'intercanvi catiònic, el pH o la presència d'altres metalls o de lligands orgànics i inorgànics. Aquests factors poden afectar a l'especiació dels metalls, que en alguns casos està directament relacionada amb la toxicitat. Per exemple, el Cr(VI) és altament tòxic en plantes i animals mentre que el Cr(III) no és tòxic per a les plantes i és essencial per als animals [19].

Típicament però, aquests factors ambientals afecten a la toxicitat ja que alteren la biodisponibilitat dels metalls o, en altres paraules, la facilitat que tenen els metalls per incorporar-se als organismes. Per exemple, els sòls amb una elevada densitat de càrrega negativa com els argilosos, enllacen cations metàl·lics per compensar la seva càrrega, fent que aquests metalls deixin de ser biodisponibles. No obstant, com aquests enllaços són febles i reversibles es veuen afectats pel pH (a pH àcids els protons desplacen els metalls i els

alliberen) i per la presència d'altres metalls (s'estableixen processos competitius entre els diferents metalls). Un altre exemple seria la formació de complexos metall-lligand amb una major mobilitat a l'aire, l'aigua i el sòl, augmentant-ne la seva biodisponibilitat. La formació d'aquests complexos depèn, entre altres factors, del pH i del contingut de matèria orgànica. Els principals lligands inorgànics són els hidròxids i els clorurs mentre que entre els lligands orgànics trobem diversos àcids (cítric, oxàlic...), les fitoquelatines o les metal·lotioneïnes [20].

En el cas dels éssers humans, podem dividir les intoxicacions per metalls en dos grans grups en funció del tipus d'exposició: (i) intoxicació per exposició a elevats nivells de metalls i (ii) intoxicació per exposició prolongada a baixos nivells de metalls. Dos dels exemples més coneguts d'exposicions a elevats nivells de metalls són la malaltia *itai-itai* a Toyama (Japó), on es va produir una intoxicació massiva amb cadmi deguda a la contaminació dels rius per l'activitat minera, i la malaltia de minamata a Kumamoto (Japó), en què una indústria química va abocar metilmercuri que es va bioacumular als peixos i va provocar una intoxicació alimentària. Aquestes situacions però, es poden controlar si s'apliquen les mesures preventives adients. De fet, actualment en països desenvolupats aquests episodis d'intoxicació són molt poc freqüents, es donen només esporàdicament fruït d'accidents o negligències. En països poc desenvolupats o amb una indústria emergent però, encara cal instaurar mesures preventives per tal de disminuir les exposicions ambientals i industrials. Aquest seria el cas de la Índia, on a la zona de Bangladesh l'aigua de consum té uns nivells d'arsènic molt elevats. La intoxicació per exposició prolongada a baixos nivells de metalls és molt més difícil de prevenir i detectar ja que els símptomes triguen anys a aparèixer [17,21].

Els metalls poden incorporar-se al nostre organisme a través de l'aire, l'aigua, l'alimentació o l'adsorció a través de la pell. La principal via d'exposició varia en funció del col·lectiu considerat, en el cas dels nens seria l'alimentació mentre que en adults que treballen a la indústria predomina la intoxicació per adsorció a través de la pell [17].

Un cop a l'interior del cos humà els metalls interfereixen en la funció d'alguns metal·loenzims i en algunes vies biològiques importants. Tot i que els símptomes varien en funció del metall, és comú que una intoxicació greu per metalls acabi derivant en danys en el sistema nerviós central, malalties

cardiovasculars, problemes renals, càncer o afectacions al fetus. En casos menys greus, la intoxicació per metalls s'ha associat també a altres malalties que, tot i no ser mortals, afecten significativament la qualitat de vida com l'artritis, l'Alzheimer, la impotència, la diabetis, la fatiga, les pèrdues de memòria o l'insomni [17,21].

1.3 Legislació

Tal com ja s'ha exposat anteriorment, actualment s'estan realitzant molts esforços per reduir les emissions antropogèniques de metalls al medi ambient. La implementació de diverses regulacions ha permès reduir les emissions d'alguns metalls però, donada la seva elevada persistència al medi ambient, els nivells de metalls actuals són encara molt superiors als nivells que trobaríem de manera natural. Aquest fet, juntament amb els efectes nocius dels metalls sobre la salut humana, fa que no només sigui necessari establir un control sobre les emissions de metalls sinó que també calgui controlar la presència de metalls al medi ambient i en productes de consum humà.

A nivell ambiental existeixen diverses normatives vigents que regulen els nivells màxims admissibles de metalls en aire, aigües i sòls. Pel que fa a l'aire, el Reial Decret 102/2011 estableix els objectius de qualitat a assolir per a determinades substàncies, regula la seva avaluació, manteniment i millora i estableix els mètodes i criteris comuns per avaluar-los. En concret, en aquesta normativa es consideren quatre metalls, l'arsènic, el plom, el níquel i el cadmi, els valors objectius per un any dels quals es mostren a la taula 1.2.

Taula 1.2. Valors objectius com a mitjana de l'any per als metalls i metal·loides considerats en el Reial Decret 102/2011.

Element	Valor objectius (ng m^{-3})
Arsènic	6
Cadmi	5
Níquel	20
Plom	500

En el cas de l'aigua, l'any 2000 es va establir la directiva marc de l'aigua (2000/60/EC) on s'establien les normes de qualitat ambiental que havien de complir les aigües superficials a Europa. Actualment, aquesta directiva s'aplica a Espanya a través del Reial Decret 817/2015, que afegeix la regulació de l'arsènic, el coure, el crom, el seleni i el zinc a les regulacions del cadmi, plom, mercuri i níquel ja establertes a la directiva europea. A la taula 1.3 es mostren els valors permesos per a cada metall en funció del tipus d'aigua superficial.

Taula 1.3. Normes de qualitat ambiental en aigües superficials referides a metalls i metal·loides establertes en el Reial Decret 817/2015.

	Mitjana anual (μg L^{-1})		CMA (μg L^{-1})
Element	**Aigües superficials continentals** [a]	**Altres aigües superficials**	**Aigües superficials**
Cadmi i compostos [b]	0,25	0,2	1,5
Plom i compostos [c]	7,2 (1,2)	7,2 (1,3)	ND (14)
Mercuri i compostos	ND	ND	0,07
Níquel i compostos [c]	20 (4)	20 (8,6)	ND (34)
Arsènic	50	25	ND
Coure [b]	120	25	ND
Crom (VI)	5	5	ND
Crom total	50	ND	ND
Seleni	1	10	ND
Zinc [b]	500	60	ND

CMA: concentració màxima admissible, ND: no definit

[a] Les aigües superficials continentals inclouen els rius, els llacs i altres aigües artificials.

[b] Els valors varien en funció de la duresa de l'aigua. S'han considerat les aigües dures (>100 mg $CaCO_3$ L^{-1} pel coure i el zinc i >200 mg $CaCO_3$ L^{-1} pel cadmi)

[c] El valor entre parèntesi fa referència a la fracció biodisponible.

Respecte als sòls, en el marc del pla nacional de recuperació de sòls contaminats (1995-2005) es van detectar a Espanya 4532 zones potencialment contaminades i, amb aquestes, la necessitat d'establir uns criteris normalitzats de valoració de la contaminació de sòls. Així, el Reial Decret 9/2005 va establir aquests criteris per a diverses substàncies orgàniques i va instar a les comunitats autònomes a establir-los per als metalls. A Catalunya, l'Agència de Residus de Catalunya va ser l'encarregada d'establir els nivells genèrics de referència per als metalls en sòls per a la protecció de la salut humana i els ecosistemes, que varien en funció

del tipus de zona i de l'ús que se li dóna al sòl. Aquests valors, que es troben recollits al Decret Legislatiu 1/2009, es mostren a la taula 1.4.

Taula 1.4. Valors genèrics de referència per a metalls i metal·loides emprats per a l'avaluació de la contaminació de sòls a Catalunya segons el Decret Legislatiu 1/2009. Els valors s'expressen en mg kg^{-1} de sòl sec.

	Protecció dels ecosistemes en funció del tipus de zona		**Protecció de la salut humana en funció de l'ús del sòl**		
Element	**Agropecuària i forestal**	**Altres**	**Industrial**	**Urbà**	**Altres**
Antimoni	6,0	6,0	30	6	6
Arsènic	30	60	30	30	30
Bari	500	270	1000	880	500
Beril·li	10	4,5	90	40	10
Cadmi	2,5	0,6	55	5,5	2,5
Cobalt	25	25	90	45	25
Coure	90	55	1000	310	90
Crom (III)	400	85	1000	1000	400
Crom (VI)	1,0	1,0	25	10	1
Estany	50	7	1000	1000	50
Mercuri	2,0	2,0	30	3	2
Molibdè	3,5	3,5	70	7	3,5
Níquel	45	45	1000	470	45
Plom	60	60	550	60	60
Seleni	0,7	0,5	70	7	0,7
Tal·li	1,5	1,5	45	4,5	1,5
Vanadi	135	135	1000	190	135
Zinc	170	110	1000	650	170

D'altra banda, si considerem els productes de consum humà també existeixen determinades normatives que regulen la presència de metalls i metal·loides. L'aigua potable es regeix pel Reial Decret 140/2003 mentre que la resta de productes alimentaris han de complir el reglament 1881/2006 de la comissió europea, corregit pel reglament 48/2014 en el cas del cadmi. A la taula 1.5 es mostren els valors màxims permesos de metalls i metal·loides en aigua potable i alguns dels valors més representatius referents a productes alimentaris.

Taula 1.5. Valors màxims permesos per a metalls i metal·loides en aigua potable (μg L^{-1}) i diversos productes alimentaris (μg kg^{-1}) segons el Reial Decret 140/2003 i el reglament europeu 1881/2006 respectivament.

Element	Aigua potable	Carn	Peix	Cereals i llegums	Fruites i hortalisses
Antimoni	5,0				
Arsènic	10				
Cadmi	5,0	50	50	100	50
Coure	2000				
Crom	50				
Mercuri	1,0		500		
Níquel	20				
Plom	10	100	300	200	100
Seleni	10				

Finalment, el tercer bloc de productes de consum humà on es regula la presència de metalls i metal·loides són els productes farmacèutics. En aquest cas la normativa va ser establida per l'Agència Europea de Medicaments (EMA) d'acord amb el Consell Internacional sobre harmonització de requisits tècnics per al registre de productes farmacèutics de consum humà, que engloba autoritats d'Europa, Japó i Estats Units així com diverses farmacèutiques. A la taula 1.6 es mostren alguns dels valors més representatius d'aquesta normativa.

Taula 1.6. Valors màxims permesos per a metalls i metal·loides en productes farmacèutics (μg g^{-1}) segons les pautes ICH QD3 del 28 de març de 2019.

Element	Concentració oral	Concentració parenteral	Concentració per inhalació
Antimoni	120	9	2
Arsènic	1,5	1,5	0,2
Cadmi	0,5	0,2	0,3
Coure	300	30	3
Crom	1100	110	0,3
Mercuri	3	0,3	0,1
Níquel	20	2	0,5
Pal·ladi	10	1	0,1
Plom	0,5	0,5	0,5
Tal·li	0,8	0,8	0,8

1.4 Determinació a nivell traça

Actualment a la bibliografia podem trobar múltiples metodologies analítiques per a la determinació de metalls a nivell traça. A la figura 1.4 es mostra una classificació d'aquestes metodologies en funció del seu principi químic, l'espècie que s'analitza i l'objectiu de l'anàlisi.

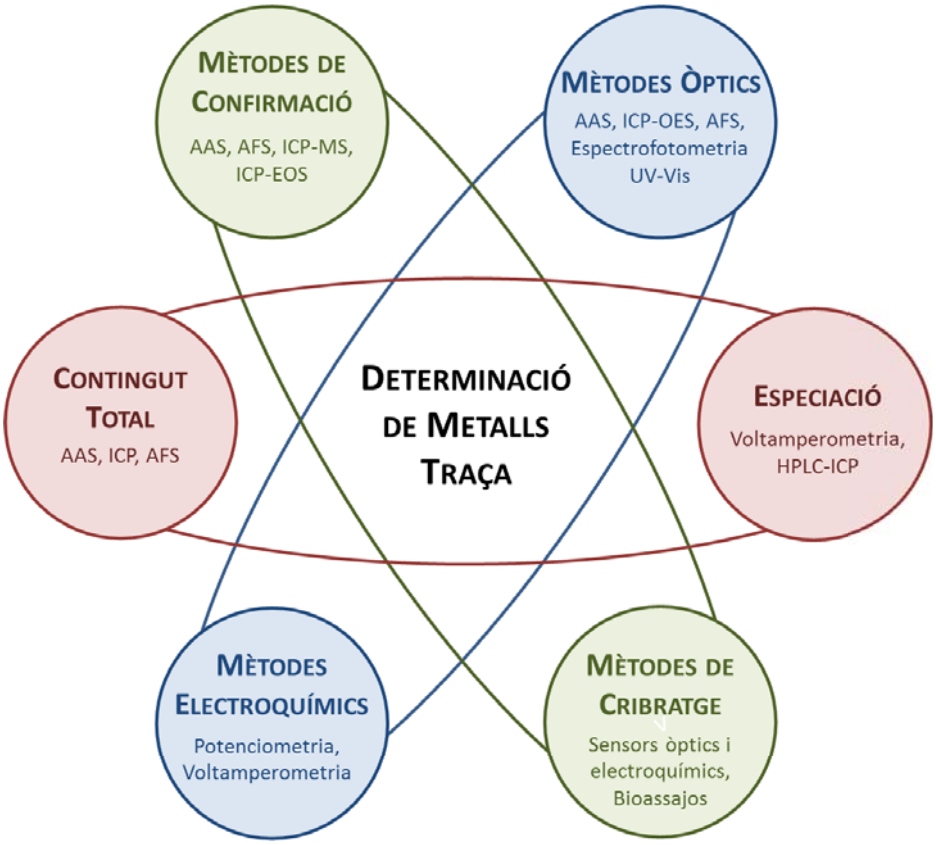

Figura 1.4. Classificació dels mètodes de determinació de metalls a nivell traça en funció del principi químic, l'espècie analitzada i l'objectiu de l'anàlisi.

En termes de principi químic podem classificar els mètodes per a la determinació de metalls a nivell traça en mètodes òptics i mètodes electroquímics. Entre els mètodes òptics prenen especial importància els mètodes d'espectrometria atòmica on la mostra és atomitzada o ionitzada amb flama o plasma acoblat inductivament (ICP, *inductively coupled plasma*) i

posteriorment detectada mitjançant diferents modes òptics (absorció, emissió o fluorescència). Dins d'aquest grup les tècniques més emprades són l'espectrometria d'absorció atòmica (AAS, *atomic absorption spectroscopy*) i el plasma acoblat inductivament amb espectrometria d'emissió òptica (ICP-OES, *inductively coupled plasma optical emission spectroscopy*) o espectrometria de masses (ICP-MS, *inductively coupled plasma mass spectrometry*) [22]. Existeixen també mètodes basats en altres principis òptics com la colorimetria o la quimioluminescència [23]. D'altra banda, dins dels mètodes electroquímics les tècniques més habituals són la potenciometria i la voltamperometria. En el primer cas els mètodes solen basar-se en l'ús d'elèctrodes d'ió selectiu (ISEs, *ion-selective electrode*) o transistors d'efecte de camp (FETs, *field-effect transistor*) mentre que en el segon cas predominen els mètodes de redissolució on els metalls són preconcentrats a la superfície de l'elèctrode, permetent així assolir límits de detecció més baixos [24].

Pel que fa a l'espècie analitzada podem classificar els mètodes d'anàlisi entre els que determinen el contingut total de metall i els que determinen una espècie en concret (un ió determinat, una forma orgànica concreta…). En el primer grup predominen els mètodes d'espectrometria atòmica mentre que en el segon grup trobaríem les tècniques voltamperomètriques, que permeten diferenciar entre espècies a partir del seu potencial de reducció, i qualsevol tècnica òptica compatible amb una separació prèvia, típicament basada en la cromatografia iònica. Aquests últims mètodes són particularment interessants ja que, tal com s'ha comentat a l'apartat 1.2, l'especiació d'un metall pot afectar la seva biodisponibilitat i toxicitat.

Finalment, si tenim en compte l'objectiu de l'anàlisi podem diferenciar entre mètodes de confirmació i mètodes de cribratge. Els mètodes de confirmació es caracteritzen per una elevada exactitud i sensibilitat i per uns baixos límits de detecció. En general, són també mètodes que requereixen grans equips i instal·lacions i personal especialitzat, fet que acaba resultant en un cost econòmic important. Un exemple de mètodes de confirmació serien els mètodes d'espectrometria atòmica. Els mètodes de cribratge, en canvi, són mètodes pensats per a l'anàlisi d'un gran nombre de mostres que prioritzen una anàlisi ràpida, econòmica, simple i, a ser possible, automatitzable i *on-site*. Els mètodes de cribratge més habituals per a la determinació de metalls es basen en els sensors òptics, els sensors electroquímics i els bioassajos [23].

La principal tècnica d'anàlisi emprada en aquesta tesi doctoral ha estat la voltamperometria de redissolució anòdica (ASV, *anodic stripping voltammetry*). Es tracta d'una tècnica electroquímica que permet la determinació de metalls a nivell traça, presenta una bona sensibilitat i selectivitat i permet diferenciar entre espècies i analitzar simultàniament diversos ions metàl·lics. A més, l'ASV presenta també tots els avantatges intrínsecs dels mètodes de cribratge.

2

Els sensors voltamperomètrics

Clàssicament, les mesures voltamperomètriques de metalls es basaven en l'ús d'una cel·la electroquímica amb un elèctrode de referència (plata/clorur de plata o calomelans), un elèctrode auxiliar (carboni o platí) i un elèctrode de treball normalment de gota penjant de mercuri (HDME, *hanging drop mercury electrode*). Un dels principals avantatges d'aquest elèctrode és la seva elevada reproductibilitat, fruït de la renovació de la gota de mercuri, que permet emprar una superfície nova a cada mesura, evitant així problemes de contaminació. A més, el HDME és particularment adient per a la determinació de metalls ja que permet treballar en una àmplia finestra de potencials catòdics i preconcentrar els metalls en forma d'amalgama [25–28].

No obstant, degut a l'elevada toxicitat dels vapors, les sals i els compostos orgànics de mercuri, la Unió Europea va començar a regular el seu ús l'any 2005, sent el reglament (UE) 2017/852 del parlament europeu la normativa més recent que regula el seu ús, emmagatzematge i comerç. Així, tot i que aquesta normativa no prohibeix explícitament l'ús del mercuri en elèctrodes de treball per voltamperometria, sí que genera una certa reticència que, juntament amb la dificultat d'acoblar el HDME a sistemes de flux o adaptar-lo per a mesures

on-site i amb les seves escasses possibilitats de modificació química, ha encoratjat el desenvolupament d'elèctrodes de treball alternatius [28,29].

En aquest sentit, una de les primeres alternatives a l'elèctrode de mercuri que es van proposar per a la determinació de metalls van ser els elèctrodes sòlids. Tot i presentar una menor reproductibilitat de la seva superfície (es requereixen tediosos procediments de polit per renovar-la i evitar efectes de memòria), els elèctrodes sòlids són més fàcilment adaptables a mesures en flux o *on-site* i presenten àmplies possibilitats de modificació química. Existeixen molts tipus d'elèctrodes sòlids però els més habituals són els basats en metalls nobles (sobretot or i platí) i els de base de carboni. Els elèctrodes de metalls nobles no són especialment adients per a la determinació de metalls ja que presenten una finestra de potencials catòdics molt limitada per la formació d'hidrogen a baixos potencials però són un bon complement al HDME ja que permeten arribar a potencials més positius i, per tant, estudiar un major nombre de substàncies orgàniques. Els elèctrodes basats en carboni, en canvi, presenten una cinètica més lenta que els proporciona una finestra de treball més àmplia, arribant als potencials negatius necessaris per a l'anàlisi de metalls. A més, el carboni és un material econòmic i, a diferència del HDME, les mesures amb elèctrodes de carboni no es veuen tan afectades per la presència d'oxigen [29].

Així doncs, en els darrers anys els sensors voltamperomètrics han evolucionat significativament i han rebut especial atenció per ser molt sensibles i selectius i permetre la realització de mesures ràpides sense requerir d'instrumentació voluminosa ni sofisticada, fet que abarateix el cost de l'anàlisi. Dins de l'evolució dels sensors voltamperomètrics són especialment significatius els avenços que s'han produït en el disseny i fabricació de les unitats sensores per tal de poder adaptar-los més fàcilment a mesures *on-site* i en el desenvolupament de nous materials electròdics que permeten treballar a diferents finestres de potencial i ofereixen major sensibilitat i/o selectivitat.

2.1 Disseny i fabricació

Degut a la seva simplicitat i rapidesa, les tècniques electroanalítiques són una bona opció per a l'anàlisi *on-site* en diversos camps d'aplicació (clínic, industrial,

mediambiental, agrari…). No obstant, per poder adaptar-los a les mesures *on-site* cal que els sensors desenvolupats compleixin un seguit de criteris [30]:

- Portabilitat: és preferible emprar sensors petits amb sistemes integrats que ja incorporin els tres elèctrodes i es puguin connectar fàcilment a instrumentació portàtil.

- Estabilitat: el sensor ha de proporcionar mesures reproduïbles en el temps sense que es produeixi una deriva del senyal o un desgast de la superfície.

- Selectivitat i especificitat: el sensor ha de ser capaç de diferenciar els anàlits d'interès de la resta de components de la mostra ja que normalment no es realitza un pretractament de la mostra.

- Adaptació a canvis del medi: la resposta del sensor no es pot veure afectada per lleugers canvis de temperatura, oxigen…

Tot i que actualment existeixen al mercat diversos dispositius que permeten adaptar-se a aquestes necessitats particulars de l'anàlisi *on-site*, probablement els elèctrodes serigrafiats (*screen-printed electrodes,* SPE) siguin una de les opcions més populars.

Els SPEs són dispositius plans que contenen els tres elèctrodes (treball, auxiliar i referència) impresos en un mateix suport (Figura 2.1). Per a la fabricació d'aquests dispositius es parteix d'un suport aïllant (típicament de ceràmica, plàstic o paper) i s'utilitzen diverses plantilles i tintes en sèrie per imprimir les diferents parts del sensor, aplicant un tractament tèrmic després de cada capa de tinta per tal de solidificar-la. Finalment, es protegeixen els contactes elèctrics amb un material aïllant [31,32]. Aquest procés es troba esquematitzat pel cas d'un SPE de carboni a la figura 2.2.

Aquest procés de fabricació atorga una gran versatilitat als SPEs. D'una banda, la composició de la tinta emprada per a l'elèctrode de treball determinarà la selectivitat i sensibilitat del sensor. Tot i que el més habitual és emprar tintes de carboni o or, també es poden emprar altres tintes (plata, platí...) o modificar-les afegint altres metalls, enzims, polímers, agents complexants, nanomaterials… per millorar la resposta del sensor en una determinada anàlisi. Algunes

d'aquestes modificacions es poden realitzar també un cop ja s'ha imprès el sensor [32–34].

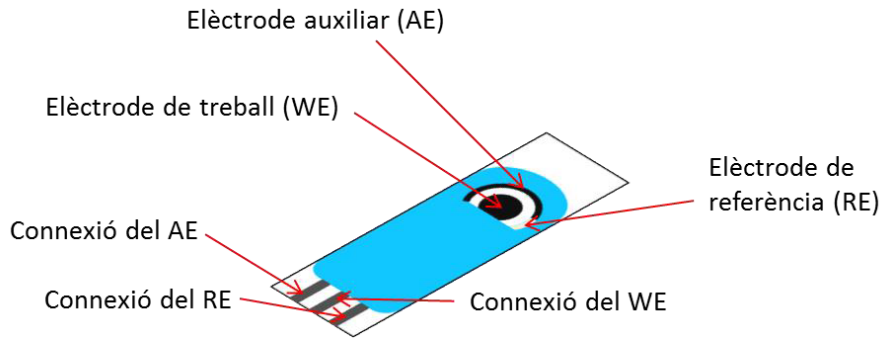

Figura 2.1. Components principals d'un elèctrode serigrafiat de carboni.

D'altra banda, l'ús de diferents plantilles durant la impressió del sensor permet obtenir sensors de diferents mides, geometries i configuracions que permeten adaptar-se millor a les necessitats de cada anàlisi. Les configuracions més simples inclouen un sol elèctrode de treball en forma de disc, anell o banda però també podem trobar configuracions molt més complexes que contemplen una disposició dels elèctrodes pensada per a l'anàlisi en flux, més d'un elèctrode de treball o, fins i tot, una placa ELISA (*Enzyme-linked immunoSorbent assay*) sencera [31,34,35].

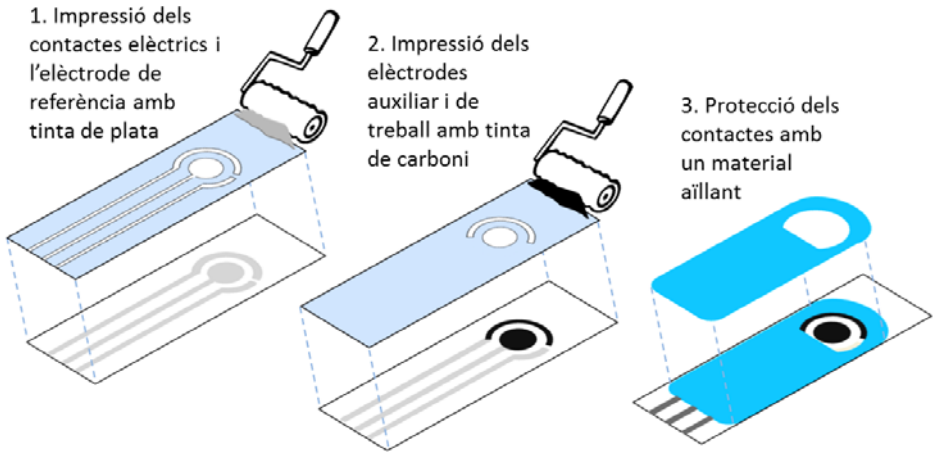

Figura 2.2. Esquematització del procés de fabricació d'un elèctrode serigrafiat de carboni.

Un altre gran avantatge del procés de fabricació dels SPEs és que permet la producció en massa d'un gran nombre de dispositius amb una elevada reproductibilitat i estabilitat a un baix cost [31,32]. Aquest fet ha permès que actualment diverses empreses (Metrohm-DropSens, Pine Research Instrumentation, PalmSens, BioSens Technology, Micrux Technologies…) comercialitzin SPEs amb diferents configuracions i materials. A més, el baix cost dels SPEs permet anar renovant l'elèctrode de manera sovintejada i evitar així tant els problemes de contaminació creuada com els tediosos procediments de polit que requereixen els elèctrodes sòlids per renovar la superfície.

2.2 L'elèctrode de treball

Tal com s'ha esmentat anteriorment, un dels avantatges que proporcionen els elèctrodes serigrafiats és la possibilitat de modificar el seu elèctrode de treball, ja sigui introduint els modificadors directament a la tinta o bé modificant la seva superfície un cop ja està imprès. Aquestes modificacions de l'elèctrode de treball influeixen fortament en la resposta dels sensors i permeten millorar la seva sensibilitat i/o selectivitat i treballar a diferents condicions experimentals (potencial, pH…).

En el cas de la determinació de metalls s'han reportat molts tipus d'elèctrodes de treball diferents. A la figura 2.3 es mostren les principals estratègies de modificació amb què s'ha treballat al llarg d'aquesta tesi doctoral. Cal tenir en compte que aquestes estratègies no són excloents entre elles sinó que, en general, se solen combinar dues o més estratègies de modificació.

En concret, a continuació s'aprofundirà en les següents estratègies: desenvolupament d'elèctrodes modificats químicament, formació de pel·lícules metàl·liques i desenvolupament d'elèctrodes basats en diferents tipus de nanomaterials (nanopartícules metàl·liques, nanoal·lòtrops de carboni i silici porós).

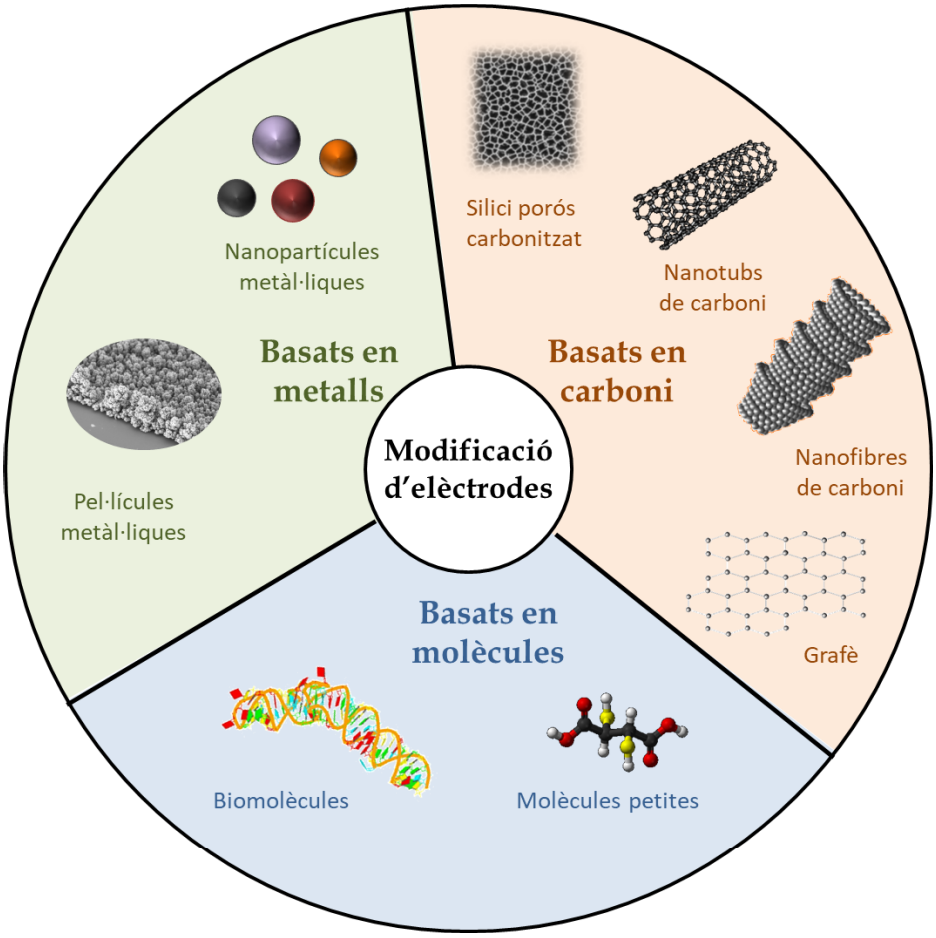

Figura 2.3. Principals estratègies de modificació de l'elèctrode de treball emprades en aquesta tesi doctoral.

2.2.1 Elèctrodes modificats químicament

L'objectiu principal de la modificació química de la superfície d'un elèctrode és augmentar la seva sensibilitat i selectivitat. Aquestes millores poden anar acompanyades també d'una millora en la reproductibilitat i l'estabilitat. Per tal d'augmentar la selectivitat d'un sensor es poden seguir principalment tres estratègies [36]:

- Electrocatàlisi: quan l'anàlit presenta una transferència electrònica lenta sobre la superfície de l'elèctrode cal aplicar potencials substancialment superiors al potencial redox per obtenir senyals analítics útils. Aquests potencials tan elevats disminueixen la sensibilitat (empitjora la relació senyal/soroll) i la selectivitat (hi ha més espècies interferents) del sensor. Immobilitzant un mediador electrocatalític sobre la superfície de l'elèctrode es pot augmentar la cinètica de la transmissió electrònica entre l'anàlit i l'elèctrode i evitar així l'ús de potencials tan elevats.

- Preconcentració: de manera anàloga a l'etapa de preconcentració de les tècniques voltamperomètriques de redissolució, en aquesta estratègia es modifica la superfície de l'elèctrode amb un material que faciliti l'acumulació selectiva de l'anàlit. Aquesta estratègia és especialment útil quan l'anàlit es troba a baixes concentracions.

- Permeació selectiva: al treballar amb mostres complexes podem tenir espècies interferents o espècies que passivin l'elèctrode. En aquesta estratègia es modifica la superfície de l'elèctrode per tal que només les espècies amb una determinada càrrega, mida o polaritat puguin accedir-hi. Així, es dificulta el transport de les espècies interferents sense restringir massa el transport de l'anàlit.

En el cas de la determinació de metalls a nivell traça prenen especial importància les estratègies de preconcentració i permeació selectiva. En aquest cas, es modifica la superfície de l'elèctrode per tal de millorar el reconeixement selectiu dels ions metàl·lics, que es pot basar en l'afinitat química, l'atrapament en una cavitat o una combinació de les dues [37].

Un exemple d'afinitat química per a metalls el trobaríem en la modificació d'elèctrodes amb pèptids. Els pèptids són lligands efectius, i sovint específics, per a una gran varietat de metalls ja que contenen un gran nombre d'àtoms potencialment donadors al llarg del seu esquelet i de les cadenes laterals dels aminoàcids. En qualsevol pèptid els metalls podran interaccionar a través dels grups carboxílic i amino terminals i a través del grup amida resultant de l'enllaç peptídic. L'afinitat pels metalls pot augmentar també si les cadenes laterals contenen grups tiols ja que aquests presenten una elevada afinitat per a diversos ions metàl·lics ($Hg^{2+} \approx Ag^{+} >> Cu^{2+} > Pb^{2+} \approx Cd^{2+} > Zn^{2+} >> Ca^{2+} \approx Mg^{2+}$) [38,39].

D'altra banda, el reconeixement degut a l'atrapament en una cavitat el podem trobar, per exemple, en la modificació d'elèctrodes amb èters corona. En aquest cas cal considerar tant la mida de la cavitat de l'èter corona com la mida de l'ió metàl·lic. La ràtio entre el diàmetre de l'ió metàl·lic i la cavitat de l'èter hauria d'estar entre 0,75 i 0,90 per tal que la interacció metall-èter corona sigui favorable [40].

Un aspecte clau en la modificació química d'un elèctrode és la immobilització de la molècula sobre la superfície de l'elèctrode. En concret, la modificació d'elèctrodes amb molècules que contenen grups tiol sol realitzar-se mitjançant la formació de monocapes autoensamblades (SAM, *self-assembled monolayer*). Les SAM es formen espontàniament sobre la superfície de l'elèctrode quan es compleixen unes condicions experimentals determinades i presenten l'avantatge de poder preparar-se fàcil i ràpidament, a més de poder emprar-se en sistemes miniaturitzats i econòmics. No obstant, en el cas dels grups tiol aquesta modificació s'ha de realitzar sobre elèctrodes d'or i aquesta estratègia dóna lloc a elèctrodes que només són estables en un interval de potencial molt estret (típicament des de -0,6 V a +0,6V), fet que impedeix la seva aplicació a la determinació de diversos metalls per ASV [41–43].

Una alternativa a les SAM que permet treballar, entre altres, amb superfícies de carboni i dóna lloc a elèctrodes més estables consisteix en immobilitzar la molècula sobre una superfície prèviament modificada amb sals de diazoni. La funcionalització de superfícies de carboni amb sals d'aril diazoni va ser descrita per primera vegada per Pinson *et al.* l'any 1992 [44]. Aquesta funcionalització té lloc mitjançant un procés d'*electrografting*, terme emprat per descriure qualsevol reacció electroquímica que permet enllaçar una capa orgànica a un substrat sòlid conductor. En el cas particular de les sals de diazoni, aquestes es redueixen donant lloc a un radical fenil que s'enllaça a la superfície de l'elèctrode de carboni mitjançant la formació d'un enllaç covalent carboni-carboni tal com es mostra a la figura 2.4 [45–48].

Les sals de diazoni es poden generar *in-situ* fent reaccionar l'amina corresponent amb $NaNO_2$ en medi àcid, evitant així haver d'aïllar i purificar la sal de diazoni. D'altra banda, en funció de l'amina de partida es poden introduir diferents grups funcionals i obtenir elèctrodes amb diferents propietats. Alguns grups ionitzables com el –COOH, $–NH_2$, $–SO_3H$ o $–N(C_2H_5)_2$ poden emprar-se per complexar metalls directament o per immobilitzar altres molècules.

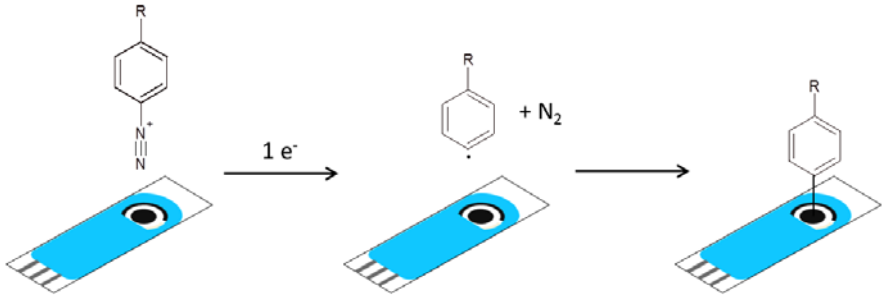

Figura 2.4. Funcionalització d'un SPE de carboni amb una sal de diazoni.

Una de les estratègies més conegudes consisteix en funcionalitzar la superfície de l'elèctrode amb grups –COOH que, un cop activats, permeten immobilitzar molècules que continguin un grup NH_2 mitjançant la formació d'un enllaç peptídic [46]. L'activació dels grups carboxílics es pot dur a terme mitjançant l'esterificació amb hidroclorur de N-(3-dimetilaminopropil)-N'-etilcarbodiimida (EDC) i N-hidroxisulfosuccinimida (sulfo-NHS). Es tracta de dos reactius comercials que permeten treballar en medi aquós i actuen com a agents de *cross-linking*, reaccionant amb els àcids carboxílics terminals per donar lloc a un èster intermedi poc propens a hidrolitzar-se que reacciona amb amines amb un rendiment al voltant del 90% (figura 2.5) [41,42].

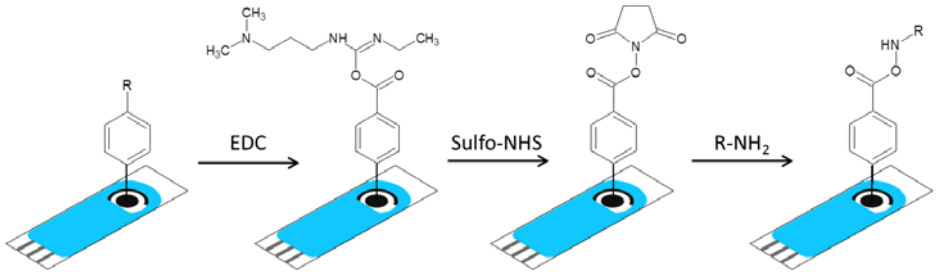

Figura 2.5. Activació dels àcids carboxílics amb EDC i sulfo-NHS.

Una estratègia menys coneguda consisteix en funcionalitzar la superfície de l'elèctrode amb grups $–NO_2$, que posteriorment es poden reduir a grups $–NH_2$ per permetre la immobilització de molècules que continguin grups –COOH, també a través de la formació d'un enllaç peptídic assistit per EDC i sulfo-NHS.

2.2.2 Pel·lícules metàl·liques

Les primeres pel·lícules metàl·liques es basaven en el mercuri i pretenien superar algunes de les limitacions del HMDE ja que són mecànicament més estables i versàtils (es poden fabricar en diferents mides i configuracions de cel·la) que les gotes de mercuri, proporcionen una ràtio superfície-volum més elevada emprant menors quantitats de mercuri, són més adients per a mesures en continu i permeten modificar la seva superfície amb recobriments permeoselectius, agents quelants o intercanviadors iònics [28].

Posteriorment, altres pel·lícules metàl·liques van aparèixer com a alternativa a les de mercuri en la finestra de potencials catòdics. Així, l'objectiu en aquest cas no era tant augmentar la selectivitat del sensor sinó poder treballar a potencials negatius amb bona sensibilitat.

En aquest sentit, les primeres pel·lícules metàl·liques no basades en mercuri per a tècniques voltamperomètriques de redissolució van ser reportades l'any 2000 i es basaven en el bismut [49]. El bismut és un metall molt menys tòxic que el mercuri i que proporciona un senyal analític semblant. Es pot aplicar a mesures per ASV gràcies a la seva capacitat per formar aliatges i compostos intermetàl·lics amb altres metalls i a mesures per voltamperometria de redissolució per adsorció (AdSV, *adsorptive stripping voltammetry*) gràcies a les seves propietats adsortives [50,51]. Alguns dels principals avantatges que presenten aquests elèctrodes basats en pel·lícules metàl·liques de bismut respecte al HDME són la menor sensibilitat a l'oxigen que permet realitzar determinacions sense haver de purgar les mostres, el seu caràcter sòlid a temperatura ambient que li confereix major estabilitat i, en alguns casos, una millor separació entre pics de diferents metalls (ex. Cd i Tl) [50,52]. La no necessitat de purgar les mostres juntament amb la major estabilitat fan aquests elèctrodes més adequats per a mesures *on-site* o en flux que el HDME. El principal desavantatge dels elèctrodes basats en pel·lícules de bismut respecte al HDME és la disminució de la finestra de potencials. Tot i que manté la mateixa finestra de potencial catòdics, limitada per la reducció de l'hidrogen, la regió anòdica es veu significativament disminuïda ja que el potencial d'oxidació del bismut és aproximadament -0,5 V, bastant menor que el del mercuri (figura 2.6) [52].

Posteriorment a les pel·lícules de bismut, l'any 2007 es van reportar les primeres pel·lícules d'antimoni [53]. Tot i ser més tòxic que el bismut, l'antimoni segueix sent bastant menys tòxic que el mercuri i els elèctrodes basats en pel·lícules d'antimoni mantenen moltes de les propietats dels elèctrodes basats en pel·lícules de bismut (baixa sensibilitat a l'oxigen, àmplia finestra de potencials catòdics…). A més, presenten un seguit d'avantatges addicionals com una ampliació de l'interval anòdic ja que el potencial d'oxidació de l'antimoni és superior al del bismut (aproximadament -0,2 V, figura 2.6), la capacitat de treballar a pHs més àcids (≤ 2) i un senyal de redissolució de l'antimoni molt petit [53,54].

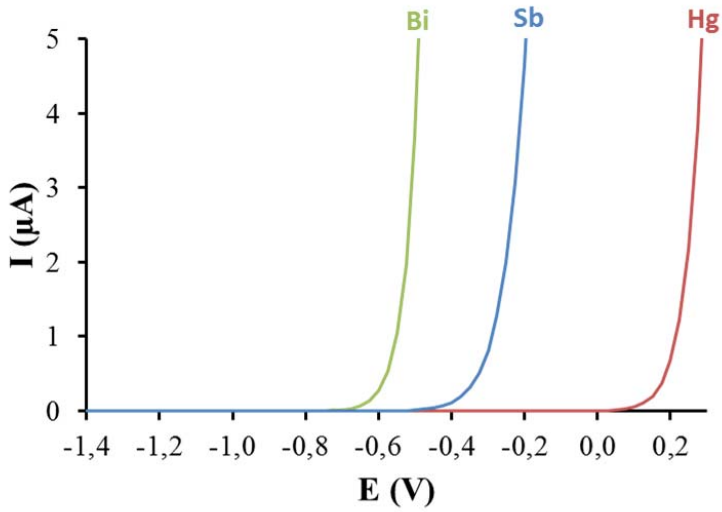

Figura 2.6. Finestres de potencials anòdics per a elèctrodes basats en pel·lícules de bismut, antimoni i mercuri.

Tot i que els elèctrodes basats en pel·lícules de bismut o d'antimoni són els que s'han estudiat amb més profunditat, a la bibliografia també trobem altres elèctrodes basats en pel·lícules metàl·liques d'altres elements, com per exemple, l'estany [55], el coure [56] o el plom [57], que han donat bons resultats per a la determinació voltamperomètrica de metalls.

A l'hora de preparar un elèctrode de pel·lícula metàl·lica cal tenir en compte dos grans aspectes: el substrat sobre el qual es depositarà la pel·lícula i el mètode de deposició [54,58]. En termes de substrats, el més habitual és emprar substrats basats en carboni (carboni vitrificat, elèctrodes serigrafiats de carboni,

nanomaterials de carboni, mina de llapis…). Pel que fa al mètode de deposició de la pel·lícula principalment trobem 4 mètodes. Els dos primers són electrodeposicions *in-situ* o *ex-situ* realitzades sobre la superfície de l'elèctrode mentre que els altres dos, la modificació a partir d'un precursor i el mètode *sputtering*, requereixen introduir modificacions durant el procés de fabricació de l'elèctrode.

- Electrodeposició *ex-situ:* la pel·lícula metàl·lica es forma en una etapa prèvia a la mesura, submergint l'elèctrode en una solució de Bi^{3+} o Sb^{3+} i aplicant el potencial necessari per reduir els ions M^{3+} a M^0. Les condicions reportades són bastant variables però, en termes generals, els paràmetres que cal optimitzar són la concentració de bismut o antimoni, el pH (sol ser al voltant de 4-5 pel bismut i 2 per l'antimoni), el contraió (nitrats, clorurs, acetats…) i la tècnica electroquímica (típicament s'aplica un potencial constant al voltant de -0,8 V per al bismut i -0,5 V per a l'antimoni durant 100-600 s, però també es pot fer aplicant una intensitat constant o per voltamperometria cíclica) [50,59].

- Electrodeposició *in-situ:* la formació de la pel·lícula metàl·lica té lloc alhora que es deposita l'anàlit a l'elèctrode i la pel·lícula es reoxida un cop s'han reoxidat els anàlits durant l'escombratge anòdic. En aquest cas s'addiciona Bi^{3+} o Sb^{3+} a la solució de mesura que conté la mostra amb una concentració significativament superior a la del metall anàlit. Respecte el mètode *ex-situ* disminueix el temps d'anàlisi ja que no cal l'etapa prèvia de formació de la pel·lícula, augmenta la reproductibilitat ja que s'empra una pel·lícula nova en cada mesura i, en alguns casos, augmenta la sensibilitat i resolució dels pics. Per contra, el seu camp d'aplicació és més restringit ja que només es pot emprar en mesures on l'excés de bismut o d'antimoni no interfereixin i on les condicions experimentals per a la mesura i la formació de la pel·lícula siguin semblants [50,59].

- Modificació a partir d'un precursor: durant la fabricació de l'elèctrode s'addiciona un precursor de bismut (Bi_2O_3, $Bi(NO_3)_3$, $Bi(AlO_2)_3$ o citrat de bismut) o d'antimoni (Sb_2O_3) al substrat de carboni. Prèviament a la mesura s'aplica un potencial negatiu per reduir aquest precursor a bismut o antimoni metàl·lic i formar la pel·lícula metàl·lica [50,54,58].

- Mètode *sputtering*: la pel·lícula de bismut o d'antimoni es forma directament sobre un substrat de silici o ceràmica mitjançant una deposició física en fase vapor. Alguns avantatges d'aquest mètode són que no requereix ions bismut o antimoni ni un substrat conductor ja que el bismut o l'antimoni actuen alhora com a element sensor i com a transductor [60].

2.2.3 Nanopartícules metàl·liques

En general es considera que una nanopartícula (NP) metàl·lica és una partícula metàl·lica que conté entre 3 i 10^7 àtoms i no supera els 100 nm en cap de les seves dimensions [61]. Les NPs poden adoptar moltes formes diferents (esferes, cubs, piràmides, estrelles, barres…) i presenten característiques úniques que poden diferir significativament respecte les propietats del metall sòlid. Un clar exemple el trobem en l'or, on el metall és groc i no presenta propietats magnètiques mentre que les NPs d'or són vermelles i s'ha observat un comportament magnètic en partícules de 2-3 nm [62]. En general, les NPs presenten unes propietats mecàniques, elèctriques, òptiques, catalítiques i magnètiques úniques entre les quals cal destacar la seva elevada ràtio superfície-volum, la seva elevada conductivitat i eficiència catalítica, l'elevada reactivitat de la seva superfície i la seva capacitat d'adsorció [63,64]. Aquestes propietats poden variar significativament en funció de la mida i la forma de la NP. Per exemple, un conjunt de NPs petites ben dispersades sol tenir major activitat catalítica que NPs agregades amb una mida més gran [64]. D'altra banda, una forma allargada permet una major deslocalització dels electrons mentre que formes amb múltiples cantonades (triangles, hexàgons, cubs…) donen lloc a acumulacions de càrrega puntual i formes com l'estrella presenten una major activitat catalítica [62].

Les propietats úniques de les NPs metàl·liques les fan especialment atractives per a la modificació de sensors electroquímics. La incorporació de NPs metàl·liques a la superfície de l'elèctrode proporciona un increment de l'àrea superficial i de la velocitat de transferència de massa i electrons que es tradueix en una millora de les seves propietats analítiques (sensibilitat, límit de detecció, estabilitat, capacitat de detecció simultània…) [61,64].

En el cas de la determinació de metalls s'han obtingut bons resultats emprant elèctrodes modificats amb diferents tipus de NPs metàl·liques, sent les NPs d'or, plata, antimoni i bismut les més habitual. A la literatura també podem trobar NPs híbrides (contenen dos metalls) i d'òxids metàl·lics com MnO_2, ZnO, NiO, Fe_3O_4, ZrO_4, SnO_2, TiO_2 o MgO, entre altres [37,64].

Per a la modificació de sensors amb NPs metàl·liques cal tenir en compte dos grans aspectes: el mètode de síntesi de les NPs i l'estratègia emprada per a la incorporació de les NPs al sensor electroquímic. En termes de mètodes de síntesi existeixen dues grans estratègies en funció del punt de partida: el *top-down* i el *bottom-up*. Tal com s'esquematitza a la figura 2.7, en el plantejament *top-down* es parteix del metall sòlid i es va reduint la seva mida fins a obtenir les NPs mentre que en el plantejament *bottom-up* les NPs es formen a partir d'àtoms o molècules, proporcionant un major control sobre la mida i la forma de la NP [65]. Aquesta última estratègia és la que se sol emprar quan les NPs metàl·liques se sintetitzen químicament en solució. En aquests casos es parteix d'un precursor del metall i un agent reductor per formar les NPs i s'empra un agent estabilitzant per protegir-les del medi, evitar la seva aglomeració i controlar la seva mida i forma [66].

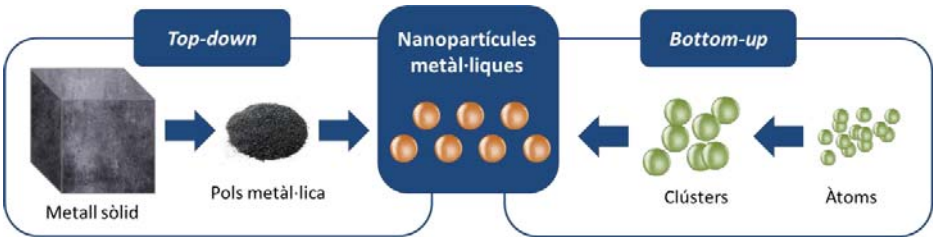

Figura 2.7. Esquematització de les estratègies *top-down* i *bottom-up* per a la síntesi de nanopartícules metàl·liques.

Pel que fa a la modificació del sensor electroquímic amb NPs es poden seguir diferents estratègies, la més senzilla de les quals és el *drop-casting,* que consisteix en dipositar una gota de la solució de NPs sobre la superfície de l'elèctrode i deixar evaporar el dissolvent de manera controlada. Altres estratègies més complexes serien, per exemple, la incorporació de les NPs a la tinta abans de la impressió del sensor o la síntesi *in-situ* de les NPs sobre la superfície de l'elèctrode mitjançant un procés d'electrodeposició.

2.2.4 Nanoal·lòtrops de carboni

Els nanoal·lòtrops de carboni són una de les famílies de nanomaterials més estudiades. Des del descobriment del ful·lerè l'any 1985 i dels nanotubs de carboni (CNTs) sis anys després, s'ha avançat molt en aquest camp, descobrint nous nanoal·lòtrops i estudiant les seves propietats i possibles aplicacions. Tal com es mostra a la figura 2.8, una de les possibles maneres de classificar els diversos nanoal·lòtrops de carboni es basa en la dimensionalitat de la seva estructura. Així, tenim estructures amb zero dimensions (0D) com el ful·lerè, amb una 1D com els CNTs, amb 2D com el grafè i amb 3D com el grafit [67].

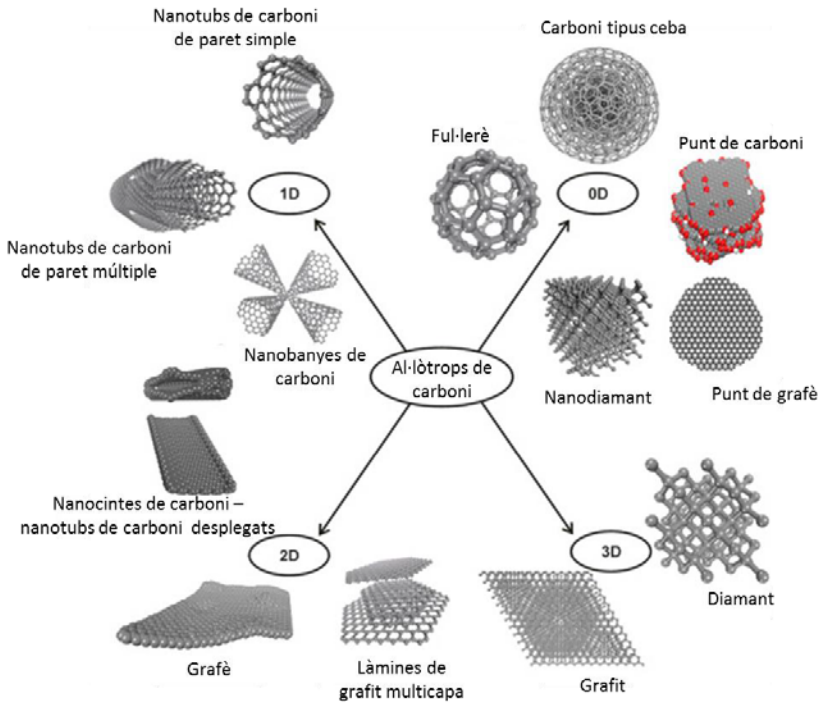

Figura 2.8. Classificació dels al·lòtrops de carboni en funció de la seva dimensionalitat Adaptat de [67].

Com a nanomaterials, els nanoal·lòtrops comparteixen moltes propietats amb les NPs metàl·liques. Així, trobem també una elevada ràtio superfície-volum i moltes de les propietats mecàniques, elèctriques, òptiques, catalítiques i magnètiques que mostraven les NPs metàl·liques. En aquest cas, cal destacar el seu caràcter orgànic i biocompatible i la seva elevada conductivitat, estabilitat

física i química i resistència a la calor [62,68]. Aquestes propietats fan que els nanoal·lòtrops de carboni siguin especialment atractius per a la modificació de sensors electroquímics, on no només proporcionen un increment de l'àrea superficial sinó que també permeten treballar amb un baix soroll de fons i una finestra de potencials bastant ample, fet que els fa adequats per a la determinació de moltes substàncies diferents [69]. En el cas de la determinació d'ions metàl·lics, els nanoal·lòtrops de carboni més emprats són:

- Nanotubs de carboni (CNT): es caracteritzen per tenir una hibridació sp^2 i una estructura tubular i es poden dividir en dos grans grups: els nanotubs de paret simple (SWCNT), que podrien representar-se com una làmina de grafè enrotllada sobre si mateixa, i els nanotubs de paret múltiple (MWCNT), que podrien representar-se com diverses làmines de grafè enrotllades concèntricament [67].

- Nanofibres de carboni (CNF): són semblants als CNTs però presenten una estructura cònica o cilíndrica enlloc de tubular [67].

- Grafè: presenta una estructura bidimensional formada per àtoms de carboni amb hibridació sp^2 que donen lloc a una extensió indefinida d'una xarxa hexagonal que recorda a l'estructura d'una bresca de mel [68].

- Nanodiamants: són NPs de carboni amb una hibridació sp^3 que presenten un domini cristal·lí amb una topologia semblant al diamant [67].

Els CNTs, les CNFs i el grafè són fàcilment funcionalitzables, fet que permet millorar considerablement la seva sensibilitat i selectivitat per a la determinació d'ions metàl·lics. En el cas dels nanodiamants, s'han obtingut molt bons resultats després de dopar-los amb bor [70].

2.2.5 Silici porós

El silici porós (pSi) va ser descobert accidentalment l'any 1956 per Arthur i Ingeborg Uhlir quan intentaven desenvolupar un mètode electroquímic per polir plaques de silici. Sota determinades condicions es formaven dipòsits vermells,

marrons o negres sobre la placa de silici [71]. No obstant, aquest fet va quedar descrit com una curiositat i no va ser fins els anys 90, quan es van identificar efectes de confinament quàntic [72] i propietats fotoluminescents [73], que el silici porós va atreure realment l'interès de la comunitat científica.

Existeixen diversos mètodes per fabricar el silici porós però un dels més habituals és l'atac electroquímic en una solució d'àcid fluorhídric. Es tracta d'una estratègia *top-down* ja que es parteix de plaques de silici i es va eliminant material per formar els porus. En primer lloc s'elimina la capa d'òxid que es forma a l'exposar el silici a l'oxigen atmosfèric i se submergeix la placa en una solució aquosa o etanòlica d'àcid fluorhídric. Això provoca que es generin enllaços Si–H a la superfície de la placa de silici, que seguidament es reemplacen per enllaços Si–F. Aquest intercanvi té lloc mitjançant un procés d'anodització que pot ser galvanostàtic o potenciostàtic. Un cop format un enllaç Si–F, es pot unir un nou ió fluorur alliberant una molècula d'hidrogen. La incorporació d'aquests àtoms de fluor, que són molt electronegatius, debilita els enllaços Si–Si i, per reacció amb el HF, permet eliminar àtoms de silici i formar els porus. En global, la reacció que té lloc durant aquest procés és

$$Si + 4HF_2^- + h^+ \rightarrow SiF_6^{2-} + 2HF + H_2 + e^-$$

on h^+ representa un forat electrònic. Variant diferents paràmetres com la proporció d'àcid fluorhídric o el temps i intensitat/potencial de l'etapa d'anodització es poden obtenir porus amb diferent diàmetre i profunditat [74–76].

En molts casos però, el silici porós obtingut no es pot emprar directament ja que es tracta d'un material poc estable que s'oxida fàcilment en presència d'oxigen. Aquest problema es pot solucionar mitjançant un procés de carbonització tèrmica, que permet obtenir un material estable fins i tot en medis agressius. Durant la carbonització tèrmica s'aplica un tractament tèrmic en presència d'una font de carboni (típicament acetilè) per tal de substituir els enllaços Si–H (inestables) per enllaços Si–C (estables). L'estructura i les propietats del silici porós carbonitzat depenen molt del tractament tèrmic aplicat però en general podem diferenciar entre dues grans classes [77,78]:

- Silici porós tèrmicament hidrocarbonitzat (THCpSi): s'obté a temperatures inferiors a 650 °C. No s'elimina tot l'hidrogen i, per tant,

coexisteixen enllaços Si–H i Si–C, donant lloc a una superfície hidrofòbica.

- Silici porós tèrmicament carbonitzat (TCpSi): s'obté a temperatures superiors a 750 °C. S'eliminen tots els hidrògens donant lloc a una superfície hidrofílica que, en condicions ambientals, es recobreix d'una fina capa d'òxid.

El silici porós és un material molt versàtil amb aplicacions tan diverses com l'alliberament de fàrmacs, les bateries o els sensors, entre d'altres. Algunes de les propietats que el fan atractiu en el camp dels sensors són la seva disponibilitat i biocompatibilitat, el seu procés de fabricació ràpid i simple i la seva elevada àrea superficial, així com la possibilitat d'ajustar la mida i el gruix dels porus i de funcionalitzar la seva superfície. S'han obtingut molt bons resultats a l'emprar el silici porós en sensors òptics i elèctrics però hi ha molt pocs estudis amb sensors electroquímics on, fins al moment, només s'han reportat alguns biosensors amb silici porós funcionalitzat [76–79].

3

Les llengües electròniques

El concepte de llengua electrònica neix, de manera anàloga al seu predecessor nas electrònic, amb la idea d'imitar el sentit humà del gust en l'anàlisi de mostres líquides. Així tal com es mostra a la figura 3.1, d'una banda, tindrem un conjunt de sensors que pretenen reproduir la capacitat que tenen les nostres papil·les gustatives per respondre a una gran varietat de substàncies i, d'altra banda, un tractament de dades complex que imita la capacitat del nostre cervell per rebre aquesta informació i reconèixer i comparar els diferents gustos [80,81].

Més concretament, i segons la definició de la Unió Internacional de Química Pura i Aplicada (IUPAC), les llengües electròniques són un instrument analític format per (i) un conjunt de sensors químics no específics i poc selectius amb gran estabilitat i sensibilitat creuada per a diferents espècies en solució, i (ii) per un model apropiat de reconeixement de patrons i/o calibratge multivariant per al processament de dades [82].

Pel que fa al tipus de sensors emprat, tot i que s'han reportat llengües electròniques basades en sensors òptics, elèctrics i gravimètrics, el més habitual són les llengües electròniques basades en sensors electroquímics i, més

concretament, potenciomètrics o voltamperomètrics [83]. Les llengües electròniques potenciomètriques van ser les primeres en desenvolupar-se i estan formades per un conjunt d'ISEs no específics. No obstant, la baixa sensibilitat dels ISEs dificulta la seva aplicació per a la determinació de components traça en mostres complexes. En canvi, les llengües electròniques voltamperomètriques (llengües voltamperomètriques d'ara en endavant) proporcionen una sensibilitat més elevada i, a més, proporcionen molta més informació. Així, per cada valor de potencial que s'obtenia amb una mesura potenciomètrica, ara tindrem un voltamperograma sencer format per centenars de valors d'intensitat. Aquest increment en la quantitat d'informació obtinguda sovint es tradueix en un increment considerable de la selectivitat entre mostres o anàlits. No obstant, aquestes elevades quantitats d'informació també requereixen de tractaments de dades més complexes i d'ordinadors més potents [81].

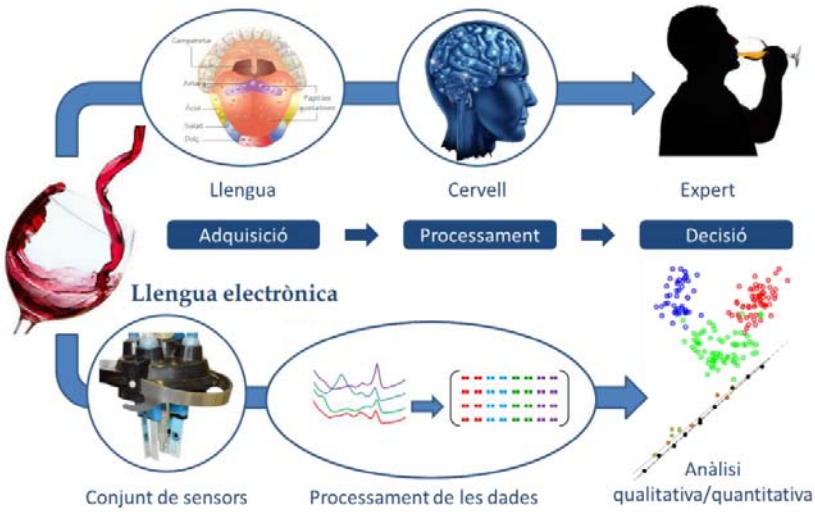

Figura 3.1. Esquematització del funcionament d'una llengua electrònica en comparació amb el funcionament del gust.

3.1 Consideracions experimentals

Quan es treballa amb un conjunt de sensors el més habitual és utilitzar un potenciòstat multicanal que permet mesurar amb diversos elèctrodes de treball

simultàniament. La disposició dels elèctrodes es pot adaptar en funció de les necessitats de l'anàlisi. A tall d'exemple, a la figura 3.2. es mostren tres possibles opcions. En el primer cas (figura 3.2a) es treballa simultàniament amb 8 sensors i la disposició dels sensors està pensada per poder analitzar 8 mostres simultàniament; cada elèctrode de treball té un elèctrode de referència i un elèctrode auxiliar associat i la distància entre sensors està pensada per treballar amb micropipetes multicanal. En el segon cas (figura 3.2b) el muntatge permet treballar simultàniament amb 4 sensors referits al mateix elèctrode de referència extern i a un mateix elèctrode auxiliar, que en aquest cas és l'elèctrode auxiliar intern d'un dels SPEs. El tercer cas (figura 3.2c) és una versió miniaturitzada del segon, que presenta els avantatges de disposar d'un elèctrode de referència intern i de requerir quantitats molt més petites de mostra. No obstant, si es vol treballar amb elèctrodes modificats el segon escenari (figura 3.2b) ofereix molta més versatilitat ja que es poden tractar els 4 sensors de manera independent.

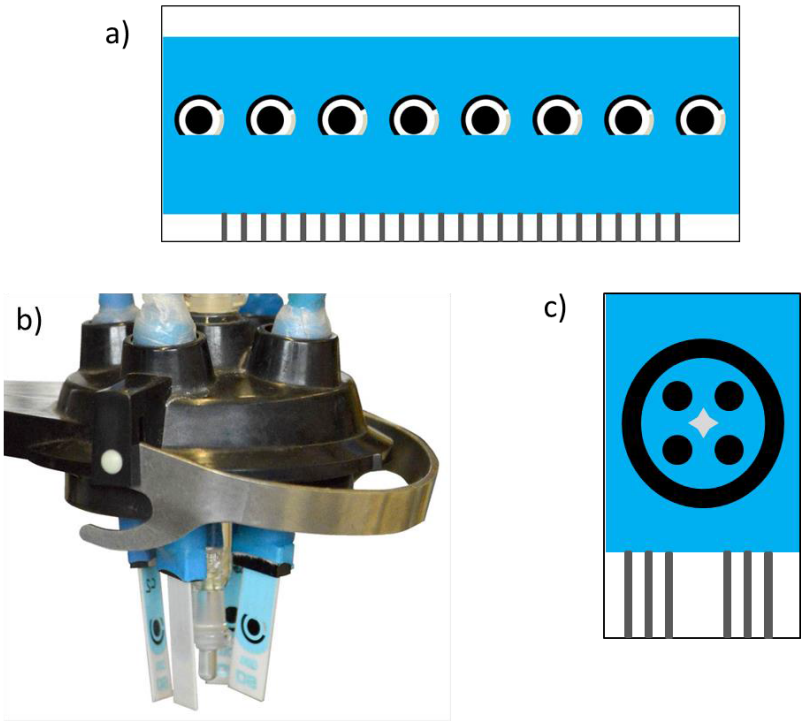

Figura 3.2. Exemples de diferents disposicions que es poden emprar quan es treballa amb un conjunt de sensors.

En funció de la relació que existeix entre els diferents elèctrodes de treball podem trobar tres situacions diferents [84]:

- Sensors redundants. Sovint s'utilitzen com a element diagnòstic del sistema analític. El mal funcionament d'un sensor pot evidenciar la seva degradació o problemes en un sol canal mentre que la fallada simultània de diversos sensors posa de manifest altres errors del sistema (fugues, soroll elèctric, mostres errònies…). Un altre escenari seria la determinació simultània de diverses mostres, que pot ser especialment útil quan es vol establir un perfil de concentracions a l'espai.

- Sensors independents. Cada sensor del conjunt respon a un únic anàlit del sistema, permetent realitzar diverses anàlisis en paral·lel. Permet disminuir considerablement el temps d'anàlisi i la quantitat de reactius i mostra però cal assegurar que no hi hagi interferències entre els diferents sensors per tal d'obtenir resultats correctes.

- Sensors amb resposta creuada. Tots els sensors responen als diferents anàlits però amb diferent sensibilitat. Aquesta és l'única situació que es considera en una llengua electrònica. La baixa selectivitat dels sensors es veu compensada amb el tractament de dades.

Per tant, en el desenvolupament d'una llengua voltamperomètrica és important parar especial atenció en la tria dels sensors. Una estratègia que s'ha comprovat que dóna bons resultats és l'estudi de la resposta independent de cada sensor per a cada anàlit. Idealment tots els sensors han de respondre a tots els anàlits amb una sensibilitat lleugerament diferent per tal de garantir una resposta creuada. Cal evitar la introducció de sensors redundants en una llengua voltamperomètrica ja que aquests augmenten el volum de dades i la complexitat del seu tractament sense aportar nova informació.

3.2 Calibratge i validació

Juntament amb la tria dels sensors voltamperomètrics i l'optimització de la seva mesura, l'altra etapa crucial en una llengua voltamperomètrica és el tractament de dades. Els models de calibratge multivariant seleccionats dependran de si es tracta d'una anàlisi qualitativa o quantitativa però, independentment de la

finalitat de l'anàlisi, el desenvolupament d'una llengua electrònica ha d'incloure tres etapes: (i) construcció del model de calibratge, (ii) validació del model i (iii) aplicació a mostres desconegudes.

Per tal de calibrar i validar el model es divideixen les mostres de calibratge en dos sets. El set de calibratge o entrenament s'emprarà per construir el model mentre que el set de validació o test permetrà comprovar la seva validesa i assegurar que no s'ha sobreajustat el model. En aquest punt cal remarcar que per a una correcta validació del model les mostres del set de validació no poden emprar-se durant el seu calibratge.

D'altra banda, com s'ha comentat anteriorment, les llengües voltamperomètriques donen lloc a un volum de dades molt elevat. Això fa que normalment calgui realitzar una compressió prèvia de les dades abans de construir el model. En aquest sentit, alguns mètodes que han donat bons resultats són la selecció de variables, l'anàlisi de components principals (PCA, *principal component analysis*), la transformada ràpida de Fourier (FFT, *fast Fourier transform*) i la transformada d'ona discreta (DWT, *discrete wavelet transform*) [85].

3.2.1 Anàlisi qualitativa

La majoria d'aplicacions qualitatives de les llengües voltamperomètriques estan relacionades amb el camp de l'alimentació. Es treballa sobretot amb mostres líquides (aigües de consum, vins, olis, tes, cafès, sucs, llets…) i els objectius més habituals són garantir la qualitat i/o preservació dels productes, discriminar mostres pertanyents a diferents denominacions d'origen o la detecció de fraus. Tot i que menys freqüentment, també trobem aplicacions qualitatives de les llengües voltamperomètriques en el camp mediambiental, biomèdic i industrial [81,86].

Dins de l'anàlisi qualitativa podem distingir dos grans grups de mètodes quimiomètrics: els mètodes no supervisats i els mètodes supervisats [80–82,87]. Els mètodes no supervisats utilitzen les característiques generals de les dades per estudiar possibles agrupacions i veure si les mostres d'una mateixa classe tendeixen a agrupar-se entre elles i diferenciar-se de la resta de mostres. El

mètode més emprat per a aquesta estratègia és el PCA però també es poden emprar altres mètodes com l'anàlisi de clústers o el mapa autoorganitzat (SOM, *self-organizing map*). Tots ells permeten reduir la dimensionalitat de les dades i eliminar redundàncies per facilitar-ne la seva visualització. Tot i que estrictament parlant els mètodes no supervisats no permeten classificar les mostres, aquests mètodes faciliten l'estudi inicial de les dades i solen emprar-se com a pas previ a l'aplicació d'un mètode supervisat.

Els mètodes supervisats, en canvi, utilitzen una agrupació de les mostres designades *a priori* per tal de crear un model que permeti separar les diferents classes. Per tant, són mètodes que sí que permeten classificar les mostres i han de ser correctament calibrats i validats. Els mètodes de calibratge multivariant més emprats són la regressió per mínims quadrats parcials amb anàlisi discriminant (PLS-DA, *partial least squares - discriminant analysis*), l'anàlisi discriminant lineal (LDA, *linear discriminant analysis*) i la màquina de vector de suport (SVM, *support vector machine*). Pel que fa a la distribució de les mostres entre els sets de calibratge i validació, habitualment es destinen un 60-70 % de les mostres per al calibratge i un 30-40 % per a la validació. La distribució de les mostres entre els dos sets sol ser aleatòria però cal assegurar que totes les classes considerades quedin representades en els dos sets.

La bondat del model s'avalua a partir de la seva capacitat de predir correctament les mostres emprades per a la validació del model i els criteris que s'empren són la sensibilitat (mostres de cada classe assignades correctament), l'especificitat (mostres d'altres classes rebutjades correctament) i la ràtio de classificació global (total de mostres correctament classificades).

3.2.2 Anàlisi quantitativa

Les llegües electròniques, a diferència de les llengües biològiques en què es van inspirar inicialment, també permeten realitzar determinacions quantitatives. Aquest tipus de determinacions no estan tan monopolitzades pel camp de l'alimentació sinó que s'han estès també a molts altres camps (control de qualitat, medi ambient, anàlisi clínica, indústria…) [81,84,86]. En general, podem diferenciar dos grans tipus d'aplicacions quantitatives de les llengües voltamperomètriques:

- Determinació de paràmetres o índex globals: en aquests casos es pretén determinar efectes o percepcions del total de la mostra, sense que aquestes estiguin directament relacionades amb un únic anàlit. Alguns exemples serien la determinació de la toxicitat, la frescor dels aliments o la capacitat antioxidant.

- Determinació d'anàlits concrets: en aquests casos es determinen anàlits coneguts en matrius complexes o en presència d'interferències. Es tracta d'una alternativa a l'aplicació de tècniques de separació, que pot ser especialment útil per a l'anàlisi automatitzada i contínua.

Per a l'anàlisi quantitativa, els mètodes de calibratge més habituals són la regressió per mínims quadrats (PLS, *partial least squares regression*) per al tractament de dades lineals i les xarxes neuronals artificials (ANN, *artificial neural networks*) per a dades no lineals. En aquest cas, també és imprescindible calibrar i validar correctament el model per poder aplicar-lo. La ràtio de distribució de mostres entre els sets de calibratge i validació sol ser semblant al mencionat anteriorment per als models qualitatius supervisats (entre 60:40 i 70:30) però el criteri de distribució de les mostres és lleugerament diferent. Un primer grup d'estratègies considera una única distribució de les mostres entre els sets de calibratge i validació, que pot ser aleatòria o prefixada. Per exemple, es pot emprar un disseny experimental per tal de definir l'interval de concentracions que cobriran les mostres de calibratge i distribuir les mostres de validació aleatòriament dins d'aquest interval o emprar l'algoritme Kennard-Stone [88], que selecciona les mostres de calibratge per tal d'obtenir una representació uniforme de totes les mostres. D'altra banda, existeix un segon grup d'estratègies on es realitzen múltiples divisions de les mostres entre els sets de calibratge i validació i després s'obté la mitjana dels resultats. Alguns exemples d'aquesta segona estratègia serien el *k-fold*, on tot el set de dades es divideix en *k* subsets i cada cop s'empra un subset diferent com a set de validació, o el submostreig aleatori repetit, on cada cop es realitza una distribució aleatòria de les mostres entre els dos sets [80,88].

Tal com veiem en els models qualitatius supervisats, la bondat del model s'avalua a partir de la seva capacitat de predir correctament les mostres emprades per a la validació del model. En aquest cas, els criteris emprats són els paràmetres de la recta de regressió obtinguda al representar els valors obtinguts respecte els valors esperats. Idealment, en aquesta recta l'ordenada a

l'origen hauria de ser 0 i el coeficient de correlació i el pendent haurien de ser 1. D'altra banda, un altre paràmetre que sol considerar-se és l'arrel de l'error quadràtic mitjà (RMSE, *root mean square error*), que quantifica la diferència entre els valors predits i els valors reals segons l'equació 3.1, on n correspon al nombre de mostres, l al nombre d'anàlits i y i $\hat{y}$ als valors predits i reals respectivament [80].

$$RMSE = \sqrt{\frac{\sum_{ij}(y_{ij} - \hat{y}_{ij})^2}{l \cdot n - 1}}$$

PART II
METODOLOGIA ANALÍTICA

4

Tècniques instrumentals

4.1 Tècniques voltamperomètriques

Al llarg d'aquesta tesi doctoral s'han emprat tècniques voltamperomètriques tant amb finalitats quantitatives com qualitatives. A nivell quantitatiu s'ha emprat principalment la voltamperometria d'impulsos diferencials (DPV, *differential pulse voltammetry*) que, per a l'anàlisi d'ions metàl·lics, s'ha combinat amb tècniques de voltamperomètriques de redissolució (ASV o AdSV). D'altra banda, a nivell qualitatiu s'ha emprat la voltamperometria cíclica (CV, *cyclic voltammetry*) per caracteritzar la resposta electroquímica de diferents elèctrodes i fer un seguiment dels processos de modificació química de la seva superfície.

4.1.1 Voltamperometria cíclica

La CV és probablement la tècnica electroquímica més emprada per a finalitats qualitatives ja que permet obtenir informació termodinàmica i cinètica a la

vegada que permet identificar ràpidament els potencials redox de les espècies electroactives estudiades així com l'efecte del medi.

El senyal d'excitació que s'aplica a l'elèctrode de treball durant una CV consisteix en un escombratge de potencial triangular: el potencial s'augmenta linealment des d'un potencial inicial fins a un potencial final, punt en què s'inverteix el sentit de l'escombratge per retornar al potencial inicial. Durant l'escombratge directe (cap a potencials més positius) l'anàlit s'oxida donant lloc a un pic anòdic (intensitats positives) mentre que al realitzar l'escombratge invers l'anàlit es redueix donant lloc a pics catòdics (intensitats negatives). Depenent de la informació que ens interessi i l'anàlit considerat es pot invertir el sentit dels escombratges directe i invers i realitzar un o més cicles.

Els principals paràmetres que permeten obtenir informació d'un voltamperograma cíclic són el potencial i la intensitat del pic anòdic (E_a, I_a) i catòdic (E_c, I_c), que es troben definits a la figura 4.1. Quan considerem un sistema ideal reversible, aquests paràmetres haurien de complir les següents relacions [89,90]:

- La intensitat del pic anòdic i catòdic són iguals ($I_a = I_c$), sempre i quan la forma oxidada i reduïda de l'anàlit no s'acumulin a l'elèctrode.
- La intensitat dels pics és proporcional a l'arrel quadrada de la velocitat d'escombratge.
- La separació entre els potencials dels dos pics és 0,059/*n* on *n* és el nombre d'electrons transferits durant la reacció.
  ($\Delta E = E_a - E_c = 0{,}059/n$).
- El potencial dels pics és independent de la velocitat d'escombratge.

L'estudi de sistemes reversibles per CV també permet estudiar la resposta electroquímica de l'elèctrode de treball, estudi especialment útil quan s'avaluen les diferents etapes del procés de modificació d'un elèctrode o quan es proven nous materials com a superfície electròdica. El sistema redox reversible més emprat en aquests estudis és el $[Fe(CN)_6]^{3-}$/ $[Fe(CN)_6]^{4-}$, que és un model aniònic, però també es poden emprar altres sistemes com, per exemple, el $[Ru(NH_3)_6]^{2+}$/ $[Ru(NH_3)_6]^{3+}$ (model catiònic) o la hidroquinona/quinona (HQ/Q) (model neutre i sensible al pH).

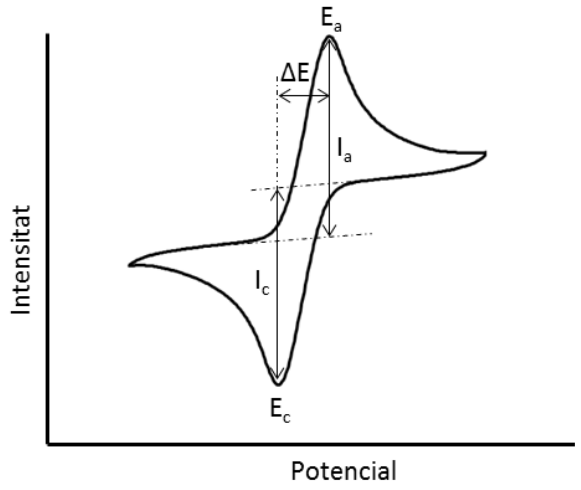

Figura 4.1. Definició dels principals paràmetres d'un voltamperograma cíclic.

4.1.2 Voltamperometria diferencial d'impulsos

Les tècniques voltamperomètriques d'impulsos són més adequades per a l'anàlisi quantitativa ja que proporcionen una millor relació corrent faradaica / corrent no-faradaica, fet que permet arribar a detectar concentracions més baixes.

Existeixen diferents tècniques voltamperomètriques segons la forma del senyal d'excitació. En el cas de la DPV, aquest senyal consisteix en una rampa lineal de potencial sobre la qual se superposen impulsos de potencial constant a intervals de temps constant. Els paràmetres que cal definir són el temps ($t_p \approx 50 – 100$ ms) i el potencial de l'impuls ($E_p \approx 10 – 100$ mV) i l'interval de temps ($t_{int} \approx 0.5 – 4$ s) i potencial ($E_{int} \approx 5 – 10$ mV) entre esglaons (Figura 4.2). La relació entre aquests dos últims paràmetres definirà la velocitat d'escombratge ($s_{rate} = E_{int}/t_{int}$).

La intensitat es mesura dues vegades, just abans d'aplicar l'impuls de potencial (I_1) i al final d'aquest (I_2). Al representar la diferència entre elles ($I_2 – I_1$) s'obté una resposta en forma de pic, l'altura o l'àrea del qual és proporcional a la concentració de l'anàlit [89,90].

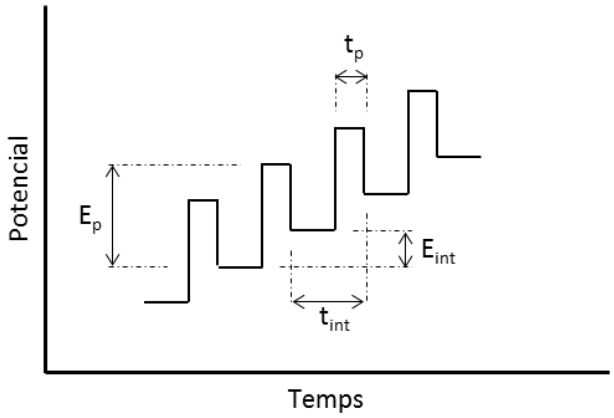

Figura 4.2. Esquematització dels principals paràmetres que defineixen el senyal d'excitació a la DPV.

4.1.3 Voltamperometria de redissolució

Les tècniques voltamperomètriques de redissolució proporcionen encara millors límits de detecció que la DPV, doncs permeten determinar concentracions de l'ordre de 10^{-10} mol L^{-1}. Aquestes tècniques consten bàsicament d'una primera etapa de preconcentració on el metall es deposita electròdicament a la superfície de l'elèctrode i d'una segona etapa de redissolució que té lloc mitjançant un escombratge de potencial. L'etapa de preconcentració es duu a terme amb agitació constant per tal de facilitar el transport de l'anàlit fins a la superfície de l'elèctrode.

En el cas dels elèctrodes de gota de mercuri es necessita una etapa de repòs entre les etapes de preconcentració i redissolució per tal d'assegurar que l'anàlit es distribueixi homogèniament dins la gota de mercuri. Aquesta etapa consisteix en aplicar el potencial de deposició durant uns 30 segons mantenint la solució en repòs però pot estalviar-se o reduir-se força si s'empra qualsevol altre elèctrode de treball.

En el cas de la determinació d'ions metàl·lics, les dues tècniques de redissolució més habituals són l'ASV i l'AdSV. Aquestes dues tècniques es diferencien

principalment per la naturalesa de l'etapa de preconcentració, que afectarà al potencial de deposició i al sentit de l'escombratge durant l'etapa de redissolució (figura 4.3).

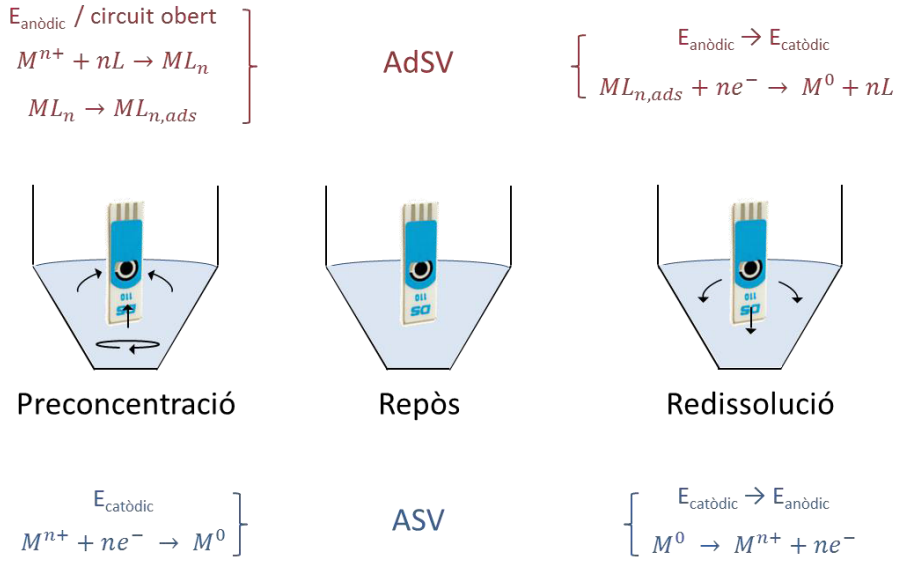

Figura 4.3. Esquematització de la ASV i la AdSV.

Voltamperometria de redissolució anòdica

En l'ASV l'etapa de preconcentració es basa en una electrodeposició catòdica de l'ió metàl·lic. Durant aquesta primera etapa s'aplica un potencial catòdic constant per tal de reduir els ions metàl·lics al seu estat fonamental i poder acumular-los a la superfície de l'elèctrode on s'estabilitzen per formació d'una amalgama en el cas del HDME o per afinitat amb algun component de la superfície en el cas dels elèctrodes modificats. Els dos paràmetres principals que cal optimitzar són el potencial (E_d) i el temps (t_d) de deposició. El E_d ha de ser lleugerament més negatiu que el potencial condicional de l'ió metàl·lic que es vol determinar per tal d'assegurar que aquest es redueix tan aviat com arriba a la superfície de l'elèctrode. Triant adequadament el E_d es pot evitar la reducció d'altres ions metàl·lics que requeririen potencials més negatius, aconseguint així una preconcentració més selectiva. Pel que fa al t_d, se sol establir un compromís

entre el senyal de l'anàlit i el temps de l'anàlisi. Deposicions molt curtes no permeten preconcentrar prou metall a la superfície de l'elèctrode mentre que deposicions molt llargues augmenten el temps d'anàlisi i afavoreixen l'aparició de fenòmens no desitjats (formació de compostos intermetàl·lics, saturació de l'elèctrode…).

Durant l'etapa de redissolució es realitza un escombratge de potencials des de l'E_d i cap a potencials més positius. Durant aquest escombratge el metall es reoxida donant lloc a un pic d'intensitats positives l'àrea o la intensitat del qual és proporcional a la concentració de metall depositat a l'elèctrode, que al seu torn és proporcional a la concentració del metall a la solució. Durant aquest escombratge de potencials se solen emprar tècniques voltamperomètriques d'impulsos, sent la DPV i la voltamperometria d'ona quadrada (SWV, *square wave voltammetry*) les dues tècniques més habituals en la determinació d'ions metàl·lics [89,90].

Alguns dels ions metàl·lics que es determinen habitualment per ASV són el Pb^{2+}, Cd^{2+}, Zn^{2+}, $Cu^{+/2+}$, Tl^{+}, In^{3+} i Bi^{3+}, entre d'altres.

Voltamperometria de redissolució per adsorció

L'AdSV s'utilitza especialment per a aquells metalls que, un cop reduïts a la forma elemental, no presenten afinitat per la superfície de l'elèctrode i no s'hi acumulen. Així, en la AdSV l'etapa de preconcentració es basa en l'adsorció d'un complex del metall que sí presenta afinitat per la superfície. Aquesta etapa es pot dur a terme aplicant un potencial constant o a circuit obert i, habitualment, l'etapa de redissolució té lloc a través d'un escombratge cap a potencials més negatius per reduir el metall complexat. Donat que aquesta tècnica implica la formació d'un complex metall – lligand, cal tenir especialment en compte certs paràmetres com el pH, el solvent, la força iònica i la temperatura entre d'altres. D'altra banda, els calibratges per AdSV solen desviar-se de la linealitat a concentracions superiors a 10^{-6} mol L^{-1} ja que s'assoleix un recobriment total de la superfície de l'elèctrode. En el cas de voler treballar a concentracions més elevades es pot disminuir el recobriment de la superfície emprant temps d'acumulació més curts o menors velocitats d'agitació [89,90].

Alguns dels ions metàl·lics que es determinen habitualment per ASV són el Ni^{2+}, Pd^{2+}, Co^{2+} i Cr^{6+}. A la taula 4.1 es mostren algunes parelles metall – lligand habituals en AdSV, juntament amb el medi en què es realitza cada determinació.

Taula 4.1. Parelles metall – lligand habituals en AdSV [89].

Metall	Lligand	Electròlit suport
Cobalt	Nioxima	HEPES
Crom	Àcid dietilentriamina-pentacètic	Acètic/acetat
Ferro	Violeta de solocrom RS	Acètic/acetat
Manganès	Negre d'eriocrom T	PIPES
Níquel	Dimetilglioxima	Amoni/amoníac
Platí	Formazona	Àcid sulfúric
Urani	Oxina	PIPES
Vanadi	Catecol	PIPES

4.2 Tècniques de microscòpia electrònica

Al llarg d'aquesta tesi doctoral s'han emprat tècniques de microscòpia electrònica per a la caracterització dels sensors basats en nanomaterials o pel·lícules metàl·liques. La microscòpia electrònica de rastreig (SEM, *scanning electron microscopy*) s'ha emprat per a la caracterització dels elèctrodes serigrafiats abans i després de la modificació, mentre que la microscòpia electrònica de transmissió (TEM, *transmission electron microscopy*) s'ha utilitzat per caracteritzar la mida i la forma de les nanopartícules metàl·liques. La taula 4.2 mostra les principals diferències entre les dues tècniques

4.2.1 Microscòpia electrònica de rastreig

La SEM és el tipus de microscòpia electrònica més emprat per a la caracterització de materials. Es tracta d'una tècnica que permet escanejar la superfície del material amb una elevada resolució i una profunditat de desenes de µm, proporcionant així imatges amb aparença tridimensional. Aquesta

tercera dimensió és especialment útil per a la caracterització de materials porosos ja que permet mesurar la profunditat dels porus.

L'escaneig es fa seguint una trajectòria de línies paral·leles on es fa incidir un feix d'electrons, enfocat amb precisió i amb una energia d'acceleració entre 1 i 40 kV, sobre una mostra gruixuda i opaca. La interacció d'aquest feix d'electrons amb la mostra genera dos tipus d'electrons: (i) els electrons retrodispersats, que són els electrons del feix incident que han sigut dispersats per la mostra i proporcionen informació sobre la composició elemental i (ii) els electrons secundaris, que són els electrons emesos per la mostra i proporcionen informació morfològica de la superfície. Per a cada posició, els electrons emesos s'enregistren al detector i el senyal s'amplifica per reconstruir la imatge [91].

Taula 4.2. Principals diferències entre SEM i TEM.

	SEM	TEM
Tipus d'electrons	Retrodispersats i secundaris	Transmesos
Il·luminació	Rastreig de la mostra punt a punt	Il·luminació directa de tota la mostra
Energia d'acceleració	1 – 40 kV	60 – 300 kV
Resolució	0,4 nm	0,05 nm
Formació de la imatge	El detector captura i compta els electrons	Reproducció directa de la imatge en una pantalla fluorescent
Tipus d'imatge	3D de la superfície	Projecció 2D de l'estructura interna
Gruix de la mostra	Qualsevol	< 100 nm
Preparació de la mostra	Molt poca/cap	Complexa

4.2.2 Microscòpia electrònica de transmissió

La TEM és un altre tipus de microscòpia electrònica habitualment emprada per a la caracterització de materials. En aquesta tècnica també es fa incidir un feix d'electrons sobre la mostra però, a diferència de la SEM, en aquest cas s'il·lumina tota la mostra de cop i s'aplica una major energia d'acceleració (entre

60 i 300 kV), fet que permet assolir una resolució bastant més alta (es poden arribar a resoldre al voltant de 0,05 nm).

D'altra banda, una mesura de TEM enregistra el feix d'electrons un cop ha travessat la mostra per tal d'obtenir informació sobre els electrons transmesos a través de la mostra i reprodueix la imatge directament sobre una pantalla fluorescent. Per tant, no només proporciona informació sobre la seva superfície sinó també de la seva estructura interna (estructura cristal·lina, morfologia…). Aquest fet però, implica treballar amb mostres molt fines (menys de 100 nm) i, per tant, la preparació de la mostra en TEM sol ser bastant més complexa que en SEM [91].

5

Tractament de dades

Com ja és ben sabut les determinacions analítiques basades en l'anàlisi instrumental requereixen l'ús de mètodes de calibratge. Quan hi ha respostes instrumentals univariants, els tres mètodes de calibratge més habituals són la recta de calibratge externa, l'addició estàndard (per minimitzar els efectes de matriu) i el patró intern (per minimitzar les derives de senyal, entre d'altres). Tots aquests mètodes es poden aplicar fàcilment en mostres que impliquen un anàlit o diversos anàlits si les seves respostes no s'interfereixen entre si. Tanmateix, quan hi ha interaccions entre les espècies i/o senyals solapats es dificulta l'aplicació d'aquestes metodologies univariants i és necessari l'ús d'estratègies multivariants que inclouen un tractament de dades basat en tècniques quimiomètriques.

Al llarg d'aquesta tesi doctoral s'han emprat mètodes de tractament de dades univariants i multivariants. En concret, s'han emprat mètodes de calibratge univariants, sobretot l'addició estàndard, durant el desenvolupament de sensors, on els sistemes models estudiats (normalment cadmi(II) i plom(II)) presenten dos pics completament separats, i mètodes de calibratge

multivariants en les mesures de llengües voltamperomètriques, on els metalls estudiats presenten pics fortament solapats.

En aquest darrer cas, el mètode de calibratge multivariant seleccionat ha estat el PLS, que està esquematitzat a la figura 5.1. Es tracta d'un mètode lineal en què s'empren combinacions lineals de les variables originals per tal de reduir el nombre de variables. A diferència del PCA i la regressió de components principals (PCR, *principal component regression)*, on només la matriu de dades (**X**) es descompon en *scores* i *loadings*, en aquest cas es descomponen tant la matriu de dades (**X**) com la matriu dels paràmetres a predir (**Y**) i les noves variables, anomenades variables latents (LVs, *latent variable*), es calculen per tal de maximitzar la covariància entre **X** i **Y**. Aquesta descomposició de les dues matrius implica que el PLS assumeix que l'error no està focalitzat a la matriu **X** sinó que el trobem igualment present a la matriu **Y**. En funció del nombre de variables a predir, distingirem entre PLS1 (1 variable) i PLS2 (diverses variables) [92,93].

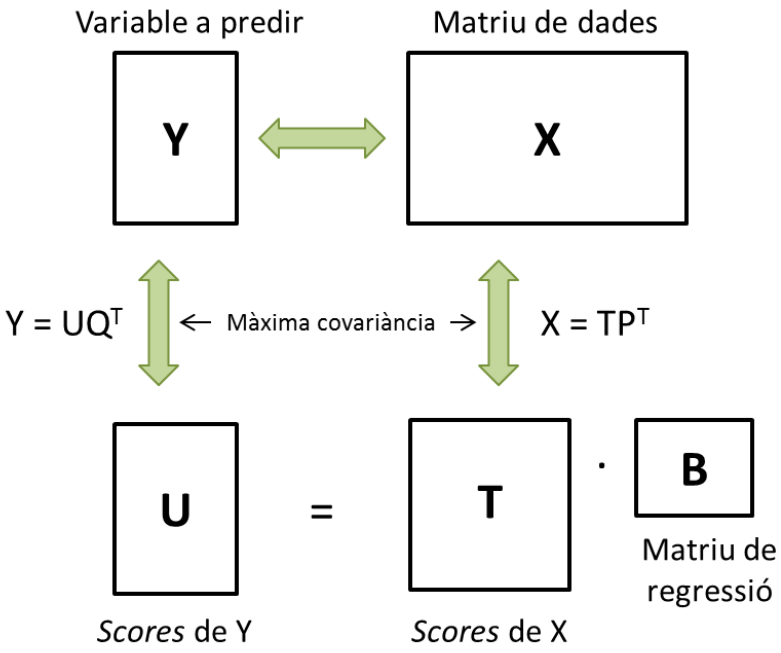

Figura 5.1. Esquematització del PLS.

5.1 Preprocessat de les dades

El preprocessat de les dades és un pas previ a la construcció del model on es transformen les dades originals en una forma més adequada per a l'anàlisi. De fet, el preprocessat pot marcar la diferència entre un bon i un mal model.

Quan es treballa amb dades provinents de diversos sensors, el primer que cal fer és agrupar-les en una sola matriu. Aquesta agrupació es pot fer en 3 dimensions (figura 5.2a) o desplegant-les per tal de treballar amb només dues dimensions (figura 5.2b). En aquest últim cas, es pot tractar les dades directament amb PLS, sense haver de recórrer a mètodes més complexes com el N-PLS.

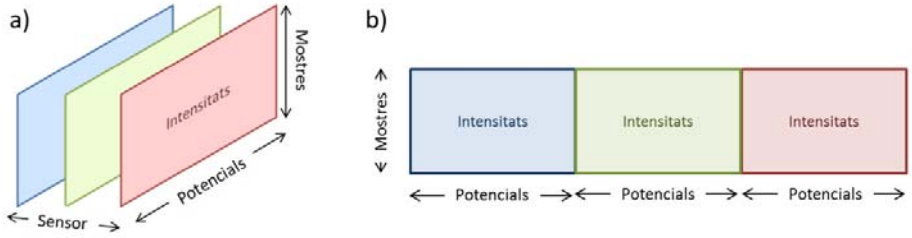

Figura 5.2. Agrupació de les dades provinents de diferents sensors en (a) 3 dimensions i (b) 2 dimensions.

En el cas de treballar amb dades voltamperomètriques, alguns dels preprocessats més habituals estan enfocats a seleccionar només la zona útil del voltamperograma, disminuir el soroll o corregir derives de la línia base. D'altra banda, l'ús de la primera derivada pot ser especialment útil quan tenim pics parcialment solapats ja que accentua les diferències de forma i amplada de cada un dels pics.

Un algoritme més complex que també és útil per al preprocessat de dades en llengües voltamperomètriques és la correcció ortogonal del senyal (OSC, *orthogonal signal correction*). L'OSC és especialment útil quan la primera LV del model PLS explica molta més variació de la matriu de dades que de la variable a predir ja que permet eliminar gran part de la variància de **X** que no està relacionada amb **Y**. Per fer-ho, s'empra un algoritme molt semblant al del PLS però, enlloc de calcular les LVs que maximitzen la covariància entre **X** i **Y**, es calculen les LVs que minimitzen aquesta covariància. Així, podem extreure la

informació de **X** no relacionada amb **Y** i restar-la de la matriu de dades original [94].

D'altra banda, tal com s'ha comentat al capítol 3, un dels inconvenients de les llengües voltamperomètriques és que, a l'ajuntar els voltamperogrames resultants de diversos sensors, la quantitat de dades obtinguda és força elevada. Així, en ocasions és necessari emprar mètodes de compressió de dades, sent la FTT i la DWT algunes de les opcions més habituals. Una altra opció que també dóna bons resultats és l'ús de models jeràrquics, on en una primera etapa es divideixen les dades en blocs (o sensors en aquest cas) i s'aplica PCA o PLS a cadascun d'ells per separat. Els *scores* obtinguts per cada bloc s'utilitzen com a nous descriptors per a un segon model PLS, aconseguint reduir considerablement la quantitat d'informació de partida [95].

5.2 Sistemes de calibratge

El calibratge i la validació són dues etapes fonamentals en l'anàlisi instrumental. A nivell univariant, com ja s'ha dit, els tres mètodes de calibratge més habituals són la recta de calibratge externa, l'addició estàndard i el patró intern.

En el cas de l'anàlisi multivariant, el mètode de calibratge més habitualment emprat seria l'anàleg a la recta de calibratge externa ja que s'empra un conjunt de mostres de calibratge i la concentració de la mostra problema es calcula per interpolació. En aquest cas és especialment important validar correctament el model i aquesta validació es realitza a dos nivells:

- Validació creuada: S'utilitzen només les mostres del set de calibratge, emprant una part d'elles per calibrar el model i l'altra per avaluar la seva capacitat de predicció. Aquest procediment es repeteix emprant diferents particions de les mostres i el model definitiu s'obté a partir de la mitjana de totes les particions. És una bona estratègia per triar el nombre de LVs necessàries però proporciona resultats massa optimistes respecte a la capacitat predictiva del model.

- Validació externa: S'empra un conjunt de mostres extern a les mostres de calibratge, proporcionant així un resultat molt més acurat respecte a la capacitat predictiva del model.

Aquest tipus de calibratge però, només funciona correctament en absència d'efecte matriu o quan les mostres de calibratge tenen una composició semblant a les mostres problema. En aquest sentit, el calibratge amb ajust de matriu (*matrix matching*) pot ser una bona solució ja que se simula la matriu de la mostra en les mostres de calibratge. No obstant, no sempre és possible reconstruir o simular aquesta matriu, fet que dificulta la generalització d'aquesta estratègia.

En l'anàlisi univariant, el problema de l'efecte matriu es pot resoldre amb el calibratge per addició estàndard. L'extrapolació d'aquest mètode de calibratge a l'anàlisi multivariant no està clarament definit però existeixen algunes propostes que es presenten a continuació:

- Mètode d'addició estàndard generalitzat (GSMA, g*eneralized standard addition method)*: és un mètode que parteix de la suposició que la resposta d'un sensor és conseqüència d'una combinació lineal de les respostes de diferents espècies, ja siguin anàlits o interferents. Aquesta suposició permet treballar amb una matriu d'increment de resposta (obtinguda restant la resposta inicial a la resposta de cada addició) que, juntament amb la matriu de concentracions afegides, permet obtenir una matriu de sensibilitats a partir de la qual es calcula la concentració inicial a la mostra. Originalment aquest mètode estava basat en el calibratge per mínims quadrats (CLS, *least-square calibration*) però posteriorment es va estendre a PLS, permetent així treballar amb mostres més complexes o amb més soroll i evitar la restricció de tenir sempre més sensors o addicions que anàlits [96,97].

- Calibratge multivariant per addició estàndard: és un mètode que aplica un model PLS directament a la resposta de la mostra i de les successives addicions per després extrapolar a la resposta d'un blanc i trobar la concentració de la mostra original (figura 5.3). Es tracta d'una aproximació molt més semblant a l'addició estàndard univariant però té dos grans inconvenients: (i) requereix del senyal del blanc i (ii) en cas de treballar amb múltiples anàlits, cal addicionar-los alternativament per tal que el model PLS sigui capaç d'associar quina zona del senyal correspon a cadascun d'ells [98].

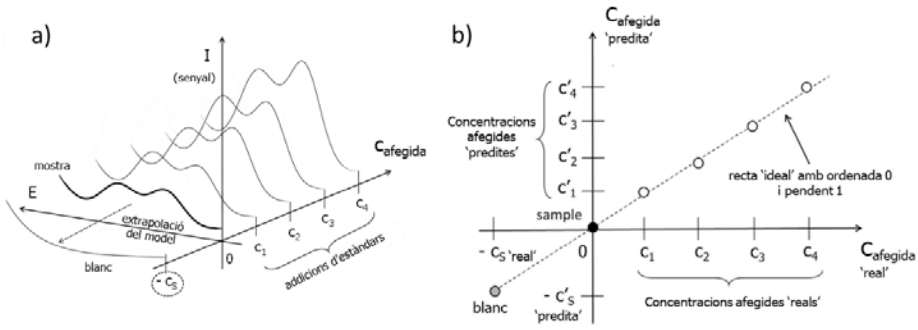

Figura 5.3. (a) Esquematització gràfica del calibratge multivariant per addició estàndard i (b) comparació de les concentracions reals en front de les predites. La mostra està representada per una línia més gruixuda a (a) i un punt negre a (b). Adaptat de [98].

PART III
EXPERIMENTAL

6

Instrumentació i reactius

6.1 Instrumentació

Al llarg d'aquesta tesi doctoral s'han emprat diferents instruments i elèctrodes per a la realització de les mesures electroquímiques en funció de l'objectiu de cada determinació. A la taula 6.1 es llisten els instruments i elèctrodes emprats, juntament amb els proveïdors corresponents. Tots els elèctrodes serigrafiats emprats tenen un diàmetre de 4 mm i s'han connectat al potenciòstat a través d'un cable flexible que permet adaptar les connexions. A continuació es detallen les diferents configuracions que s'han utilitzat:

- Mesures voltamperomètriques en un sol canal: potenciòstat μAutolab Type III o PGSTAT12 (EcoChemie, Països Baixos) i interfase IME 663 connectats a un stand polarogràfic 663 VA (Metrohm, Suïssa). Les mesures es realitzen en una cel·la voltamperomètrica amb un elèctrode de treball referit a un elèctrode de referència Ag/AgCl/KCl (3 mol L^{-1}) i un elèctrode auxiliar de platí externs (figura 6.1 a).

- Mesures voltamperomètriques en un sol canal amb volums petits: potenciòstat μAutolab Type III (EcoChemie, Països Baixos). Les mesures

es realitzen dipositant una gota de 50 µL de la solució de mesura de manera que cobreixi els tres elèctrodes del SPE (figura 6.1b).

- Mesures voltamperomètriques multicanal: potenciòstat PGSTAT12 (EcoChemie, Països Baixos) amb configuració multicanal. Les mesures es realitzen amb dos o quatre elèctrodes de treball referits a un mateix elèctrode de referència Ag/AgCl/KCl (3 mol L^{-1}) extern i emprant l'elèctrode auxiliar intern d'un dels SPEs (figura 6.1c).

- Mesures voltamperomètriques amb silici porós: potenciòstat CH sèries 600D (CH Instruments, EUA). Les mesures es realitzen emprant una cel·la de tefló que permet delimitar l'àrea de l'elèctrode de treball a 7,5 mm de diàmetre i emprant un elèctrode de referència de Ag/AgCl/NaCl (3 mol L^{-1}) i un fil de platí com a elèctrode auxiliar (figura 6.1d).

Taula 6.1. Llistat d'instruments i elèctrodes emprats

Nom	Casa comercial
Potenciòstats	
µAutolab Type III (1 canal)	EcoChemie (Països Baixos)
PGSTAT12 (4 canals)	EcoChemie (Països Baixos)
CHI600D (1 canal)	CH Instruments (EUA)
Elèctrodes de referència i auxiliars	
Ag/AgCl/KCl (3 mol L^{-1})	Metrohm (Suïssa)
Ag/AgCl/NaCl (3 mol L^{-1})	BAS Inc (EUA)
Platí	Metrohm (Suïssa)
Elèctrodes de treball	
SPE de carboni (ref. 110, DS SPCE)	Dropsens (Espanya)
SPE de CNF (ref. 110CNF, DS SPCE)	Dropsens (Espanya)
SPE de grafè (ref. 110GPH, DS SPCE)	Dropsens (Espanya)
SPE de MWCNT (ref. 110SWCNT, DS SPCE)	Dropsens (Espanya)
SPE de bismut *sputtered* (ref. Bi10, DS SPE)	Dropsens (Espanya)
Silici porós tèrmicament carbonitzat	Fabricació pròpia al laboratori

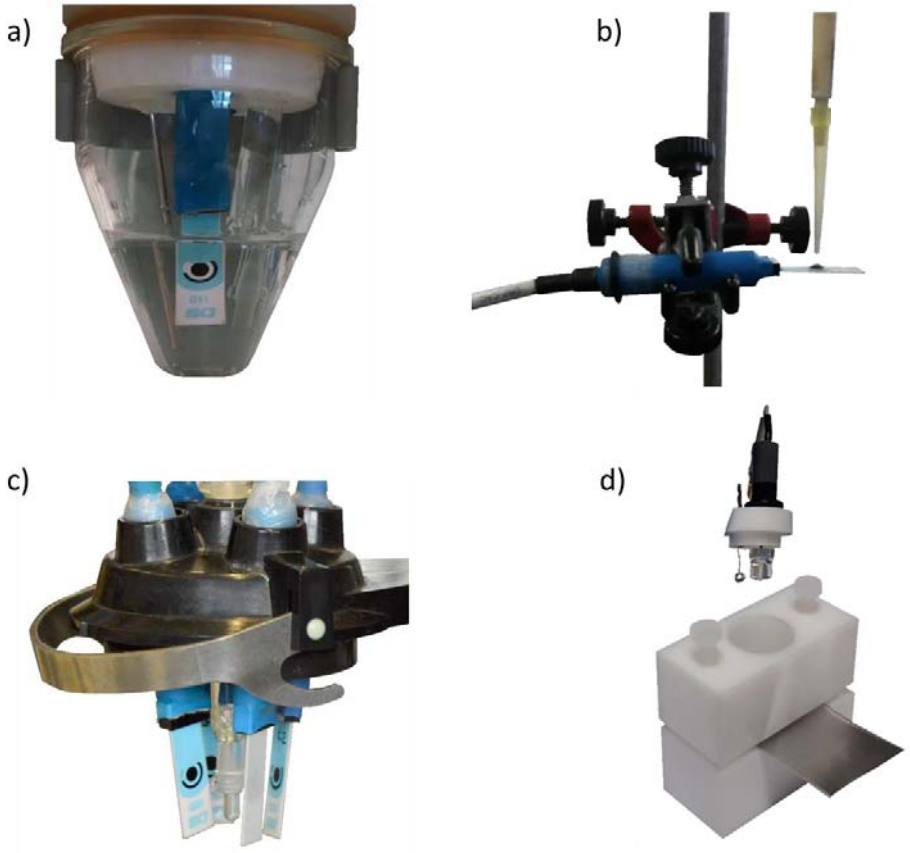

Figura 6.1. Configuracions de treball emprades: (a) mesures en un sol canal (b) mesures en un sol canal amb volums petits, (c) mesures multicanal i (d) mesures amb silici porós.

Per al control de l'instrument i l'adquisició de dades s'ha utilitzat el software GPES (versió 4.9) de la casa EchoChemie o el software CHI (versió 14.05) de la casa CH Instruments en funció del potenciòstat utilitzat. L'anàlisi univariant s'ha realitzat mitjançant Microsoft Excel i per a l'anàlisi multivariant s'ha emprat Matlab amb la PLS-toolbox.

Per a la caracterització microscòpica de les superfícies electròdiques s'han emprat els microscopis electrònics de rastreig JSM 7100FE (Jeol, Japó), Gemini SEM (Zeiss, Alemanya) o Nova Nano SEM 430 (FEI, EUA). La caracterització microscòpica de les solucions de NPs metàl·liques s'ha realitzat amb els microscopis electrònics de transmissió JEM 2100 o 2011 (Jeol, Japó).

Les mesures de ICP-MS s'han realitzat amb l'espectròmetre nexION 350D (Perkin-Elmer, EUA) i les de pH amb un pH-metre micro pH 2000 (Crison, Espanya).

Per a la fabricació del silici porós s'han emprat oblees de silici de 6 polzades (Siltronix, França) i un equip de gravat de silici en humit MPSB (AMMT Gmb, Alemanya).

6.2 Reactius

Al llarg d'aquesta tesi doctoral s'han emprat solucions patró d'ions metàl·lics (taula 6.2) provinents de solucions estàndard comercials o preparades a partir de les sals corresponents. En aquest últim cas, les concentracions s'han establert per estandardització complexomètrica o per ICP-MS.

Taula 6.2. Origen de les solucions patró d'ions metàl·lics.

Metall	Font	Proveïdor/Estandardització
Cd(II)	$Cd(NO_3)_2 \cdot 4H_2O$	Complexometria
Pb(II)	$Pb(NO_3)_2 \cdot 4H_2O$	Complexometria
Zn(II)	$Zn(NO_3)_2 \cdot 4H_2O$	Complexometria
Cu(II)	$Cu(NO_3)_2 \cdot 3H_2O$	Complexometria
In(III)	$In_2(SO_4)_3 \cdot 5H_2O$	ICP-MS
Tl(I)	TlCl	ICP-MS
Bi(III)	Solució comercial 1000 mg L^{-1}	Sigma-Aldrich (EUA)
Sb(III)	Solució comercial 1000 mg L^{-1}	Sigma-Aldrich (EUA)
Pd(II)	Solució comercial 1000 mg L^{-1}	Sigma-Aldrich (EUA)

D'altra banda, a la taula 6.3 es mostren la resta de reactius emprats, classificats segons la seva funció. Es tracta sempre de reactius de qualitat analítica i totes les solucions s'han preparat amb aigua ultrapura (Milli-Q plus 185 system, Millipore).

Taula 6.3. Llistat de reactius emprats classificats segons la seva funció.

Nom	Fórmula	Proveïdor
Modificació química d'elèctrodes		
Àcid aminobenzoic (ABA)	$C_7H_7NO_2$	Sigma-Aldrich (EUA)
4-Nitroanilina (PNA)	$C_6H_6N_2O_2$	Sigma-Aldrich (EUA)
Nitrit de sodi	$NaNO_2$	Sigma-Aldrich (EUA)
Hidroclorur de N-(3-dimetilaminopropil)-N'-etilcarbodiimida (EDC)	$C_8H_{17}N_3$	Applichem (Alemanya)
N-hidroxisulfosuccinimida (sulfo-NHS)	$C_4H_4NNaO_6S$	Sigma-Aldrich (EUA)
Àcid 2-(N-morfolin-etansulfònic) (MES)	$C_6H_{13}NO_4S$	Merck (Alemanya)
Glutatió (GSH), forma reduïda >99%	$C_{10}H_{17}N_3O_6S$	Merck (Alemanya)
L-Cisteïna (Cys), >99%	$C_3H_7NO_2S$	Sigma-Aldrich (EUA)
L-Cistina (Cyst)	$C_6H_{12}N_2O_4S_2$	Fluka (Suïssa)
Selenocistina (SeCyst)	$C_6H_{12}N_2O_4Se_2$	Sigma-Aldrich (EUA)
4-Carboxibenzo-18-corona-6	$C_{17}H_{24}O_8$	Acros (Bèlgica)
Síntesi de nanopartícules de plata		
Nitrat de plata	$AgNO_3$	Sigma-Aldrich (EUA)
Sulfonat sòdic de poliestirè (PSSS)	$Na_n[C_8H_7SO_3^-]_n$	Sigma-Aldrich (EUA)
Citrat de sodi	$Na_3C_6H_5O_7$	Sigma-Aldrich (EUA)
Borohidrur de sodi	$NaBH_4$	Sigma-Aldrich (EUA)
Àcid ascòrbic	$C_6H_8O_6$	Sigma-Aldrich (EUA)

Taula 6.3 (continuació). Llistat de reactius emprats classificats segons la seva funció.

Nom	Fórmula	Proveïdor
Sals inorgàniques		
Ferricianur de potassi	$K_3[Fe(CN)_6]$	Panreac (Espanya)
Ferrocianur de potassi trihidratat	$K_4[Fe(CN)_6]\cdot 3H_2O$	Merck (Alemanya)
Acetat de sodi	CH_3COONa	Merck (Alemanya)
Nitrat de potassi	KNO_3	Sigma-Aldrich (EUA)
Dihidrogenfosfat de potassi	KH_2PO_4	Sigma-Aldrich (EUA)
Hidrogenfosfat de sodi	Na_2HPO_4	Sigma-Aldrich (EUA)
Hidròxid de sodi	NaOH	Sigma-Aldrich (EUA)
Molècules orgàniques		
Hidroquinona (HQ)	$C_6H_6O_2$	Sigma-Aldrich (AUS)
Catecol (CC)	$C_6H_6O_2$	Sigma-Aldrich (AUS)
Resorcinol (RC)	$C_6H_6O_2$	Sigma-Aldrich (AUS)
Dimetilglioxima (DMG)	$C_4H_8N_2O_2$	Sigma-Aldrich (EUA)
Àcids		
Àcid clorhídric	HCl	Merck (Alemanya)
Àcid acètic	CH_3COOH	Merck (Alemanya)
Àcid perclòric	$HClO_4$	Sigma-Aldrich (EUA)
Àcid nítric	HNO_3	Merck (Alemanya)
Àcid fluorhídric	HF	Scharlau (AUS)
Dissolvents orgànics		
Metanol	CH_3OH	Sigma-Aldrich (EUA)
Etanol	CH_3CH_2OH	Panreac (Espanya)
Dimetilformamida (DMF)	$(CH_3)_2$-N-CHO	Merck (Alemanya)

Finalment, per a l'avaluació de l'aplicabilitat dels sensors en mostres reals s'han emprat tres materials de referència diferents:

- LGC6016: Aigua provinent de l'estuari Severn, molt a prop de Avonmouth (Regne Unit), que és una zona molt industrialitzada. Ha estat obtinguda de LGC Standards (Regne Unit).

- ERM® – CA713: Aigua residual provinent d'una instal·lació de tractament d'aigües residuals a Bèlgica. Ha estat preparada per l'Institute for Reference Materials and Measurements (IRMM) del Joint Research Centre (JCR) i subministrada per Sigma-Aldrich (EE.UU).

- BCR® – 610: Aigua subterrània preparada per l'IRMM i subministrada per Sigma-Aldrich (EE.UU).

A la taula 6.4 es mostren les concentracions dels ions metàl·lics presents a cadascun dels tres materials.

Taula 6.4. Ions metàl·lics presents en els materials de referència certificats. Les concentracions estan expressades en μg L^{-1} i les incerteses es mostren entre parèntesi.

	LGC6016	**ERM® – CA713**	**BCR® – 610**
Cadmi	101 (2)	5,09 (0,20)	2,94 (0,08)
Coure	190 (4)	101 (7)	45,7 (1,5)
Plom	196 (3)	49,7 (4,9)	7,78 (0,13)
Manganès	976 (31)	95 (4)	--
Níquel	186 (3)	50,3 (1,4)	22,6[a]
Arsènic	--	10,8 (0,3)	10,8 (0,4)
Crom	--	20,9 (1,3)	--
Ferro	--	445 (27)	--
Mercuri	--	1,84 (0,11)	--
Seleni	4,9 (1,1)	--	
Alumini	--	--	159 (4)
Zinc	55[a]	78[a]	

[a]No es proporcionen incerteses

7

Procediments experimentals

7.1 Modificació d'elèctrodes serigrafiats

7.1.1 Elèctrodes modificats químicament

Al llarg d'aquesta tesi doctoral s'han modificat elèctrodes químicament amb diferents molècules que mostren afinitat pels ions metàl·lics (figura 7.1). Per fer-ho s'han seguit tres protocols de modificació diferents en funció de si la molècula s'ha enllaçat a través del grup carboxílic o amino i de si la modificació s'ha realitzat en cel·la o en gota. En tots els casos, s'han caracteritzat les diferents etapes del procés de modificació per CV emprant una solució 2 mmol L^{-1} de ferricianur i 2 mmol L^{-1} de ferrocianur en tampó fosfat 0,1 mol L^{-1} (pH 7,4).

Enllaç a través del grup amino, modificació en cel·la

El principi de la modificació a través de grup amino es mostra exemplificat pel cas de la cisteïna a la figura 7.2. En primer lloc es funcionalitza la superfície de l'elèctrode de carboni o de nanofibres de carboni realitzant un *electrografting* amb una sal d'aril diazoni. Aquesta sal se sintetitza *in situ* addicionant gota a

gota 5 meq de $NaNO_2$ aquós a una solució freda d'ABA en HCl 1 mol L^{-1}. La solució resultant es deixa agitant 30 min en un bany de gel i a continuació se n'introdueixen 20 mL en una cel·la electroquímica juntament amb l'elèctrode que es vol modificar, un elèctrode auxiliar i un elèctrode de referència. L'*electrografting* es realitza aplicant entre 15 i 30 cicles de CV de 0 V a -1 V a una velocitat d'escombratge de 200 mV s^{-1} sense agitar. L'elèctrode funcionalitzat resultant es neteja amb aigua mili-Q i etanol.

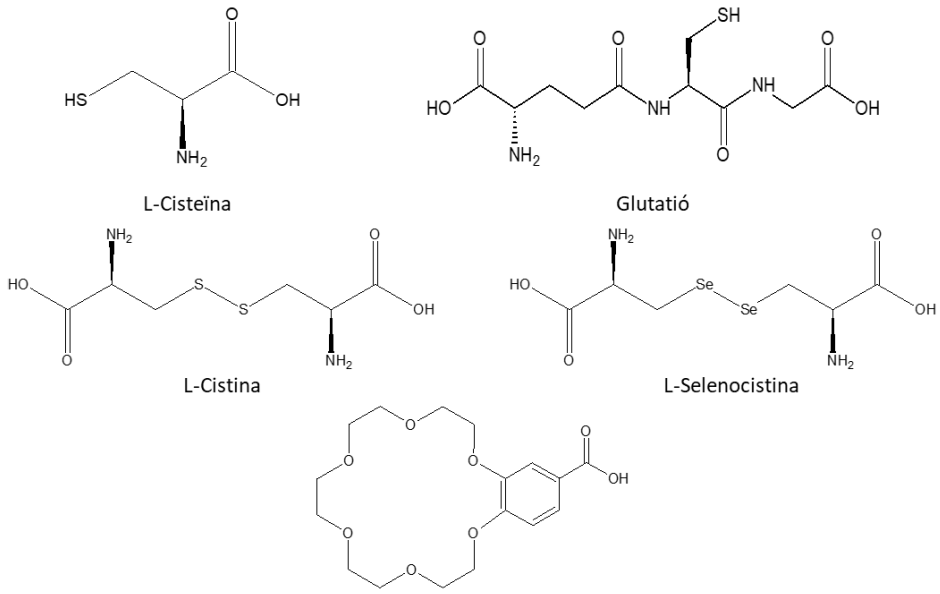

Figura 7.1. Molècules emprades per a la modificació química d'elèctrodes serigrafiats

Per tal d'activar els grups carboxílics terminals generats durant el procés d'*electrografting* es col·loquen 10 µL d'una solució 5 mg mL^{-1} EDC i 7,5 mg mL^{-1} sulfo-NHS en tampó MES 0,1 mol L^{-1} pH 4,5 sobre l'elèctrode de treball del SPE i es deixa reaccionar durant 1 h a temperatura ambient.

Passada l'hora es neteja l'elèctrode amb aigua, es col·loquen 10 µL de la solució del modificador sobre l'elèctrode de treball i es deixa reaccionar tota la nit a la nevera (4 °C). La concentració i el dissolvent d'aquesta última solució varien en funció del modificador considerat.

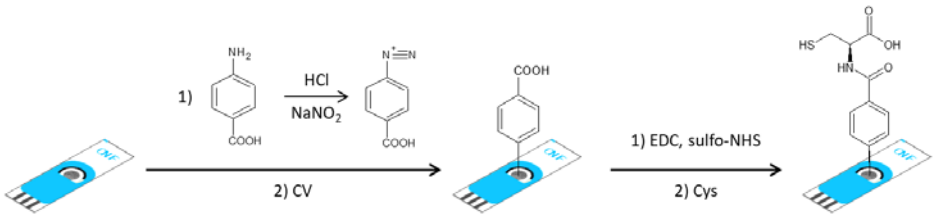

Figura 7.2. Esquematització de la modificació química per enllaç a través del grup amino emprant la cisteïna com a exemple.

Enllaç a través del grup amino, modificació en gota

Aquest protocol és una adaptació del protocol anterior on el procés d'*electrografting* es realitza amb només 50 µL de la solució de sal d'aril diazoni, reduint així considerablement les quantitats de reactius. Per fer-ho, se sintetitza la sal d'aril diazoni també *in-situ,* addicionant gota a gota 0,5 meq de $NaNO_2$ aquós a una solució freda d'ABA en HCl 1 mol L^{-1}. La solució resultant es deixa agitant 30 min en un bany de gel i a continuació es dipositen 50 µL de la solució de sal de diazoni sobre el SPE de manera que cobreixi els tres elèctrodes. L'*electrografting* es realitza aplicant 10 cicles de CV de 0 V a -1 V a una velocitat d'escombratge de 200 mV s^{-1} sense agitar. L'elèctrode funcionalitzat resultant es neteja amb aigua mili-Q i etanol.

L'activació dels grups carboxílics i l'enllaç del modificador es realitzen seguint el procediment explicat en el protocol anterior.

Enllaç a través del grup carboxílic, modificació en cel·la

El principi de la modificació a través de grup carboxílic es mostra exemplificat pel cas de la cisteïna a la figura 7.3. Aquest cop la sal d'aril diazoni se sintetitza *in-situ* addicionant gota a gota 0,1 eq de $NaNO_2$ aquós a una solució freda de PNA en HCl 1 mol L^{-1}. La solució resultant es deixa agitant 30 min en un bany de gel i a continuació se n'introdueixen 20 mL en una cel·la electroquímica juntament amb l'elèctrode que es vol modificar, un elèctrode auxiliar i un elèctrode de referència. L'*electrografting* es realitza aplicant 15 cicles de CV de 0 V a -1 V a una velocitat d'escombratge de 200 mV s^{-1} sense agitar. L'elèctrode funcionalitzat resultant es neteja amb aigua mili-Q i etanol.

A continuació s'intercanvia la solució de la cel·la per HCl 0,01 mol L^{-1} i es redueixen els grups nitro generats a la superfície de l'elèctrode a grups amino aplicant 5 cicles de CV de -0,4 V a -1,2 V a 200 mV s^{-1} sense agitar. L'elèctrode funcionalitzat resultant es neteja amb aigua mili-Q i etanol.

Paral·lelament al procés d'*electrografting*, s'activen els grups carboxílics del modificador fent-lo reaccionar durant 1 h a la nevera amb una solució que conté 82,5 mg mL^{-1} d'EDC i 122,5 mg mL^{-1} de sulfo-NHS en tampó MES 0,1 mol L^{-1} pH 4,5.

Finalment, la formació de l'enllaç peptídic entre els grups carboxílic del modificador i els grups amino generats a la superfície té lloc dipositant 10 µL de la solució del modificador sobre l'elèctrode de treball del SPE i deixant-ho reaccionar tota la nit a la nevera (4˚C).

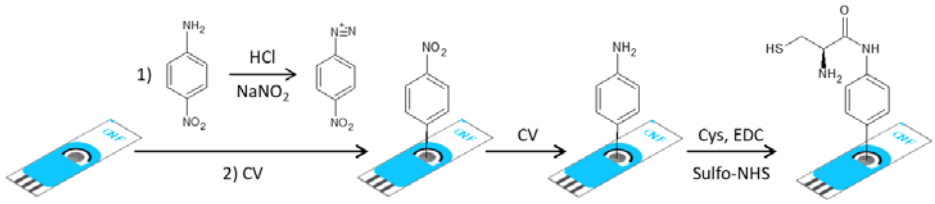

Figura 7.3. Esquematització de la modificació química per enllaç a través del grup carboxílic emprant la cisteïna com a exemple.

7.1.2 Pel·lícules metàl·liques

Al llarg d'aquesta tesi doctoral s'han emprat tres tipus de modificacions d'elèctrodes basades en la formació de pel·lícules metàl·liques: la pel·lícula d'antimoni *in-situ* (*in-situ*-SbSPE*)*, la pel·lícula d'antimoni *ex-situ* (*ex-situ*-SbSPE) i la pel·lícula de bismut *ex-situ* (*ex-situ*-BiSPE). Les pel·lícules *ex-situ* requereixen una etapa de preparació de l'elèctrode prèvia a la mesura voltamperomètrica mentre que amb les pel·lícules *in-situ* les dues etapes es produeixen simultàniament.

En tots els casos la formació de la pel·lícula té lloc en una cel·la voltamperomètrica i emprant un elèctrode de referència i auxiliar externs. La solució de treball es desoxigena purgant amb nitrogen i a continuació s'aplica el

potencial de deposició necessari per reduir el Bi(III) o el Sb(III) a Bi o Sb metàl·lic. A la taula 7.1 es detallen els paràmetres emprats per a cada tipus de pel·lícula.

Taula 7.1. Paràmetres emprats per a la formació de les diferents pel·lícules metàl·liques.

Elèctrode	Solució de partida	Purga	Deposició
in-situ-SbSPE	0,5 mg L^{-1} de Sb(III) Metalls anàlit	2-15 min	Definides per cada determinació
ex-situ-SbSPE	50 mg L^{-1} de Sb(III) 0,01 mol L^{-1} HCl pH 2	10 min	E_d = -0,50 V t_d = 300 s t_r = 20 s
ex-situ-BiSPE	100 mg L^{-1} de Bi(III) 0,2 mol L^{-1} acètic/acetat pH 4,5	10 min	E_d = -0,80 V t_d = 300 s t_r = 20 s

7.1.3 Nanopartícules metàl·liques

Al llarg d'aquesta tesi doctoral s'han emprat dos grups de NPs de plata per a la modificació de SPEs. El primer grup correspon a NPs sintetitzades a partir de productes naturals, concretament les tiges dels gotims de raïm que queden com a residus del procés de verema, i que han estat proporcionades pel grup de Metalls i Mediambient de la Universitat de Girona.

El segon grup de NPs s'ha sintetitzat a partir de reactius químics en col·laboració amb el grup de Recuperació de Recursos i Gestió Ambiental de la Universitat Politècnica de Catalunya. Per a la primera síntesi, on s'obtenen NPs esfèriques, s'addicionen 5 mL de $AgNO_3$ 0,5 mmol L^{-1}, a una velocitat de 2 mL min^{-1} i amb agitació constant, sobre 5,55 mL d'una solució aquosa de 2,25 mmol L^{-1} de citrat de sodi, 22,5 mg L^{-1} de PSSS i 0,54 mmol L^{-1} de $NaBH_4$. Aquestes NPs esfèriques posteriorment s'utilitzen com a precursores per a una segona síntesi, on s'obtenen NPs prismàtiques. En aquest cas, s'addicionen 3 mL de $AgNO_3$ 0,5 mmol L^{-1}, a una velocitat de 1 mL min^{-1} i amb agitació constant, sobre una solució formada per 5 mL d'aigua, 2,5 mL de les NPs esfèriques i 75 µL d'àcid ascòrbic 10 mmol L^{-1}. Finalment, les NPs prismàtiques s'estabilitzen amb 0,5 mL de citrat de sodi 25 mmol L^{-1}.

Tant les NPs de plata d'origen natural com les d'origen sintètic, s'han incorporat al SPE mitjançant la tècnica del *dropcasting*, dipositant una gota de 40 µL de la solució de NPs sobre la superfície de l'elèctrode de treball i deixant-la assecar durant 30 min a l'estufa a 50 ˚C.

7.2 Fabricació d'elèctrodes de silici porós

Al llarg d'aquesta tesi doctoral s'han emprat dos tipus d'elèctrodes de silici porós, THCpSi i TCpSi. En els dos casos el procés de fabricació consta d'una primera etapa comuna on es formen els porus i d'una segona etapa on s'estabilitza el pSi. En funció de les condicions emprades en l'etapa d'estabilització s'obtindrà THCpSi o TCpSi.

La fabricació del pSi s'ha realitzat a partir d'oblees de silici de 6 polzades de diàmetre mitjançant un procés d'anodització en una solució de HF:etanol (1:1). Inicialment es forma una primera capa de sacrifici aplicant una densitat de corrent de 61 mA cm^{-2} durant 30 s. Aquesta capa s'elimina amb NaOH 1 mol L^{-1} i la cel·la es neteja amb aigua i etanol absolut i s'asseca amb nitrogen. A continuació, s'aplica una densitat de corrent de 53 mA cm^{-2} durant 20 s, que permet obtenir pSi amb un diàmetre de porus de 72 ± 15 nm i una profunditat de 500 nm. Finalment, es neteja el pSi amb etanol i es conserva en un dessecador fins al procés d'estabilització.

Per a l'estabilització del pSi per hidrocarbonització, el pSi es col·loca en un tub de quars a temperatura ambient i s'aplica un flux de N_2 durant 45 min seguit d'un flux d'una mescla de N_2:acetilè (1:1) durant 15 min. A continuació es col·loca el tub de quars en un forn tubular prèviament escalfat a 525 ˚C i es manté el flux de la mescla N_2: acetilè (1:1) durant 15 minuts més. Finalment, es deixa refredar fins a temperatura ambient sota un flux de N_2.

Per a l'estabilització del pSi per carbonització, inicialment s'hidrocarbonitza seguint el mateix procediment que en el cas anterior i, un cop refredat a temperatura ambient, es torna aplicar un flux de N_2: acetilè (1:1) durant 10 min a temperatura ambient seguit d'un flux de N_2 a 800 ˚C durant 10 minuts. Finalment, es deixa refredar fins a temperatura ambient també sota un flux de N_2. En tots els casos, la velocitat del flux és de 2 mL min^{-1}.

7.3 Caracterització d'elèctrodes

7.3.1 Caracterització electroquímica

La caracterització electroquímica de les diferents etapes del procés de modificació tant dels elèctrodes modificats químicament com dels elèctrodes de pSi s'ha realitzat per CV. En tots els casos s'ha estudiat la resposta del sensor en presència del sistema redox reversible $[Fe(CN)_6]^{3-}$ / $[Fe(CN)_6]^{4-}$, amb una concentració 2 mmol L^{-1} de les dues espècies i en tampó fosfats 0,01 o 0,1 mol L^{-1} (pH 7,4). Les mesures de CV s'han realitzat amb una velocitat d'escombratge de 100 mV s^{-1}.

7.3.2 Caracterització microscòpica

Com ja s'ha comentat anteriorment a l'apartat 6.1, la caracterització microscòpica tant de la superfície dels elèctrodes desenvolupats com de les solucions de NPs s'ha realitzat per SEM o TEM. Concretament, la SEM s'ha emprat per a la caracterització de la modificació de SPEs amb pel·lícules i NPs metàl·liques i per a la caracterització d'elèctrodes de pSi mentre que la caracterització de les NPs metàl·liques s'ha realitzat per TEM. Per a les mesures de SEM s'ha emprat una resolució de 1 µm i potencials d'acceleració de 5 o 20 mV mentre que les mesures de TEM s'han realitzat a 200 kV.

7.4 Mesures voltamperomètriques

L'aplicabilitat dels sensors desenvolupats s'ha estudiat per a la determinació voltamperomètrica simultània d'ions metàl·lics o del sistema catecol, hidroquinona i resorcinol en el cas de les mesures amb pSi. L'anàlit estudiat en cada cas determina la selecció de la tècnica voltamperomètrica (ASV, AdSV o DPV).

Els principals paràmetres que s'han optimitzat en les mesures voltamperomètriques són el medi on es realitza la mesura i els paràmetres associats a l'etapa de deposició o acumulació (temps i potencial). A la taula 7.2 es recullen les condicions emprades per als diferents sistemes. Pel que fa a

l'escombratge de potencials, que en tots els casos s'ha realitzat per DPV, s'han emprat valors habituals per als diferents paràmetres: temps d'impuls de 50 ms, intervals de potencial de 5 mV i potencials d'impuls de 50 o 100 mV.

Taula 7.2. Condicions emprades per a les mesures voltamperomètriques dels diferents sistemes estudiats.

Sistema	Tècnica	Medi	E_d / E_{acc} (V)	t_d / t_{acc} (s)
Pb^{2+}, Cd^{2+}	ASV	Acètic acetat 0,1 mol L^{-1}, pH 4,5	-1,4	120
Pb^{2+}, Cd^{2+}	ASV	HCl i KNO_3 0,01 mol L^{-1}, pH 2	-1,5	120
Tl^{+}, In^{3+}	ASV	Acètic acetat 0,1 mol L^{-1}, pH 4,5	-1,4 / -1,3	120
Pb^{2+}, Cu^{2+}	ASV	Acètic acetat 0,1 mol L^{-1}, pH 4,5	-1,1	120
Pb^{2+}, Cd^{2+}, Tl^{+}, In^{3+}, Bi^{3+}, Zn^{2+}	ASV	Acètic acetat 0,1 mol L^{-1}, pH 4,5	-1,4	120
Pd^{2+}	AdSV	Acètic acetat 0,1 mol L^{-1}, pH 4,5	-0,6	180
HQ, CC, RC	DPV	Tampó fosfats 0,01 mol L^{-1}, pH 7,4	--	30

Al determinar ions metàl·lics per tècniques voltamperomètriques de redissolució amb elèctrodes serigrafiats és habitual que els metalls s'acumulin a la superfície de l'elèctrode. Així, sovint cal introduir una etapa de neteja entre mesures per tal d'oxidar els metalls acumulats i poder reutilitzar el sensor sense que la seva resposta es vegi afectada per aquesta acumulació no desitjada. L'etapa de neteja sol consistir en l'aplicació d'un potencial més positiu durant un període de temps curt (15-60 s) que es pot realitzar en la mateixa cel·la de mesura o en un medi més agressiu com $HClO_4$ o HNO_3.

L'avaluació de l'aplicabilitat dels sensors desenvolupats i la comparació de les seves característiques s'ha realitzat, per als diferents anàlits estudiats, a partir dels següents paràmetres de qualitat analítica:

- Sensibilitat: pendent de la recta de calibratge.
- Límit de detecció (LOD): 3 vegades la desviació estàndard de l'ordenada a l'origen entre el pendent de la recta de calibratge.
- Límit de quantificació (LOQ): 10 vegades la desviació estàndard de l'ordenada a l'origen entre el pendent de la recta de calibratge.
- Interval lineal: des del LOQ fins a l'últim punt de la recta de calibratge on es conserva la linealitat.
- Coeficient de determinació (R^2).
- Repetitivitat: variació del senyal, expressada en desviació estàndard relativa (%RSD), al realitzar entre 5 i 15 mesures d'una solució amb un mateix sensor.
- Reproductibilitat a un nivell de concentració: variació del senyal, expressada en %RSD, al realitzar entre 5 i 10 mesures d'una solució amb 2 o 3 sensors diferents.
- Reproductibilitat al llarg d'un interval de concentracions: variació del pendent de la recta de calibratge mesurada amb 3 sensors diferents i expressada en %RSD.

Finalment, en el cas dels sensors que han proporcionat millors resultats també s'ha estudiat l'aplicabilitat per a la determinació d'ions metàl·lics en mostres reals emprant materials de referència certificats o mostres fortificades. En aquest últim cas, els resultats obtinguts voltamperomètricament s'han comparat amb els resultat obtinguts per ICP-MS. En tots els casos, per minimitzar els efectes de matriu de les mostres s'ha emprat el mètode de calibratge univariant per addició estàndard i s'ha aplicat el mínim tractament de mostra possible (només la dilució necessària per ajustar el pH òptim).

7.5 Calibratges multivariants

7.5.1 Calibratge extern

El calibratge multivariant extern s'ha emprat per a la quantificació de mescles d'ions metàl·lics que donen lloc a pics solapats. La distribució de les mostres de calibratge s'ha realitzat en tots els casos basant-se en un disseny experimental mentre que les mostres de validació s'han distribuït dins de l'interval de concentracions considerat. A la figura 7.4 es mostra el disseny experimental

emprat per a dos i sis metalls, amb les mostres de calibratge i validació representades per símbols plens i buits respectivament.

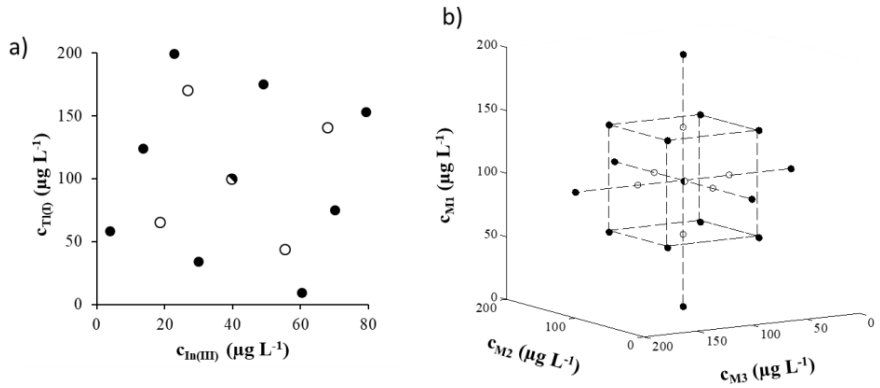

Figura 7.4. Disseny experimental emprat per al calibratge multivariant de sistemes amb 2 (A) i 6 (B) metalls. Mostres de calibratge (●) i de validació (○).

Un cop mesurades totes les mostres, es construeixen les matrius desplegant les dades provinents dels diferents sensors (vegeu figura 5.2b) i es procedeix amb el pretractament de les dades i construcció del model PLS:

- Determinació voltamperomètrica de Tl^+ i In^{3+}: s'han emprat 2 sensors per al calibratge: un elèctrode de CNF modificat amb una pel·lícula d'antimoni *ex-situ* i un elèctrode de CNF modificat amb l'èter corona 4-carboxibenzo-18-corona-6. Per al preprocessat de les dades s'han emprat correccions de línia base, suavitzats, la primera derivada i l'autoescalat. Per als models PLS1 del Tl(I) i In(III) s'han emprat 3 i 5 LVs respectivament.

- Determinació voltamperomètrica de Cd^{2+}, Pb^{2+}, Tl^+ i Bi^{3+} en presència de Zn^{2+} i In^{3+}: s'han emprat 4 sensors per al calibratge: un elèctrode de CNF, un elèctrode de CNF modificat amb una pel·lícula d'antimoni *ex-situ* i dos elèctrodes de CNF modificats químicament amb cisteïna i glutatió. Per al preprocessat de les dades s'ha emprat l'OSC i, degut al gran volum de dades, s'ha treballat amb un model PLS jeràrquic.

7.5.2 Addició estàndard

El calibratge multivariant per addició estàndard s'ha emprat per a la determinació de mostres complexes amb mescles d'ions metàl·lics que donen lloc a pics solapats. Concretament, el sistema estudiat per a aquesta estratègia ha esta la mescla de Tl(I) i In(III) en mostres de tònica emprant un elèctrode de CNF modificat amb una pel·lícula de bismut *ex-situ* i un elèctrode de CNF modificat amb selenocistina.

En aquest cas, inicialment se simula el blanc al qual després s'extrapolarà mesurant la mostra amb un t_d = 0 s. A continuació es mesura la mostra original per triplicat amb el t_d optimitzat i finalment es realitzen addicions alternes dels metalls considerats. Un cop mesurades totes les addicions, es forma una matriu amb les mesures de la mostra i les addicions, desplegant les dades provinents dels dos sensors, i es construeixen models PLS1 emprant les concentracions afegides com a variable a predir. Finalment, s'extrapola el model al senyal del blanc per obtenir la concentració dels metalls a la mostra. En aquest cas, el pretractament de les dades contempla correccions de línia base, la primera derivada i l'autoescalat i per als models PLS1 s'han emprat 5 i 3 LVs per al Tl(I) i l'In(III) respectivament.

PART IV

Resultats i discussió

8

Desenvolupament de sensors voltamperomètrics

Aquest capítol engloba nou treballs centrats en el desenvolupament de nous sensors voltamperomètrics. Els diferents treballs segueixen un esquema similar on inicialment es caracteritzen els sensors desenvolupats per tècniques electroquímiques i/o microscòpiques i a continuació se n'avaluen les seves prestacions analítiques. Generalment, en cada treball es comparen dos o més sensors que permeten estudiar diferents aspectes del procés de modificació del sensor i al final s'avalua l'aplicabilitat en mostres reals del sensor que proporciona millors resultats.

Per a la discussió dels resultats, aquests nou treballs s'han agrupat en funció del tipus de sensor desenvolupat: elèctrodes modificats químicament (4 treballs), elèctrodes basats en pel·lícules metàl·liques (2 treballs), elèctrodes modificats amb NPs metàl·liques (2 treballs) i elèctrodes de pSi (1 treball). En cada apartat, la discussió està dividida en dos subapartats, un primer referit a la caracterització dels elèctrodes i un segon referit a l'aplicació analítica.

Glutathione modified screen-printed carbon nanofiber electrode for the voltammetric determination of metal ions in natural samples.

C. Pérez-Ràfols, N. Serrano, J. M. Díaz-Cruz, C. Ariño, M. Esteban

Talanta 155 (2016) 8-13

https://doi.org/10.1016/j.talanta.2016.04.011

Talanta 155 (2016) 8–13

Contents lists available at ScienceDirect

Talanta

journal homepage: www.elsevier.com/locate/talanta

Glutathione modified screen-printed carbon nanofiber electrode for the voltammetric determination of metal ions in natural samples

Clara Pérez-Ràfols, Núria Serrano *, José Manuel Díaz-Cruz, Cristina Ariño, Miquel Esteban

Departament de Química Analítica, Facultat de Química, Universitat de Barcelona, Martí i Franquès 1-11, E-08028 Barcelona, Spain

ARTICLE INFO

Article history:
Received 23 February 2016
Received in revised form
29 March 2016
Accepted 5 April 2016
Available online 7 April 2016

Keywords:
Peptide-modified sensors
Electrochemical grafting
Screen-printed electrodes
Metal determination
Stripping voltammetry
Glutathione

ABSTRACT

This work reports the development of a glutathione modified electrode via electrografting on a screen-printed carbon nanofiber substrate (GSH-SPCNFE). GSH-SPCNFE was compared to a classical screen-printed carbon electrode modified with glutathione (GSH-SPCE) for the simultaneous voltammetric determination of Cd(II) and Pb(II). Their electrochemical characterization and analytical performance suggest that SPCNFE could be a much better support for GSH immobilization. The applicability of GSH-SPCNFE for the determination of low concentration levels of Pb(II) and Cd(II) ions in environmental samples was successfully tested in a certified wastewater reference material by means of stripping voltammetry with a very high reproducibility and good trueness.

1. Introduction

The great variety of natural and anthropogenic sources of heavy metals, as well as their inability to be degraded, results in concerning levels of contamination of the environment. This, coupled to these metals being a serious threat to human health, makes necessary to have proper methods for their determination [1]. In this sense, stripping techniques and, in particular anodic stripping voltammetry (ASV), are especially suitable for trace heavy metal ions determination in natural samples because they provide excellent detection limits and high reproducibility and sensitivity and they are capable of multielement determination with a relatively low cost [2]. Traditionally, stripping techniques were connected to the use of mercury-based working electrodes due to their high reproducibility and wide cathodic potential range [3]. However, concerns about mercury toxicity have led to focus on the development of more environmentally friendly working electrodes. In this area, chemically modified electrodes are of great interest. In the design of these electrodes, many different strategies for designing recognition interfaces can be followed. In recent years, though, monolayers strategies, dominated by alkanethiol self-assembled monolayers (SAMs), have become increasingly popular. However, alkanethiols SAMs present some limitations including a narrow potential range for metal ion determination as well as poor long term stability [4]. Another viable strategy for molecule immobilization that can overcome these limitations and has proven its usefulness in the development of metal ion sensors is based on aryl diazonioum salt monolayers anchored on the electrode surface [4–6]. This strategy leads to stable electrodes that can be used for a wide number of measurements without signs of degradation [7–9] and allows to incorporate a wide range of functional groups to the electrode surface [10].

Peptides are known as effective, and often specific, ligands for metal ions. Their ability to bind metals is a consequence of the great number of donor atoms not only in their peptide backbone but also in their aminoacid side chains [11–13]. Particularly, the complexation of heavy metals with thiol rich peptides like glutathione (GSH) or its fragments has been largely studied by electroanalytical techniques (Table 2 in [13]). Thus, thiol rich peptides and related structures can be an interesting choice as recognition molecule in metal ion sensors [7,8].

The modification of electrodes with aryl diazonium salts has been applied to many sorts of carbon surfaces including glassy carbon [7,14,15], graphite [8,9], diamond [16,17] and screen-printed carbon electrodes [18–20] among others. Great advancements have been achieved in the last years in the field of screen-printed electrodes (SPEs) allowing the mass production of reproducible, economical and disposable devices. The whole electrode system, including reference, auxiliary and working electrodes, is usually printed on the same strip. Other important features of these SPEs are related to its miniaturized size and their capability to be

* Corresponding author.
E-mail address: nuria.serrano@ub.edu (N. Serrano).

http://dx.doi.org/10.1016/j.talanta.2016.04.011
0039-9140/

connected to portable instrumentation, which makes them suitable for on-site analysis. Furthermore, SPEs offer the possibility to use many different compositions of printing inks that can strongly influence their performance [21,22]. This versatility in printing inks composition also allows the incorporation of nanomaterials like carbon nanotubes or carbon nanofibers to the SPEs, which are ideal for sensor application since they are conductive, easily functionalized and possess very large surface areas. In particular, carbon nanofibers are unique in the fact that their whole surface area can be activated [23]; recent studies have shown that they can be a great choice of substrate in sensors design, enabling to achieve better analytical performances [24,25].

In this paper, all the above-mentioned benefits have been considered for the first time in the development of a glutathione modified electrode via electrografting on a screen-printed nanomaterial substrate leading to a glutathione modified screen-printed carbon nanofiber electrode (GSH-SPCNFE) which will be compared to a classical screen-printed carbon electrode modified with glutathione (GSH-SPCE) in terms of their electrochemical characterization and their analytical performance in the simultaneous determination of Cd(II) and Pb(II) as a model metal ion system. Taking advantage of the better analytical performance of the GSH-SPCNFE, its applicability has been tested through the simultaneous determination of Pb(II) and Cd(II) ions in a certified wastewater reference material.

2. Experimental

2.1. Chemicals

2-(N-morpholino)-ethanesulfonic acid (MES), potassium ferrocyanide $K_4[Fe(CN)_6]\cdot 3H_2O$, hydrochloric acid, sodium acetate, acetic acid and glutathione (GSH), in the reduced form, with purity greater than 99% were purchased from Merck (Darmstadt, Germany). *N*-hydroxysulfosuccinimide (sulfo-NHS), *N*-(3-dimethylaminopropyl)-*N′*-ethylcarbodiimide hydrochloride (EDC), 4-aminobenzoic acid (ABA), perchloric acid, potassium dihydrogen phosphate, sodium nitrite, sodium monophosphate, methanol and certified reference material, wastewater ERM®-CA713, were supplied by Sigma-Aldrich (St. Louis, MO, USA). Potassium ferricyanide $K_3[Fe(CN)_6]$ was provided by Panreac (Barcelona, Spain). All reagents were of analytical grade. Pb(II) and Cd(II) stock solutions 10^{-2} mol L^{-1} were prepared from $Pb(NO_3)_2\cdot 4H_2O$ and $Cd(NO_3)_2\cdot 4H_2O$ respectively and standardized complexometrically [26]. Ultrapure water (Milli-Q plus 185 system, Millipore) was used in all experiments.

2.2. Apparatus

An Autolab System PGSTAT12 (EcoChemie, The Netherlands) attached to a Metrohm 663 VA Stand (Metrohm, Switzerland) and a personal computer with GPES version 4.9 data acquisition software (EcoChemie) was used for stripping measurements.

Ag|AgCl|KCl (3 mol L^{-1}) and Pt wire (Metrohm, Switzerland) were used as reference and auxiliary electrode respectively. The working electrode was a modified glutathione electrode prepared from carbon screen-printed electrode (GSH-SPCE) or carbon nanofibers modified screen-printed electrode (GSH-SPCNFE), both with 4 mm diameter and provided by Dropsens (Oviedo, Spain) (ref. 110, DS SPCE and 110CNF, DS SPCE respectively).

Screen-printed electrodes were connected to the Autolab System by means of a flexible cable (ref. CAC, DropSens).

A Crison micro pH 2000 pH-meter was used for pH measurements.

All measurements were carried out in a glass cell at room temperature (20 °C) without oxygen removal.

2.3. Procedures

2.3.1. Preparation of modified SPEs

Glutathione modified SPEs were prepared based on a two-step procedure previously described [7] with slight modifications.

2.3.1.1. Diazonium salt electrografting. Aryl diazonium salt was generated *in situ* by adding 2 mmol L^{-1} of sodium nitrite to a cooled solution of 73 mmol L^{-1} of ABA in 1 mol L^{-1} aqueous HCl. The resultant solution was allowed to stir in an ice bath for about 30 min before the electrochemical grafting process [27] was conducted. For this purpose, the SPE was immersed in 20 mL of the diazonium salt solution and 15 cyclic voltammetry (CV) cycles from 0 V to −1 V at 0.2 V s^{-1} were applied. In order to remove any physisorbed compounds the functionalized electrodes were thoroughly rinsed with Mili-Q water and methanol.

2.3.1.2. Covalent immobilization of glutathione via carbodiimide coupling. 10 μL of a 26 mmol L^{-1} EDC and 35 mmol L^{-1} sulfo-NHS solution in 100 mmol L^{-1} MES buffer (pH 4.5) were dropped onto the functionalized SPE and left to incubate for 1 h to activate the carboxyl groups of the electrografted diazonium salt. The activated carboxyl groups reacted overnight at 4 °C with the amine terminal groups of glutathione by placing 10 μL of a 2.9 mg/100 mL glutathione solution in 0.1 mol L^{-1} MES buffer (pH 4.5).

2.3.2. Voltammetric measurements

In stripping voltammetric measurements of Cd(II) and Pb(II) using a GSH-SPE, target metal ions were deposited for a deposition time (t_d) of 120 s at a deposition potential (E_d) of −1.4 V, applied with stirring. Deposition was followed by a rest period (t_r) of 5 s and determinations were done by scanning the potential from −1.4 to −0.45 V using pulse times of 50 ms, step potentials of 5 mV and pulse amplitudes of 50 mV.

Linear calibration plots were obtained by increasing metal ion concentrations in 0.1 mol L^{-1} acetate buffer (pH 4.5) solution.

In the analysis of the certified wastewater sample, a volume of the sample in 0.1 mol L^{-1} acetate buffer (pH 4.5) was placed in the cell and the scan was recorded (dilution factor 10/17). Calibration was performed by the standard addition method, five aliquots of metal standard solutions were further added and the respective curves were recorded.

In both linear calibration plots and analysis of the certified wastewater sample, a cleaning step was performed before each set of measurement by applying a conditioning potential (E_{cond}) of −0.3 V for 15 s in 0.1 mol L^{-1} $HClO_4$.

3. Results and discussion

3.1. Electrochemical characterization

Electrochemical characterization of both GSH-SPCE and GSH-SPCNFE was performed at each functionalization step by CV using ferrocyanide/ferricyanide as redox probe in 100 mmol L^{-1} phosphate buffer (pH 7.4). The potential was scanned between −0.6 V and 0.6 V at 100 mV s^{-1} without stirring. As expected, bare CNF resulted in more intense peaks than bare SPCE (Fig. 1), which can be attributed to its enhanced surface area. In both electrodes, a current decrease could be observed after electrografting (Fig. 1) due to the formation of a blocking layer [28]. There is not a clear agreement about the number of CV cycles that should be performed during the electrografting process. In fact, values ranging from 1 to 200 cycles can be found in the literature [29,30]. In this

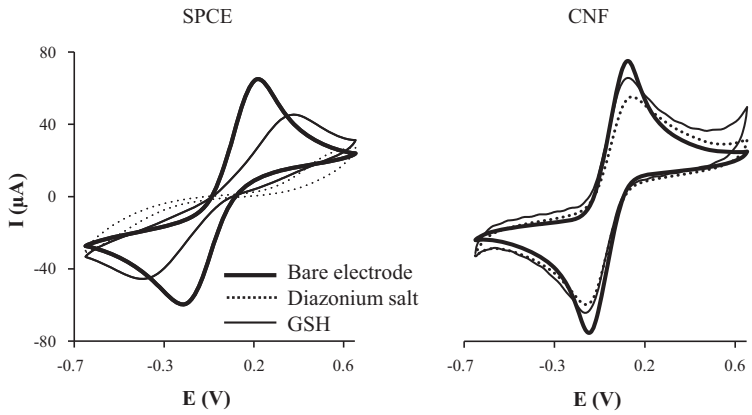

Fig. 1. CVs plots recorded at each functionalization step for GSH-SPCE and GSH-SPCNFE. Measurements were performed in a 2 mmol L^{-1} ferrocyanide/ferricyanide solution in phosphate buffer.

paper, the optimum number of CV cycles to be applied was investigated. It was proved that once the peak corresponding to the reduction of the diazonium salt disappears, increasing the number of cycles does not improve the electrode performance whereas it prolongs the functionalization process. For this reason, 15 cycles were selected as the optimum value. For both GSH-SPCE and GSH-SPCNFE, covalent binding of glutathione resulted in intermediate currents (Fig. 1). These modified electrodes can be stored for some weeks without signs of degradation.

3.2. Repeatability and reproducibility

Several electrochemical parameters, such as E_d, t_d and pH, were firstly optimized to ensure the detection of both Cd(II) and Pb(II) ions at each GSH-modified electrodes in the selected concentration range. DPASV measurements of a solution containing 50 μg L^{-1} of Pb(II) and Cd(II) were carried out at different E_d and t_d values ranging from −1.2 V to −1.5 V and from 30 s to 300 s respectively, looking for a compromise between peak area and analysis time. Two different media, acetate buffer (pH 4.5) and HCl (pH 2), were also tested. Well-defined peaks were obtained at pH 4.5 whereas the electrode was damaged for measurements at pH 2. In all cases, the compromise conditions were an E_d of −1.4 V applied with stirring for 120 s at pH 4.5 (acetate buffer).

Fig. 2 shows a comparison of the analytical performance of the GSH-SPCE (thin line) and GSH-SPCNFE (thick line) for the simultaneous determination of a solution containing 80 μg L^{-1} Cd

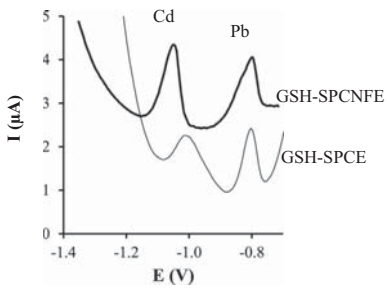

Fig. 2. DPASV measurements of 80 μg L^{-1} Pb(II) and Cd(II) on GSH-SPCNFE (thick line) and GSH-SPCE (thin line), applying a E_d of −1.4 V during 120 s at 0.1 mol L^{-1} acetate buffer (pH 4.5).

(II) and Pb(II). Well-defined peaks can be observed for both Cd(II) and Pb(II) ions with all electrodes. However, more intense peaks are obtained using the GSH-SPCNFE, particularly in the case of Cd (II). This fact can be attributed to CNF substrate being able to immobilize a higher amount of ligand due to its enhanced surface area [24].

Repeatability and reproducibility of both GSH-SPCE and GSH-SPCNFE were tested by measuring a solution of 80 μg L^{-1} Cd(II) and Pb(II) in acetate buffer (pH 4.5). Repeatability was calculated from 5 repetitive measurements using the same glutathione-modified electrode whereas reproducibility was calculated from two different glutathione-modified units within a series of 5 repetitive measurements. In the case of repeatability GSH-SPCNFE yielded an RSD % of 5.1% and 7.6% for Cd(II) and Pb(II) respectively whereas GSH-SPCE yielded an RSD% of 8.2% for Cd(II) and 8.3% for Pb(II). Good values of reproducibility were also obtained for GSH-SPCNFE (6.8% and 8.9% for Cd(II) and Pb(II) respectively). However, reproducibility calculated for GSH-SPCE yielded more than 20% for both Cd(II) and Pb(II). This poor reproducibility is probably associated with the modification procedure, particularly with the covalent immobilization of GSH step. In the case of GSH-SPCNFE, whenever 10 μL of EDC/sulfo-NHS or GSH solutions are dropped onto the electrode, a persistent well-formed drop can be observed. GSH-SPCE, however, is not able to sustain the drop and the 10 μL of solution spread out of the working electrode surface without guaranteeing that the working electrode is always covered by the same amount of ligand, resulting in less reproducible devices.

Repeatability and reproducibility values achieved for GSH-SPCNFE are of the same order of those reported for glassy carbon modified with penicillamine [7] or epoxy graphite modified with crown ethers [9], both following the same modification strategy.

3.3. Calibration data

First of all, the influence of the presence of Pb(II) in the determination of Cd(II) and vice versa was studied. In this sense, individual calibrations of Cd(II) and Pb(II) ions ranging from 1.2 to 150.1 μg L^{-1} and calibrations of considered metal ions in presence of 100 μg L^{-1} of either Cd(II) or Pb(II) by stripping voltammetry were carried out on GSH-SPCNFE. Sensitivities (a.u./μg L^{-1}) obtained as the slope value of the calibration curves of Cd(II) and Pb (II) with and without the presence of the other metal ion were 0.67 and 0.63 for Cd(II), and 1.05 and 3.02 for Pb(II), respectively. At the view of these results, it can be concluded that the presence

Table 1
Calibration data for separate determination of Pb(II) and Cd(II) on GSH-SPCE and GSH-SPCNFE at E_d of −1.4 V, t_d of 120 s and pH 4.5.

	GSH-SPCNFE		GSH-SPCE	
	Pb (II)	Cd (II)	Pb (II)	Cd (II)
Sensitivity (a.u. μg^{-1} L)	3.02 (0.04)	0.63 (0.01)	1.07 (0.02)	1.22 (0.05)
R^2	0.999	0.999	0.998	0.997
Linear range ($\mu g\ L^{-1}$)[a]	10.1–150.1	10.8–150.1	11.7–153.0	43.8–153.0
LOD ($\mu g\ L^{-1}$)	3.0	3.2	3.5	13.2

[a] The lowest value of the linear range was considered from the LOQ.

of Pb(II) does not affect the determination of Cd(II), whereas the presence of high concentrations of Cd(II) slightly influence in the sensitivity (slope) towards Pb(II).

Sensitivity, limit of detection (LOD) and limit of quantification (LOQ) for the separate determination of Pb(II) and Cd(II) obtained by stripping voltammetry on GSH-SPCNFE were compared with those achieved on GSH-SPCE (Table 1). For this reason, linear calibration curves were carried out by measuring at the optimized conditions nine increasing concentrations of Pb(II) and Cd(II) ranging from 1.2 to 150.1 $\mu g\ L^{-1}$ in GSH-SPCNFE and from 1.1 to 153.0 $\mu g\ L^{-1}$ in GSH-SPCE. LOD and LOQ were calculated as 3 and 10 times the standard deviation of the intercept over the slope of the calibration curve respectively. As shown in Table 1, good linear responses of peak area *versus* metal ion concentration were obtained for both Pb(II) and Cd(II) with GSH-SPCE and a slightly higher sensitivity was observed for Cd(II) than for Pb(II). However, although LODs achieved for both Cd(II) and Pb(II) were at levels of $\mu g\ L^{-1}$, the LOD obtained for Pb(II) was much better than that obtained for Cd(II). In fact, in comparison with other peptide-modified electrodes reported in the literature [8, 31], the LOD obtained for Pb(II) in this work is similar or even lower whereas Cd (II) LOD is quite higher. These results were remarkably improved when GSH was immobilized onto a carbon nanofiber substrate. As it can be seen in Table 1, although sensitivity for Cd(II) decreased in GSH-SPCNFE, a much lower LOD was achieved, resulting therefore in a wider linear range. The LOD of 3.2 $\mu g\ L^{-1}$ obtained now for Cd(II) is of the same order and in some cases better than those reported with other peptide modified electrodes [8,31] as well as with other similar electrodes modified following the same strategy like penicillamine-modified glassy carbon electrode [7] or crown ether-modified epoxy-graphite electrodes [9]. It should be pointed out though, that in many of these reported LODs an unpractical deposition time of 300 s or even 600 s instead of 120 s was applied. Thus, GSH-SPCNFE can provide similar or even better LODs with faster determinations. Regarding to Pb(II), LOD was also slightly improved with GSH-SPCNFE, which also provided a much higher sensitivity.

These improvements observed for GSH-SPCNFE could be attributed to the fact that, unlike SPCE, the whole surface area of carbon nanofibers can be activated and, therefore, a higher amount of ligand can be immobilized on the surface of the electrode [24].

Therefore, the reported calibration data, coupled with the better reproducibility previously observed, suggest that SPCNFE could be a much better platform for peptide immobilization in general, and particularly for GSH, than the classical SPCE. Furthermore, GSH-SPCNFE could be fully suitable and a valuable alternative to more conventional electrodes for the simultaneous determination of Cd(II) and Pb(II) at trace levels in natural samples. It must be emphasized that unlike glassy carbon or epoxy-graphite electrodes, SPEs do not require any polishing prior to GSH immobilization. On the other hand, the durability of the GSH immobilization on every screen-printed platform for a large set of

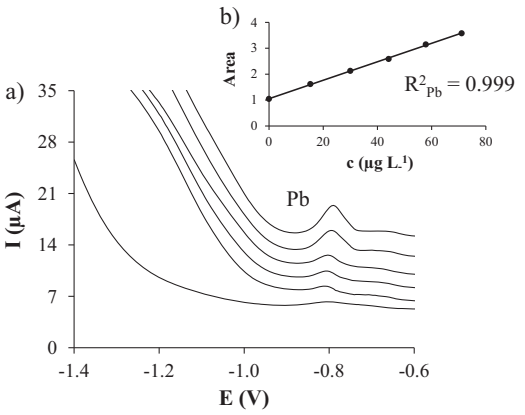

Fig. 3. a) Stripping voltammetric measurements in a wastewater sample by using a GSH-SPCNFE at pH 4.5 with E_d of −1.4 V during a t_d of 120 s and t_r of 5 s; and, b) Pb (II) standard addition plot.

measurements (more than 20) without loss of sensitivity enables the voltammetric determination of metal ions with the same GSH-SPE unit.

3.4. Application to the analysis of a wastewater reference material

At the view of the reproducibility and the analytical performance of both GSH modified screen-printed electrodes, GSH-SPCNFE was considered for the simultaneous determination of Cd (II) and Pb(II) in natural samples and its applicability was tested by measuring a wastewater certified reference material (ERM®-CA713). It should be mentioned though, that the Cd(II) concentration in this available reference material was below the quantification limit. For this reason, only Pb(II) was determined in the presence of Cd(II).

Pb(II) determination was performed by means of the standard addition method. DPASV measurements were carried out under the above optimized conditions, including five metal additions. Representative stripping voltammograms acquired in the analysis of the wastewater reference material using GSH-SPCNFE are shown in Fig. 3a. Well-defined peaks that behave equally to the calibration data were obtained and, as it is shown in Fig. 3b, good correlation of the representative DPASV measurements performed with GSH-SPCNFE was also observed for Pb(II).

Three replicates of the voltammetric determination of the certified wastewater reference material using GSH-SPCNFE were performed. The obtained metal concentration data are reported in Table 2. Good concordance between all the replicates, as well as with the certified Pb(II) ion value was obtained. It should be

Table 2
Total concentrations of Pb(II) and Cd(II) determined in certified wastewater (ERM®-CA713) by stripping voltammetry on GSH-SPCNFE by standard addition calibration method applying an E_d of −1.4 V and t_d of 120 s at pH 4.5.

	Lead			Cadmium	
	c ($\mu g\ L^{-1}$)	RSD (%)	Relative error (%)	c ($\mu g\ L^{-1}$)	RSD (%)
GSH-SPCNFE	50.1	1.2	0.8	n.q.	–
Certified metal value	49.7	3.4	–	5.09	3.9

n=3 for RSD (%); n.q. not quantified.

pointed out that the selected reference material contains other metals like Cr, Cu, Fe, Mn and Ni at similar or higher concentrations than Pb(II) that do not seem to interfere with the determination of Pb(II).

These good results confirm the applicability of GSH-SPCNFE for the determination of Pb(II) in the presence of Cd(II) in natural samples being, therefore, a valuable alternative to the most conventional electrodes with the additional advantage that the SPCNFEs which are the basis of the GSH-SPCNFE are commercially available and do not need any polishing prior to the immobilization of the peptide.

4. Conclusions

This work reports the development of a glutathione modified screen-printed sensor in which the peptide was successfully immobilized through aryl diazonium electrochemical grafting onto a nanomaterial substrate electrode based on carbon nanofiber (GSH-SPCNFE). The repeatability and reproducibility of GSH-SPCNFE compared to a classical screen-printed carbon electrode modified with glutathione (GSH-SPCE) as well as its analytical performance were much better due to both the enhanced surface area attributed to CNF substrate and the modification process itself. Furthermore, the modified GSH-SPCNFE can be used for a large set of measurements without signs of degradation or loss of sensitivity requiring only the performance of a simple cleaning stage between each set of measurements. The LODs and LOQs achieved for Pb(II) and Cd(II) determination with a GSH-SPCNFE are similar or even better than those reported with other peptides or chelating agents applying a t_d of 120 s instead of the 300 s [8,9] or even 600 s [31] used in earlier studies. On the other hand, the basis of the GSH-SPCNFE is a commercial screen-printed support modified with carbon nanofibers, it means that the developed sensor has the additional advantages of the screen-printed electrodes, that is their accessibility, low-cost character and suitability for on-site analysis. Moreover, unlike glassy carbon or epoxy-graphite electrodes, SPEs do not require any polishing prior to peptide immobilization. Finally, the applicability of the developed GSH-SPCNFE was successfully verified by the determination of Pb(II) concentration in a certified wastewater reference material with very high trueness and good reproducibility inferred by the relative error (0.8%) and the relative standard deviation (1.2%). With respect to Cd(II), it was not possible to quantify it since its concentration in the available certified reference material was below the obtained LOQ. Nevertheless, at the sight of the results it can be concluded that GSH-SPCNFE is an attractive alternative to the more conventional glutathione modified electrodes for Cd(II) and Pb(II) determination at low $\mu g\ L^{-1}$ levels in environmental samples. Therefore, the use of SPEs modified with CNF is postulated as a promising support for the immobilization of other chelating agents via electrografting for metal ion determination. Finally, it should be taken into consideration that the developed electrode can be also used for metal determination in combination with others forming a multi-sensor array in search for a multivariate response.

Acknowledgments

This work is supported by the Ministry of Economy and Competitiveness (Project CTQ2012–32863) and the Generalitat of Catalonia (Project 2014SGR269). Clara Pérez-Ràfols acknowledges the Generalitat of Catalonia for a Ph.D grant.

References

[1] E. Lawrence, A.R.W. Jackson, J.M. Jackson, Longman dictionary of environmental science, Addison Wesley Longman, United Kingdom, 1998.
[2] J. Wang, Stripping analysis: principles, instrumentation and applications, VCH (1985).
[3] J. Barek, A.G. Fogg, A. Muck, J. Zima, Polarography and voltammetry at mercury electrodes, Crit. Rev. Anal. Chem. 31 (2001) 291–309.
[4] J.J. Gooding, Advances in interfacial design for electrochemical biosensors and sensors: Aryl diazonium salts for modifying carbon and metal electrodes, Electroanalysis 20 (2008) 573–582.
[5] M. Delamar, R. Hitmi, J. Pinson, J.M. Savbnt, Covalent modification of carbon surfaces by grafting of functionalized aryl radicals produced from electrochemical reduction of diazonium salts, J. Am. Chem. Soc. 114 (1992) 5883–5884.
[6] S. Baranton, D. Bélanger, Electrochemical derivatization of carbon surface by reduction of in situ generated diazonium cations, J. Phys. Chem. B. 109 (2005) 24401–24410.
[7] C. Pérez-Ràfols, N. Serrano, J.M. Díaz-Cruz, C. Ariño, M. Esteban, Penicillamine-modified sensor for the voltammetric determination of Cd(II) and Pb(II) ions in natural samples, Talanta 144 (2015) 569–573.
[8] N. Serrano, B. Prieto-Simón, X. Cetó, M. Del Valle, Array of peptide-modified electrodes for the simultaneous determination of Pb(II), Cd(II) and Zn(II), Talanta 125 (2014) 159–166.
[9] N. Serrano, A. González-Calabuig, M. del Valle, Crown ether-modified electrodes for the simultaneous stripping voltammetric determination of Cd(II), Pb (II) and Cu(II), Talanta 138 (2015) 130–137.
[10] G. Liu, T.N. Quynh, E. Chow, T. Böcking, D.B. Hibbert, J.J. Gooding, Study of factors affecting the performance of voltammetric copper sensors based on Gly-Gly-His modified glassy carbon and gold electrodes, Electroanalysis 18 (2006) 1141–1151.
[11] J.J. Gooding, D.B. Hibbert, W. Yang, Electrochemical metal ion sensors. Exploiting amino acids and peptides as recognition elements, Sensors 1 (2001) 75–90.
[12] J.J. Gooding, Peptide-modified electrodes for detecting metal ions, in: Arben Merkoçi, S. Alegret (Eds.), Electrochemical Sensor Analysis, Elsevier, The Netherlands, 2007, pp. 189–210.
[13] N. Serrano, J.M. Díaz-Cruz, C. Ariño, M. Esteban, Recent contributions to the study of phytochelatins with an analytical approach, Trends Anal. Chem. 73 (2015) 129–145.
[14] G. Liu, J. Liu, T. Böcking, P.K. Eggers, J.J. Gooding, The modification of glassy carbon and gold electrodes with aryl diazonium salt: the impact of the electrode materials on the rate of heterogeneous electron transfer, Chem. Phys. 319 (2005) 136–146.
[15] M. Bourourou, H. Barhoumi, A. Maaref, N. Jaffrezic-Renault, Electrochemical study of modified glassy carbon electrode with carboxyphenyl diazonium salt in aqueous solutions, Sens. Transducers 27 (2014) 22–28.
[16] Y. Zhou, J. Zhi, Development of an amperometric biosensor based on covalent immobilization of tyrosinase on a boron-doped diamond electrode, Electrochem. Commun. 8 (2006) 1811–1816.
[17] S.Q. Lud, M. Steenackers, R. Jordan, P. Bruno, D.M. Gruen, P. Feulner, et al., Chemical grafting of biphenyl self-assembled monolayers on ultrananocrystalline diamond, J. Am. Chem. Soc. 128 (2006) 16884–16891.
[18] M. Revenga-Parra, T. García-Mendiola, J. González-Costas, E. González-Romero, A.G. Marín, J.L. Pau, F. Pariente, E. Lorenzo, Simple diazonium chemistry to develop specific gene sensing platforms, Anal. Chim. Acta 813 (2014) 41–47.
[19] L. Civit, H.M. Nassef, A. Fragoso, C.K. O'Sullivan, Amperometric determination of ascorbic acid in real samples using a disposable screen-printed electrode modified with electrografted o-aminophenol film, J. Agric. Food Chem. 56 (2008) 10452–10455.
[20] M. Moreno-Guzmán, I. Ojeda, R. Villalonga, A. González-Cortés, P. Yáñez-Sedeño, J.M. Pingarrón, Ultrasensitive detection of adrenocorticotropin hormone (ACTH) using disposable phenylboronic-modified electrochemical immunosensors, Biosens. Bioelectron. 35 (2012) 82–86.
[21] J. Barton, M.B.G. García, D.H. Santos, P. Fanjul-Bolado, A. Ribotti, M. McCaul, et al., Screen-printed electrodes for environmental monitoring of heavy metal ions: a review, Microchim. Acta 183 (2016) 503–517.
[22] A. Hayat, J.L. Marty, Disposable screen printed electrochemical sensors: tools for environmental monitoring, Sensors 14 (2014) 10432–10453.
[23] V. Vamvakaki, K. Tsagaraki, N. Chaniotakis, Carbon nanofiber-based glucose biosensor, Anal. Chem. 78 (2006) 5538–5542.
[24] S.A. Lim, M.U. Ahmed, A carbon nanofiber-based label free immunosensor for high sensitive detection of recombinant bovine somatotropin, Biosens. Bioelectron. 70 (2015) 48–53.
[25] C. Pérez-Ràfols, N. Serrano, J.M. Díaz-Cruz, C. Ariño, M. Esteban, New approaches to *anti*mony film screen-printed electrodes using carbon-based nanomaterials substrates, Anal. Chim. Acta 916 (2016) 17–23.
[26] A.I. Vogel, Textbook of Quantitative Chemical Analysis, 5th ed., Pearson Education Limited, United States, 1989.
[27] D. Bélanger, J. Pinson, Electrografting: a powerful method for surface modification, Chem. Soc. Rev. 40 (2011) 3995–4048.
[28] E. Ahlberg, B. Helgée, V.D. Parker, The reaction of aryl radicals with mettalic electrodes, Acta Chem. Scand. B 34 (1980) 181–186.
[29] S. Eissa, L. L'Hocine, M. Siaj, M. Zourob, A graphene-based label-free voltammetric immunosensor for sensitive detection of the egg allergen ovalbumin,

Analyst 138 (2013) 4378.
[30] C. Ocaña, M. del Valle, A comparison of four protocols for the immobilization of an aptamer on graphite composite electrodes, Microchim. Acta 181 (2014) 355–363.
[31] D. Ebrahimi, E. Chow, J.J. Gooding, D.B. Hibbert, Multi-analyte sensing: a chemometrics approach to understanding the merits of electrode arrays versus single electrodes, Analyst 133 (2008) 1090–1096.

A chemically-bound glutathione sensor bioinspired by the defense of organisms against heavy metal contamination: Optimization of the immobilization conditions.

C. Pérez-Ràfols, N. Serrano, J. M. Díaz-Cruz, C. Ariño, M. Esteban

Chemosensors 5 (2017) 12-20 (*Open Access*)

https://doi.org/10.3390/chemosensors5020012

chemosensors

MDPI

Article

A Chemically-Bound Glutathione Sensor Bioinspired by the Defense of Organisms against Heavy Metal Contamination: Optimization of the Immobilization Conditions

Clara Pérez-Ràfols, Núria Serrano *, José Manuel Díaz-Cruz, Cristina Ariño and Miquel Esteban

Departament d'Enginyeria Química i Química Analítica, Facultat de Química, Universitat de Barcelona, Martí i Franquès 1-11, E-08028 Barcelona, Spain; claraperezrafols@ub.edu (C.P.-R.); josemanuel.diaz@ub.edu (J.M.D.-C.); cristina.arino@ub.edu (C.A.); miquelestebanc@ub.edu (M.E.)
* Correspondence: nuria.serrano@ub.edu; Tel.: +34-93-403-3706

Academic Editor: Manel Del Valle
Received: 23 February 2017; Accepted: 25 March 2017; Published: 2 April 2017

Abstract: The influence of the experimental conditions (glutathione concentration and incubation time and temperature) concerning the covalent immobilization of glutathione via carbodiimide coupling on the behavior of a glutathione modified screen-printed carbon electrode obtained by electrografting is evaluated. The optimized parameters fasten the modification process and improve the performance of the sensor as compared to the usual procedure. This suggests the convenience of a tailored preparation of metal sensors based on metal-binding biomolecules such as glutathione.

Keywords: heavy metal sensors; voltammetry; glutathione; electrografting; screen-printed electrodes

1. Introduction

Environmental contamination by heavy metals is a serious problem enhanced by the large quantity and variety of natural and anthropogenic sources of these species, their accumulation in organisms and their negative effects on human health [1]. Against such contamination, organisms have developed biochemical mechanisms of defense, based on the synthesis of molecules with high affinity for heavy metal ions than can chemically bind them to decrease their toxicity and to favor their elimination. The basis of such biochemical defense includes high concentrations of small molecules, mainly aminothiols like cysteine (Cys), cysteine-glycine (Cys-Gly) or glutathione (GSH), and low concentrations of larger molecules which are enzymatically synthesized from the previous ones as a response to heavy metal contamination. In the case of plants, algae and fungi, such larger molecules are phytochelatins, of general structure $(\gamma\text{-Glu-Cys})_n\text{Gly}$ with n usually ranging from 2 to 5 [2–4]. In the case of mammals metallothioneins, a more complex combination of aminoacids with a high proportion of cysteine, play a similar role as phytochelatins [2].

While organisms reinforce their mechanisms to minimize the effects of heavy metal contamination, analytical chemists try to develop more effective methods to determine and monitor the concentration of heavy metals in environmental and biological samples. Although techniques like atomic absorption or ICP are especially powerful in the analysis of metals [5,6], they should be complemented by portable, low-cost techniques for these applications where simplicity, ease of use, economy and possibility of measuring *on-line* or in-situ are required. Among these techniques, voltammetry is a sensitive, cheap and versatile choice, especially when it includes analyte preconcentration by reduction (anodic stripping voltammetry, ASV) or by adsorption (adsorptive stripping voltammetry, AdSV) [7]. For a long time, stripping voltammetric measurements were mostly carried out with mercury drop or mercury film electrodes [8]. However, in the last years, the toxicity of mercury has encouraged

its replacement by alternative materials such as bismuth and antimony films on carbon supports or conventional solid electrodes chemically modified with nanoparticles and molecules having some affinity for heavy metals [9–11]. More recently, the popularization of screen-printed electrodes (SPE) and their commercial availability in a wide variety of materials has largely expanded the field of application of modified electrodes as substitutes for mercury [12]. Commercial screen-printed electrodes are an excellent substrate for modification. They are cheap and reproducible and their disposable character avoids tedious and time-consuming polishing and cleaning steps which are mandatory in the modification of conventional solid electrodes.

Among the different strategies proposed for the stripping analysis of heavy metals beyond the use of mercury, some efforts have been devoted to mimic the defense mechanisms of plants and preconcentrate the target metals by binding them to the electrode with the same molecules used for metal bioaccumulation. Thus, the molecule immobilization procedure is a key aspect in the design of these electrodes [13]. In this regard, the literature describes different strategies including the formation of alkanethiol self-assembled monolayers (SAMs) and the molecule immobilization based on aryl diazonium salt anchored on the electrode surface, which is a more viable approach that can overcome the major limitations of SAMs and has proven its usefulness in the development of metal ion sensors [14–16]. For example, the development of modified sensors in which glutathione (GSH) and its fragments Cys-Gly and γ-Glu-Cys were immobilized through aryl diazonium electrochemical grafting onto the surface of graphite-epoxy composite electrodes (GEC), was used for the simultaneous determination of Cd(II), Pb(II) and Zn(II) [17]. More recently, the procedure was successfully adapted to the special characteristics of screen-printed electrodes to develop a glutathione-modified carbon nanofiber screen-printed electrode [18].

In the present work we revisit the glutathione-modified electrode to gain a deeper insight on the main factors concerning the immobilization of the peptide by electrografting. In this way, we try not only to improve the analytical performance of this sensor, but also to deduce some practical guidelines for the immobilization of more complex metal-binding biomolecules.

2. Materials and Methods

2.1. Chemicals

Potassium ferrocyanide $K_4[Fe(CN)_6]\cdot 3H_2O$, 2-(*N*-morpholino)-ethanesulfonic acid (MES), sodium acetate, acetic acid, hydrochloric acid and glutathione (GSH), in the reduced form, with purity greater than 99% were supplied from Merck (Darmstadt, Germany). *N*-hydroxysulfosuccinimide (sulfo-NHS), 4-aminobenzoic acid (ABA), perchloric acid, *N*-(3-dimethylaminopropyl)-*N*′-ethylcarbodiimide hydrochloride (EDC), potassium dihydrogen phosphate, sodium monophosphate, sodium nitrite and methanol were provided by Sigma-Aldrich (St. Louis, MO, USA). Potassium ferricyanide $K_3[Fe(CN)_6]$ was purchased from Panreac (Barcelona, Spain). All reagents were of analytical grade. Cd(II) and Pb(II) stock solutions 10^{-2} mol·L^{-1} were prepared from $Cd(NO_3)_2\cdot 4H_2O$ and $Pb(NO_3)_2\cdot 4H_2O$ respectively and standardized complexometrically [19]. Ultrapure water (Milli-Q plus 185 system, Millipore) was used in all experiments.

2.2. Instrumentation

An Autolab System PGSTAT12 (EcoChemie, Utrecht, The Netherlands) attached to a Metrohm 663 VA Stand (Metrohm, Herisau, Switzerland) and using GPES 4.9 software package (EcoChemie) was used for differential pulse anodic stripping voltammetric (DPASV) measurements.

For experiments, the working electrode was a modified glutathione electrode prepared from carbon nanofibers modified screen-printed electrode (GSH-SPCNFE) of 4 mm diameter and supplied by Dropsens (Oviedo, Spain) (ref. 110CNF, DS SPCE). A flexible cable (ref. CAC, DropSens) was used to connect screen-printed electrodes to the Autolab System. The auxiliary electrode was a Pt wire (Metrohm, Switzerland) and the reference electrode was Ag | AgCl | KCl (3 mol·L^{-1}).

A Crison micro pH 2000 pH-meter was used for pH measurements, and all measurements were performed in a glass cell at room temperature (20 °C) without oxygen removal.

2.3. Preparation of the Glutathione Modified Screen-Printed Carbon Nanofiber Electrode (GSH-SPCNFE)

GSH-SPCNFEs were prepared based on a two-step procedure previously reported [18] and briefly described below. Factors concerning the immobilization of glutathione onto the functionalized SPE such as concentration of glutathione, and incubation time and temperature for the binding of the activated carboxyl groups and glutathione were considered for optimization.

2.3.1. Diazonium Salt Electrografting

The aryl diazonium salt was generated in-situ by adding 2 mmol·L^{-1} of sodium nitrite to a cooled solution of 73 mmol·L^{-1} of ABA in 1 mol·L^{-1} aqueous HCl. This solution was mixed in an ice bath for 30 min before the electrochemical grafting process [20] was conducted. For this purpose, the SPCNFE was immersed in the diazonium salt solution and 15 cyclic voltammetry (CV) cycles were applied from 0 V to −1 V at 0.2 V·s^{-1}. The functionalized electrodes were thoroughly rinsed with Mili-Q water and methanol in order to remove any physisorbed compounds.

2.3.2. Covalent Immobilization of Glutathione via Carbodiimide Coupling

The carboxylic groups were activated by dropping 10 µL of a 35 mmol·L^{-1} sulfo-NHS and 26 mmol·L^{-1} EDC solution in 100 mmol·L^{-1} MES buffer (pH 4.5) onto the electrode surface and leaving it for 1 h. Then the electrodes were rinsed with Mili-Q water. The activated carboxyl groups reacted 30 min, 2 h or 24 h at 4 °C or 25 °C with the amine terminal groups of glutathione by placing 10 µL of a glutathione solution of a concentration of 1.45, 2.90 or 5.80 mg/100 µL in 0.1 mol·L^{-1} MES buffer (pH 4.5).

The electrochemical characterisation of each GSH-SPCNFE was carried out using 2 mmol·L^{-1} ferrocyanide/ferricyanide as redox probe in 100 mmol·L^{-1} phosphate buffer (pH 7.4) at each functionalization step by CV leading voltammograms that confirm the modifications taking place on the electrode surface (figure not shown).

2.4. Voltammetric Measurements

The linear calibration plots for the simultaneous determination of Pb(II) and Cd(II) on GSH-SPCNFE were obtained from DPASV measurements, performed at a deposition potential (E_d) of −1.4 V during a deposition time (t_d) of 120 s with stirring and followed by a rest period (t_r) of 5 s, by increasing metal ion concentrations in 0.1 mol·L^{-1} acetate buffer (pH 4.5) solution. Determinations were done by scanning the potential from −1.4 to −0.3 V using pulse times of 50 ms, a step potential of 5 mV and pulse amplitudes of 50 mV.

3. Results and Discussion

The preparation of the GSH-SPCNFE by electrografting methodology is based on two main steps. The first one, the diazonium salt electrografting, is mainly dependent on both the substrate and the support of the working electrode. There is not a clear agreement about the number of CV cycles (ranging from 1 to 200) that should be performed during the electrografting process [18]. Thus, the number of CV cycles as well as their scan rate should be optimized according to the working electrode. In our case, for a SPCNFE this step was previously optimized to 15 cycles at 200 mV·s^{-1} [18]. The second step, the covalent immobilization of the ligand via carbodiimide coupling, is crucial in the modification of working electrodes with different ligands through the aryl diazonium salt electrografting. In the case of electrodes modified with glutathione, slightly different conditions have been reported in the literature for this step, with concentrations of glutathione ranging from 2.5 to 5 mg/100 µL MES buffer pH 4.5, either at 4 °C or without temperature control and

usually overnight [17,18,21–24]. The influence of these three parameters (glutathione concentration, incubation temperature and incubation time) in the performance of the resulting sensor was studied taking the conditions used in [18] (2.9 mg/100 μL MES, 4 °C and overnight) as starting point and using the determination of Cd(II) and Pb(II) as a model of application.

First of all, three different glutathione concentrations, 1.45, 2.90 and 5.80 mg/100 μL MES, were tested maintaining the incubation time and temperature at 24 h and 4 °C respectively. Figure 1 shows the obtained voltammetric responses with each resulting sensor for a solution containing 77 $\mu g \cdot L^{-1}$ of both Cd(II) and Pb(II). As it can be observed, well-shaped peaks were obtained using 1.45 and 2.90 mg GSH/100 μL MES whereas 5.80 mg GSH/100 μL MES resulted in less defined and smaller peaks. This fact could be due to an excess of glutathione blocking the active sites. This blocking also affects the interaction of Pb(II) and Cd(II) with the surface of the electrodes, resulting in a slight shift in the potential, which is also highlighted by the worse baseline. Also, the performance of the resulting sensors was evaluated in terms of sensitivity, limit of detection (LOD) and linearity range for both Cd(II) and Pb(II) (Table 1). Looking for a linear proportionality between metal concentration and analytical response, the use of peak intensity or peak area as analytical response was evaluated during the experimental research of this work. The second approach showed a better linearity, particularly for Pb(II) ions, than the peak intensity. Therefore the peak area approach was used as analytical response in this study. Sensitivities were calculated as the slope of the calibration curve and LODs were calculated as 3 times the standard deviation of the intercept over the slope of the calibration curve. In all cases, linear calibration curves were obtained up to 125.2 and 150.1 $\mu g \cdot L^{-1}$ for Cd(II) and Pb(II) respectively. As shown in Table 1, the highest sensitivity for Pb(II) and Cd(II) were obtained using 1.45 and 5.80 mg GSH/100 μL MES respectively whereas the lowest LODs were obtained using 2.90 and 5.80 mg GSH/100 μL MES respectively. Taking into account the better defined peaks achieved using either 1.45 or 2.90 mg GSH/100 μL MES compared to those obtained using 5.80 mg GSH/100 μL MES and the lower LODs provided by 2.90 in comparison to 1.45 mg GSH/100 μL MES, 2.90 mg GSH/100 μL MES was selected as the optimal glutathione concentration. It should be pointed out though, that if a more expensive peptide was to be used as a ligand, a concentration of 1.45 mg/100 μL MES would result in a less expensive sensor without highly affecting its analytical performance.

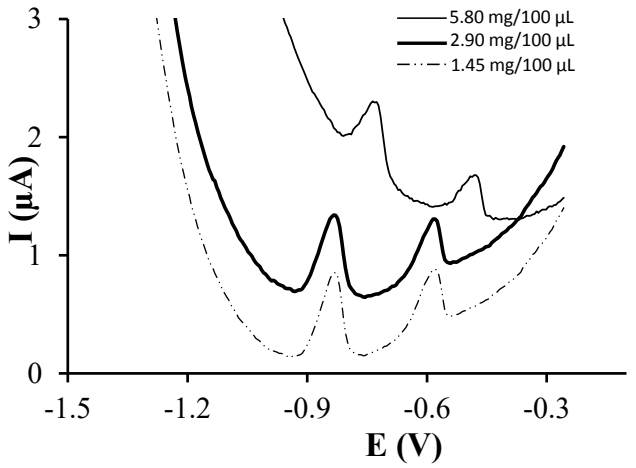

Figure 1. Differential pulse anodic stripping voltammetric (DPASV) measurements of 77 $\mu g \cdot L^{-1}$ Pb(II) and Cd(II) on GSH-SPCNFE applying a E_d of −1.4 V during 120 s at 0.1 $mol \cdot L^{-1}$ acetate buffer (pH 4.5). GSH-SPCNFE modified with a glutathione solution of a concentration 1.45, 2.90 or 5.80 mg/100 μL in 0.1 $mol \cdot L^{-1}$ MES buffer (pH 4.5) during 24 h at 4 °C.

Table 1. Calibration data for the simultaneous determination of Pb(II) and Cd(II) on GSH-SPCNFE at E_d of −1.4 V, t_d of 120 s and pH 4.5 at different GSH immobilization conditions.

			Pb(II)			Cd(II)		
GSH Concentration (mg/100 μL)	**Time (h)**	**T (°C)**	**Sensitivity (a.u. $\mu g^{-1} \cdot L$)**	**R^2**	**LOD ($\mu g \cdot L^{-1}$)**	**Sensitivity (a.u. $\mu g^{-1} \cdot L$)**	**R^2**	**LOD ($\mu g \cdot L^{-1}$)**
1.45	24	4	0.347 (0.004)	0.9993	2.74	0.670 (0.008)	0.9993	2.65
2.90	24	4	0.314 (0.003)	0.9996	2.49	0.702 (0.007)	0.9995	2.25
5.80	24	4	0.330 (0.004)	0.9994	3.11	0.718 (0.006)	0.9997	2.12
2.90	0.5	4	0.369 (0.003)	0.9996	2.18	0.659 (0.005)	0.9997	1.80
2.90	2	4	0.415 (0.003)	0.9997	2.24	0.687 (0.005)	0.9998	1.65
2.90	2	25	0.535 (0.004)	0.9997	2.07	1.014 (0.008)	0.9997	1.96

Once the glutathione concentration was selected, the effect of the incubation time was studied. Figure 2 shows the voltammograms obtained for a solution containing 77 $\mu g \cdot L^{-1}$ of both Cd(II) and Pb(II) using incubation times of 30 min, 2 h and 24 h. Well-defined peaks were obtained in all cases. Again, linear calibration curves were obtained from 1 and up to 125.2 and 150.1 $\mu g \cdot L^{-1}$ for Cd(II) and Pb(II) respectively. Sensitivities associated to Cd(II) increased using longer incubation times whereas Pb(II) sensitivity increased when the incubation time was varied from 30 min to 2 h but decreased when it was extended to 24 h. On the other hand, the lowest LODs were obtained using incubation times of 30 min and 2 h for Pb(II) and Cd(II) respectively. Therefore, these results suggest that 30 min is not enough time to reach the full analytical performance of the modified sensor whereas an incubation time of 24 h considerably increases the manufacturing process without providing a much better analytical performance. Thus, an incubation time of 2 h was selected.

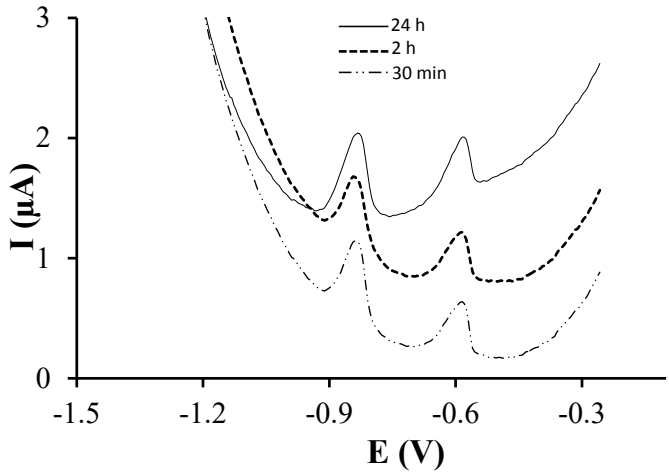

Figure 2. DPASV measurements of 77 $\mu g \cdot L^{-1}$ Pb(II) and Cd(II) on GSH-SPCNFE applying a E_d of −1.4 V during 120 s at 0.1 $mol \cdot L^{-1}$ acetate buffer (pH 4.5). GSH-SPCNFE modified with a glutathione solution of a concentration 2.90 mg/100 μL in 0.1 $mol \cdot L^{-1}$ MES buffer (pH 4.5) during 30 min, 2 h or 24 h at 4 °C.

Finally, the effect of the incubation temperature was also evaluated. Figure 3 shows the voltammograms obtained for a solution containing 77 $\mu g \cdot L^{-1}$ of both Cd(II) and Pb(II) using incubation temperatures of 4 °C and 25 °C. As it can be observed, an incubation temperature of 25 °C resulted in more intense peaks for both Cd(II) and Pb(II) ions. Also, as it can be observed in Table 1,

higher sensitivities were achieved for both Cd(II) and Pb(II) using an incubation temperature of 25 °C whereas lower LODs were obtained using 4 and 25 °C for Cd(II) and Pb(II) respectively. Therefore, 25 °C was selected as the optimal incubation temperature. It should be pointed out that, out of the three parameters studied, the incubation temperature is the one that mostly affects the target ions sensitivities. However, although increasing the temperature from 4 to 25 °C improves the sensitivity, it should be taken into account that higher temperatures could affect the integrity of glutathione.

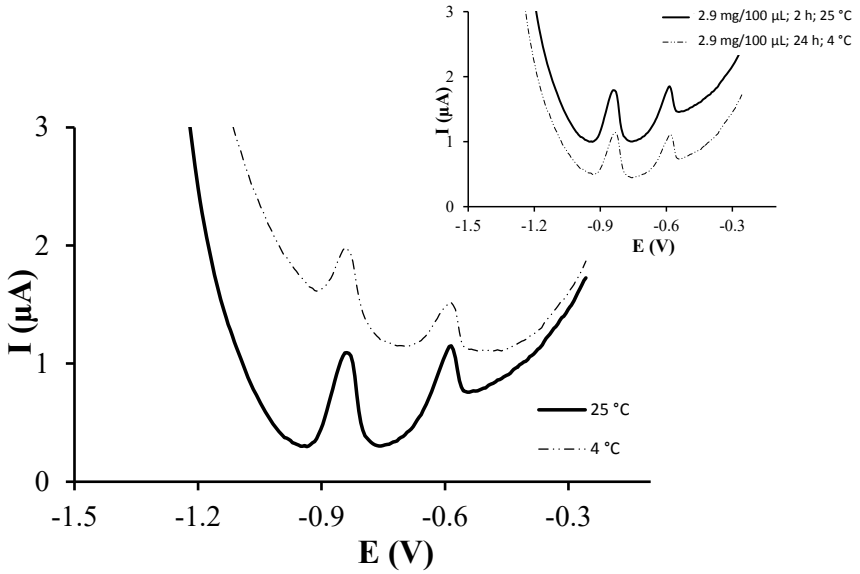

Figure 3. DPASV measurements of 77 µg·L^{-1} Pb(II) and Cd(II) on GSH-SPCNFE applying a E_d of −1.4 V during 120 s at 0.1 mol·L^{-1} acetate buffer (pH 4.5). GSH-SPCNFE modified with a glutathione solution of a concentration 2.90 mg/100 µL in 0.1 mol·L^{-1} MES buffer (pH 4.5) during 2 h at 4 or 25 °C. Inset: comparison between the response of the GSH-SPCNFE under ideal and base conditions.

Therefore, these reported results suggest that the better conditions for the covalent immobilization of glutathione during the preparation of GSH-SPCNFE are a concentration of 2.9 mg GSH/100 µL, an incubation time of 2 h and an incubation temperature of 25 °C. As it can be observed in Figure 4, these optimized conditions result in a sensor that provides well-defined peaks that increase linearly with concentration for both Cd(II) and Pb(II) ions. Also, the optimized sensor provides more intensive peaks compared to that modified using the starting conditions (inset in Figure 3) as well as higher sensitivities and lower LODs for both Cd(II) and Pb(II) ions (Table 1). It should be pointed out though, that the optimal incubation time and glutathione concentration could slightly vary depending on the type and the area of the carbon surface where the modification is performed.

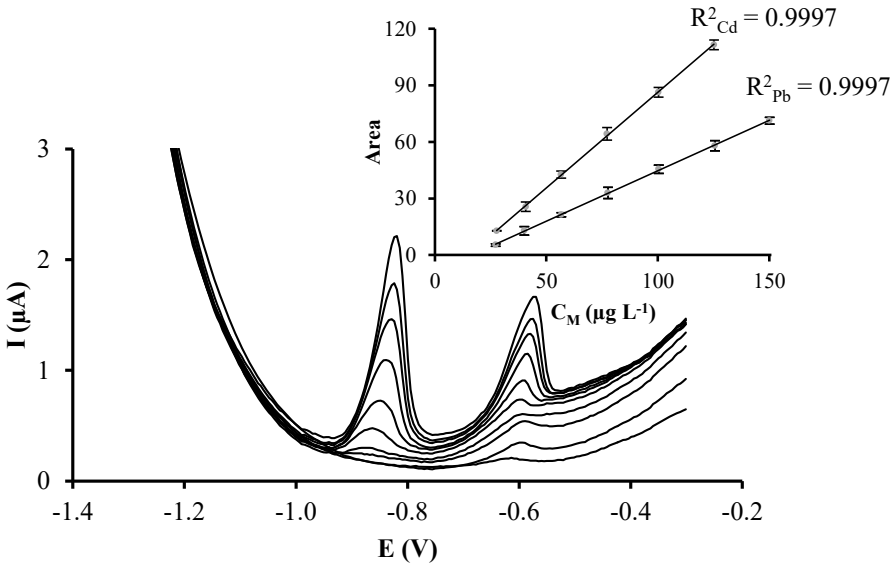

Figure 4. DPASV measurements of increasing concentrations of Pb(II) and Cd(II) simultaneously recorded on GSH-SPCNFE applying a E_d of −1.4 V during 120 s at 0.1 mol·L^{-1} acetate buffer (pH 4.5). GSH-SPCNFE modified with a glutathione solution of a concentration 2.90 mg/100 µL in 0.1 mol·L^{-1} MES buffer (pH 4.5) during 2 h at 25 °C. Inset: Pb(II) and Cd(II) calibration plots.

4. Conclusions

The results described so far suggest that, beyond the standard receipts for electrode modification by electrografting and taking into account that the first step should be optimized according to the working electrode, the systematic optimization of the experimental conditions concerning the covalent immobilization of a particular ligand via carbodiimide coupling step can substantially improve the performance of the sensor.

In the case of glutathione immobilization, the incubation temperature has evolved as a relevant parameter. A typical room temperature of 25 °C produces better results than the usual refrigerator temperature of 4 °C, possibly due to faster kinetics. As for the incubation time, it can be notoriously reduced from 24 to 2 h keeping an optimal sensing performance. Finally, the usual concentration of ligand (2.9 mg/100 µL) has shown to be very close to the optimum value. A decrease of such concentration produces a slight increase of detection and quantification limits. Anyway the relatively low impact of reducing the amount of ligand could justify this option in the case of rare or expensive substances. As for the increase of the ligand concentration until 5.8 mg/100 µL, it causes a dramatic enhancement of the baseline and its curvature, which deteriorates sensor performance. This suggests that the concentration of the ligand should be carefully optimized depending on the nature of both subtract and modifier. In this sense, mol·L^{-1} units would be more convenient than mg/100 µL for a better comparison among ligands with different molecular weight (e.g., glutathione and phytochelatins of different chain length).

Thus, in general, we can conclude that the use of tailored modification procedures which adapt experimental conditions such as the incubation temperature, the incubation time and the concentration of the ligand can considerably improve the performance of modified sensors based on the electrografting methodology, especially in studies where different members of a family of compounds are compared. This is a key point to take into account in further investigation on the

bioinspired application of glutathione and related molecules as ligands in the development of heavy metal sensors.

Acknowledgments: This work is supported by the University of Barcelona and by the Generalitat of Catalonia (Project 2014SGR269). Clara Pérez-Ràfols acknowledges the Spanish Ministry of Economy and Competitiveness for a Ph.D. grant.

Author Contributions: C. Pérez-Ràfols, N. Serrano and J.M. Díaz-Cruz conceived and designed the experiments and made a first draft of the paper, C. Pérez-Ràfols performed the experiments and the data treatment, C. Pérez-Ràfols, N. Serrano, J.M. Díaz-Cruz, C. Ariño and M. Esteban discussed the results and revised the writing of the paper from the first draft to the definitive version.

Conflicts of Interest: The authors declare no conflict of interest.

References

1. Lawrence, E.; Jackson, A.R.W.; Jackson, J.M. *Longman Dictionary of Environmental Science*; Addison Wesley Longman: Essex, UK, 1998.
2. Cobbett, C.S.; Goldsbrough, P. Phytochelatins and metallothioneins: Roles in heavy metal detoxification and homeostasis. *Annu. Rev. Plant Biol.* **2002**, *53*, 159–182. [CrossRef] [PubMed]
3. Grill, E.; Loffler, S.; Winnacker, E.L.; Zenk, M.H. Phytochelatins, the heavy-metal binding peptides of plants, are synthesized from glutathione by a specific γ-glutamylcysteine dipeptidyl transpeptidase (phytochelatin synthase). *Proc. Natl. Acad. Sci. USA* **1989**, *86*, 6838–6842. [CrossRef] [PubMed]
4. Serrano, N.; Díaz-Cruz, J.M.; Ariño, C.; Esteban, M. Recent contributions to the study of phytochelatins with an analytical approach. *Trends Anal. Chem.* **2015**, *73*, 129–145. [CrossRef]
5. Soodan, R.K.; Pakade, Y.B.; Nagpal, A.; Katnoria, J.K. Analytical techniques for estimation of heavy metals in soil ecosystem: A tabulated review. *Talanta* **2014**, *125*, 405–410. [CrossRef] [PubMed]
6. Bings, N.H.; Bogaerts, A.; Broekaert, J.A.C. Atomic Spectroscopy. *Anal. Chem.* **2013**, *85*, 670–704. [CrossRef] [PubMed]
7. Wang, J. *Stripping Analysis: Principles, Instrumentation and Applications*; VCH: New York, NY, USA, 1985.
8. Barek, J.; Fogg, A.G.; Muck, A.; Zima, J. Polarography and voltammetry at mercury electrodes. *Crit. Rev. Anal. Chem.* **2001**, *31*, 291–309. [CrossRef]
9. Serrano, N.; Alberich, A.; Díaz-Cruz, J.M.; Ariño, C.; Esteban, M. Coating methods, modifiers and applications of bismuth screen-printed electrodes. *Trends Anal. Chem.* **2013**, *46*, 15–29. [CrossRef]
10. Serrano, N.; Díaz-Cruz, J.M.; Ariño, C.; Esteban, M. Antimony-based electrodes for analytical determinations. *Trends Anal. Chem.* **2016**, *77*, 203–213. [CrossRef]
11. March, G.; Nguyen, T.D.; Piro, B. Modified electrodes used for electrochemical detection of metal ions in environmental analysis. *Biosensors* **2015**, *5*, 241–275. [CrossRef] [PubMed]
12. Barton, J.; González-García, M.B.; Hernández-Santos, D.; Fanjul-Bolado, P.; Ribotti, A.; McCaul, M.; Diamond, D.; Magni, P. Screen-printed electrodes for environmental monitoring of heavy metal ions: A review. *Microchim. Acta* **2016**, *183*, 503–517. [CrossRef]
13. Wawrzyniak, U.E.; Ciosek, P.; Zaborowski, M.; Liu, G.; Gooding, J.J. Gly-Gly-His Immobilized on Monolayer Modified Back-Side Contact Miniaturized Sensors for Complexation of Copper Ions. *Electroanalysis* **2013**, *25*, 1461–1471. [CrossRef]
14. Gooding, J.J. Advances in interfacial design for electrochemical biosensors and sensors: Aryl diazonium salts for modifying carbon and metal electrodes. *Electroanalysis* **2008**, *20*, 573–582. [CrossRef]
15. Delamar, M.; Hitmi, R.; Pinson, J.; Savbnt, J.M. Covalent modification of carbon surfaces by grafting of functionalized aryl radicals produced from electrochemical reduction of diazonium salts. *J. Am. Chem. Soc.* **1992**, *114*, 5883–5884. [CrossRef]
16. Baranton, S.; Bélanger, D. Electrochemical derivatization of carbon surface by reduction of in situ generated diazonium cations. *J. Phys. Chem. B* **2005**, *109*, 24401–24410. [CrossRef] [PubMed]
17. Serrano, N.; Prieto-Simón, B.; Cetó, X.; del Valle, M. Array of peptide-modified electrodes for the simultaneous determination of Pb(II), Cd(II) and Zn(II). *Talanta* **2014**, *125*, 159–166. [CrossRef] [PubMed]
18. Pérez-Ràfols, C.; Serrano, N.; Díaz-Cruz, J.M.; Ariño, C.; Esteban, M. Glutathione modified screen-printed carbon nanofiber electrode for the voltammetric determination of metal ions in natural samples. *Talanta* **2016**, *155*, 8–13. [CrossRef] [PubMed]

19. Vogel, A.I. *Textbook of Quantitative Chemical Analysis*, 5th ed.; Pearson Education Limited: Harlow, UK, 1989.
20. Bélanger, D.; Pinson, J. Electrografting: A powerful method for surface modification. *Chem. Soc. Rev.* **2011**, *40*, 3995–4048. [CrossRef] [PubMed]
21. Liu, G.; Böcking, T.; Gooding, J.J. Diazonium salts: Stable monolayers on gold electrodes for sensing applications. *J. Electroanal. Chem.* **2007**, *600*, 335–344. [CrossRef]
22. Chow, E.; Ebrahimi, D.; Gooding, J.J.; Hibbert, D.B. Application of N-PLS calibration to the simultaneous determination of Cu^{2+}, Cd^{2+} and Pb^{2+} using peptide modified electrochemical sensors. *Analyst* **2006**, *131*, 1051–1057. [CrossRef] [PubMed]
23. Ebrahimi, D.; Chow, E.; Gooding, J.J.; Hibbert, D.B. Multi-analyte sensing: A chemometrics approach to understanding the merits of electrode arrays versus single electrodes. *Analyst* **2008**, *133*, 1090–1096. [CrossRef] [PubMed]
24. Chow, E.; Hibbert, D.B.; Gooding, J.J. Voltammetric detection of cadmium ions at glutathione-modified gold electrodes. *Analyst* **2005**, *130*, 831–837. [CrossRef] [PubMed]

Selenocystine modified screen-printed electrode as an alternative sensor for the voltammetric determination of metal ions.

J. Puy-Llovera, C. Pérez-Ràfols, N. Serrano, J. M. Díaz-Cruz, C. Ariño, M. Esteban

Talanta 175 (2017) 501-506

https://doi.org/10.1016/j.talanta.2017.07.089

Talanta 175 (2017) 501–506

Contents lists available at ScienceDirect

Talanta

journal homepage: www.elsevier.com/locate/talanta

Selenocystine modified screen-printed electrode as an alternative sensor for the voltammetric determination of metal ions

Jaume Puy-Llovera, Clara Pérez-Ràfols, Núria Serrano*, José Manuel Díaz-Cruz, Cristina Ariño, Miquel Esteban

Departament d'Enginyeria Química i Química Analítica, Facultat de Química, Universitat de Barcelona, Martí i Franquès 1-11, E–08028 Barcelona, Spain

ARTICLE INFO

Keywords:
Chemically modified electrode
Electrochemical grafting
Metal determination
Stripping voltammetry
Selenocystine
L-Cystine

ABSTRACT

A novel selenium based screen-printed electrode was developed based on the immobilization of selenocystine on aryl diazonium salt monolayers anchored to a carbon-nanofiber screen-printed electrode support (SeCyst-SPCNFE). SeCyst-SPCNFE was analytically compared to a screen-printed carbon nanofiber electrode modified with L-Cystine (Cyst-SPCNFE) for the determination of Pb(II) and Cd(II) by stripping voltammetric techniques. Their analytical performance suggests that SeCyst-SPCNFE could be a much better alternative for metal ion determination at trace levels than Cyst-SPCNFE. The proposed electrode was successfully applied for the simultaneous voltammetric determination of trace Pb(II) and Cd(II) in a wastewater reference material with a very high reproducibility (3.2%) and good trueness (2.6%).

1. Introduction

In recent years, there has been an increasing ecological and global public health attention associated with environmental contamination by metal ions. Thus, the determination of trace heavy metals with adverse health effects in human metabolism presents obvious concerns due to their persistence in the environment and documented potential for serious health consequences. Therefore, their non-biodegradability and accumulation in organism demand suitable methods for heavy metal monitoring [1,2]. Stripping voltammetric methods are the most efficient electrochemical techniques for trace and species analysis due to their high sensitivity, selectivity and reproducibility, being also suitable for multimetal ion determination in environmental samples with a relatively low cost [3]. The performance of voltammetry is strongly influenced by the working electrode material. For many years, stripping techniques and, in particular anodic stripping voltammetry (ASV), applied to the determination of trace metal ions were associated with the use of working mercury electrodes due to the extensive cathodic potential range [4]. However, the disposal of the mercury containing device and the incorrect handling can lead to the formation of mercury vapours that as solution of soluble mercury salts are toxic and represent a significant health and environmental hazard. This fact, together with the poor versatility of mercury drops as sensing devices, has led to the search for alternative working electrodes that exhibit an analogous electrochemical behaviour but lower toxicity. Indeed, the development of electrochemical sensors for the detection and quantification of metal ions in natural samples has paid increasing attention to chemically modified electrodes (CME) based on environmentally friendly supports and modifiers.

The immobilization procedure is a crucial point in the design of CMEs [5]. In this sense, the immobilization based on aryl diazonium salt electrografting has proven its benefits in the development of sensors for metal ion determination [6–8]. This immobilization procedure is based on two main steps: i) the diazonium salt electrografting which is mainly dependent on both the support and the substrate of the working electrode; and ii) the covalent immobilization of the ligand via carbodiimide coupling which is affected by the selected ligand.

Nowadays, the screen-printing technology is a recognized method for the fabrication of sensors and biosensors for metal ion determination. Its accessible and low-cost character permits the production of numerous highly-reproducible single-use screen-printed electrodes (SPEs). SPEs usually include a working electrode (whose surface can be modified), a counter electrode and a reference electrode printed on the same strip [9–13]. The commercial availability of screen-printed electrodes (SPE) made of different inks, including also nanomaterial, has largely expanded the field of application of modified electrodes as substitutes for mercury.

It is well-known the affinity of peptides to different metal ions due to the great number of potential donor atoms contained in both the

* Corresponding author.
E-mail address: nuria.serrano@ub.edu (N. Serrano).

http://dx.doi.org/10.1016/j.talanta.2017.07.089
Received 12 June 2017; Received in revised form 25 July 2017; Accepted 28 July 2017
Available online 29 July 2017

backbone of the peptide and the amino acid side chains [6,14]. Particularly, in the case of thiol rich peptides, the thiol groups as well as the carboxylate groups and the amino groups play a key role in this respect [15]. Likewise, electrochemical studies of selenium-containing compounds revealed that selenium groups are also involved in the chelation of metal ions [5,14,16,17]. Thus, taking into account the effectiveness of peptides to interact with a great variety of metal ions, the development and use of peptide modified electrodes for the determination of metal ions in natural media constitute an issue of major concern [6,14].

In this paper, we present for the first time the development of a selenocystine modified sensor via electrografting on a screen-printed carbon-nanofiber substrate (SeCyst-SPCNFE). This sensor will be applied to the voltammetric determination of Cd(II) and Pb(II) as a model metal ion system and compared to a sensor modified with L-Cystine (Cyst-SPCNFE) providing a better analytical performance. Finally, the applicability of SeCyst-SPCNFE will be tested in a certified wastewater sample.

2. Experimental

2.1. Chemicals

4-aminobenzoic acid (ABA), N-hydroxysulfosuccinimide (sulfo-NHS), selenocystine, certified reference material: wastewater ERM®-CA713, sodium hydroxide and sodium nitrite were provided by Sigma-Aldrich (St. Louis, MO, USA). L-cystine was acquired from Fluka, 2-(N-morpholino)-ethanesulfonic (MES), potassium ferrocyanide $K_4[Fe(CN)_6]\cdot 3H_2O$, dimethylformamide (DMF), hydrochloric acid, acetic acid and sodium acetate were purchased from Merck (Darmstadt, Germany). Potassium ferricyanide $K_3[Fe(CN)_6]$ and ethanol were supplied by Panreac (Barcelona, Spain). N-(3-dimethyllaminopropyl)-N′-ethylcarbodiimide hydrochloride (EDC) was obtained from AppliChem (Darmstadt, Germany). All reagents were of analytical grade. 10^{-2} mol L^{-1} stock solutions of Pb(II) and Cd(II) were prepared from $Pb(NO_3)_2\cdot 4H_2O$ and $Cd(NO_3)_2\cdot 4H_2O$ respectively and standardized complexometrically [18]. Ultrapure water (Milli-Q plus 185 system, Millipore) was used in all experiments.

2.2. Apparatus

An Autolab System PGSTAT12 (EcoChemie, The Netherlands) attached to a Metrohm 663 VA Stand (Metrohm, Switzerland) and a personal computer with GPES version 4.9 data acquisition software (EcoChemie) was used for stripping measurements.

Ag/AgCl/KCl (3 mol L^{-1}) and Pt wire (Metrohm, Switzerland) were used as reference and auxiliary electrodes respectively. The working electrodes used were a modified L-Cystine (Cyst-SPCNFE) and selenocystine (SeCyst-SPCNFE) electrodes, which were prepared from carbon nanofibers modified screen-printed electrodes with 4 mm diameter provided by Dropsens (Oviedo, Spain) (ref. 110CNF, DS SPCE).

Screen-printed electrodes were connected to the Autolab System by means of a flexible cable (ref. CAC, DropSens).

A Crison micro pH 2000 pH-meter was used for pH measurements.

All measurements were carried out in a glass cell without oxygen removal.

2.3. Procedures

2.3.1. Preparation of modified SPEs

The preparation of peptide modified SPEs was based on a two-step procedure previously described [19] with slight modifications (Fig. 1). A carbon nanofiber modified screen-printed electrode (SPCNFE) was considered as a platform for electrode modification, since it has been reported that its much larger effective surface area provides sensors with a better analytical performance [19–21].

2.3.1.1. Diazonium salt electrografting. Aryl diazonium salt was generated in situ by adding 0.2 mmol L^{-1} of sodium nitrite to a cooled ABA 73 mmol L^{-1} solution in 1 mol L^{-1} aqueous HCl. The resulting solution was stirred in an ice bath for about 5 min before the electrochemical grafting process was carried out. For this purpose, 10 μL of the solution were dropped onto the surface of the SPCNFE and 10 cyclic voltammetric (CV) cycles from 0 V to −1 V at 0.2 V s^{-1} were applied. In order to remove any physisorbed compounds, the functionalized electrodes were thoroughly rinsed with Mili-Q water.

2.3.1.2. Covalent immobilization of peptides via carbodiimide coupling. 10 μL of a 26 mmol L^{-1} EDC and 35 mmol L^{-1} sulfo-NHS solution in 100 mmol L^{-1} MES buffer (pH 4.5) were dropped onto the functionalized SPE and left to incubate for 1 h to activate the carboxyl groups of the electrografted diazonium salt. The activated carboxyl groups reacted overnight at 4 °C with the amine terminal groups of peptides by adding 10 μL of a 94 mmol L^{-1} of peptide solution in either ethanol absolute, NaOH 1 mol L^{-1}, HCl 1 mol L^{-1} or DMF 99.8%.

2.3.2. Voltammetric measurements

In DPASV measurements using Cyst-SPCNFE and SeCyst-SPCNFE, Cd(II) and Pb(II) were deposited onto the peptide modified SPEs by applying a deposition potential (E_d) of −1.4 V with stirring of the measuring solution during a deposition time (t_d) of 120 s, and followed by a rest period (t_r) of 5 s. Determinations were performed by scanning the potential from −1.4 to −0.3 V using pulse times of 50 ms, step potentials of 5 mV and pulse amplitudes of 100 mV.

Linear calibration plots were obtained by increasing metal ion concentrations in 0.1 mol L^{-1} acetate buffer solution (pH 4.5).

In the analysis of the certified wastewater sample, a volume of the sample was added to a 0.1 mol L^{-1} acetate buffer (pH 4.5). The resulting solution was placed in the cell and the scan was recorded. Calibration was performed by the standard addition method. Four aliquots of metal standard solution were added and the respective curves were recorded.

In the analysis of both calibration and certified wastewater samples, a cleaning step was performed before each set of measurements by applying a conditional potential (E_{cond}) of −0.3 V for 15 s in 0.1 mol L^{-1} $HClO_4$.

3. Results and discussion

3.1. Covalent immobilization of cystine and selenocystine

The modification of carbon electrodes with Cyst and SeCyst was based on the aryl diazonium salt electrografting. This modification strategy has been previously reported for the immobilization of several thiols on carbon substrates [5,7,19,22,23] and it usually includes a final step where the thiol is dissolved in MES buffer so it can react with the carboxylic groups previously generated on the electrode surface. However, the poor solubility of Cyst and SeCyst in MES buffer does not allow this last reaction to take place. For this reason, several alternative solvents such as ethanol, hydrochloric acid, sodium hydroxide and dimethylformamide were tested and the performance of the resulting sensors was evaluated for the simultaneous determination of Cd(II) and Pb(II).

Several electrochemical parameters, such as E_d, t_d and pH, were firstly optimized to ensure the detection of both Cd(II) and Pb(II) ions in the selected concentration range. DPASV measurements of a solution containing 50 μg L^{-1} of Pb(II) and Cd(II) were carried out at different E_d and t_d values ranging from −1.2 V to −1.5 V and from 30 s to 300 s respectively, looking for a compromise between peak height and analysis time. In all cases, the compromise conditions

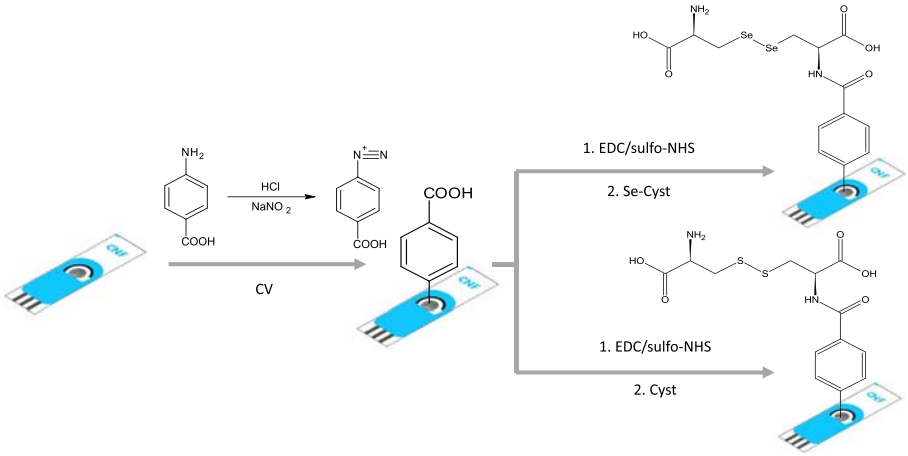

Fig. 1. Scheme of the preparation of SeCyst-SPCNFE and Cyst-SPCNFE by electrochemical grafting.

were an E_d of −1.4 V applied with stirring for 120 s at pH 4.5 (acetate buffer).

Fig. 2 shows the voltammograms obtained for a solution containing 100 μg L^{-1} Pb(II) and Cd(II) using the resulting SeCyst-SPCNFEs. As it can be observed similar responses, with small and poorly defined peaks, were obtained when SeCyst was dissolved in HCl or NaOH. This poor response could be attributed to the fact that in these media, although highly soluble, SeCyst is not in its zwitterionic form, which difficults its binding with the carboxylic groups attached to the electrode surface. Much better defined peaks were obtained when DMF or ethanol were used and a considerable increase in intensity could be observed for ethanol, in which SeCyst presented a higher solubility. A similar trend can be observed when Cyst-SPCNFE is considered. In this case, however, no peaks were observed for either metal ion using HCl as solvent and the peaks obtained when ethanol was used were not as intense as the ones obtained with SeCyst-SPCNFE (inset in Fig. 2)

Calibration data for the simultaneous determination of Cd(II) and Pb(II) ions using SeCyst-SPCNFE and Cyst-SPCNFE modified using the four considered solvents are reported in Table 1. Linear calibration curves were carried out at the optimized conditions by measuring increasing concentrations of Cd(II) and Pb(II) ranging from 1 to 150 μg L^{-1} (Fig. 3). Sensitivities were calculated as the slope of the calibration curve and limits of detection (LOD) and quantification (LOQ) as 3 and 10 times, respectively, the standard deviation of the intercept over the slope of the calibration curve. The LOQ was considered as the lowest value of the linear concentration range. Again, an improvement of the sensors performance, inferred by the higher sensitivity and the lower LODs, can be observed when the peptides are dissolved in ethanol. This improvement is particularly high in the case of SeCyst-SPCNFE. Therefore, ethanol was selected as the optimal solvent for the covalent immobilization of both Cyst and SeCyst to the carbon electrode surface.

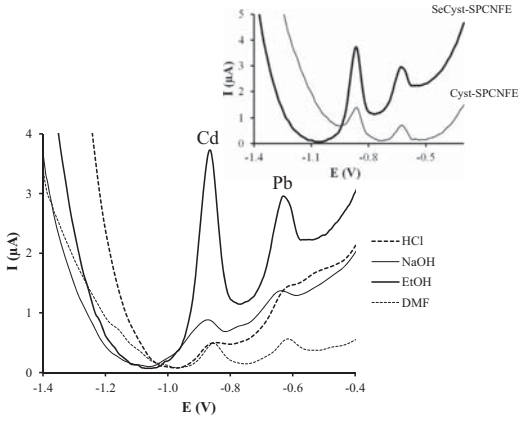

Fig. 2. DPASV measurements of 100 μg L^{-1} Pb(II) and Cd(II) at pH 4.5 and applying an E_d of −1.4 V and t_d of 120 s on SeCyst-SPCNFE modified using NaOH, HCl, ethanol and DMF. Inset: comparison of the performance of SeCyst-SPCNFE and Cyst-SPCNFE modified with ethanol.

Table 1
Calibration data for the simultaneous determination of Pb(II) and Cd(II) on Cyst-SPCNFEs and SeCyst-SPCNFEs modified using different solvents. DPASV were carried out at E_d of −1.4 V, t_d 120 s and pH 4.5.

	Cyst-SPCNFE		SeCyst-SPCNFE	
	Cd(II)	**Pb(II)**	**Cd(II)**	**Pb(II)**
EtOH absolute				
Sensitivity (nA μg^{-1} L)	14.2 (0.3)	7.6 (0.1)	32.4 (0.4)	14.3 (0.2)
R^2	0.997	0.999	0.999	0.999
Linear range (μg L^{-1})	19.1–150.0	15.1–150.0	10.7–150.0	10.8–150.0
LOD (μg L^{-1})	5.7	4.5	3.2	3.2
HCl 1 mol L^{-1}				
Sensitivity (nA μg^{-1} L)	–	–	4.8 (0.2)	2.8 (0.1)
R^2	–	–	0.995	0.996
Linear range (μg L^{-1})	–	–	46.7–150.0	37.9–150.0
LOD (μg L^{-1})	–	–	14.0	11.4
DMF 99.8%				
Sensitivity (nA μg^{-1} L)	10.2 (0.5)	7.0 (0.3)	6.1 (0.2)	3.05 (0.09)
R^2	0.994	0.992	0.997	0.996
Linear range (μg L^{-1})	49.2–150.0	45.3–150.0	29.9–150.0	31.2–150.0
LOD (μg L^{-1})	14.7	13.6	9.0	9.4
NaOH 1 mol L^{-1}				
Sensitivity (nA μg^{-1} L)	8.3 (0.4)	3.6 (0.2)	4.8 (0.1)	3.84 (0.09)
R^2	0.993	0.993	0.996	0.998
Linear range (μg L^{-1})	51.8–150.0	43.4–150.0	30.8–150.0	25.1–150.0
LOD (μg L^{-1})	15.5	13.0	9.2	7.5

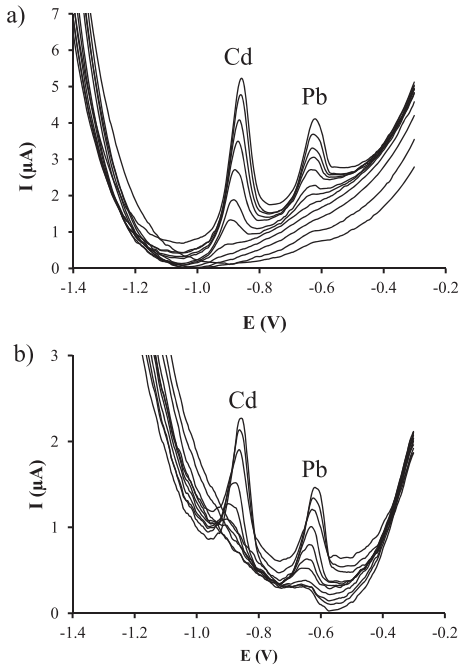

Fig. 3. Stripping voltammetric measurements of increasing concentrations of Pb(II) and Cd(II) ranging from 1 to 150 µg L^{-1} on SeCyst-SPCNFE (a) and Cyst-SPCNFE (b) at pH 4.5 applying an E_d of −1.4 V and t_d of 120 s.

3.2. Influence of the chosen ligand

Once the solvent for the covalent immobilization of Cyst and SeCyst was optimized, the analytical performance of SeCyst-SPCNFE and Cyst-SPCNFE for the simultaneous determination of Pb(II) and Cd(II) as model metal ions was compared in terms of repeatability, reproducibility, sensitivity, linear range and LODs.

In order to study the repeatability and reproducibility of SeCyst-SPCNFE and Cyst-SPCNFE, DPASV measurements of a solution containing 65 µg L^{-1} of Cd(II) and Pb(II) in acetate buffer at pH 4.5 were carried out. Repeatability, estimated from 15 repetitive measurements with the same SeCyst-SPCNFE modified electrode, yielded a RSD% of 6.5% and 9.4% for Cd(II) and Pb(II) respectively whereas Cyst-SPCNFE yielded a RSD% of 27.4% and 34.9% for Cd(II) and Pb(II) respectively. Reproducibility was calculated within a series of 10 repetitive measurements from two modified electrodes and yielded a RSD% of 11.1% for Cd(II) and 9.1% for Pb(II) and 28.5% for Cd(II) and 34.1% for Pb(II) for SeCyst-SPCNFE and Cyst-SPCNFE respectively. Although both repeatability and reproducibility are rather poor in the case of Cyst-SPCNFE, SeCyst-SPCNFE presents good values that are similar to repeatability and reproducibility values previously reported for electrodes modified with thiols [7,19,22] or crown ethers [8,24] following a similar strategy. On the other hand, the durability of the SeCyst immobilization on every screen–printed platform for a large set of measurements (more than 20) without loss of sensitivity enables the voltammetric determination of metal ions with the same SeCyst-SPCNFE unit.

The evolution of Cd(II) and Pb(II) ions signals with simultaneously increasing concentrations using SeCyst-SPCNFE and Cyst-SPCNFE can be observed in Fig. 3a and b respectively. In all cases, well-defined peaks without splitting were obtained. Sensitivities, linear ranges and LODs for both SeCyst-SPCNFE and Cyst-SPCNFE are reported in Table 1. As it can be observed, good linear responses were obtained up to 150 µg L^{-1} in all cases. On the other hand, both electrodes are more sensitive to Cd(II) than Pb(II) and SeCyst-SPCNFE provides higher sensitivities than Cyst-SPCNFE for both metal ions. A possible explanation of these facts could be found in the Hard Soft Acid Base (HSAB) theory of Pearson [25]. In this sense, both selenides and sulfides are considered soft bases, with selenides being softer, whereas Cd(II) is a soft acid and Pb(II) is borderline. According to this theory, in which soft bases have more affinity with soft acids, Cd(II) would react better than Pb(II) and selenides would be more reactive than sulfides.

Good LODs, which allow the detection of both Pb(II) and Cd(II) below the legal limits of drinking water (10 and 5 µg L^{-1} respectively) [26], were achieved using SeCyst-SPCNFE. In the case of Cyst-SPCNFE however, slightly higher LODs were obtained and the LOD for Cd(II) does not allow its detection below the legal limits. The LODs achieved with SeCyst-SPCNFE are also similar to those reported for Cd(II) and Pb(II) with carbon electrodes modified following a similar strategy with thiols [7,19,22,23] or crown ethers [8] (between 1.5 and 3.3 µg L^{-1} for Pb(II) and 1.96 and 4.7 µg L^{-1} for Cd(II)), with antimony [27], bismuth [28] or mercury [9] films deposited on carbon screen printed electrodes (between 0.03 and 10 µg L^{-1} for Pb(II) and 0.2 and 8 µg L^{-1} for Cd(II)), with carbon nanomaterial based electrodes [29] (between 1 and 20.7 µg L^{-1} for Pb(II) and 0.001 and 2.8 µg L^{-1} for Cd(II)) or with metal nanoparticles based electrodes [29] (between 0.2 and 4.9 µg L^{-1} for Pb(II) and 0.9 and 4.9 µg L^{-1} for Cd(II)).

Therefore, the better analytical performance, especially in terms of sensitivity, repeatability and reproducibility, achieved by SeCyst-SPCNFE, suggest that the immobilization of selenium based ligands onto carbon electrodes could be much better alternative for the determination of trace heavy metals ions.

Furthermore, the different analytical response achieved with SeCyst-SPCNFE in comparison to the one obtained with Cyst-SPCNFE hints that carbon electrodes modified with selenium based ligands could also be combined with other types of sensors (metal film electrodes, nanomaterial based- electrodes, thiol or crown-ethers modified electrodes...) for the development of new voltammetric electronic tongues applied to the resolution of complex metal mixtures.

3.3. Application to the analysis of a residual water reference material

At the view of the above results, given the better repeatability and reproducibility, the higher sensitivity and the lower LODs provided by

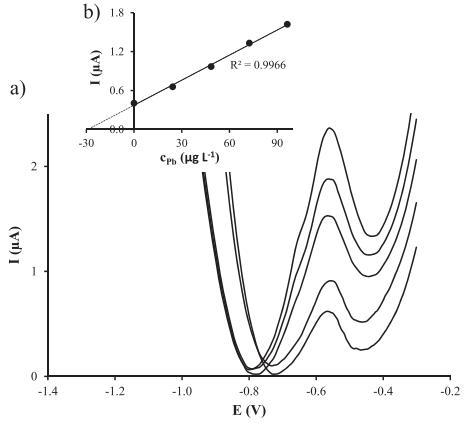

Fig. 4. a) Stripping voltammetric measurements in a wastewater sample by using a SeCyst-SPCNFE at pH 4.5 with E_d of −1.4 V during a t_d of 120 s; and, b) Pb(II) standard addition plot.

Table 2
Total concentrations of Pb(II) and Cd(II) determined in certified wastewater (ERM® – CA713) by stripping voltammetry on SeCyst-SPCNFE by standard addition calibration method applying an E_d of −1.4 V and t_d of 120 s at pH 4.5.

	Lead(II)			Cadmium(II)	
	c (μg L^{-1})	RSD (%)	Relative error (%)	c (μg L^{-1})	RSD (%)
SeCyst-SPCNFE	51.0	3.2	2.6	n.q.	—
Certified metal value	49.7	3.4	—	5.09	3.9

n = 3 for RSD (%); n.q. not quantified.

SeCyst-SPCNFE, this electrode was selected as a better option to study its applicability for the simultaneous determination of trace Pb(II) and Cd(II) in a wastewater reference material (ERM® – CA713) by means of the standard addition method. It should be pointed out though, that since Cd(II) concentration in this available reference material was below the LOQ, only Pb(II) could be determined. Thus, DPASV measurements using the above optimized conditions were carried out including four additions of Pb(II). Representative voltammograms obtained in the analysis of the wastewater samples using SeCyst-SPCNFE are shown in Fig. 4a. As it can be observed, Pb(II) behaves in a similar way to that observed in the calibration samples. Also, as it can be observed in Fig. 4b, a good correlation of the representative stripping measurements was observed for Pb(II). It should be mentioned that the presence of other metal ions in the reference material such as As, Cr, Cu, Fe, Hg, Mn, Ni or Se does not seem to interfere in the Pb(II) determination.

The obtained metal concentration data from three replicates of the certified wastewater material using SeCyst-SPCNFE are reported in Table 2. As it can be observed, a good concordance between the Pb(II) concentrations from the three replicates, as well as with the certified metal value, was obtained. These good results confirm the applicability of SeCyst-SPCNFE for the determination of Pb(II) in the presence of Cd(II) in natural samples. Therefore, the use of selenium based sensors for the determination of trace metal ions can be a valuable alternative to other ligands like thiols or crown ethers, since they provide a distinctive response that could be really useful in the development of new voltammetric electronic tongues.

4. Conclusions

In this work, the possibility of using selenium based sensors for the determination of trace metal ions was studied through the development of a selenocystine modified screen-printed carbon nanofiber electrode (SeCyst-SPCNFE) and its application to the simultaneous voltammetric determination of Pb(II) and Cd(II) as a model system. Furthermore, the performance of the resulting sensor was compared to that of an electrode modified with cystine (Cyst-SPCNFE).

First of all, the solvent used for the covalent immobilization of both ligands was optimized and, out of all the solvent tested, the best results were achieved using ethanol. In comparison with Cyst-SPCNFE, SeCyst-SPCNFE provided better repeatability and reproducibility as well as higher sensitivities and lower LODs. These good results demonstrate that selenium based sensors can be successfully used for metal ion determination as an alternative to more conventional thiol rich peptide modified electrodes. Moreover, the distinctive response provided by SeCyst-SPCNFE compared to Cyst-SPCNFE makes selenium based sensors good candidates to be included in voltammetric electronic tongues applied to the resolution of complex metal mixtures.

Finally, the applicability of SeCyst-SPCNFE for the analysis of real samples was successfully proven by the determination of Pb(II) in a certified wastewater reference materials, in which good reproducibility and high trueness inferred by the low relative standard deviation (3.2%) and relative error (2.6%) were achieved.

Acknowledgments

This work is supported by the Generalitat of Catalonia (Project 2014SGR269). Clara Pérez-Ràfols acknowledges the Spanish Ministry of Economy and Competitiveness for a Ph.D grant (reference FPU15/02140).

References

[1] E. Lawrence, A.R.W. Jackson, J.M. Jackson, Longman Dictionary of Environmental Science, Addison Wesley Longman, Harlow, UK, 1998.
[2] I.D.L. Foster, S.M. Charlesworth, Heavy metals in the hydrological cycle: trends and explanation, Hydrol. Process. 10 (1996) 227–261.
[3] J. Wang, Stripping Analysis: Principles, Instrumentation and Applications, VCH, Deerfield Beach, FL, 1985.
[4] J. Barek, A.G. Fogg, A. Muck, J. Zima, Polarography and voltammetry at mercury electrodes, Crit. Rev. Anal. Chem. 31 (2001) 291–309. http://dx.doi.org/10.1080/20014091076776.
[5] U.E. Wawrzyniak, P. Ciosek, M. Zaborowski, G. Liu, J.J. Gooding, Gly-Gly-His immobilized on monolayer modified back-side contact miniaturized sensors for complexation of copper ions, Electroanalysis 25 (2013) 1461–1471. http://dx.doi.org/10.1002/elan.201200667.
[6] J.J. Gooding, D.B. Hibbert, W. Yang, Electrochemical metal ion sensors. Exploiting amino acids and peptides as recognition elements, Sensors 1 (2001) 75–90. http://dx.doi.org/10.3390/s10300075.
[7] N. Serrano, B. Prieto-Simón, X. Cetó, M. del Valle, Array of peptide-modified electrodes for the simultaneous determination of Pb(II), Cd(II) and Zn(II), Talanta 125 (2014) 159–166. http://dx.doi.org/10.1016/j.talanta.2014.02.052.
[8] N. Serrano, A. González-Calabuig, M. del Valle, Crown ether-modified electrodes for the simultaneous stripping voltammetric determination of Cd(II), Pb(II) and Cu(II), Talanta 138 (2015) 130–137. http://dx.doi.org/10.1016/j.talanta.2015.01.044.
[9] J. Barton, M.B.G. García, D.H. Santos, P. Fanjul-Bolado, A. Ribotti, M. McCaul, et al., Screen-printed electrodes for environmental monitoring of heavy metal ions: a review, Microchim. Acta 183 (2016) 503–517. http://dx.doi.org/10.1007/s00604-015-1651-0.
[10] M. Li, Y.T. Li, D.W. Li, Y.T. Long, Recent developments and applications of screen-printed electrodes in environmental assays-a review, Anal. Chim. Acta. 734 (2012) 31–44. http://dx.doi.org/10.1016/j.aca.2012.05.018.
[11] J.P. Metters, R.O. Kadara, C.E. Banks, New directions in screen printed electroanalytical sensors: an overview of recent developments, Analyst 136 (2011) 1067–1076. http://dx.doi.org/10.1039/c0an00894j.
[12] O.D. Renedo, M.A. Alonso-Lomillo, M.J.A. Martínez, Recent developments in the field of screen-printed electrodes and their related applications, Talanta 73 (2007) 202–219. http://dx.doi.org/10.1016/j.talanta.2007.03.050.
[13] K. Duarte, C.I.L. Justino, A.C. Freitas, A.M.P. Gomes, A.C. Duarte, T.A.P. Rocha-Santos, Disposable sensors for environmental monitoring of lead, cadmium and mercury, TrAC Trends Anal. Chem. 64 (2015) 183–190. http://dx.doi.org/10.1016/j.trac.2014.07.006.
[14] J.J. Gooding, Peptide-modified electrodes for detecting metal ions, in: S. Alegret, A. Merkoçi (Eds.), Electrochemical Sensor Analysis, Elsevier, Amsterdam, 2007, pp. 189–210. http://dx.doi.org/10.1016/S0166-526X(06)49010-3.
[15] N. Serrano, J.M. Díaz-Cruz, C. Ariño, M. Esteban, Recent contributions to the study of phytochelatins with an analytical approach, TrAC Trends Anal. Chem. 73 (2015) 129–145. http://dx.doi.org/10.1016/j.trac.2015.04.031.
[16] R. Gusmão, J.M. Díaz-Cruz, C. Ariño, M. Esteban, Chemometric analysis of voltammetric data on metal ion binding by selenocystine, J. Phys. Chem. A 116 (2012) 6526–6531. http://dx.doi.org/10.1021/jp2123696.
[17] R. Gusmão, R. Prohens, J.M. Díaz-Cruz, C. Ariño, M. Esteban, Combination of chemometrically assisted voltammetry, calorimetry, and circular dichroism as a new method for the study of bioinorganic substances: application to selenocystine metal complexes, J. Biol. Inorg. Chem. 17 (2012) 321–329. http://dx.doi.org/10.1007/s00775-011-0853-0.
[18] A.I. Vogel, Textbook of Quantitative Chemical Analysis, 5th ed., Pearson Education Limited, Harlow, GB, 1989.
[19] C. Pérez-Ràfols, N. Serrano, J.M. Díaz-Cruz, C. Ariño, M. Esteban, Glutathione modified screen-printed carbon nanofiber electrode for the voltammetric determination of metal ions in natural samples, Talanta 155 (2016) 8–13. http://dx.doi.org/10.1016/j.talanta.2016.04.011.
[20] C. Pérez-Ràfols, N. Serrano, J.M. Díaz-cruz, C. Ariño, M. Esteban, New approaches to antimony film screen-printed electrodes using carbon-based nanomaterials substrates, Anal. Chim. Acta. 916 (2016) 17–23. http://dx.doi.org/10.1016/j.aca.2016.03.003.
[21] C. Pérez-Ràfols, N. Serrano, J.M. Díaz-Cruz, C. Ariño, M. Esteban, A screen-printed voltammetric electronic tongue for the analysis of complex mixtures of metal ions, Sens. Actuators B Chem. 250 (2017) 393–401. http://dx.doi.org/10.1016/j.snb.2017.04.165.
[22] C. Pérez-Ràfols, N. Serrano, J. Manuel Díaz-Cruz, C. Ariño, M. Esteban, Penicillamine-modified sensor for the voltammetric determination of Cd(II) and

Pb(II) ions in natural samples, Talanta 144 (2015) 569–573. http://dx.doi.org/10.1016/j.talanta.2015.06.083.
[23] C. Pérez-Ràfols, N. Serrano, J.M. Díaz-Cruz, C. Ariño, M. Esteban, A chemically bound glutathione sensor bioinspired by the defense of organisms against heavy metal contamination: optimization of the immobilization conditions, Chemosensors 5 (2017) 12–19.
[24] A. González-Calabuig, D. Guerrero, N. Serrano, M. del Valle, Simultaneous voltammetric determination of heavy metals by use of crown ether-modified electrodes and chemometrics, Electroanalysis 28 (2016) 663–670. http://dx.doi.org/10.1002/elan.201500512.
[25] R.G. Pearson, Hard and soft acids and bases, HSAB, Part I, J. Chem. Educ. 45 (1968) 581–587. http://dx.doi.org/10.1021/ed045p581.
[26] H.G. Gorchev, G. Ozolins, Guidelines for Drinking-Water Quality, 2011, ⟨https://dx.doi.org/10.1016/S1462-0758(00)00006-6⟩.
[27] N. Serrano, J.M. Díaz-Cruz, C. Ariño, M. Esteban, Antimony- based electrodes for analytical determinations, TrAC Trends Anal. Chem. 77 (2016) 203–213. http://dx.doi.org/10.1016/j.trac.2016.01.011.
[28] N. Serrano, A. Alberich, J.M. Díaz-Cruz, C. Ariño, M. Esteban, Coating methods, modifiers and applications of bismuth screen-printed electrodes, TrAC – Trends Anal. Chem. 46 (2013) 15–29. http://dx.doi.org/10.1016/j.trac.2013.01.012.
[29] G. Aragay, A. Merkoçi, Nanomaterials application in electrochemical detection of heavy metals, Electrochim. Acta. 84 (2012) 49–61. http://dx.doi.org/10.1016/j.electacta.2012.04.044.

Expanding the possibilities of electrografting modification of voltammetric sensors through two complementary strategies.

C. Pérez-Ràfols, M. Rosal, N. Serrano, C. Ariño, M. Esteban, J. M. Díaz-Cruz

Electrochimica Acta 319 (2019) 878-884

https://doi.org/10.1016/j.electacta.2019.07.034

Electrochimica Acta 319 (2019) 878–884

Contents lists available at ScienceDirect

Electrochimica Acta

journal homepage: www.elsevier.com/locate/electacta

Expanding the possibilities of electrografting modification of voltammetric sensors through two complementary strategies

Clara Pérez-Ràfols, Miguel Rosal, Núria Serrano*, Cristina Ariño, Miquel Esteban, José Manuel Díaz-Cruz

Departament d'Enginyeria Química i Química Analítica, Facultat de Química, Universitat de Barcelona, Martí i Franquès 1-11, E–08028 Barcelona, Spain

ARTICLE INFO

Article history:
Received 19 June 2019
Received in revised form
4 July 2019
Accepted 9 July 2019
Available online 11 July 2019

Keywords:
Electrochemical grafting
Peptide-modified sensors
Screen-printed electrodes
Stripping voltammetry
Metal determination

ABSTRACT

Two different modification strategies by means of aryl diazonium salt electrografting were compared for the development of voltammetric sensors. In this sense, L-cysteine was immobilized onto a screen-printed carbon-based electrode surface through either its $-NH_2$ or its $-COOH$ group and the performance of the resulting modified sensors was tested for the simultaneous determination of Pb(II) and Cd(II) by anodic stripping voltammetry. The results obtained indicate that attachment through the $-COOH$ group of cysteine, despite being a much less frequent electrografting strategy, improves the analytical performance of the resulting sensor achieving lower LODs, at low $\mu g\ L^{-1}$ levels, for Cd(II) and Pb(II). Furthermore, this strategy allows the quantification of both metal ions below the legal limits established by the European Water Framework Directive, which represents a great improvement with respect to similar sensors reported in the literature.

1. Introduction

The problems associated with metal ions contamination have been known for years. During the last decades, metal emissions have significantly decreased, mainly due to their banning in some specific products (e.g. lead in gasoline or mercury regulations) or the decrease of their use and/or smelting [1,2]. However, the amount of metals emitted to the environment is still preoccupying and this, coupled to their non-biodegradable character, makes it still important to develop new analytical methods for the determinations of *on-site* trace metal ions.

Among all the available analytical techniques for metal ions determination, electrochemical techniques and, more specifically anodic stripping voltammetry (ASV), are particularly suitable. ASV measurements fulfil all the analytical requirements (high reproducibility and repeatability, low detection limits, high sensitivity, multielement determination…) and at the same time provide fast measurements with relatively low cost and portable equipment [3]. These last features are further enhanced by the coupling of ASV measurements with screen-printed electrodes (SPE), which are miniaturized, versatile, disposable and economical devices that can be mass-produced in a reproducible manner [4,5].

ASV measurements are strongly influenced by the chosen working electrode. Several types of working electrodes have been successfully reported for metal ion determination including metal films, sputtered electrodes, chemically modified electrodes, biosensors and metal nanoparticles or carbon nanostructured electrodes [6–12].

Among all of these, chemically modified electrodes present the advantage that sensitivity and selectivity can be regulated by the incorporation of a convenient functional group onto the electrode surface. In this sense, several types of complexing agents such as EDTA [13–15], dimethylglyoxime [16], crown ethers [17,18] or thiolic compounds [19–22] have been used as electrode modifiers for metal ion determination. In particular, peptides are effective ligands for a great variety of metal ions because they contain a large number of potentially donor atoms. In any peptide, a metal ion can interact through the amino groups, the amide nitrogen and/or the carboxylic group present on its backbone and, additionally, this peptide-metal interaction can be further enhanced by other donor groups present in the side chains. This would be the case, for example, of thiol-rich peptides [23,24].

A good strategy reported in the literature for the immobilization of peptides and ligands in general onto carbon surfaces is based on the aryl diazonium salt electrografting [25]. This strategy allows the covalent linking of the modifier to the surface providing structural

* Corresponding author.
E-mail address: nuria.serrano@ub.edu (N. Serrano).

https://doi.org/10.1016/j.electacta.2019.07.034
0013-4686/

flexibility, chemical stability and control on the immobilization orientation resulting in sensors with great reproducibility and durability [26]. Although carbon surfaces can be functionalized with different aryl diazonium salts, the most usual electrografting approach found in the literature is based on the *in-situ* generation of 4-carboxybenzenediazonium, which results on the functionalization of the electrode surface with carboxylic groups that allows the immobilization of modifiers containing an amino group through a peptide bond facilitated by cross-linking agents. A less common electrografting approach is based on the *in-situ* generation of 4-nitrobenzenediazonium. In this case, the electrode surface is functionalized with amino groups allowing the immobilization of modifiers through different functional groups such as carboxylic acids.

In order to compare these two electrografting based-strategies for sensor modification, in this work L-cysteine (L-Cys) was immobilized onto a screen-printed carbon-based electrode surface through either the generation of 4-carboxybenzenediazonium or 4-nitrobenzenediazonium and the performance of the resulting electrodes was studied for the simultaneous determination of Cd(II) and Pb(II).

2. Experimental

2.1. Chemicals

Hydrochloric acid, acetic acid, sodium acetate, 2-(N-morpholino)-ethanesulfonic acid (MES) and potassium ferrocyanide were supplied by Merck (Darmstadt, Germany). N-(3-dimethylaminopropyl)-N′-ethylcarbodiimide hydrochloride (EDC), N-hydroxysulfosuccinimide (sulfo-NHS), 4-nitroaniline (PNA), 4-aminobenzoic acid (ABA), sodium nitrite, potassium dihydrogen phosphate, sodium monophosphate and L-cysteine (L-Cys) with a purity greater than 99% were obtained from Sigma-Aldrich (St. Louis, MO, USA). Potassium ferricyanide was purchased from Panreac (Barcelona, Spain). Cd(II) and Pb(II) stock solutions 10^{-2} mol L^{-1} were prepared from $Cd(NO_3)_2 \cdot 4H_2O$ and $Pb(NO_3)_2 \cdot 4H_2O$ respectively and standardized complexometrically [27]. In all cases analytical grade reagents were used and solutions were prepared with ultrapure water (Milli-Q plus 185 system, Millipore).

2.2. Apparatus

Stripping voltammetric measurements were carried out on an Autolab System PGSTAT12 (EcoChemie, The Netherlands) attached to a Metrohm 663 VA Stand (Metrohm, Switzerland). GPES software version 4.9 (EcoChemie) was used for data acquisition.

Ag|AgCl|KCl (3 mol L^{-1}) reference electrode and Pt wire counter electrode were acquired from Metrohm (Switzerland). A carbon nanofiber screen-printed electrode (SPCNFE, 4 mm diameter), supplied by Dropsens (Spain), was modified with Cys and used as working electrode. A flexible cable (ref. CAC, DropSens) was employed for the connection of screen-printed electrodes.

pH measurements were carried out on a Crison micro pH 2000 pH-meter and all measurements were performed in a glass cell at room temperature (20 °C) without oxygen removal.

2.3. Preparation of modified SPEs

Cys modified SPEs were prepared by two different methods according to the schemes shown in Fig. 1. Both methods are based on the electrografting of an aryl diazonium salt followed by the covalent immobilization of Cys.

2.3.1. Preparation of (ABA)Cys-SPCNFE

The preparation of (ABA)Cys-SPCNFE is described elsewhere [28]. Briefly, 2 mmol L^{-1} $NaNO_2$ was added drop by drop to a cooled solution of 73 mmol L^{-1} of ABA in 1 mol L^{-1} aqueous HCl and left to stir in an ice bath for 30 min to generate the aryl diazonium salt. Then, the electrografting process was conducted in this solution by CV; applying 15 cycles from 0 to −1 V at 200 mV s^{-1}.

After rinsing the electrodes with Mili-Q water and ethanol, the carboxyl groups generated on the electrode surface were activated by dropping 10 μL of a 5 mg mL^{-1} EDC and 7.5 mg mL^{-1} sulfo-NHS solution in 0.1 mol L^{-1} MES buffer (pH 4.5) onto the functionalized electrodes and leaving it to incubate for 1 h. Finally, 10 μL of a 2.9 mg/100 μL Cys solution in 0.1 mol L^{-1} MES buffer (pH 4.5) were dropped onto the electrode and left to react overnight at 4 °C.

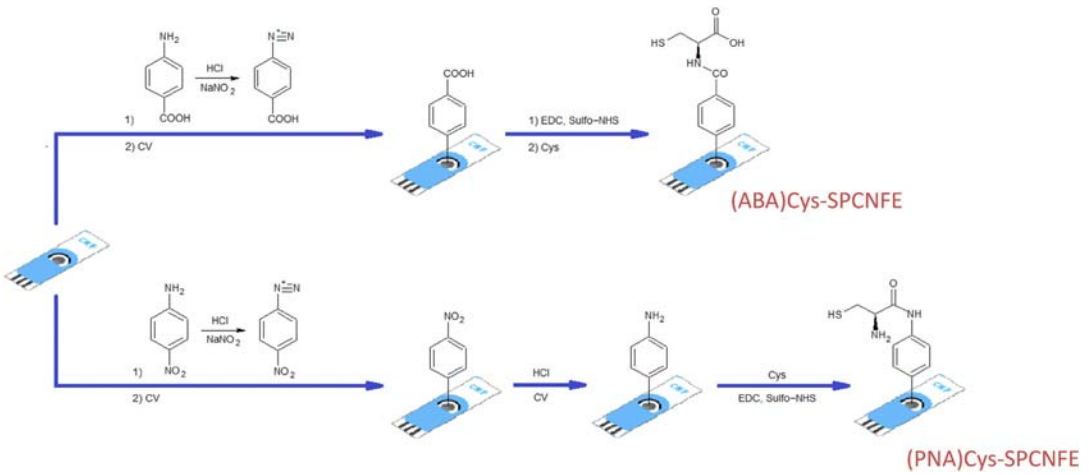

Fig. 1. Schematic representation of the two methods used for the modification of SPCNFE with l-cysteine.

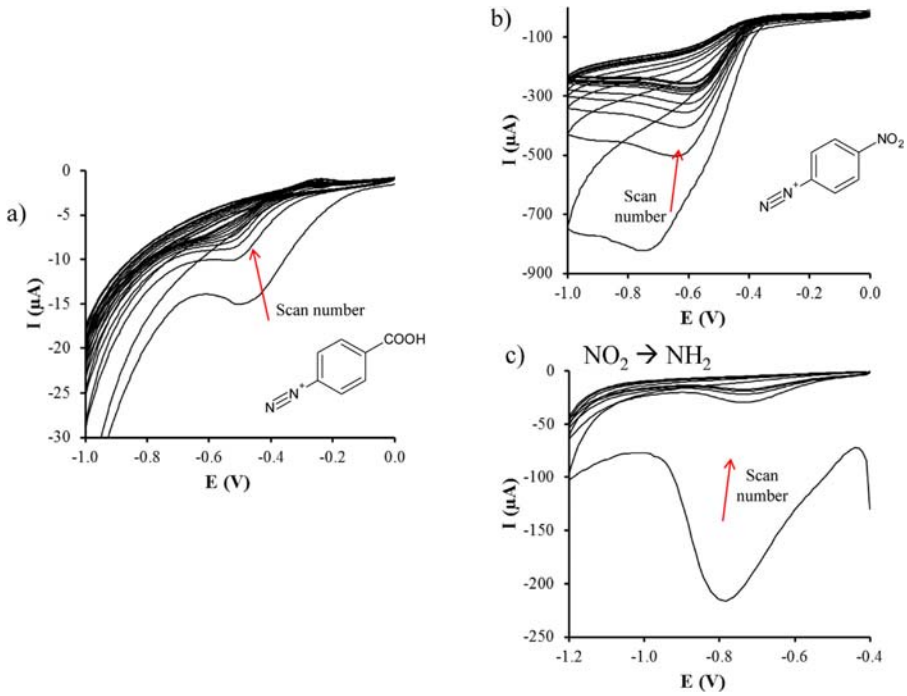

Fig. 2. CV at a SPCNFE during the electrografting of the diazonium salt synthetized from (a) ABA and (b) PNA. (c) CV corresponding to the reduction of the NO_2 group. A scan rate of 200 mV s^{-1} was used in all cases.

2.3.2. Preparation of (PNA)Cys-SPCNFE

10 mmol L^{-1} $NaNO_2$ was added drop by drop to a cooled solution of 12 mmol L^{-1} of PNA in 1 mol L^{-1} aqueous HCl and left to stir in an ice bath for 30 min to generate the aryl diazonium salt. Then, the electrografting process was conducted in this solution by CV; applying 15 cycles from 0 to −1 V at 200 mV s^{-1}.

After rinsing the electrodes with Mili-Q water and ethanol, the nitro groups were reduced with 5 cycles of CV from −0.4 to −1.2 V at 200 mV s^{-1} in 10 mmol L^{-1} HCl. After CV, the electrodes were rinsed again with Mili-Q water and ethanol.

Finally, the amino groups reacted overnight at 4 °C with 10 μL of a 2.9 mg/100 μL Cys solution in 0.1 mol L^{-1} MES buffer (pH 4.5) previously activated with 8.25 mg/100 μL EDC and 5.25 mg/100 μL sulfo-NHS for 1 h.

2.4. Voltammetric measurements

Differential pulse anodic stripping voltammetric (DPASV) measurements of Cd(II) and Pb(II) using (ABA)Cys-SPCNFE and (PNA) Cys-SPCNFE were performed in acetate buffer 0.1 mol L^{-1} pH 4.5 or 5, depending on the considered sensor, applying a deposition potential (E_d) of −1.0 V for a deposition time of 120 s with stirring. Deposition was followed by a rest period (t_r) of 5 s and a scan from −1.0 to −0.3 V with pulse times of 50 ms, pulse amplitudes of 100 mV and step potentials of 5 mV was recorded. In order to remove any remaining bound metals, an electrochemical cleaning stage consisting on the application of a conditioning potential (E_{cond}) of 0 V for 60 s was introduced between measurements.

Electrode characterizations at different modification steps and pHs was performed by CV using 2 mmol L^{-1} ferrocyanide/ferricyanide in 100 mmol L^{-1} phosphate buffer as a redox probe. The potential was scanned from −0.5 to 0.7 V at 100 mV s^{-1}.

3. Results and discussion

3.1. Electrodes modification

As a first step, aryl diazonium salts were generated *in situ* from ABA and PNA in 1 mol L^{-1} HCl and grafted onto the SPCNFE surface. CV measurements observed during the reduction of the diazonium salts are presented in Fig. 2a and b for 4-carboxybenzenediazonium and 4-nitrobenzenediazonium respectively. In both cases, a broad irreversible peak that decreases with every scan can be observed. This decrease in the peak intensity is due to the formation of an organic layer on the surface of the electrode, which prevents the access of the diazonium cations [25].

Additionally, for the preparation of (PNA)Cys-SPCNFE, the electrografting process was followed by the reduction of the nitro groups generated onto the electrode surface. This reduction was performed by CV in 0.01 mol L^{-1} HCl and, as it is shown in Fig. 2c, a broad irreversible cathodic peak can be observed at −0.775 V, which is characteristic of the six electron reduction reaction of the nitro groups to the amino groups [29]. The disappearance of this peak in the following cycles shows that the reduction of the nitro groups was completed.

These steps allowed the generation of either carboxylic or amino groups onto the electrode surface, which were later used to immobilize Cys through the formation of a peptide bond assisted by

EDC/sulfo-NHS crosslinking agents. This way, (ABA)Cys-SPCNFE has a free thiol and a free carboxylic group whereas in (PNA)Cys-SPCNFE the thiol and amino groups are available, which will be protonated or deprotonated depending on the working pH value (Fig. 1).

3.2. Effect of pH on the electrode surface

The immobilization of Cys through the amino group in (ABA)Cys-SPCNFE and through the carboxylic group in (PNA)Cys-SPCNFE, both assisted by EDC/sulfo-NHS crosslinking agents, leads to the availability of different pH-dependent groups for each electrode. Thus, the electrode response was studied at different pHs.

For this purpose, CV measurements were carried out in a 2 mmol L^{-1} ferrocyanide/ferricyanide at several pHs. Since ferrocyanide/ferricyanide is a non-pH dependent redox probe, the difference in the peak intensities can be explained by the electrostatic interactions of the electrode surface and the redox probe. Fig. 3 shows the evolution of anodic current peaks *vs.* pH for (ABA)Cys-SPCNFE, (PNA)Cys-SPCNFE and bare SPCNFE. As it can be seen, at pH 3 the highest response corresponds to (PNA)Cys-SPCNFE, which could be associated to the positive charge of the amino group in **D** that creates a favourable electrostatic interaction with $[Fe(CN)_6]^{3-/4-}$. In both (ABA)Cys-SPCNFE and bare SPCNFE the surface charge should be neutral and the lower response for (ABA)Cys-SPCNFE could be attributed to the presence of the cysteine-based layer that hinders the access of $[Fe(CN)_6]^{3-/4-}$. As the pH increases from 3 to 6, a current decrease is observed for both (ABA)Cys-SPCNFE and (PNA)Cys-SPCNFE. Although this behaviour cannot be associated to the theoretical acid-base equilibriums, a possible explanation could be related to the first steps of the modification procedure. As it can be seen in Fig. 1, in the case of (ABA)Cys-SPCNFE and (PNA)Cys-SPCNFE, the electrode surface is functionalized with benzoic acid and aniline units, respectively, prior to cysteine attachment. Although most of these units are later linked to cysteine through the EDC/sulfo-NHS crosslinking agents, it is possible that some of them remain unmodified. These unmodified units would have theoretical pK_a values of 4.2 (benzoic acid) and 4.9 (aniline), which would explain the above-mentioned current decrease. In the case of bare SPCNFE, no surface functionalization was performed and, therefore, this current decrease is not observed.

In the pH region from 6 to 11 the slight current decrease observed can be explained by the acid-base equilibriums of cysteine forms. Particularly, in the case of (ABA)Cys-SPCNFE, this decrease can be associated to the deprotonation of the thiol group (**B** − **C**), with an experimental pK_a value, calculated from the dI/dpH *vs.* pH, close to 9. On the other hand, for (PNA)Cys-SPCNFE only one experimental pK_a value close to 8 was observed, which could be attributed to the loss of both amino (**D** − **E**) and thiol (**E** − **F**) protons.

3.3. Application to the determination of metal ions

Both (ABA)Cys-SPCNFE and (PNA)Cys-SPCNFE were tested for the determination of Pb(II) and Cd(II) as a model metal ion system by DPASV. First of all, some experimental parameters including pH, E_d and t_d were optimized. Fig. 4 shows the response evolution *vs* pH of both considered sensors for a solution containing 50 μg L^{-1} of Pb(II) and Cd(II). pH is a critical parameter in this type of determination since it affects most of the processes involved such as protonation/deprotonation of functional groups with affinity for metal ions (-SH, $-NH_2$, $-COOH$), electrostatic interactions between the metal ion and the electrode surface and metal hydrolysis. For (ABA)Cys-SPCNFE the optimal pH was established at 5, which can be justified by presence of COO^- groups on the electrode surface that allow a favourable electrostatic interaction with the metal ions. At lower pHs this COO^- groups are protonated and this electrostatic interaction is not present whereas at higher pHs metal ion hydrolysis can be observed. A similar behaviour is shown by (PNA)Cys-SPCNFE, although in this case the lower response at pHs lower than 4 could be explained by the non-favourable electrostatic interaction with metal ions caused by the positively charged protonated aniline units present on the surface.

Regarding E_d, different voltammetric measurements were carried out from −1.4 V to −1.0 V in a solution containing 50 μg L^{-1} of Pb(II) and Cd(II) using both (ABA)Cys-SPCNFE and (PNA)Cys-

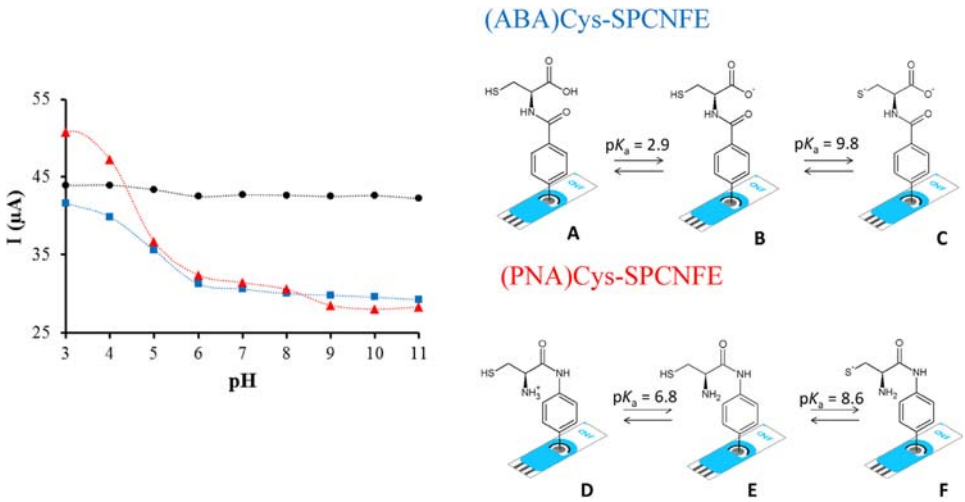

Fig. 3. Effect of pH on the peak current of CV measurements recorded in a 2 mM ferrocyanide/ferricyanide solution at 100 mv s^{-1} at a SPCNFE (black circles), (ABA)Cys-SPCNFE (blue squares) and (PNA)Cys-SPCNFE (red triangles).

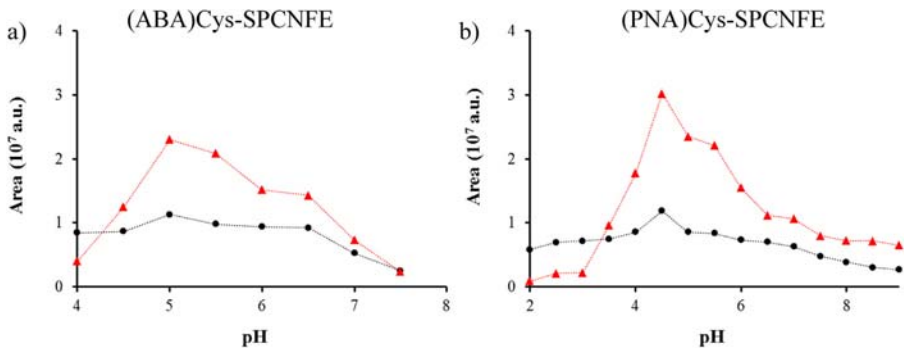

Fig. 4. Effect of pH on the peak area of DPASV measurements recorded in a 50 μg L^{-1} Cd^{2+} (red triangles) and Pb^{2+} (black circles) solution at a (a) (ABA)Cys-SPCNFE and (b) (PNA)Cys-SPCNFE. In all cases an E_d of -1.0 V and a t_d of 120 s were used.

SPCNFE. In both cases, the highest current response for both Cd(II) and Pb(II) was found at an E_d of −1.0 V and, therefore, this value was selected for further experiments. Finally, t_d was also studied from 30 to 300 s and a t_d of 120 s was selected as a compromise between peak area and analysis time.

Once the experimental conditions were optimized the analytical performance of both sensors was studied considering repeatability, reproducibility, sensitivity, linear range and limits of detection (LOD) and quantification (LOQ). All these values are summarized in Table 1.

Repeatability was computed from 5 repetitive measurements carried out with the same sensor on a solution containing 50 μg L^{-1} of Pb(II) and Cd(II) in acetate buffer achieving similar RSD(%) values for both metal ions and both sensors, lower than 1.6% in all cases. Reproducibility was estimated from the slope of three independent calibration curves carried out from 1 to 150 μg L^{-1} of Pb(II) and Cd(II) using three different sensors. The obtained values were lower than 1.3% in all cases, which proves that both modification strategies produce very reproducible sensors, being slightly better in the case of (PNA)Cys-SPCNFE.

Simultaneous Pb(II) and Cd(II) calibration curves were performed at the optimal experimental conditions from 1 to 150 μg L^{-1} using both (ABA)Cys-SPCNFE and (PNA)Cys-SPCNFE. As it can be seen in Fig. 5 two separate and well-defined peaks were obtained for both considered metal ions. Similar shapes and intensities were obtained for Cd(II) using both sensors whereas in the case of Pb(II) a more gaussian-shaped peak with higher intensities was observed using (PNA)Cys-SPCNFE.

Table 1
Calibration data for the simultaneous determination of Pb(II) and Cd(II) on (ABA)Cys-SPCNFE and (PNA)Cys-SPCNFE at acetate buffer pH 5 and 4.5 respectively applying an E_d of −1.0 V and a t_d of 120 s. Standard deviations are denoted by parenthesis.

	(ABA)Cys-SPCNFE		(PNA)Cys-SPCNFE	
	Cd(II)	**Pb(II)**	**Cd(II)**	**Pb(II)**
Sensitivity (a.u. μg^{-1} L)	5.39 (0.05)	2.75 (0.01)	4.63 (0.03)	3.44 (0.01)
R^2	0.998	0.999	0.999	1.000
Linear range (μg L^{-1})[a]	7.3–153.9	3.7–153.9	4.6–153.9	3.4–153.9
LOD (μg L^{-1})	2.2	1.1	1.4	1.0
Repeatability (%)	1.52	1.58	1.39	1.33
Reproducibility (%)	1.29	1.15	0.82	0.92

[a] LOQ was considered as the lowest value of the linear range.

Regarding sensitivity, computed as the slope of the calibration curve, both sensors present a higher sensitivity for Cd(II) than for Pb(II) which is in agreement with the hard-soft classification scheme, where softer ligands such as thiols present more affinity to softer metals like Cd(II) [23]. This higher preference for Cd(II) is accentuated in the case of (ABA)Cys-SPCNFE. On the other hand, LODs and LOQs, calculated as three and ten times the standard deviation of the intercept over the slope of the calibration curve respectively, were in all cases at μg L^{-1} levels. It should be pointed out that both sensors are able to quantify Pb(II) at lower concentrations than the established legal limit (10 μg L^{-1} according to the European Water Framework Directive 2000/60/EC) whereas only (PNA)Cys-SPCNFE can quantify Cd(II) at the more demanding limit established by the same directive for this metal (5 μg L^{-1}). This fact could be justified by the presence of amino groups in (PNA)Cys-SPCNFE that also have a strong binding preference for soft metals like Cd(II) [23].

Therefore, considering both peak shapes and analytical performance, we can conclude that attaching cysteine through its carboxylic group, i.e. (PNA)Cys-SPCNFE, is a better option than attaching it through the amino group since it provides a better sensor for the determination of metal ions at trace concentration levels, being able to simultaneously quantify both Cd(II) and Pb(II) at the legal limits established by the European Water Framework Directive. Moreover, it should be highlighted that the developed (PNA)Cys-SPCNFE sensor clearly improves the results previously reported for peptide-modified sensors [19–21,30], none of which provides a LOQ below the legal limit, without increasing the analysis time (t_d is the same or even lower than that used in the cited works).

In general terms, after studying the behaviour of both electrografting approaches, it can be said that the approach based on 4-nitrobenzenediazonium, although being less common, is not only an alternative strategy to the most usual electrografting procedure based on 4-carboxybenzenediazonium but can also give rise to improved sensors in some cases. It should also be pointed out that, although requiring an additional modification step to reduce the nitro groups to amino groups (Fig. 1), the total sensor development time is similar or even slightly shorter than the procedure based on 4-carboxybenzenediazonium, with the additional advantage of allowing the attachment of modifiers with carboxylic groups that otherwise would require the use of a lysine spacer to assist their immobilization with the more usual electrografting based on 4-carboxybenzenediazonium.

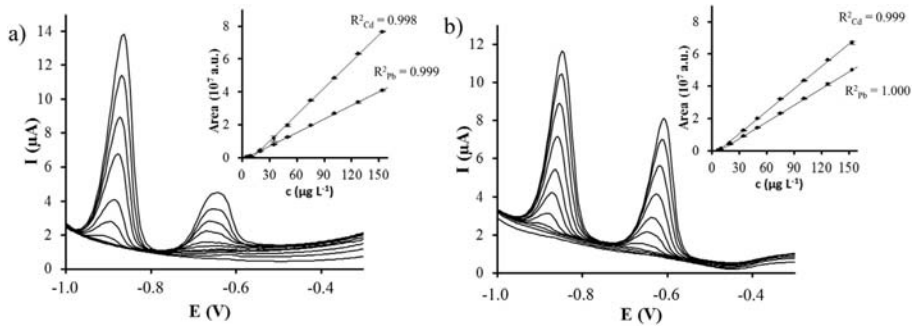

Fig. 5.

4. Conclusions

At the view of the obtained results we can conclude that Cys was successfully linked to the SPCNFE surface through both its $-NH_2$ and −COOH groups using aryl diazonium electrografting based strategies giving rise to two different sensors. The sensor performance was studied as a function of pH showing slightly different behaviour according to the free functional groups available in each case. Moreover, both sensors were analytically tested for metal ion determination using Pb(II) and Cd(II) as a model system. Firstly, the working pH was established, being 4.5 and 5.0 the optimal value for (PNA)Cys-SPCNFE and (ABA)Cys-SPCNFE respectively. At these pH conditions, metals are not affected by hydrolysis and the electrostatic interactions between metal ions and the electrode surface are favourable.

From an analytical point of view, although both developed sensors are very repetitive and reproducible and can be used for a large number of measurements without signs of degradation, (PNA) Cys-SPCNFE presents a better voltammetric behaviour conferred by the better shaped Pb(II) peak. Both (PNA)Cys-SPCNFE and (ABA) Cys-SPCNFE are sensitive sensors that are able to detect Pb(II) and Cd(II) at trace levels with LODs around 1 and 2 $\mu g\,L^{-1}$ for Pb(II) and Cd(II) respectively, resulting in suitable sensors for the detection of Pb(II) and Cd(II) at very low concentrations. However, (PNA)Cys-SPCNFE presents the additional feature of being capable of quantifying both metal ions below the legal limits established by the European Water Framework Directive, which represents a great improvement with respect to similar sensors reported in the literature. Thus, despite being a much less common electrografting strategy for the development of voltammetric sensors, the approach based on 4-nitrobenzenediazonium is also a valuable procedure that should be further taken into account.

Finally, it should be pointed out that the combination of both electrografting approaches clearly expands the versatility of the covalent modification strategies for the development of voltammetric sensors since it allows the attachment of modifiers with different functional groups, therefore broadening the list of modifiers that can be covalently linked to an electrode surface.

Acknowledgments

This work is supported by the Generalitat of Catalonia (Project 2017SGR311). Clara Pérez-Ràfols acknowledges the Spanish Ministry of Education, Culture and Sports for a Ph.D grant (reference FPU15/02140) and Clara Pérez-Ràfols and Miguel Rosal thank the Water Research Institute (IdRA) of the University of Barcelona for its support.

References

[1] E. Callender, Heavy metals in the environment-historical trends, in: B.S. Lollar (Ed.), Environ. Geochemistry, Elsevier-Pergamon, Oxford, 2005, p. 67, https://doi.org/10.2134/jeq1993.00472425002200010029x.
[2] I.D.L. Foster, S.M. Charlesworth, Heavy metals in the hydrological cycle: trends and explanation, Hydrol. Process. 10 (1996) 227–261.
[3] J. Wang, Stripping Analysis: Principles, instrumentation and applications, VCH, Deerfield Beach, FL, 1985.
[4] J. Barton, M.B.G. García, D.H. Santos, P. Fanjul-Bolado, A. Ribotti, M. McCaul, et al., Screen-printed electrodes for environmental monitoring of heavy metal ions: a review, Microchim. Acta. 183 (2016) 503–517, https://doi.org/10.1007/s00604-015-1651-0.
[5] O.D. Renedo, M.A. Alonso-Lomillo, M.J.A. Martínez, Recent developments in the field of screen-printed electrodes and their related applications, Talanta 73 (2007) 202–219, https://doi.org/10.1016/j.talanta.2007.03.050.
[6] C. Ariño, N. Serrano, J.M. Díaz-Cruz, M. Esteban, Voltammetric determination of metal ions beyond mercury electrodes, A review, Anal. Chim. Acta. 990 (2017) 11–53, https://doi.org/10.1016/j.aca.2017.07.069.
[7] A. Waheed, M. Mansha, N. Ullah, Nanomaterials-based electrochemical detection of heavy metals in water: current status, challenges and future direction, TrAC Trends Anal. Chem. (Reference Ed.) 105 (2018) 37–51, https://doi.org/10.1016/j.trac.2018.04.012.
[8] A. Economou, C. Kokkinos, Advances in stripping analysis of metals, in: Electrochem. Strateg. Detect. Sci., The Royal Society of Chemistry, Cambridge, 2016, pp. 1–18, https://doi.org/10.1039/9781782622529-00001.
[9] K.C. Honeychurch, Screen-printed electrochemical sensors and biosensors for monitoring metal pollutants, Insciences J 2 (2012) 1–51, https://doi.org/10.5640/insc.020101.
[10] J. Mehta, S.K. Bhardwaj, N. Bhardwaj, A.K. Paul, P. Kumar, K.H. Kim, et al., Progress in the biosensing techniques for trace-level heavy metals, Biotechnol. Adv. 34 (2016) 47–60, https://doi.org/10.1016/j.biotechadv.2015.12.001.
[11] C. Kokkinos, A. Economou, I. Raptis, C.E. Efstathiou, T. Speliotis, Novel disposable bismuth-sputtered electrodes for the determination of trace metals by stripping voltammetry, Electrochem. Commun. 9 (2007) 2795–2800, https://doi.org/10.1016/j.elecom.2007.09.022.
[12] V. Sosa, N. Serrano, C. Ariño, J.M. Díaz-Cruz, M. Esteban, Sputtered bismuth screen-printed electrode: a promising alternative to other bismuth modifications in the voltammetric determination of Cd(II) and Pb(II) ions in groundwater, Talanta 119 (2014) 348–352, https://doi.org/10.1016/j.talanta.2013.11.032.
[13] M.A. Rahman, M.-S. Won, Y.-B. Shim, Characterization of an EDTA bonded conducting polymer modified electrode: its application for the simultaneous determination of heavy metal ions, Anal. Chem. 75 (2003) 1123–1129, https://doi.org/10.1021/ac0262917.
[14] M. Heitzmann, C. Bucher, J.-C. Moutet, E. Pereira, B.L. Rivas, G. Royal, et al., Complexation of poly(pyrrole-EDTA like) film modified electrodes: application to metal cations electroanalysis, Electrochim. Acta 52 (2007) 3082–3087, https://doi.org/10.1016/j.electacta.2006.09.041.
[15] G.O. Buica, C. Bucher, J.C. Moutet, G. Royal, E. Saint-Aman, E.M. Ungureanu, Voltammetric sensing of mercury and copper cations at poly(EDTA-like) film modified electrode, Electroanalysis 21 (2009) 77–86, https://doi.org/10.1002/elan.200804386.
[16] M. Rosal, X. Cetó, N. Serrano, C. Ariño, M. Esteban, J.M. Díaz-Cruz, Dimethylglyoxime modified screen-printed electrodes for nickel determination, J. Electroanal. Chem. 839 (2019) 83–89, https://doi.org/10.1016/j.jelechem.2019.03.025.

[17] A. González-Calabuig, D. Guerrero, N. Serrano, M. del Valle, Simultaneous voltammetric determination of heavy metals by use of crown ether-modified electrodes and chemometrics, Electroanalysis 28 (2016) 663–670, https://doi.org/10.1002/elan.201500512.
[18] N. Serrano, A. González-Calabuig, M. del Valle, Crown ether-modified electrodes for the simultaneous stripping voltammetric determination of Cd(II), Pb(II) and Cu(II), Talanta 138 (2015) 130–137, https://doi.org/10.1016/j.talanta.2015.01.044.
[19] C. Pérez-Ràfols, N. Serrano, J.M. Díaz-Cruz, C. Ariño, M. Esteban, Glutathione modified screen-printed carbon nanofiber electrode for the voltammetric determination of metal ions in natural samples, Talanta 155 (2016) 8–13, https://doi.org/10.1016/j.talanta.2016.04.011.
[20] C. Pérez-Ràfols, N. Serrano, J.M. Díaz-Cruz, C. Ariño, M. Esteban, Penicillamine-modified sensor for the voltammetric determination of Cd(II) and Pb(II) ions in natural samples, Talanta 144 (2015) 569–573, https://doi.org/10.1016/j.talanta.2015.06.083.
[21] N. Serrano, B. Prieto-Simón, X. Cetó, M. del Valle, Array of peptide-modified electrodes for the simultaneous determination of Pb(II), Cd(II) and Zn(II), Talanta 125 (2014) 159–166, https://doi.org/10.1016/j.talanta.2014.02.052.
[22] E. Chow, D. Ebrahimi, J.J. Gooding, D.B. Hibbert, Application of N-PLS calibration to the simultaneous determination of Cu(2+), Cd(2+) and Pb(2+) using peptide modified electrochemical sensors, Analyst 131 (2006) 1051–1057, https://doi.org/10.1039/b604690h.
[23] E. Chow, J.J. Gooding, Peptide modified electrodes as electrochemical metal ion sensors, Electroanalysis 18 (2006) 1437–1448, https://doi.org/10.1002/elan.200603558.
[24] J.J. Gooding, Peptide-modified electrodes for detecting metal ions, in: Electrochem. Sens. Anal., Alegret and Merkoçi, Elsevier, Amsterdam, 2007, pp. 189–210, https://doi.org/10.1016/S0166-526X(06)49010-3.
[25] D. Bélanger, J. Pinson, Electrografting: a powerful method for surface modification, Chem. Soc. Rev. 40 (2011) 3995–4048, https://doi.org/10.1039/c0cs00149j.
[26] C. Ocaña, M. del Valle, A comparison of four protocols for the immobilization of an aptamer on graphite composite electrodes, Microchim. Acta. 181 (2014) 355–363, https://doi.org/10.1007/s00604-013-1126-0.
[27] A.I. Vogel, Textbook of quantitative chemical analysis, fifth ed., Pearson Education Limited, Harlow, GB, 1989.
[28] C. Pérez-Ràfols, N. Serrano, J.M. Díaz-Cruz, C. Ariño, M. Esteban, A screen-printed voltammetric electronic tongue for the analysis of complex mixtures of metal ions, Sens. Actuators B Chem. 250 (2017) 393–401, https://doi.org/10.1016/j.snb.2017.04.165.
[29] M. Delamar, G. Désarmot, O. Fagebaume, R. Hitmi, J. Pinson, J. Savéant, Modification of carbon fiber surfaces by electrochemical reduction of aryl diazonium salts: application to carbon epoxy composites, Carbon N. Y. 35 (1997) 801–807.
[30] J. Puy-Llovera, C. Pérez-Ràfols, N. Serrano, J.M. Díaz-Cruz, C. Ariño, M. Esteban, Selenocystine modified screen-printed electrode as an alternative sensor for the voltammetric determination of metal ions, Talanta 175 (2017) 501–506, https://doi.org/10.1016/j.talanta.2017.07.089.

New approaches to antimony film screen-printed electrodes using carbon-based nanomaterials substrates.

C. Pérez-Ràfols, N. Serrano, J. M. Díaz-Cruz, C. Ariño, M. Esteban

Analytica Chimica Acta 916 (2016) 17-23

https://doi.org/10.1016/j.aca.2016.03.003

Analytica Chimica Acta 916 (2016) 17–23

Contents lists available at ScienceDirect

Analytica Chimica Acta

journal homepage: www.elsevier.com/locate/aca

New approaches to antimony film screen-printed electrodes using carbon-based nanomaterials substrates

Clara Pérez-Ràfols, Núria Serrano*, José Manuel Díaz-Cruz, Cristina Ariño, Miquel Esteban

Departament de Química Analítica, Facultat de Química, Universitat de Barcelona, Martí i Franquès 1-11, E–08028 Barcelona, Spain

HIGHLIGHTS

- *In-situ* SbSPEs are used for the determination of Cd(II) and Pb(II) ions.
- Carbon nanomaterial-modified SPEs were used as electrode platforms for the Sb film.
- Better LODs and LOQs are achieved when using carbon nanofibers as support.
- SbSPCE-CNF was successfully applied for Cd(II) and Pb(II) in real sample analysis.

GRAPHICAL ABSTRACT

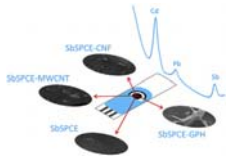

ARTICLE INFO

Article history:
Received 25 November 2015
Received in revised form
18 February 2016
Accepted 1 March 2016
Available online 5 March 2016

Keywords:
Antimony film electrodes
Screen-printed electrodes
Anodic stripping voltammetry
Heavy metal ions

ABSTRACT

Three different commercial carbon nanomaterial-modified screen-printed electrodes based on graphene, carbon nanotubes and carbon nanofibers were pioneeringly tested as electrode platforms for the plating with Sb film. They were microscopically and analytically compared to each other and to the most conventional unmodified carbon screen-printed electrode (SPCE). The obtained detection and quantification limits suggest that the *in-situ* antimony film electrode prepared from carbon nanofibers modified screen-printed electrode (SbSPCE-CNF) produces a better analytical performance as compared to the classical SPCE modified with antimony for Pb(II) and Cd(II) determination, approving its appropriateness for measuring low μg L^{-1} levels of the considered metals. *In-situ* SbSPCE-CNF was successfully used for the simultaneous determination of Pb(II) and Cd(II) ions, by means of differential pulse anodic stripping voltammetry, in a certified reference estuarine water sample with a very high reproducibility and good trueness.

1. Introduction

Heavy metals are present in the environment from both natural and human sources. Their bioaccumulation and persistence constitutes a serious threat to human health, and this demands suitable methods for heavy metal monitoring [1]. The usual techniques for metal ion determination include atomic absorption spectrometry (AAS), inductively coupled plasma optical emission spectrometry (ICP-OES), X-ray fluorescence (XRF), inductively coupled plasma mass spectrometry (ICP-MS) and stripping techniques such as anodic stripping voltammetry (ASV), adsorptive stripping voltammetry (AdSV) and stripping chronopotentiometry (SCP). Particularly, ASV is accepted as one of the most suitable techniques for measuring trace metals in samples of biological and environmental interest, due to its sensitivity and reproducibility for metal ion determination, the low detection limits, its capability to

* Corresponding author.
E-mail address: nuria.serrano@ub.edu (N. Serrano).

http://dx.doi.org/10.1016/j.aca.2016.03.003
0003-2670/

multielement analysis, and its relatively low cost [2]. For many years, stripping methods were connected with the use of mercury-based electrodes as a working electrode, since they are very reproducible and have a wide cathodic window [3]. However, the potential risks of toxicity, contamination and disposal associated with the use of mercury have forced to search for other working electrode materials. In 2000, bismuth-based electrodes were introduced for voltammetric analysis of metal ions and, over the years, they were stablished as a successful alternative to mercury-based electrodes for analytical determinations [4,5]. Nevertheless, in 2007, antimony was also proposed as a promising electrode material with a similar performance than that of mercury and bismuth-based electrodes. Subsequent studies revealed some remarkable features under chosen conditions of antimony film electrodes (SbFEs) such as wide operational potential window, favorably negative overvoltage of hydrogen evolution, suitable operation in solutions of more acidic pH than that reported for bismuth film electrodes (BiFEs) and a very small stripping signal for antimony itself. Moreover, antimony is much less toxic than mercury [6–8].

For the preparation of the Sb electrodes, both the substrate on which the Sb will be plated and the Sb-coating method are two essential aspects that have to be taken into consideration. The available Sb-coating methods are analogous to those used for BiFEs, being the *in-situ*, *ex-situ* and bulk the most representative approaches [8,9]. Regarding the substrate, carbon-based substrates revealed better performance than metal electrode materials, being glassy carbon followed by carbon paste the most used supports for the preparation of the film [8,10], although gold and platinum disk electrode [10] as well as boron doped diamond (BDD) were also used [11].

In the last years the screen-printing microfabrication technology has undergone a great progress allowing the mass production of numerous highly-reproducible single-use screen-printed electrodes (SPEs) with an accessible and low-cost character. These SPEs usually comprise a three-electrode configuration printed on the same strip. Some other important characteristics are related to its miniaturized size and the option of connecting it to portable instrumentation permitting the on-site determination of analytes. Furthermore, the design versatility and the possibility of using a great diversity of compositions of printing inks, as well as the easy modification of their surface are important advantages of these devices [5,12].

Thus, the coupling of Sb film with disposable SPEs presents an attractive option for the determination of heavy metal ions. However, most of the studies devoted to the application of antimony screen-printed electrodes (SbSPE) for the determination of trace metals use the conventional bare carbon screen-printed electrode (SPCE) as a support for the preparation of the film [8], whereas the use of SPCEs with the working electrode surface modified with nanomaterials, which are of great interest for the development of electrochemical sensors, as a support for plating the Sb film are very scarce. To the best of our knowledge only a tentative study was carried out using an screen-printed antimony film electrode modified with multi-walled carbon nanotubes for the determination of Hg(II) and Pb(II) [13].

With the aim to improve the properties of SbSPCE using nanomaterials as electrode platform, this study discusses the effect of different substrate electrodes as multi-walled carbon nanotubes modified screen-printed electrode (SPCE-MWCNT), graphene modified screen-printed electrode (SPCE-GPH) and carbon nanofibers modified screen-printed electrodes (SPCE-CNF) on which the Sb film will be plated for the stripping performance of the simultaneous determination of Cd(II) and Pb(II) as model metal ions. Moreover, SbSPCE-MWCNT, SbSPCE-GPH and SbSPCE-CNF were microscopically and analytically compared with the conventional SbSPCE. Finally, SbSPCE-CNF as the optimal *in-situ* SbSPE was applied for the first time for the simultaneous monitorizacion of Pb(II) and Cd(II) ions in a certified estuarine water sample.

2. Experimental

2.1. Chemicals

Sb(III) 1,000 mg L^{-1} atomic absorption standard solution was purchased from Merck (Darmstadt, Germany). All other reagents used were Panreac (Barcelona, Spain) and Merck analytical grade. Daily standard solutions of Cd(II) and Pb(II) were prepared by appropriate dilution of stock solutions 10^{-2} mol L^{-1}, prepared from $Pb(NO_3)_2 \cdot 4H_2O$ and $Cd(NO_3)_2 \cdot 4H_2O$ respectively and standardized complexometrically [14]. KNO_3 0.01 mol L^{-1} was used as supporting electrolyte and hydrochloric acid (pH 2) and acetate buffer (pH 4.5) solutions were employed for pH control. In all experiments, ultrapure water (Milli-Q plus 185 system, Millipore) was used.

Certified reference material, estuarine water LGC6016, was purchased from LGC Standards. As it is indicated in the certificate of measurement, estuarine water was collected from the Severn Estuary, UK, near Avonmouth (a heavily industrialized area). The water was filtered through a 0.45 μm membrane filter and then stabilized by the addition of concentrated nitric acid to achieve a pH of 2.

2.2. Apparatus

An Autolab System PGSTAT12 (EcoChemie, The Netherlands) attached to a Metrohm 663 V A Stand (Metrohm, Switzerland) was used to perform differential pulse anodic stripping voltammetric (DPASV) measurements. GPES version 4.9 software (EcoChemie) was used for data acquisition.

The auxiliary and the reference electrode (to which all potentials are referred) were Pt wire and Ag|AgCl|KCl (3 mol L^{-1}), respectively (Metrohm, Switzerland). The working electrode used was an *in-situ* antimony film electrode prepared from different carbon-based commercial screen-printed disk electrodes of 4 mm diameter provided by Dropsens (Spain): carbon screen-printed electrodes (ref. 110, DS SPCE), graphene modified screen-printed electrodes (ref. 110GPH, DS SPCE), multi-walled carbon nanotubes modified screen-printed electrodes (ref. 110CNT, DS SPCE) and carbon nanofibers modified screen-printed electrodes (ref. 110CNF, DS SPCE).

A flexible cable ref. (CAC, DropSens) was used to connect the screen-printed electrodes to the Autolab System.

All measurements were carried out under a purified nitrogen atmosphere (Linde N50) in a glass cell at room temperature (20 °C).

Scanning electron microscope JSM 7100FE from JEOL (Japan) was used for the surface morphology characterization.

2.3. Experimental procedure

2.3.1. In-situ preparation of SbSPE

In-situ modification of the screen-printed electrodes was carried out by directly adding a 0.5 mg L^{-1} Sb(III) solution to the sample solution usually containing 0.01 mol L^{-1} hydrochloric acid and the target metals. Then, Sb(III) is codeposited onto the bare based-carbon electrode together with Cd(II) and Pb(II) ions at the deposition potential (E_d) and deposition time (t_d) defined by the own analytical determination.

2.3.2. Procedure

DPASV determinations of Cd(II) and Pb(II) using an *in-situ* SbSPE

were performed at an E_d of −1.5 V (vs. Ag/AgCl), applied with stirring, during a t_d of 120 s and followed by a rest period (t_r) of 5 s. Determinations were done by scanning the potential from −1.5 to −0.1 V (vs. Ag/AgCl) using pulse times of 50 ms, step potentials of 5 mV and pulse amplitudes of 50 mV.

In order to obtain the linear calibration plots for the simultaneous determination of Pb(II) and Cd(II) by DPASV using an *in-situ* SbSPE, metal concentrations were increased in a solution of 0.01 mol L^{-1} HCl and 0.01 mol L^{-1} KNO_3.

In the analysis of the certified estuarine water sample, a volume of the sample (LGC6016) in 0.1 mol L^{-1} acetate buffer (pH 4.5) was placed in the cell and deaerated with pure nitrogen for 15 min in order to avoid the effect of oxygen in voltammetric measurements. Then, the estuarine water sample scan was recorded. In the case of calibration the standard addition method was applied, five aliquots of Pb(II) and Cd(II) standard solutions were further added and the respective curves were recorded.

In both linear calibration plots and analysis of the certified estuarine water sample, the solution was deaerated and mechanically stirred for 120 s after each addition and a cleaning step was performed before each measurement by applying a conditioning potential (E_{cond}) of 0.5 V (vs. Ag/AgCl) for 15 s.

3. Results and discussion

3.1. Morphological surface characterization: SEM analysis

Fig. 1 compares the SEM images obtained at 10.000x magnification of the different commercial bare carbon-based SPE substrates (Fig. 1a–d) and the different Sb film coated SPEs (Fig. 1e–h). The scanning electron micrograph of a typical unmodified SPCE (Fig. 1a) exhibits a uniform rough surface with grains in contrast with the ribbon-like tube appearance in the form of small bundles of SPCE-CNF (Fig. 1b), the twisted spaghetti-like character of SPCE-CNT (Fig. 1c), and the characteristic hexagonal arrangement of the SPCE-GPH (Fig. 1d). The special surface morphologies shown by modified SPCE offer a much larger real surface area than the unmodified SPCE.

The surface morphologies of bare carbon-based SPEs look different from those of the respective SbSPEs, in which the deposited Sb can be observed (Fig. 1e–h). In all SbSPEs the Sb film was formed by firmly fixed Sb of different sizes randomly dispersed on the carbon-based SPE surface, without covering the entire surface, but resulting in a reasonably uniform Sb film as it is seen in the corresponding insets of Fig. 1e–h. However, the comparison of the scanning electron micrographs makes obvious the diverse surface morphologies of the different SbSPEs, which could certainly affect their electroanalytical performance.

3.2. Optimization of electrochemical parameters and condition media for the in-situ SbSPCE

Several key electrochemical parameters, such as t_d, E_d and Sb(III) concentration, in connection with the simultaneous detection of Pb(II) and Cd(II) by DPASV using an *in-situ* plated SbSPE were optimized. This optimization was performed using the conventional SbSPCE as a SbSPE model. 0.01 mol L^{-1} HCl solution was selected as medium since it is the most used in the literature for the simultaneous determination of Pb(II) and Cd(II) on *in-situ* antimony film electrodes coated on carbon substrates [6,8,15–17].

DPASV measurements of a 50 μg L^{-1} Pb(II) and Cd(II) in 0.5 mg L^{-1} Sb(III), 0.01 mol L^{-1} KNO_3 and 0.01 mol L^{-1} HCl, were performed at different E_d ranging from −1.2 to −1.6 V (vs. Ag/AgCl) and applying a t_d of 120 s. Pb(II) peak increased when using more negative E_d while Cd(II) increased until −1.5 V (vs. Ag/AgCl) and significantly decreased at −1.6 V (vs. Ag/AgCl). According to this study an optimal E_d of −1.5 V (vs. Ag/AgCl) was selected. Once the E_d was selected, different t_d ranging from 30 to 300 s were studied. Well-defined stripping peaks for Pb(II) and Cd(II) that increase proportionally with t_d were observed (Figure not shown). In agreement with these results, a t_d of 120 s was selected as a good compromise between the peak current and the time of the analysis.

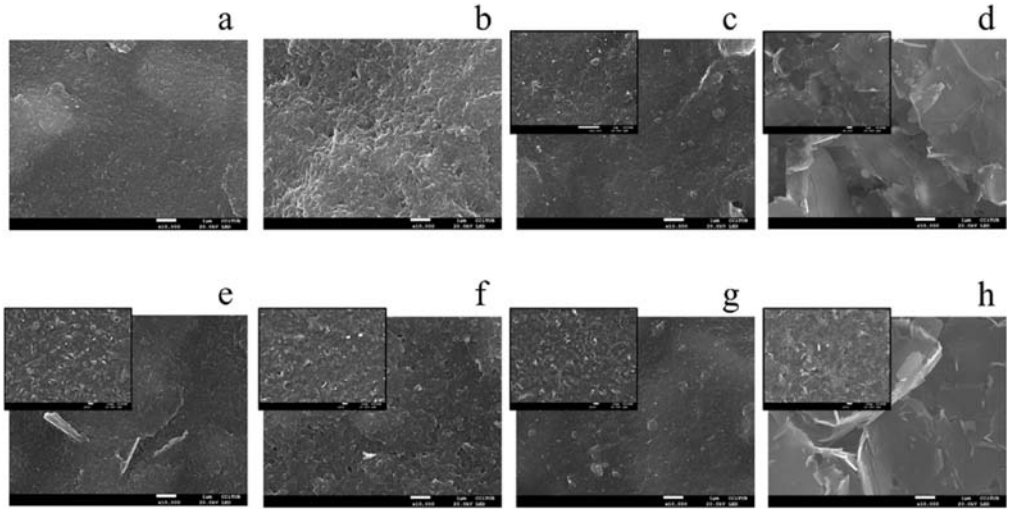

Fig. 1. Scanning electron micrographs of carbon (a), carbon nanofibers (b), carbon nanotubes (c) and graphene (d) commercial screen-printed electrodes and antimony films coated *in-situ* on these electrodes (e–h). Resolution of 1 μm, accelerating potential of 20.0 kV and magnification of 10,000 ×, 20,000 × (inset c), 5000 × (inset d) and 500 × (insets e-h) were used.

Finally, the effect of Sb(III) concentration was also studied. DPASV measurements of a 50 μg L^{-1} Pb(II) and Cd(II) solution, in 0.01 mol L^{-1} HCl, 0.01 mol L^{-1} KNO_3 and different Sb(III) concentrations ranging from 0.25 to 1.25 mg L^{-1}, were carried out applying a E_d of −1.5 V (vs. Ag/AgCl) during 120 s (Fig. 2). From 0.5 to 0.75 mg L^{-1} Sb(III) similar Cd(II) peaks, at *ca.* −0.96 V (vs. Ag/AgCl), where obtained while a decrease in the signal could be observed for higher or lower Sb(III) concentrations, obtaining the lowest signal at 0.25 followed by 1 mg L^{-1} Sb(III). On the other hand, Pb(II) peak, at *ca.* −0.69 V (vs. Ag/AgCl), started to decrease already at 0.75 mg L^{-1} Sb(III). As expected, Sb(III) peak, at *ca.* −0.23 V (vs. Ag/AgCl), increased proportionally to its concentration. After analyzing these results, an optimal Sb(III) concentration of 0.5 mg L^{-1} was selected.

3.3. Repeatability and reproducibility

Once the electrochemical parameters and the media were optimized, four different carbon substrates (bare carbon, graphene, carbon nanotubes and carbon nanofibers) were tested. Fig. 3 shows a comparison of the electroanalytical performance of the *in-situ* SbSPEs prepared on the different carbon substrates for the simultaneous determination of a solution containing 100 μg L^{-1} Pb(II) and Cd(II) in the previous optimized conditions. In all cases a well-defined peak is observed for Cd(II), obtaining the lowest signal with the *in-situ* SbSPCE-GPH (thin solid line) and the highest signal with SbSPCE-CNF (thick solid line). Related to Pb(II), a well-defined peak is also obtained with SbSPCE-CNF, SbSPCE (dashed thin line) and SbSPCE-GPH, while a double peak can be observed in the case of SbSPCE-MWCNT (dashed thick line). This fact could be attributed to the lack of uniformity of these surfaces, which allows antimony ions to deposit in different ways when the film is formed. The highest signal for Pb(II) is also obtained with the *in-situ* SbSPCE-CNF. Finally, a Sb(III) stripping peak was also detected on all *in-situ* SbSPEs, being more prominent in the case of SbSPCE-MWCNT (dashed thick line) and very small with the *in-situ* SbSPCE-GPH (thin solid line).

In order to test the repeatability and reproducibility of the *in-situ* SbSPE coated on the different carbon substrates, stripping measurements of a solution containing 50 μg L^{-1} Pb(II) and Cd(II) in 0.01 mol L^{-1} HCl, 0.01 mol L^{-1} KNO_3 and 0.5 mg L^{-1} Sb(III) were carried out. Table 1 shows the repeatability and reproducibility

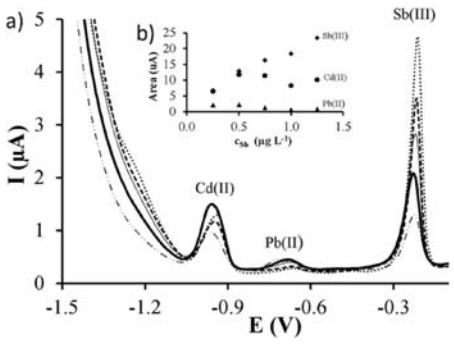

Fig. 2. a) DPASV measurements of 50 μg L^{-1} Pb(II) and Cd(II) on *in-situ* SbSPCE at 0.01 mol L^{-1} HCl and 0.25 (dotted-dashed line), 0.5 (thick line), 0.75 (thin line), 1 (dashed thick line) and 1.25 (dashed thin line) mg L^{-1} Sb(III) applying a E_d of −1.5 V (vs. Ag/AgCl) during 120 s at 0.01 mol L^{-1} KNO_3. b) Plot of peak area *vs* Sb(III) concentration.

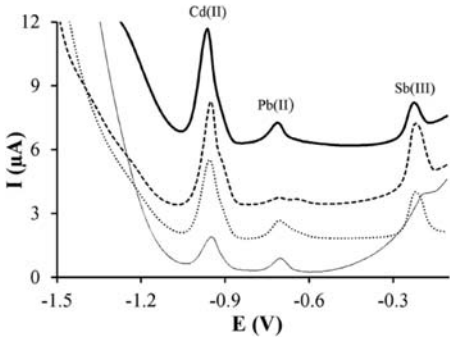

Fig. 3. DPASV voltammograms of 100 μg L^{-1} Pb(II) and Cd(II) on *in-situ* SbSPCE-GPH (thin line), SbSPCE (dashed thin line), SbSPCE-MWCNT (dashed thick line) and SbSPCE-CNF (thick line) applying a E_d of −1.5 V (vs. Ag/AgCl) during 120 s at 0.01 mol L^{-1} HCl, 0.01 mol L^{-1} KNO_3 and 0.5 mg L^{-1} Sb(III).

values calculated for Pb(II) and Cd(II) with each electrode. Repeatability was estimated using the same *in-situ* SbSPE unit for five repetitive measurements whereas reproducibility was calculated from three different *in-situ* SbSPE units within a series of five repetitive measurements. In all cases, the repetitive measurements yielded excellent repeatability, with RSDs ranging from 1.1 to 3.5% for Pb(II) and from 1.0 to 2.8 for Cd(II), obtaining the best results for the *in-situ* SbSPCE-CNF. These values are similar or even better to those reported for *in-situ* antimony films coated on glassy carbon [6], carbon paste [17] or carbon fiber microelectrodes [15]. Regarding the reproducibility, good values were also obtained with SbSPCE and SbSPCE-CNF whereas SbSPCE-GPH and SbSPCE-MWCNT presented higher RSD%. These high reproducibility values observed in SbSPCE-GPH and SbSPCE-MWCNT could be attributed to the low homogeneity between the different units commercially purchased.

3.4. Linearity, limit of detection (LOD) and limit of quantification (LOQ)

Calibration data for the simultaneous determination of Cd(II) and Pb(II) ions on the *in-situ* SbSPEs prepared on the different carbon substrates by stripping voltammetry (DPASV) are summarized in Table 2. Linear calibration curves were obtained at the optimized conditions by measuring eight increasing concentrations of Cd(II) and Pb(II) ranging from 1.1 to 100.3 and from 1.0 to 100.9 μg L^{-1} respectively. The limit of detection (LOD) was calculated as 3 times the standard deviation of the intercept over the slope of the calibration curve of the target ions. The limit of quantification (LOQ), which was considered as the lowest value of the linear concentration range, was evaluated by considering 10 times the previous ratio.

As shown in Table 2 excellent linear responses of peak area *versus* metal ion concentration were observed for both Pb(II) and Cd(II) for all the SbSPEs. LOD and LOQ were at the level of μg L^{-1} in all cases, being those obtained for Cd(II) slightly better than those obtained for Pb(II). The LODs obtained for the *in-situ* SbSPCE, which are similar to those previously reported with screen-printed supports [9], are of the same order, although slightly higher, than those reported using glassy carbon [6] or carbon paste [17] as supports for the preparation of the film, also with the *in-situ* approach and a t_d of 120 s (Table 3). The obtained LODs were even higher when using the SbSPCE-GPH (Table 2), which proves that the use of these

Table 1
Repeatability and reproducibility data for the simultaneous determination of Pb(II) and Cd(II) on *in-situ* SbSPCE, SbSPCE-GPH, SbSPCE-MWCNT and SbSPCE-CNF at pH 2 HCl, 0.01 mol L^{-1} KNO_3 and 0.5 mg L^{-1} Sb(III).

Electrode	Pb(II)		Cd(II)	
	Repeatability (RSD%)	Reproducibility (RSD%)	Repeatability (RSD%)	Reproducibility (RSD%)
SbSPCE	3.5	4.5	2.6	2.8
SbSPCE-GPH	2.9	17.2	2.8	18.0
SbSPCE-MWCNT	1.3	11.3	1.5	11.4
SbSPCE-CNF	1.1	4.4	1.0	1.2

Table 2
Calibration data for the simultaneous determination of Pb(II) and Cd(II) on *in-situ* SbSPCE, SbSPCE-GPH, SbSPCE-MWCNT and SbSPCE-CNF at pH 2 HCl, 0.01 mol L^{-1} KNO_3 and 0.5 mg L^{-1} Sb(III). The standard deviations are denoted by parenthesis.

Electrode	Pb(II)					Cd(II)				
	Sensitivity (a.u. μg^{-1} L)[a]	Intercept (a.u.)	R^2	Linear range[b] (μg L^{-1})	LOD (μg L^{-1})	Sensitivity (a.u. μg^{-1} L)[a]	Intercept (a.u.)	R^2	Linear range[b] (μg L^{-1})	LOD (μg L^{-1})
SbSPCE	0.87 (0.03)	−9 (2)	0.997	17.5–100.9	5.3	3.24 (0.05)	−37 (3)	0.999	9.5–100.3	2.8
SbSPCE-GPH	0.48 (0.02)	−10 (1)	0.994	28.8–100.9	8.6	1.37 (0.03)	−15 (2)	0.995	13.2–100.3	4.0
SbSPCE-MWCNT	0.49 (0.01)	−3.1 (0.7)	0.998	14.7–100.9	4.4	4.33 (0.06)	−48 (4)	0.999	8.6–100.3	2.6
SbSPCE-CNF	1.36 (0.01)	−14.2 (0.9)	1.000	6.9–100.9	2.1	4.74 (0.03)	−66 (2)	1.000	3.7–100.3	1.1

[a] Sensitivity was considered from the slope of the calibration curve.
[b] The lowest value of the linear range was considered from the LOQ.

Table 3
Comparative of LODs and linear ranges obtained for Cd(II) and Pb(II) using different electrode supports and coating methods for the formation of the Sb film.

Electrode support	Coating method	t_d (s)	Linear range (μg L^{-1})		LOD (μg L^{-1})		Ref.
			Cd(II)	Pb(II)	Cd(II)	Pb(II)	
Glassy carbon	*In-situ*	120	20–140	20–140	0.7	0.9	[6]
Carbon paste	*In-situ*	120	5–50	5–50	0.8	0.2	[17]
SPCE	*In-situ*	120	11.5–72.4	16.8–62.6	3.4	5.0	[9]
SPCE	*In-situ*	120	9.5–100.3	17.5–100.9	2.8	5.3	This work
SPCE-GPH	*In-situ*	120	13.2–100.3	28.8–100.9	4.0	8.6	This work
SPCE-CNF	*In-situ*	120	3.7–100.3	6.9–100.9	1.1	2.1	This work
SPCE-MWCNT	*In-situ*	120	8.6–100.3	14.7–100.9	2.6	4.4	This work
SPCE	Bulk-modified with Sb_2O_3	600	20–100	–	20	–	[18]
SPCE	Bulk-modified with Sb_2O_3	240	10–90	5–45	2.5	0.9	[19]
SPCE	Bulk-modified with SnO_2/Sb_2O_5	240	10–90	5–45	1.8	1.1	[19]
SPCE	Bulk-modified with $Sb^{III}(C_2O_4)OH$	240	10–90	5–45	3.5	1.1	[19]

commercial screen-printed carbon electrodes modified with graphene as a platform for the Sb(III) deposition does not seem to provide a more suitable Sb electrode for the simultaneous determination of Cd(II) and Pb(II). In contrast, with SbSPCE-MWCNT, a slight improvement of the LODs can be observed. However, this minimum improvement, coupled with their low reproducibility previously observed, does not justify the use of multi-walled carbon nanotubes modified screen-printed electrodes as a support for plating the Sb film, as they are much more expensive than the conventional SPCE. SbSPCE-CNF, on the other hand, provides LODs significantly lower which, coupled with its excellent repeatability and reproducibility, make it a more suitable support for the Sb film deposition even considering its higher cost. Furthermore, as it can be seen in Table 3, SbSPCE-CNF provides LODs much similar to those obtained using glassy carbon or carbon paste as support, with the advantages associated to the screen-printed electrodes (commercially available, no pretreatment required …), and similar or even better than LODs reported for screen-printed electrodes using other coating methods such as bulk modifications [18,19]. It should be pointed out that for SbSPCE-GPH, SbSPCE-MWCNT and SbSPCE-CNF no previous LOD and LOQ data for Cd(II) and Pb(II) are available in the literature.

The improvement observed for SbSPCE-MWCNT and SbSPCE-CNF could be attributed to the much larger effective surface area that present these modified carbon-based SPEs in comparison to the conventional unmodified SPCE as can be seen in the scanning electron micrographs. Regarding SbSPCE-GPH, although its surface area should be also enhanced and lower LODs should be expected,

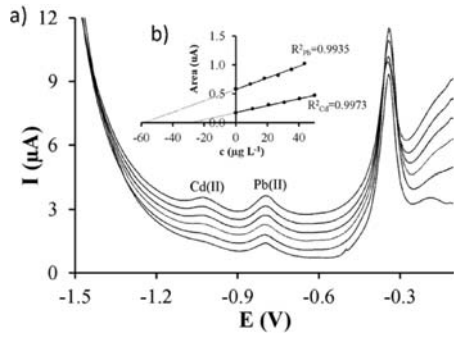

Fig. 4. a) DPASV measurements in an estuarine water sample by using an *in-situ* SbSPCE-CNF at pH 4.5 with E_d of −1.5 V (vs. Ag/AgCl) during a t_d of 120 s and t_r of 5 s; and, b) Cd(II) and Pb(II) standard addition plot.

Table 4
Total concentrations of Pb(II) and Cd(II) determined in certified estuarine water (LGC6016) by DPASV on *in-situ* SbSPCE-CNF by standard addition calibration method applying an E_d of −1.5 V and t_d of 120 s.

	Pb(II)			Cd(II)		
	c (μg L^{-1})	RSD (%)	Relative error (%)	c (μg L^{-1})	RSD (%)	Relative error (%)
Certified metal value	195.2	0.5	0.4	98.8	1.2	2.2
	196	1.5	–	101	2.0	–

n = 3 for RSD (%).

the achieved results do not agree with the above-mentioned supposition indicating maybe a problem with the commercial purchased device.

Therefore the reported calibration data suggests that SbSPCE-CNF could be fully suitable and a valuable alternative to more conventional SbSPCE for the simultaneous determination of Cd(II) and Pb(II) at trace levels in natural samples as well as in drinking water [20], being able to quantify lower concentrations than SbSPCE.

3.5. Application to the analysis of an estuarine water reference material

At the view of the above results, SbSPCE-CNF was selected to study its applicability for the determination of Cd(II) and Pb(II) in a certified estuarine water reference material (LGC6016). Considered metal ions were determined by means of the standard addition method. Then, voltammetric stripping measurements following the optimized conditions were carried out including the additions of Pb(II) and Cd(II). Fig. 4a shows representative stripping voltammograms obtained in the analysis of the estuarine water samples using SbSPCE-CNF. Cd(II) and Pb(II) peaks behave in the same way as in the calibration data: well-defined peaks for both metal ions were obtained.

Standard addition plot for both Cd(II) and Pb(II) (Fig. 4b) shows the good correlation of the representative stripping voltammetric measurements carried out using SbSPCE-CNF. It should be mentioned that the presence of other constituents of the reference material such as Cu, Mn, Ni and Zn at similar concentrations as the considered metals does not seem to interfere in the simultaneous determination of Cd(II) and Pb(II).

The metal concentration data obtained from the voltammetric determination of three replicates of the certified estuarine water sample performed using SbSPCE-CNF are reported in Table 4. A good concordance between Cd(II) and Pb(II) concentrations were obtained, as well as with the certified metal ion values. Therefore, these good results confirm the applicability of the *in-situ* antimony film electrode prepared from carbon nanofibers modified screen-printed electrodes for the simultaneous determination of Cd(II) and Pb(II) in natural samples, being an interesting and valuable alternative for the determination of these metal ions not only to the most traditional devices such as mercury and bismuth electrodes but also to the most conventional *in-situ* SbSPCE.

4. Conclusions

In this work, analytical and microscopic features of antimony film coated on different commercial carbon modified screen-printed electrodes were compared to each other and to the most conventional *in-situ* SbSPCE. Firstly, the electrochemical parameters for the simultaneous determination of Cd(II) and Pb(II) were optimized, obtaining the best voltammetric response using a E_d of −1.5 V (vs. Ag/AgCl), a t_d of 120 s and a Sb(III) concentration of 0.5 mg L^{-1}. At the above optimized conditions, all the SbSPEs provided LODs and LOQs at levels of μg L^{-1} for both metals. SbSPCE-GPH did not achieve the results obtained with the most conventional SbSPCE and only a slight improvement could be observed when using the SbSPCE-MWCNT. The best results in terms of sensitivity, repeatability, reproducibility and detection limits were obtained with the SbSPCE-CNF. Moreover, the achieved LODs and linear ranges were similar or even much better than values reported in previous studies for Sb modified electrodes using other supports or coating methods. Therefore, the *in-situ* antimony film electrode prepared from carbon nanofibers modified screen-printed electrodes could be a valuable alternative to the most conventional SbSPCE for environmental applications. Although they are somewhat more expensive, they can be also used for a large set of measurements without signs of degradation or loss of sensitivity.

Furthermore, SbSPCE-CNF was successfully applied for the determination of Cd(II) and Pb(II) in an estuarine water sample, as an example of its applicability for the analysis of natural samples, being able to quantify both Cd(II) and Pb(II) concentrations with very high reproducibility and good trueness inferred by the relative standard deviation (0.5% for Pb(II) and 1.2% for Cd(II)) and the relative error (0.4% for Pb(II) and 2.2% for Cd(II)), respectively.

Acknowledgments

This work is supported by the Ministry of Science and Innovation of Spain (Project CTQ2012−32863) and the Generalitat of Catalonia (Project 2014SGR269). Clara Pérez-Ràfols acknowledges the University of Barcelona for a PhD grant.

References

[1] E. Lawrence, A.R.W. Jackson, J.M. Jackson, Longman Dictionary of Environmental Science, Addison Wesley Longman, Harlow, UK, 1998.
[2] J. Wang, Stripping Analysis: Principles, Instrumentation and Applications, VCH, Deerfield Beach, FL, 1985.
[3] J. Barek, A.G. Fogg, A. Muck, J. Zima, Polarography and voltammetry at mercury electrodes, Crit. Rev. Anal. Chem. 31 (2001) 291–309.
[4] J. Wang, J. Lu, S.B. Hocevar, P.A.M. Farias, B. Ogorevc, Bismuth-coated carbon electrodes for anodic stripping voltammetry, Anal. Chem. 72 (2000) 3218–3222.
[5] N. Serrano, A. Alberich, J.M. Díaz-Cruz, C. Ariño, M. Esteban, Coating methods, modifiers and applications of bismuth screen-printed electrodes, Trends Anal. Chem. 46 (2013) 15–29.
[6] S.B. Hocevar, I. Svancara, B. Ogorevc, K. Vytras, Antimony film electrode for electrochemical stripping analysis, Anal. Chem. 79 (2007) 8639–8643.
[7] V. Jovanovski, S.B. Hocevar, B. Ogorevc, Ex Situ prepared antimony film electrode for electrochemical stripping measurement of heavy metal ions, Electroanalysis 21 (2009) 2321–2324.
[8] N. Serrano, J.M. Díaz-Cruz, C. Ariño, M. Esteban, Antimony- based electrodes for analytical determinations, Trends Anal. Chem. 77 (2016) 203–213.
[9] V. Sosa, C. Barceló, N. Serrano, C. Ariño, J.M. Díaz-Cruz, M. Esteban, Antimony film screen-printed carbon electrode for stripping analysis of Cd(II), Pb(II) and Cu(II) in natural samples, Anal. Chim. Acta 855 (2015) 34–40.
[10] B. Sebez, B. Ogorevc, S.B. Hocevar, M. Veber, Functioning of antimony film electrode in acid media under cyclic and anodic stripping voltammetry conditions, Anal. Chim. Acta 785 (2013) 43–49.
[11] K.E. Toghill, L. Xiao, G.G. Wildgoose, R.G. Compton, Electroanalytical determination of cadmium(II) and lead(II) using an antimony nanoparticle modified boron-doped diamond electrode, Electroanalysis 21 (2009) 1113–1118.
[12] J. Barton, M.B. González García, D. Hernández Santos, P. Fanjul-Bolado,

A. Ribotti, M. McCaul, D. Diamond, P. Magni, Screen-printed electrodes for environmental monitoring of heavy metal ions: a review, Microchim. Acta 183 (2016) 503–517.
[13] X. Niu, H. Zhao, M. Lan, Disposable screen-printed antimony film electrode modified with carbon nanotubes/ionic liquid for electrochemical stripping measurement, Electrochim. Acta 56 (2011) 9921–9925.
[14] A.I. Vogel, Textbook of Quantitative Chemical Analysis, fifth ed., Pearson Education Limited, Harlow, GB, 1989.
[15] M. Slavec, S.B. Hocevar, L. Baldrianova, E. Tesarova, I. Svancara, B. Ogorevc, K. Vytras, Antimony film microelectrode for anodic stripping measurement of cadmium(II), lead(II) and copper(II), Electroanalysis 22 (2010) 1617–1622.
[16] V. Guzsvány, H. Nakajima, N. Soh, K. Nakano, T. Imato, Antimony-film electrode for the determination of trace metals by sequential-injection analysis/anodic stripping voltammetry, Anal. Chim. Acta 658 (2010) 12–17.
[17] E. Tesarova, L. Baldrianova, S.B. Hocevar, I. Svancara, K. Vytras, B. Ogorevc, Anodic stripping voltammetric measurement of trace heavy metals at antimony film carbon paste electrode, Electrochim. Acta 54 (2009) 1506–1510.
[18] R. Pauliukaite, R. Metelka, I. Svancara, A. Krolicka, A. Brobrowski, E. Norkus, K. Kalcher, K. Vytras, Screen.printed Carbon Electrodes Bulk-modified with Bi_2O_3 or Sb_2O_3 for Trace Determination of Some Heavy Metals, Sci. Pap. Univ. Pardubice, Ser. A 10 (2004) 47–58.
[19] M. Maczuga, A. Economou, A. Bobrowski, M.I. Prodromidis, Novel screen-printed antimony and tin voltammetric sensors for anodic stripping detection of Pb(II) and Cd(II), Electrochim. Acta 114 (2013) 758–765.
[20] Spanish legislation (RD 140/2003 of 7th of February) according to the Directive 98/83/CE on water quality for human consumption.

Determination of Pd(II) using an antimony film coated on a screen-printed electrode by adsorptive stripping voltammetry.

C. Pérez-Ràfols, P. Trechera, N. Serrano, J. M. Díaz-Cruz, C. Ariño, M. Esteban

Talanta 167 (2017) 1-7

https://doi.org/10.1016/j.talanta.2017.01.084

Talanta 167 (2017) 1–7

Contents lists available at ScienceDirect

Talanta

journal homepage: www.elsevier.com/locate/talanta

Determination of Pd(II) using an antimony film coated on a screen-printed electrode by adsorptive stripping voltammetry

Clara Pérez-Ràfols, Pedro Trechera, Núria Serrano*, José Manuel Díaz-Cruz, Cristina Ariño, Miquel Esteban

Departament d'Enginyeria Química i Química Analítica, Facultat de Química, Universitat de Barcelona, Martí i Franquès 1-11, E–08028 Barcelona, Spain

ARTICLE INFO

Keywords:
Palladium
Antimony film electrode
Adsorptive stripping voltammetry
Screen-printed electrode

ABSTRACT

The use of an antimony film coated on a screen-printed carbon electrode (*ex-situ* SbSPCE) is proposed for the determination of Pd(II) at ppb levels in natural samples by adsorptive stripping voltammetry using dimethylglyoxime as chelating agent. *Ex-situ* SbSPCE produces a better analytical performance as compared to a commercially sputtered bismuth screen-printed electrode (Bi_{sp}SPE). The detection and quantification limits were 2.7 and 9.0 μg L^{-1} respectively with a good linear behaviour in the wide examined concentration range (from 1 μg L^{-1} up to 100.0 μg L^{-1}, R^2=0.998). The proposed *ex-situ* SbSPCE showed an excellent repeatability with a relative standard deviation of 0.5% for ten successive measurements and a very good reproducibility (1.6% for three different *ex-situ* SbSPCE units within series of ten repetitive assays). Moreover, the *ex-situ* SbSPCE was successfully applied for the determination of low concentration levels of Pd(II) in spiked tap water with a very high reproducibility (0.2%) and providing equivalent results to those achieved by ICP-MS measurements.

1. Introduction

Palladium is a metal that possesses strong catalytic activity, the demand of which has been more than doubled in the past ten years. It is used in electrical equipment, dental appliances, chemical catalysts and jewellery, being the maximum increase in demand for palladium in automotive emission control catalysts. In contrast to other metals, there is little information concerning concentrations of palladium in the environment. However, in the last decades it has been detected that the concentration of palladium is increasing in the overall environment mainly due to its greater use in automobile catalysts and jewellery industry [1–3]. Concentrations of palladium reported in soil samples collected from areas near major roads range from < 0.7 to 47 μg Kg^{-1} and, concentrations reported in sewage sludge range from 18 to 260 μg Kg^{-1}, although a concentration of 4700 μg Kg^{-1} has been reported in a sludge contaminated by discharges from the local jewellery industry [3]. Thus, because both its increasing use and the toxicity of compounds of Pd(II) to mammals, fishes and higher plants, the Pd(II) determination is increasingly important [4,5].

There are different techniques such as atomic absorption spectrometry [5–7], high-performance liquid chromatography with photodiode array detector [8], inductively coupled plasma [9], spectrophotometry [4,10,11], etc, available for the sensitive analysis of palladium in samples. However, these techniques have some disadvantages such as expertise required, need of sample pre-treatments, time-consuming procedures, high initial investment (equipment) and high cost of consumables. In this sense, electroanalytical methods are stated as a very good alternative. In particular, voltammetric stripping techniques provide excellent properties for the determination of metal ions with excellent detection and quantification limits. Moreover, they are highly reproducible, relatively low cost, sensitive and selective, and they present capability to multielement analysis [12]. When stripping techniques are coupled with screen-printed electrodes (SPEs), they become especially suitable for *on-site* analysis, since SPE devices usually incorporate the whole electrode system (working, reference and auxiliary). In addition, the use of SPEs instead of classical working electrodes avoids the continuous and tedious cleaning processes. In fact, SPEs have in recent years undergone great improvements, allowing the mass production of reproducible and low-cost miniaturized size devices [13–15].

Traditionally Pd(II) determination based on voltammetric methods was carried out using the hanging mercury drop electrode (HMDE) as working electrode with an excellent analytical performance [16]. Nevertheless, the potential high toxicity of mercury-based electrodes, if they are not conveniently used, has led to their replacement by other electrodes more environmentally friendly but with a similar analytical

* Corresponding author.
E-mail address: nuria.serrano@ub.edu (N. Serrano).

http://dx.doi.org/10.1016/j.talanta.2017.01.084
Received 16 November 2016; Received in revised form 25 January 2017; Accepted 30 January 2017
Available online 31 January 2017

performance. In this respect, some attempts were undertaken using some substitute voltammetric sensors. Bobrowski *et al.* reported on the applicability of a cylindrical silver-based amalgam film electrode (Hg(Ag)-FE) for the Pd(II) determination by adsorptive stripping voltammetry (AdSV) in the presence of dimethylglyoxime (DMG) [17]. Bismuth and antimony-based electrodes have been postulated over the years as an important alternative to mercury electrodes with great results for analytical purposes [18–21]. Particularly, Van der Horst *et al.* [22,24] and Silwana et al. [23] described good results for the determination of Pd(II) by the AdSV approach using a bismuth film coated on a glassy carbon electrode [22] or on a screen-printed carbon electrode [23] and, using a bismuth-silver bimetallic nanoparticles coated on a glassy carbon electrode [24]. Nevertheless, studies devoted to the application of antimony-based electrodes for analysis of Pd(II) are really scarce. In fact, from the best of our knowledge, only a glassy carbon electrode modified with a composite of reduced graphene oxide impregnated with antimony nanoparticles was proposed for this purpose [25]; but the application of antimony coated on screen-printed electrodes (SbSPE) for the Pd(II) determination is not yet attempted. It is worth noting that SbSPE, unlike antimony coated on glassy carbon electrodes (SbGCE), do not require any pre-polishing and in particular Sb film coated on screen-printed carbon electrodes (SbSPCE) can be used for a large set of measurements using the same electrode unit [26].

Thus, in the present study, antimony film coated via *ex-situ* on a commercial screen-printed carbon electrode (*ex-situ* SbSPCE) was successfully applied for the determination of Pd(II) in water samples by means of the AdSV approach using DMG as chelating agent. Furthermore, the *ex-situ* SbSPCE analytical performance was compared with that of a commercial sputtered bismuth screen-printed electrode (Bi_{sp}SPE).

2. Experimental section

2.1. Chemicals and solutions

Sb(III) 1.000 mg L^{-1} atomic absorption standard solution was obtained from Merck (Darmstadt, Germany). Working Pd(II) solutions were prepared by appropriate dilution of 1.000 g L^{-1} standard solution with HCl 0.01 mol L^{-1}. Other solutions used were: 0.1 mol L^{-1} solution of dimethylglyoxime (DMG) in 95% methanol and 0.1 mol L^{-1} acetate buffer solution (pH 4.5). All other reagents used were Sigma-Aldrich (St. Louis, MO, USA) and Panreac (Barcelona, Spain) analytical grade. Ultrapure water was obtained from a Milli-Q plus 185 system, Millipore.

Tap water samples were collected in our laboratory from the local water distribution network, managed by Agbar Company (Barcelona; http://www.agbar.es/eng/home.asp) and mostly using water coming from Llobregat River.

2.2. Instrumentation

Adsorptive stripping voltammetric (AdSV) measurements were performed using a μAutolab Type III (EcoChemie, The Netherlands) coupled to a Metrohm 663VA Stand (Metrohm, Switzerland) and a personal computer with GPES version 4.9 data acquisition software (EcoChemie).

The electrochemical cell used consisted in the conventional three-electrode system: Ag|AgCl|KCl (3 mol L^{-1}) as reference electrode, Pt wire as auxiliary electrode, and antimony or bismuth screen-printed electrode as working electrode. *Ex-situ* SbSPCE was prepared using a commercial screen-printed carbon disk electrode of 4 mm of diameter (ref. DRP-110, DS SPE) supplied by DropSens (Oviedo, Spain), and Bi_{sp}SPE was a sputtered thick film bismuth of 4 mm of diameter (ref. Bi10, DS SPE) obtained also from DropSens.

Screen-printed electrodes were connected to the Autolab System by means of a flexible cable (ref. CAC, DropSens).

A Crison micro pH 2000 pH-meter was used for pH measurements.

All electrochemical measurements were carried out at room temperature (20 °C) and the antimony film preparation was performed under a purified nitrogen atmosphere (Linde N50).

Inductively coupled plasma mass spectrometry Perkin-Elmer model Elan 6000 (USA) was used for ICP-MS measurements.

2.3. Preparation of ex-situ SbSPCE

Before measurements, the SPCE, the auxiliary, and the reference electrodes were connected to the stand and immersed into a 0.01 mol L^{-1} HCl solution containing 50 mg L^{-1} of Sb(III). After purging the solution for 600 s, a deposition potential of −0.5 V was applied for 300 s with constant stirring, followed by a rest period of 20 s, without stirring. Then, the *ex-situ* SbSPCE was rinsed with water and ready to use. This procedure was tested earlier [26], yielding a very high reproducibility and repeatability.

2.4. Voltammetric measurements

Linear calibration curves for the determination of Pd(II) using *ex-situ* SbSPCE and Bi_{sp}SPE by AdSV were constructed by adding small volumes of the Pd(II) concentrated standard solution into the electrochemical cell containing 20 mL of 0.1 mol L^{-1} acetate buffer (pH 4.5) and 2×10^{-4} mol L^{-1} DMG [17]. Unless otherwise indicated, AdSV measurements were performed applying an accumulation potential (E_{acc}) of −0.6 V during an accumulation time (t_{acc}) of 180 s with constant stirring. After a rest period (t_r) of 20 s without stirring, voltammograms were recorded by scanning the potential from −0.45 to −1.0 V (on *ex-situ* SbSPCE) and from −0.5 V to −1.2 V (on Bi_{sp}SPE), using pulse times of 50 ms, pulse amplitudes of 100 mV and a step potential of 5 mV.

Analysis of Pd(II) in the tap water sample by the proposed voltammetric method using an *ex-situ* SbSPCE were carried out measuring 3 replicates of a spiked tap water sample with Pd(II) concentration distributed in the range of the calibration curves. The standard addition method was used to eliminate matrix effects.

In both cases, linear calibration curves and analysis of tap water samples, in order to eliminate the remaining bound Pd(II)-DMG complex from the working electrode surface a conditioning potential (E_{cond}) of −1.0 V (on *ex-situ* SbSPCE) or of −1.2 V (on Bi_{sp}SPE) for 30 s was applied before each measurement.

2.5. Sample preparation

Water samples collected from the local water distribution network were spiked with 180 μg L^{-1} of Pd(II). This concentration value was further determined by ICP-MS. For voltammetric determinations, a volume of the spiked tap water sample was added into the voltammetric cell containing 0.1 mol L^{-1} acetate buffer (pH 4.5) and 2×10^{-4} mol L^{-1} DMG resulting in solution concentrations of 45 μg L^{-1} of Pd(II). The AdSV scan was recorded under the aforementioned electrochemical conditions.

3. Results and discussion

3.1. Condition media and optimization of electrochemical parameters

First it is worth noting that all experiments in this work were performed using 0.1 mol L^{-1} acetate buffer (pH 4.5) and 2×10^{-4} mol L^{-1} DMG [17], because even though the best sensitivity in some previous studies for Pd(II) determination [22,23] was obtained in 0.01 mol L^{-1} ammonia buffer (pH=9.0 [22] and pH=9.2 [23]), an analytical misbehavior of stripping signals for Pd(II) (no reproducible signals could be obtained) was observed in this study using the

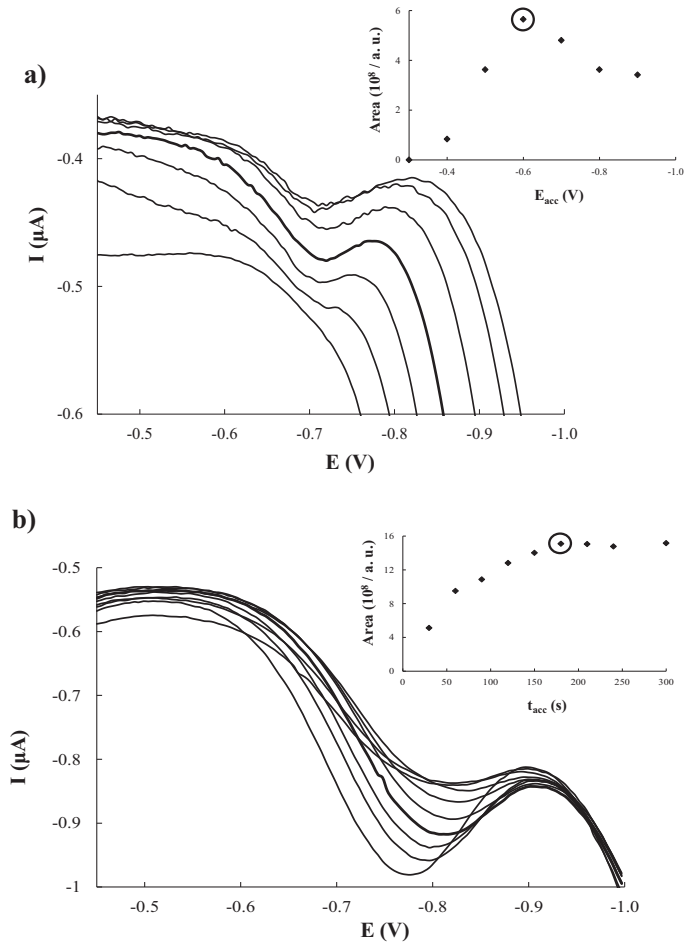

Fig. 1. Effect of accumulation potential (a) and accumulation time (b) on the peak area of Pd(II)-DMG complex signal using an *ex-situ* SbSPCE in 0.1 mol L^{-1} acetate buffer (pH 4.5) and 2×10^{-4} mol L^{-1} DMG. An E_{acc} of −0.6 V was used for t_{acc} optimization.

adsorptive approach in ammonium buffer.

Looking for the highest analytical response the effect of the accumulation potential (E_{acc}), initial potential (E_i) and accumulation time (t_{acc}) on Pd(II) determination were firstly evaluated using *ex-situ* SbSPCE by AdSV.

Then, the effect of E_{acc} over the peak area of Pd(II)-DMG complex reduction signal was tested in the range from −0.2 to −0.9 V with a t_{acc} of 120 s in a solution containing 50 µg L^{-1} Pd(II) at acetate buffer pH 4.5 and 2×10^{-4} mol L^{-1} DMG (Fig. 1a). As E_{acc} was shifted from −0.2 V to more negative potentials, peak area increased significantly up to −0.6 V. For more negative E_{acc} a diminution of peak area was progressively observed. Therefore, an E_{acc} of −0.6 V was chosen for further experiments.

The value of E_i is another critical point in the determination of Pd(II) by AdSV. Thus, the influence of the E_i over the peak area of Pd(II)-DMG complex was also evaluated in the range from −0.3 to −0.5 V (Results not shown). Maximal peak area was obtained at E_i of −0.45 V and this E_i value was chosen as optimal.

The effect of the t_{acc} over the peak area of Pd(II)-DMG complex was studied in the range of 30–300 s applying an E_{acc} of −0.6 V in the aforementioned solution (Fig. 1b). Peak area linearly increases with t_{acc} until 180 s, where the area stabilizes. Therefore, a t_{acc} of 180 s was chosen as ideal looking for a compromise between the time of the analysis and the peak area.

The selected E_{acc}, E_i and t_{acc} to ensure the determination of Pd(II) at Bi_{sp}SPE were also firstly optimized in a solution containing 50 µg L^{-1} Pd(II) at acetate buffer pH 4.5 and 2×10^{-4} mol L^{-1} DMG (Results not shown); the compromise conditions were an E_{acc} of −0.6 V applied during a t_{acc} of 180 s and an E_i of −0.5 V. It must be pointed out that using Bi_{sp}SPE more positive potentials cannot be applied to prevent the oxidation of the bismuth [27].

3.2. Analytical characterization

With the purpose of comparing the repeatability and reproducibility of the *ex-situ* SbSPCE and the Bi_{sp}SPE, AdSV measurements in a solution containing 50 µg L^{-1} Pd(II) at acetate buffer pH 4.5 and 2×10^{-4} mol L^{-1} DMG following the above-mentioned conditions were

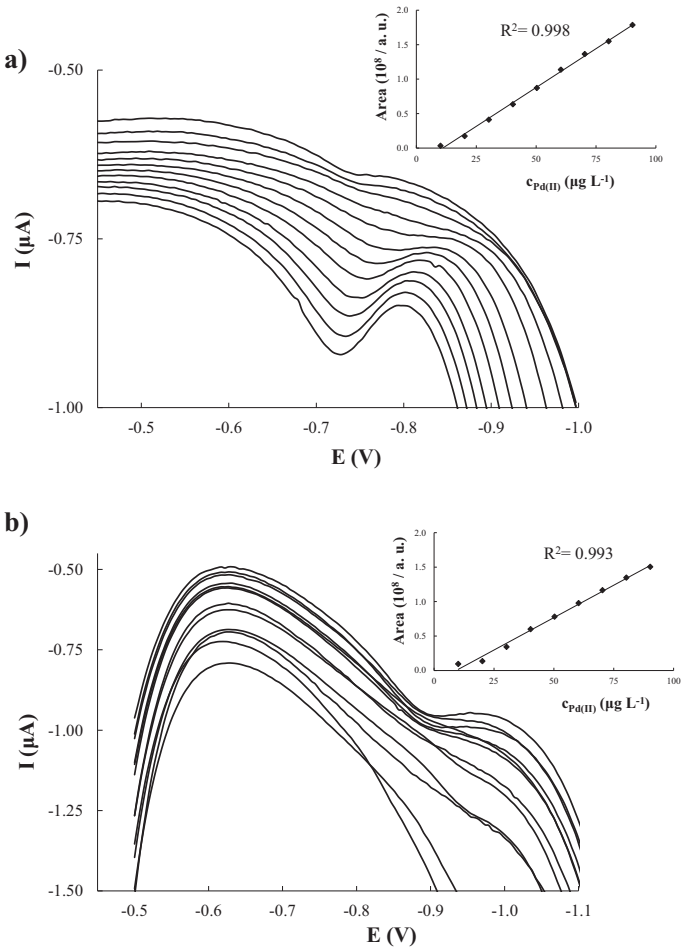

Fig. 2. Adsorptive voltammograms and calibration plots (inset) of Pd(II)-DMG system in 0.1 mol L^{-1} acetate buffer (pH 4.5) and 2×10^{-4} mol L^{-1} DMG: (a) *Ex-situ* SbSPCE; and (b) Bi_{sp}SPE.

Table 1
Calibration data for the determination of Pd(II) by DPAdSV on *ex-situ* SbSPCE and Bi_{sp}SPE at 0.1 mol L^{-1} acetate buffer (pH 4.5) and using DMG as complexing agent.

Electrode	Pd (II)			
	Sensitivity (a.u. μg^{-1} L)[a]	R^2	Linear range ($\mu g\ L^{-1}$)[b]	LOD ($\mu g\ L^{-1}$)
***Ex-situ* SbSPCE**	2.25 (0.03)	0.998	9.0–100.2	2.7
Bi_{sp}SPE	1.84 (0.05)	0.993	17.9–100.2	5.4

[a] The standard deviations are denoted by parenthesis.
[b] The lowest value of the linear range was considered from the LOQ.

carried out. Bi_{sp}SPE was selected given its commercial character and good analytical performance [28,29] as the representative bismuth screen-printed electrode. The repeatability was calculated as the relative standard deviation (RSD) of ten repetitive measurements using the same *ex-situ* SbSPCE or Bi_{sp}SPE unit yielding a RSD of 0.5% and 1.3% for *ex-situ* SbSPCE and Bi_{sp}SPE, respectively. The reproducibility estimated from three different *ex-situ* SbSPCE and Bi_{sp}SPE units within a series of ten repetitive measurements produced RSD of 1.6% and 5.0%, respectively.

Calibration plots of Pd(II)-ions ranging from 1.0 to 100.0 µg L^{-1} by AdSV on both *ex-situ* SbSPCE and Bi_{sp}SPE were constructed using a concentration of DMG as complexing agent of 2×10^{-4} mol L^{-1} and following the above optimized experimental conditions (Fig. 2A and B, respectively). When an *ex-situ* SbSPCE was used, a well-shaped and defined stripping peak close to −0.7 V was detected over the selected concentration range, whereas the use of a Bi_{sp}SPE leaded to a less symmetrical and regular signal close to −0.9 V.

Limit of detection (LOD) and limit of quantification (LOQ) were calculated as 3 and 10 times the standard deviation of the intercept over the slope of the calibration curve respectively. For their determination twelve standard concentrations of Pd(II) were used as calibration samples. The corresponding LOQ was established as the lowest value of the linear concentration range. As shown in Table 1, good linear responses of peak area *vs* Pd(II) concentration were achieved using both *ex-situ* SbSPCE and Bi_{sp}SPE and similar sensitivities (a.u./

μg L^{-1}), obtained as the slope value of the calibration curves of Pd(II), were attained. However, although LODs reached for Pd(II) were at μg L^{-1} level for both *ex-situ* SbSPCE and Bi_{sp}SPE, the LOD value obtained using the *ex-situ* SbSPCE was better than that provided by the Bi_{sp}SPE.

As it is shown in Table 1, although sensitivities are similar, a lower LOQ was achieved using *ex-situ* SbSPCE, resulting consequently in a wider linear range. Therefore, the described calibration data, together with the much better signal resolution, shape and symmetry and, the notably repeatability and reproducibility, suggest that *ex-situ* SbSPCE could be a better sensor than Bi_{sp}SPE for Pd(II) determination.

Regarding previous results, the LOD obtained for the determination of Pd(II) with an *ex-situ* SbSPCE is slightly higher in comparison to that achieved by AdSV using DMG as chelating agent with a cylindrical silver-based amalgam film electrode (Hg(Ag)-FE), 0.15 μg L^{-1} [17]. Nevertheless, it should be pointed out that in contrast: i) the Hg(Ag)-FE repeatability is significantly worse (3.0%); ii) Hg(Ag)-FE presents a shorter linear range (1–50 μg L^{-1}); and iii) unlike Hg(Ag)-FE, SPCEs which are the basis of *ex-situ* SbSPCE, do not require any polishing prior Sb deposition, with the plus of the environmental friendly character related to antimony electrodes [21]. Regarding the determination of Pd(II) using other bismuth film electrodes (BiFE), somewhat lower LODs were achieved using a glassy carbon bismuth film electrode (0.12 μg L^{-1}) [22], a SPCE coated with a bismuth film (0.008 μg L^{-1}) [23], or a glassy carbon electrode coated with bismuth-silver bimetallic nanoparticles (0.19 ng L^{-1}) [24]. However, it should be mentioned that in the present work the obtained linear range is much wider and less restricted to lower concentrations (until 100.0 μg L^{-1}) than values obtained in [22] (until 2.5 μg L^{-1}), in [23] (until 0.1 μg L^{-1}) and especially in [24] (until 1 ng L^{-1}). Moreover, the reproducibility reported using Bi film modified SPCE (BiSPCE), the unique reported electrode based on SPEs for Pd(II) determination, is really poor (8.95%) [23] compared to that obtained in this study with *ex-situ* SbSPCE (1.6%). Regarding the determination of Pd(II) with other antimony-based electrode contributions, a glassy carbon electrode modified with a composite of reduced graphene oxide impregnated with antimony nanoparticles (GCE/rGO-SbNPs) [25] provides a detection limit of 0.45 pg L^{-1}, which is considerable lower that the LOD obtained in this study. However, the examined concentration range using GCE/rGO-SbNPs is severely restricted to extremely low concentrations (40–400 pg L^{-1}) and the repeatability is again significantly worse (4.2%). Finally, it is worth noting that no studies are reported in the literatures about the use of Sb film based- electrodes for Pd(II) determination.

In the last decades a marked increase of palladium in the environment due to the increasing use of catalytic converters in automobiles has been shown in air and dust samples, i.e. the concentration of palladium in a roadside dust sample of South East England was 70 ng g^{-1} (mean) or a tunnel dust sample of Munich (Germany) was 100 ng g^{-1} (mean) [1,2]. Thus, the reported analytical performance suggests that the use of an *ex-situ* SbSPCE at the aforementioned conditions can be fully appropriate for the determination of Pd(II) at ppb levels in natural samples. In addition, the modification of a SPCE support via a film deposition is easier, less time consuming and cheaper than the preparation of a GCE modified with a nanocomposite [21]. Moreover, the *ex-situ* plating or preplated method in comparison with the *in-situ* deposition modality is also a good option if the metal speciation in the sample can be disturbed by the presence of Sb(III)-ions, with the plus that the screen-printed electrode configuration allows an easy connection to portable instrumentation making possible *on-site* analysis.

3.3. Interference study

The study of the effect of interferences is important because some metal ions can interfere with the determination of Pd(II) by complexing competitively with DMG or producing reduction peaks that overlap with or even totally suppress the Pd(II) peak. In this paper, the potential interference of Co(II), Fe(III) and Ni(II) as commonly occurring interfering ions was studied using *ex-situ* SbSPCE under the optimum conditions detailed above. From the obtained AdSV measurements until a 100:1 Co(II)-to-Pd(II) ratio it seems that Co(II) does not interfere with Pd(II) peak. It is also shown from the obtained results that in the case of Fe(III) and Ni(II) – ions the presence of similar concentrations of Pd(II) and the interfering metal ion generates a decrease on the peak area of Pd(II) close to 20%. Higher Fe(III) or Ni(II) concentration ratios produce a progressive reduction of Pd(II) peak area. This loss is about 50% for a concentration ratio of 100:1 Fe(III)-to-Pd(II), whereas for the same Ni(II)-to-Pd(II) ratio the Pd(II) peak is practically suppressed.

Compared with previous reported results using a BiSPCE, as an example of other based-SPE, the presence of Ni(II) and Fe(III) as interfering ions delivered similar effect in the Pd(II) determination [23]. In contrast, in the proposed method for Pd(II)-DMG determination using an *ex-situ* SbSPCE Co(II) does not interfere.

3.4. Tap water analysis

At the view of the preceding results, the *ex-situ* SbSPCE was considered for the determination of Pd(II) in natural waters and its applicability was tested on a spiked tap water. The determination of Pd(II) - ions was carried out by means of the standard addition method. AdSV measurements using the aforementioned conditions were performed, including four metal additions. Fig. 3 shows representative adsorptive voltammograms acquired in the analysis of the spiked tap water using *ex-situ* SbSPCE. Well- shaped peaks for the Pd(II) - ions were obtained and, as it is shown in inset of Fig. 3, good correlation of the representative AdSV measurements was also observed for Pd(II).

Three AdSV replicates of the tap water were analysed using *ex-situ* SbSPCE. The obtained results are summarised in Table 2. A good concordance, inferred by the obtained RSD%, was attained between the different replicates. In order to test the accuracy of the proposed AdSV method the sample was also analysed by ICP-MS, a well-established technique for the determination of metals, and the results obtained from both techniques were statistically compared. In this sense, a two-tailed *t*-test (equal variances) was carried out and it was concluded that the *ex-situ* SbSPCE and ICP-MS for a confidence level of 95% provide statistically similar results.

Thus, these results confirm the suitability of *ex-situ* SbSPCE for the determination of Pd(II) in natural samples, being a valuable alternative to other electrodes such as mercury or bismuth based- electrodes for the determination of Pd(II) at ppb levels in samples of environmental interest. Moreover, adsorptive stripping voltammetric measurements using an *ex-situ* SbSPCE are proposed as a cheaper and interesting alternative to more conventional techniques such as ICP-MS.

4. Conclusions

The proposed AdSV method for the determination of Pd(II) is the first approach on Sb film-based electrodes with the additional advantage of using a low-cost commercially available SPCE as a support. In this study the analytical performance of the *ex-situ* SbSPCE was compared with a commercial Bi_{sp}SPE, concluding that the *ex-situ* SbSPCE behaves much better for the determination of Pd(II) at μg L^{-1} levels. Regarding the unique SPE-based approach for Pd(II) determination previously reported, although the detection limit achieved using the *ex-situ* SbSPCE is somewhat higher it is essential to note that the reproducibility estimated from different *ex-situ* SbSPCE unit is so much better (it presents also an excellent repeatability) and, the examined linear concentration range is much wider. Moreover, *ex-situ* SbSPCE signifies a notable improvement in comparison with the other reported antimony-based electrode contributions, since the deposition

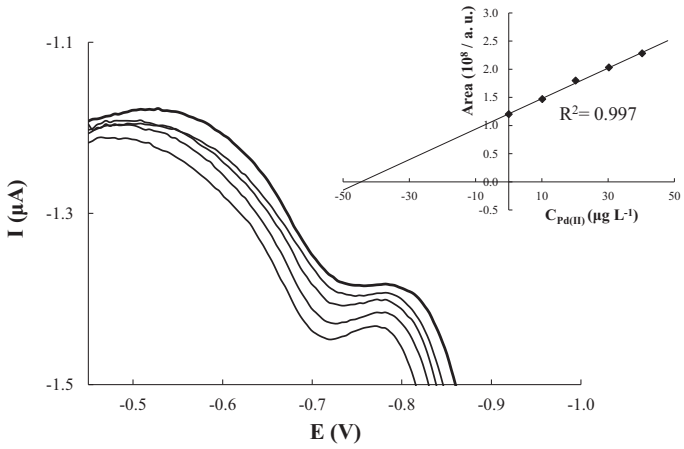

Fig. 3. AdSV measurements in tap water samples on *ex-situ* SbSPCE at pH 4.5 and 2×10^{-4} mol L^{-1} DMG using an E_{acc} of −0.6 V during a t_{acc} of 180 s and an E_i of −0.45 V. Inset: Pd(II) standard addition plot.

Table 2
Total concentration of Pd(II) determined in tap water samples by DPAdSV on *ex-situ* SbSPCE by standard addition calibration method applying an E_{acc} of −0.6 V and t_{acc} of 180 s at 0.1 mol L^{-1} acetate buffer (pH 4.5) and by ICP-MS.

	Pd (II)	
	$c_{Pd\ (II)}$ (µg L^{-1})	RSD (%)
DPAdSV	178.6	0.2
ICP-MS	178.4	0.3

n=3 for RSD (%).

of the Sb film on a SPCE does not require a pre-polishing of the carbon screen-printed surface, which is imperative when a glassy carbon electrode is used as a support. Moreover, *ex-situ* SbSPCE has also the characteristic features of SPEs such as commercial availability, low-cost, disposable character and the easy portability that makes feasible the *on-site* analysis.

The viability of the AdSV method using the *ex-situ* SbSPCE for Pd(II) determination using DMG was demonstrated using a spiked tap water sample with a very good reproducibility inferred by the RSD (%), providing also comparable results to those obtained by ICP-MS measurements.

Therefore, the above described results suggest that *ex-situ* SbSPCE can be fully suitable for the determination of Pd(II) at ppb levels in environmental samples, particularly considering the reports concerning the increased palladium concentrations in autobahns in the last decades [1–3].

Acknowledgments

This work is supported by the Ministry of Economy and Competitiveness (Project CTQ2012-32863) and the Generalitat de Catalonia (Project 2014SGR269). Clara Pérez-Ràfols acknowledges the Ministry of Education, Culture and Sports for a Ph.D. grant.

References

[1] J. Kielhorn, C. Melber, D. Keller, I. Mangelsdorf, Palladium-A review of exposure and effects to human health, Int. J. Hyg. Environ. Health 205 (2002) 417–432.
[2] H. Satoh, Palladium, in: G.F. Nordberg, B.A. Fowler, M. Nordberg, L. Friberg (Eds.), Handbook on the Toxicology of Metalsthird edition, Academic Press, Elsevier, USA, 2007, pp. 759–768.
[3] C. Melber, D. Keller, I. Mangelsdorf, Palladium: Environmental Health Criteria 226, World Health Organization, Geneva, 2002.
[4] A. Niazi, B. Jafarian, J. Ghasemi, Kinetic spectrophotometric determination of trace amounts of palladium by whole kinetic curve and a fixed time method using resazurine sulfide reaction, Spectrochim. Acta A 71 (2008) 841–846.
[5] M. Mohamadi, A. Mostafavi, A novel solidified floating organic drop microextraction based on ultrasound-dispersion for separation and preconcentration of palladium in aqueous samples, Talanta 81 (2010) 309–313.
[6] C.B. Ojeda, F.S. Rojas, J.M.C. Pavon, On-line preconcentration of palladium(II) using a microcolumn packed with a chelating resin, and its subsequent determination by graphite furnace atomic absorption spectrometry, Microchim. Acta 158 (2007) 103–110.
[7] O. Guillard, F. Favreau, B. Fauconneau, A. Chantreau, A. Pineau, Performance of ammonium dihydrogenphosphate–palladium nitrate by graphite furnace atomic absorption spectrophotometer with Zeeman correction for optimized urinary manganese determination in a biological laboratory, Anal. Biochem. 362 (2007) 284–286.
[8] H. Lin, Z.J. Huang, Q. Hu, G. Yang, G. Zhang, Determination of palladium, platinum, and rhodium by HPLC with online column enrichment using 4-carboxylphenyl-thiorhodanine as a precolumn derivatization reagent, J. Anal. Chem. 62 (2007) 58–62.
[9] M.R. Jamali, Y. Assadi, F. Shemirani, M. Salavati-Niasari, Application of thiophene-2-carbaldehyde-modified mesoporous silica as a new sorbent for separation and preconcentration of palladium prior to inductively coupled plasma atomic emission spectrometric determination, Talanta 71 (2007) 1524–1529.
[10] A.A. Ensafi, M. Keyvanfard, Kinetic-spectrophotometric determination of palladium in hydrogenation catalyst by its catalytic effect on the oxidation of pyrogallol red by hydrogen peroxide, Spectrochim. Acta A 58 (2002) 1567–1572.
[11] F. Shemirani, R.R. Kozani, M.R. Jamali, Y. Assadi, M.R.M. Hosseini, Cloud-point extraction, preconcentration, and spectrophotometric determination of palladium in water samples, Int. J. Environ. Anal. Chem. 86 (2006) 1105–1112.
[12] J. Wang, Stripping analysis: principles, instrumentation and applications, VCH, Deerfield Beach, FL, 1985.
[13] Z. Taleat, A. Khoshroo, M. Mazloum-Ardakani, Screen-printed electrodes for biosensing: a review (2008–2013), Microchim. Acta 181 (2014) 865–891.
[14] J. Barton, M.B.G. García, D.H. Santos, P. Fanjul-Bolado, A. Ribotti, M. McCaul, D. Diamond, P. Magni, Screen-printed electrodes for environmental monitoring of heavy metal ions: a review, Microchim. Acta 183 (2016) 503–517.
[15] A. Hayat, J.L. Marty, Disposable screen printed electrochemical sensors: Tools for environmental monitoring, Sensors 14 (2014) 10432–10453.
[16] C. Locatelli, Voltammetric analysis of trace levels of platinum group metals – principles and applications, Electroanalysis 19 (2007) 2167–2175 (and references therein).
[17] A. Bobrowski, M. Gawlicki, P. Kapturski, V. Mirceski, F. Spasovski, J. Zarębski, The silver amalgam film electrode in adsorptive stripping voltammetric determination of palladium(II) as its dimethyldioxime complex, Electroanalysis 21 (2009) 36–40.
[18] J. Wang, Stripping Analysis at bismuth electrodes: a review, Electroanalysis 17 (2005) 1341–1346.
[19] A. Economou, Bismuth-film electrodes: recent developments and potentialities for electroanalysis, Trends Anal. Chem. 24 (2005) 334–340.
[20] N. Serrano, A. Alberich, J.M. Díaz–Cruz, C. Ariño, M. Esteban, Coating methods, modifiers and applications of bismuth screen-printed electrodes, Trends Anal. Chem. 46 (2013) 15–29.
[21] N. Serrano, J.M. Díaz-Cruz, C. Ariño, M. Esteban, Antimony-based electrodes for analytical determinations, Trends Anal. Chem. 77 (2016) 203–213.

[22] C. van der Horst, B. Silwana, E. Iwuoha, V. Somerset, Stripping voltammetric determination of palladium, platinum and rhodium in freshwater and sediment samples from South African water resources, J. Envir. Sci. Health A 47 (2012) 2084–2093.
[23] B. Silwana, C. van der Horst, E. Iwuoha, V. Somerset, Screen-printed carbon electrodes modified with a bismuth film for stripping voltammetric analysis of platinum group metals in environmental samples, Electrochim. Acta 128 (2014) 119–127.
[24] C. Van, der Horst, B. Silwana, E. Iwuoha, V. Somerset, Bismuth–silver bimetallic nanosensor application for the voltammetric analysis of dust and soil samples, J. Electroanal. Chem. 752 (2015) 1–11.
[25] B. Silwana, C. van der Horst, E. Iwuoha, V. Somerset, Reduced graphene oxide impregnated antimony nanoparticle sensor for electroanalysis of platinum group metals, Electroanalysis 28 (2016) 1597–1607.
[26] C. Barceló, N. Serrano, C. Ariño, J.M. Díaz-Cruz, M. Esteban, Ex-situ antimony screen-printed carbon electrode for voltammetric determination of Ni(II) - ions in wastewater, Electroanalysis 28 (2016) 640–644.
[27] N. Serrano, J.M. Díaz-Cruz, C. Ariño, M. Esteban, Ex-situ deposited bismuth film on screen printed carbon electrode: a disposable device for stripping voltammetry of heavy metal ions, Electroanalysis 22 (2010) 1460–1467.
[28] V. Sosa, N. Serrano, C. Ariño, J.M. Díaz-Cruz, M. Esteban, Voltammetric determination of Pb(II) and Cd(II) ions in well water using a sputtered bismuth screen-printed electrode, Electroanalysis 26 (2014) 2168–2172.
[29] V. Sosa, N. Serrano, C. Ariño, J.M. Díaz-Cruz, M. Esteban, Sputtered bismuth screen-printed electrode: a promising alternative to other bismuth modifications in the voltammetric determination of Cd(II) and Pb(II) - ions in groundwater, Talanta 119 (2014) 348–352.

Ag nanoparticles drop-casting modification of screen-printed electrodes for the simultaneous voltammetric determination of Cu(II) and Pb(II).

C. Pérez-Ràfols, J. Bastos-Arrieta, N. Serrano, J. M. Díaz-Cruz, C. Ariño, J. de Pablo, M. Esteban

Sensors 17 (2017) 1458-1469 (*Open Access*)

https://doi.org/10.3390/s17061458

sensors

MDPI

Article

Ag Nanoparticles Drop-Casting Modification of Screen-Printed Electrodes for the Simultaneous Voltammetric Determination of Cu(II) and Pb(II)

Clara Pérez-Ràfols [1], Julio Bastos-Arrieta [2,3], Núria Serrano [1], José Manuel Díaz-Cruz [1,*], Cristina Ariño [1], Joan de Pablo [2,3,4] and Miquel Esteban [1]

1 Departament d'Enginyeria Química i Química Analítica, Facultat de Química, Universitat de Barcelona, Martí i Franquès 1-11, 08028 Barcelona, Spain; claraperezrafols@ub.edu (C.P.-R.); nuria.serrano@ub.edu (N.S.); cristina.arino@ub.edu (C.A.); miquelestebanc@ub.edu (M.E.)

2 Departament d'Enginyeria Química, Universitat Politècnica de Catalunya (UPC), Campus Diagonal Besòs, Edificio I (EEBE), Carrer Eduard Maristany 10-14, 08019 Barcelona, Spain; julio.bastos@upc.edu (J.B.-A.); joan.de.pablo@upc.edu (J.d.P.)

3 Barcelona Research Center for Multiscale Science and Engineering, 08019 Barcelona, Spain

4 Fundació CTM Centre Tecnològic, Plaça de la Ciència 2, 08240 Manresa, Spain

* Correspondence: josemanuel.diaz@ub.edu; Tel.: +34-93-402-1796

Received: 5 May 2017; Accepted: 17 June 2017; Published: 21 June 2017

Abstract: A new silver nanoparticle modified screen-printed electrode was developed and applied to the simultaneous determination of Pb(II) and Cu(II). Two different types of silver nanoparticles with different shapes and sizes, Ag nanoseeds and Ag nanoprisms, were microscopically characterized and three different carbon substrates, graphite, graphene and carbon nanofibers, were tested. The best analytical performance was achieved for the combination of Ag nanoseeds with a carbon nanofiber modified screen-printed electrode. The resulting sensor allowed the simultaneous determination of Pb(II) and Cu(II) at trace levels and its applicability to natural samples was successfully tested with a groundwater certified reference material, presenting high reproducibility and trueness.

Keywords: silver nanoparticles; screen-printed electrodes; anodic stripping voltammetry; metal ions; nanoparticle drop-casting

1. Introduction

Voltammetric stripping techniques have been widely applied to trace metal ions determination because they present excellent detection limits, great sensitivity to the presence of different metals and capacity to multimetal determination with a relatively low cost [1]. For several decades, these techniques mainly used the hanging mercury drop electrode (HMDE) as a working electrode. HMDE presents several advantages such as new drops being formed continuously, which avoids problems related to contamination, its great reproducibility or its extensive cathodic potential range (from +0.4 V to −2.5 V according to supporting electrolyte) among others [2]. However, potential toxicity risks associated to mercury use and disposal, together with the difficulty to adapt HMDE to sensor devices and flow systems, have led to the introduction of new working electrode materials throughout the years.

Bismuth film electrodes (BiFE) were proposed in 2000 as an alternative to HMDE since they offered properties close to those of mercury with the advantages of being more environmentally friendly and easily adaptable to sensor devices and flow systems [3]. BiFE, though, presents a narrower anodic potential range since the stripping peak of bismuth appears at −0.3 V. This fact prevents the use of BiFE prepared via ex situ plating or preplated method to the determination of more easily oxidizable metals like Cu(II), whereas the in situ BiFE approach, where Bi(III) ions are electrochemically deposited

on the electrode surface during the analysis, cannot be used to the determination of copper either because Bi(III) and Cu(II) ions compete for the surface sites [4,5].

The anodic potential range was slightly extended with the introduction of antimony film electrodes (SbFE) in 2007 since the stripping peak of antimony does not appear until −0.1 V [6]. This potential range, though, is still not wide enough to allow the determination of copper with an ex situ SbFE approach. Better results were obtained with an SbFE prepared via in situ, where Cu(II) was successfully determined [7]. However, the use of in situ SbFEs implies the addition of Sb(III) ions to the sample solution, causing a slight overlapping between both the Cu(II) and the Sb(III) peaks, which is not an ideal situation.

Other types of working electrodes like solid electrodes or chemically modified electrodes (CME) have been successfully applied to the determination of Cu(II). These types of electrodes usually present a much wider anodic potential range than bismuth and antimony based electrodes. Nevertheless, CMEs usually present longer manufacturing times, whereas, when working with solid electrodes, it is difficult to control their surface in a reproducible manner and the peaks appear distorted and with excessive noise [8]. It should be pointed out that the use of under potential deposition (UPD) combined with stripping techniques for analytical applications can overcome some of the major disadvantages related to solid electrodes [9].

Another field that brings more possibilities to the development of improved electrochemical sensors is the use of nanomaterials. At this small scale, materials present some unique optical, mechanical, electrical and chemical properties and, compared to electrodes based on bulk materials, nanomaterials present some enhanced properties such as increased electrode surface area, increased mass-transport rate and faster electron transfer [10]. In this sense, nanostructured modified electrodes ranging from carbon-based nanomaterials to metallic nanoparticles have been studied for metal ion determination [10–12]. Concerning metallic nanoparticles, good results have been obtained using bismuth, antimony and gold among others [10,11]. Silver nanoparticles, on the other hand, are also being explored due to their good chemical and physical properties as well as their inexpensiveness. Some good results have already been reported for the determination of Sb(III) [13], Cr(VI) [14], Pb(II) and Cd(II) [15]. Furthermore, electrodes based on silver nanoparticles present a wider anodic potential range compared to SbFEs, which makes them good candidates for the determination of Cu(II).

Silver nanoparticles electrodes can be based on different supports. In this sense, the appearance of the screen-printing technology has represented a huge progress thanks to the disposable character, good reproducibility and low-cost commercial availability of screen-printed devices. Moreover, the possibility of using a great diversity of compositions of printing inks, as well as the easy modification of their surface and the design versatility are important advantages of these devices [3,16]. These exciting benefits of screen-printed electrodes as supports over traditional based electrodes for metal ion determination have also been reported by Honeychurch et al. [17].

Inspired by both, the good properties of silver nanoparticles and the great features of screen-printed technology, in this work, we report for the first time the determination of Cu(II) with a silver-nanoparticle based- screen-printed electrode. In this reported electrode silver nanoparticles, Ag-nanoseeds and Ag-nanoprisms were simply prepared and easily incorporated to commercially available screen-printed electrodes. These silver-nanoparticles were microscopically and analytically studied. Furthermore, the determination of Pb(II) and its interaction with Cu(II) have also been considered. Additionally, the simultaneous determination of Pb(II) and Cu(II) in a certified groundwater sample was successfully achieved.

2. Materials and Methods

2.1. Chemicals

Certified reference material, groundwater (BCR®-610), was provided by Sigma-Aldrich (St. Louis, MO, USA). All other reagents used were purchased from Panreac (Barcelona, Spain) and Merck

(Darmstadt, Germany) analytical grade. Daily Cu(II) and Pb(II) standard solutions were prepared by appropriate dilution of stock solutions 10^{-2} mol·L^{-1}, prepared from $Cu(NO_3)_2 \cdot 3H_2O$ and $Pb(NO_3)_2 \cdot 4H_2O$, respectively, and complexometrically standardized [18]. Acetate buffer 0.1 mol·L^{-1} (pH 4.5) was used for pH control and ultrapure water (Milli-Q plus 185 system, Millipore, Billerica, MA, USA) was used in all experiments.

Silver nitrate, poly(sodium styrenesulphonate) (PSSS), trisodium citrate, sodium borohydride and ascorbic acid were used for the preparation of Ag-nanoseeds and Ag-nanoprims, all from Sigma-Aldrich (St. Louis, MO, USA).

2.2. Apparatus

For stripping voltammetric measurements, an Autolab System PGSTAT12 (EcoChemie, Utrecht, the Netherlands), in its multichannel configuration, attached to a Metrohm 663 VA Stand (Metrohm, Herisau, Switzerland) was used. GPES Multichannel 4.7 software package (EcoChemie, Utrecht, The Netherlands) was employed for data acquisition.

Pt wire and Ag | AgCl | KCl (3 mol·L^{-1}) (Metrohm, Herisau, Switzerland) were used as auxiliary and reference electrodes, respectively. The working electrode was either a carbon screen-printed electrode (SPCE), a carbon nanofiber modified screen-printed electrode (SPCNFE) or a graphene modified screen-printed electrode (SPGPHE) modified with silver nanoparticles and connected to the Autolab Systems by means of a flexible cable (ref. CAC, DropSens). SPCE, SPCNFE and SPGPHE were disk electrodes of 4 mm diameter purchased from Dropsens (Oviedo, Spain) (ref. 110, DS SPCE, ref. 110CNF, DS SPCE and ref. 110GPH, DS SPCE respectively).

A pH-meter Basic 20 (Crison Instruments, Barcelona, Spain) was used for pH measurements.

Surface morphology characterization was performed by a scanning electron microscope JSM 7100FE from JEOL (Tokyo, Japan).

Transmission Electron Microscopy (TEM) images were obtained using a JEM Jeol 2100 microscope (Peabody, MA, USA) at 200 kV, coupled with an Energy-Dispersive Spectrometer (Inca X-Sight from Oxford Instruments, Abingdon, UK).

2.3. Synthesis and Characterization of Ag Nanoseeds and Ag Nanoprisms

The preparation of different types of Ag nanoparticles was carried out by Seed Mediated Approach Methodology [19,20]. Seed nucleation is due to $NaBH_4$ (as strong reducing agent) that leads to the formation of small spherical nanoparticles, with trisodium citrate and PSSS as stabilizers. For nanoprism formation, ascorbic acid acts as reducing agent (softer than $NaBH_4$) with preferential axial growth in crystallization. This fact leads to the formation of the shape defined nanoprisms, with sodium tricitrate used as nanoprism stabilizer. Thus, Ag nanoseeds were produced by combining aqueous trisodium citrate (5 mL, 2.5 mmol·L^{-1}), aqueous PSSS (0.25 mL, 500 mg·L^{-1}) and aqueous $NaBH_4$ (0.3 mL, 10 mmol·L^{-1}, freshly prepared) followed by addition of aqueous $AgNO_3$ (5 mL, 0.5 mmol·L^{-1}) at a rate of 2 mL·min^{-1} while stirring continuously. Then, a specific Ag nanoprism sample was prepared by combining 5 mL distilled water, aqueous ascorbic acid (75 µL, 10 mmol·L^{-1}) and 2.5 mL of the previously synthesized Ag nanoseeds, followed by addition of aqueous $AgNO_3$ (3 mL, 0.5 mmol·L^{-1}) at a rate of 1 mL·min^{-1}. After synthesis, aqueous trisodium citrate (0.5 mL, 25 mmol·L^{-1}) was added to stabilize the particles. Milli-Q Water was used throughout all solutions.

The size distribution of the prepared nanoparticles was obtained by direct observation of the TEM images and the construction of the corresponding size distribution histograms. These measurements were performed using the ImageJ Software (1.48 V), and the histograms obtained were adjusted to a three-parameter Gaussian curve (Equation (1)), where x_0 is the mean diameter (to which most nanoparticles correspond), b is the standard deviation and a is a statistical parameter related to this fitting. Histograms were calculated using Excel 2010 (Microsoft, Redmond, WA, USA), and the

equation was adjusted with SigmaPlot 11.0 (Systat Software, San José, CA, USA). For Ag nanoprisms, heights were used as reference for the diameter value:

$$y = ae^{[-0.5(\frac{x_0-x}{b})^2]}. \quad (1)$$

2.4. Preparation of Ag-Nanoparticles-SPCNFE

Ag-nanoparticles-SPCNFE was prepared by drop-casting 40 μL of silver nanoparticles solution onto the electrode surface and drying it for 30 min at 50 °C.

2.5. Voltammetric Measurements

For voltammetric stripping determinations of Pb(II) and Cu(II) using Ag-nanoparticles-SPCNFE, both metal ions were deposited at a deposition potential (E_d) of −1.1 V, applied with stirring, during a deposition time (t_d) of 120 s. Deposition was followed by a rest period (t_r) of 5 s and then the potential was scanned from −1.1 to 0.15 V using pulse times of 50 ms, step potentials of 5 mV and pulse amplitudes of 50 mV.

Linear calibration plots for both separate and simultaneous determinations of Cu(II) and Pb(II) were performed by increasing metal ion concentrations in 0.1 mol·L^{-1} acetate buffer (pH 4.5).

The analysis of the certified groundwater sample was performed by the standard addition calibration method. First of all, a volume of the sample (BCR®-610) was adjusted to pH 4.5 with sodium acetate and the scan was recorded. Then, four aliquots of Cu(II) and Pb(II) standard solutions were added and the respective curves were recorded.

3. Results and Discussion

3.1. Electron Microscopy Characterization of Ag-Nanoparticles-SPCNFE

The incorporation of nanoparticles (NPs) in sensing systems derives to the enhancement and customization of the electrochemical features (e.g., oxidation or reduction current onto a transducing platform), which offers novel option for electroanalytical purposes in environmental and biological fields [21]. Consequently, the incorporation of Ag-NPs to commercially available screen-printed electrodes implies the increase of electrocatalytically active zones on the structure of the composite material. SEM images of the surface of SPCNFE modified with Ag-nanoseeds (Figure 1A,B) and Ag-nanoprisms (Figure 1C,D) show, in comparison to the bare SPCNFE (Figure 1E), the dispersion of these NPs all over the electrode surface (white dots). This can explain the capability to improve the electrochemical performance in comparison with the non–modified SPCNFE, as previously observed in other electrochemical systems modified with nanomaterials [22].

Seed mediated approach synthesis of nanostructures is a multistep methodology [23] based on the first fast crystallization of nanoseeds, which can be used for further nucleation and customized growth of shape defined nanoprisms of larger size [24]. TEM characterization of spherical Ag-nanoseeds (Figure 2A,B) and shaped defined Ag-nanoprisms (Figure 2C,D) provides valuable morphological information of the materials incorporated to SPCNFE matrix.

3.2. Enhanced Modification of SPE with Ag-Nanoparticles

The attachment of the silver nanoparticles to the screen-printed electrodes surface was firstly optimized using Ag-nanoseeds as a model of silver nanoparticles. Different drop volumes and drying times were tested and the best results were obtained by depositing a single drop of 40 μL of the Ag-nanoseeds solution to the electrode surface and drying it in the oven at 50 °C.

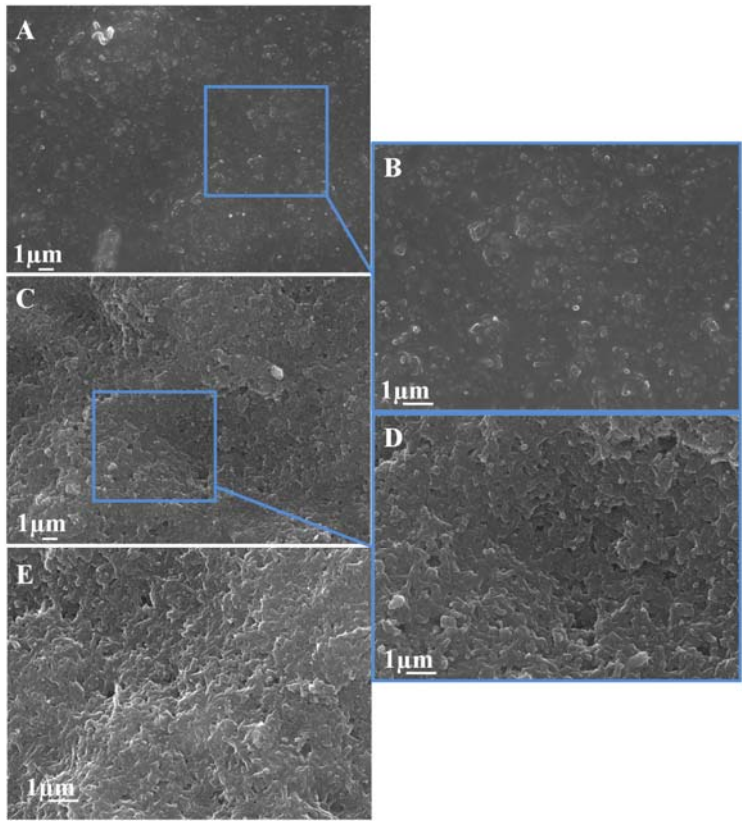

Figure 1. SEM micrographs of Ag-nanoseeds-SPCNFE (**A**,**B**), Ag-nanoprisms-SPCNFE (**C**,**D**) and bare SPCNFE (**E**). Magnification of E = A = C <<< B = D.

In order to see the enhancement of the electrochemical response provided by the silver nanoparticles screen-printed electrode, firstly, the measurements of a solution containing 100 $\mu g \cdot L^{-1}$ of Cu(II) and Pb(II) were carried out on both SPCE and Ag-nanoseeds-SPCE. As it can be seen in Figure 3, the attachment of the silver nanoparticles on the screen-printed surface considerably increases the voltammetric response for both considered metal ions, suggesting that a sensor based on the modification with Ag-nanoparticles could be a better alternative for the determination of Cu(II) and Pb(II).

Taking into account that it has been reported that the use of carbon based nanomaterials supports improves the analytical performance of sensors [25], three different carbon-based screen-printed substrates, graphite, graphene and carbon nanofibers, were compared prioritizing the repeatability and reproducibility of the resulting sensor. In this sense, stripping measurements of a solution containing 100 $\mu g \cdot L^{-1}$ of Cu(II) and Pb(II) in acetate buffer pH 4.5 were carried out. The repeatability was calculated from 10 repetitive measurements using the same Ag-nanoseeds-SPE, whereas the reproducibility was measured from three different Ag-nanoseeds-SPE units within a series of 10 repetitive measurements. Ag-nanoseeds-SPCE was the least repetitive sensor, with relative standard deviations (RSD) yielding 18.1% for Cu(II) and 20.1% for Pb(II). Better repeatability results were obtained for Ag-nanoseeds-SPCNFE (3.6% for Cu(II) and 5.5% for Pb(II)) and Ag-nanoseeds-SPGPHE (3.2% for Cu(II) and 3.1% for Pb(II)). This fact could be attributed to the enlarged surface area and

rugosity provided by the nanostructured carbon materials, which help retaining the Ag-nanoseeds onto the electrode surface.

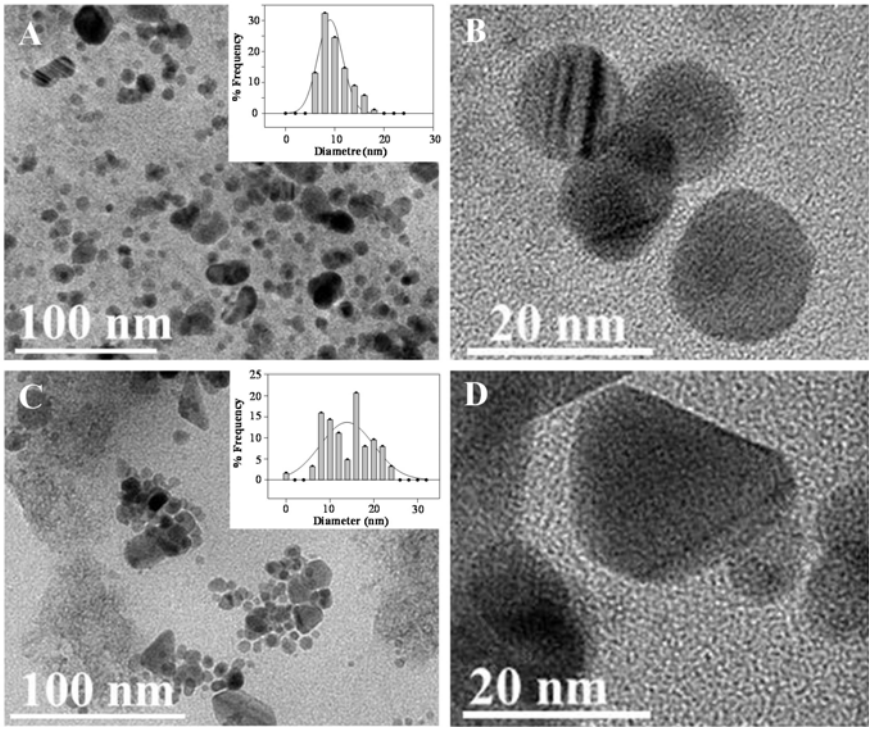

Figure 2. TEM micrographs of 9.1 ± 0.4 nm spherical Ag-nanoseeds (**A**,**B**) and triangular shaped 14.0 ± 0.9 nm Ag-nanoprisms (**C**,**D**) with the corresponding size distribution histograms (insets in **A** and **C**). Magnification of A = C <<< B = D.

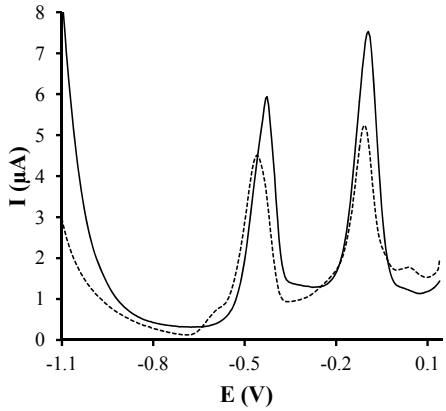

Figure 3. Stripping voltammetric measurements of a solution containing 100 $\mu g \cdot L^{-1}$ of Cu(II) and Pb(II) at pH 4.5 using an E_d of −1.1 V during a t_d of 120 s on Ag-nanoseeds-SPCE (solid line) and SPCE (dashed line).

Given the low repeatability observed for Ag-nanoseeds-SPCE, this substrate was discarded and the reproducibility was studied for both Ag-nanoseeds-SPCNFE and Ag-nanoseeds-SPGPHE. In this case, Ag-nanoseeds-SPCNFE provided better results (5.2% for Cu(II) and 8.1% for Pb(II)) compared to Ag-nanoseeds-SPGPHE (19.3% for Cu(II) and 15.2% for Pb(II)). This poor reproducibility values obtained for Ag-nanoseeds-SPGPHE could be attributed to the low homogeneity between the different units commercially purchased. This fact was previously observed for the preparation of antimony film coated on SPGPHE [26].

In view of these results, SPCNFE was selected as the optimal carbon substrate and its repeatability and reproducibility were also studied for Ag-nanoprisms, yielding 3.6% and 6.3% for Cu(II) and 5.1% and 9.3% for Pb(II), respectively. As it can be seen, similar repeatability and reproducibility were obtained for both Ag-nanoseeds and Ag-nanoprisms. Furthermore, these reproducibility values are also in agreement with reproducibility values reported with silver nanoparticles modified electrodes for Sb(III) [13], Pb(II), Cd(II) [15] and Cr(IV) [14].

3.3. Electrochemical Parameters and Calibration Data

Once the preparation of the silver nanoparticle modified electrodes was optimized, different electrochemical parameters were optimized for the simultaneous determination of Pb(II) and Cu(II). In this sense, stripping measurements of a solution containing 100 $\mu g \cdot L^{-1}$ of Cu(II) and Pb(II) in acetate buffer pH 4.5 were carried out at several deposition potentials (E_d) ranging from -0.6 to -1.2 V and using a deposition time (t_d) of 120 s as a compromise between peak area and analysis time. When applying E_d between -0.6 V and -0.9 V, two overlapped peaks were observed in the copper oxidation region. The reasons for such behavior are not clear but could be related to the stabilization of Cu(I) onto the electrode surface. Anyway, using more negative E_d, a single peak clearly corresponding to the Cu(II) oxidation was observed. This peak increased when the E_d was shifted from -0.95 to -1.1 V and decreased at more negative potentials. Therefore, an E_d of -1.1 V was selected as the optimal for the determination of Cu(II) and Pb(II).

The anodic range of the Ag-nanoparticles-SPCNFE was also studied. It was observed that the stripping peak associated to Ag/Ag(I) did not appear until 0.2 V, which perfectly allows the determination of Cu(II) which appears at ca. -0.11 V. It should be pointed out that this anodic range is wider than that provided by a silver screen-printed electrode where the stripping peak associated to the oxidation of Ag appears at ca. -0.03 V. This fact is in agreement with the behavior showed by a rotating silver electrode [25], where Cu(II) cannot either be determined and could be attributed to nanomaterials having different redox potentials than bulk materials [27].

Once the electrochemical parameters were optimized, separate calibrations of Cu(II) and Pb(II) were carried out on both Ag-nanoseeds-SPCNFE and Ag-nanoprisms-SPCNFE sensors (Figure 4). Table 1 reports the sensitivities, correlations, linear ranges and limits of detections (LOD) obtained. Sensitivities were calculated as the slope of the calibration curve, whereas LODs and LOQs were calculated as three and ten times, respectively, the standard deviation of the intercept over the slope. As it can be observed, Ag-nanoprisms-SPCNFE provides lower sensitivities compared to Ag-nanoseeds-SPCNFE, which also presents slightly better LODs. This fact could be attributed to the spherical shape of Ag-nanoseeds, which provides a larger surface area, as well as to the wetting behavior of the nanoparticle containing solutions that leads to a more homogeneously distributed layer. Nevertheless, in both cases, the obtained LODs are similar or even better than those provided in the literature using CMEs [28,29], in situ SbFE [7,30,31] or silver nanoparticles based electrodes [32] for Cu(II) and CMEs [28,33,34], SbFEs [6], BiFEs [3] or silver nanoparticles based electrodes [15,32] for Pb(II). It should also be pointed out that, although the linear range for Cu(II) is similar for both Ag-nanoseeds-SPCNFE and Ag-nanoprisms-SPCNFE, in the case of Pb(II), the electrode surface is easily saturated when the Ag-nanoprisms-SPCNFE is used, which results in a significantly narrower linear range.

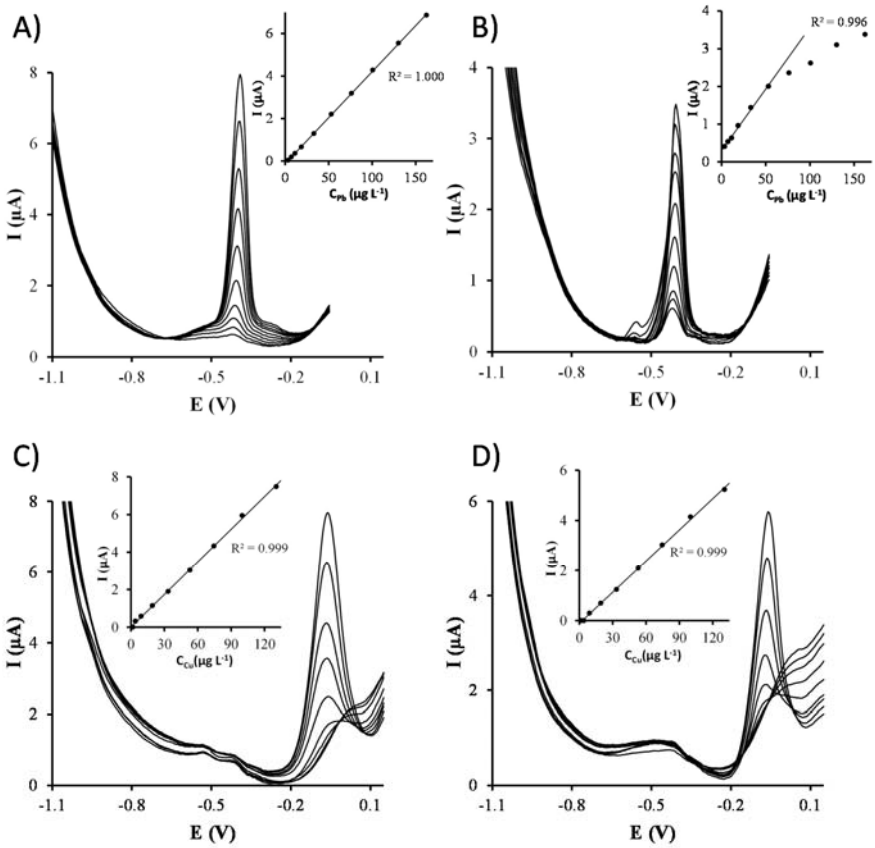

Figure 4. Stripping voltammetric measurements and calibration curves (insets) obtained for the individual calibration of Pb(II) (**A**,**B**) and Cu(II) (**C**,**D**) in acetate buffer pH 4.5 using an Ag-nanoseeds-SPCNFE (**A**,**C**) and an Ag-nanoprisms-SPCNFE (**B**,**D**) at an E_d of −1.1 V and a t_d of 120 s.

Table 1. Calibration data for both separate and simultaneous determination of Pb(II) and Cu(II) on Ag-nanoseeds-SPCNFE and Ag-nanoprisms-SPCNFE at E_d of −1.1 V, t_d of 120 s and pH 4.5. The standard deviations are denoted by parenthesis.

	Separate		Simultaneous	
	Pb(II)	**Cu(II)**	**Pb(II)**	**Cu(II)**
Ag-nanoseeds-SPCNFE				
Sensitivity ($nA \cdot \mu g^{-1} \cdot L$)	43.3 (0.2)	57.5 (0.7)	43 (1)	73 (2)
R^2	1.000	0.999	0.998	0.998
Linear range [1] ($\mu g \cdot L^{-1}$)	3.2–162.5	7.6–130.7	6.6–53.5	10.0–77.0
LOD ($\mu g \cdot L^{-1}$)	0.96	2.29	1.98	2.99
Ag-nanoprisms-SPCNFE				
Sensitivity ($nA \cdot \mu g^{-1} \cdot L$)	32.3 (0.9)	41.4 (0.6)	25.9 (0.7)	34.4 (0.5)
R^2	0.996	0.999	0.997	0.999
Linear range [1] ($\mu g \cdot L^{-1}$)	7.3–53.1	9.9–130.7	7.8–53.5	8.3–100.7
LOD ($\mu g \cdot L^{-1}$)	2.20	2.98	2.35	2.49

[1] The lowest value of the linear range was considered from LOQ.

In order to study the interaction between Cu(II) and Pb(II) ions, simultaneous calibrations of both target metal ions were also carried out on Ag-nanoseeds-SPCNFE and Ag-nanoprisms-SPCNFE (Figure 5 and Table 1). It can be observed that both metals interact with each other, resulting in changes of the sensitivities as compared to separate calibrations. The most notorious thing, though, is the shortening of the linearity range probably caused by the competition of Cu(II) and Pb(II) for the active sites of the electrode surface.

Although both Ag-nanoseeds-SPCNFE and Ag-nanoprisms-SPCNFE present a similar analytical performance regarding repeatability, reproducibility, linear range and LODs, the higher sensitivities achieved by Ag-nanoseeds-SPCNFE together with the fact that Ag-nanoseeds require fewer steps to be synthesized than Ag-nanoprisms, Ag-nanoseeds-SPCNFE was selected to test its applicability in natural samples.

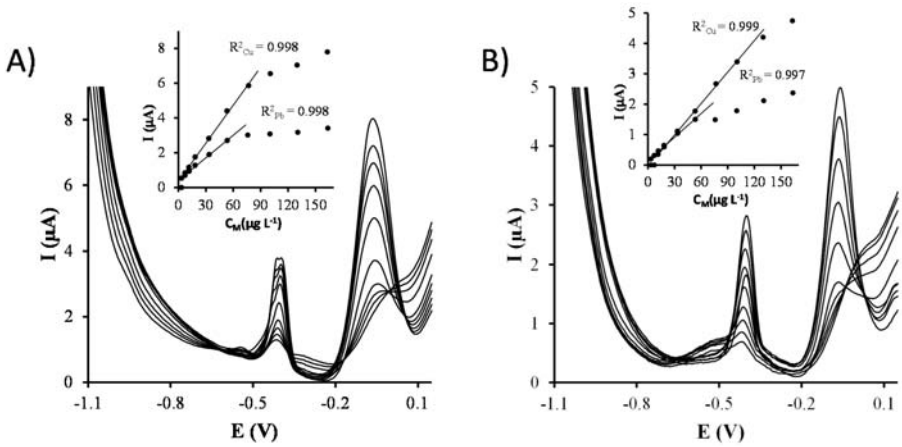

Figure 5. Stripping voltammetric measurements and calibration curves (insets) obtained for the simultaneous calibration of Pb(II) and Cu(II) in acetate buffer pH 4.5 using an Ag-nanoseeds-SPCNFE (**A**) and an Ag-nanoprisms-SPCNFE (**B**) at an E_d of −1.1 V and a t_d of 120 s.

3.4. Application to the Analysis of a Groundwater Reference Material

In view of the above discussed results, Ag-nanoseeds-SPCNFE was considered for the determination of Cu(II) and Pb(II) in natural samples. Thus, the applicability of this sensor was tested by simultaneously determining Pb(II) and Cu(II) in a groundwater certified reference material (BCR®-610). Figure 6 shows representative voltammograms for the simultaneous analysis of Cu(II) and Pb(II) in the groundwater reference material. Pb(II) and Cu(II) concentrations were determined using the standard addition method, and, as it can be observed, well defined peaks were obtained for both target ions like in the calibration samples.

Calibration curves for both Pb(II) and Cu(II) are shown in the inset of Figure 6. Good correlations were obtained in both cases. Three replicates of the simultaneous voltammetric determination of Cu(II) and Pb(II) in the groundwater certified material using Ag-nanoseeds-SPCNFE were carried out. The obtained concentration data is reported in Table 2. As it can be observed, good concordance between the replicates, inferred by the relative standard deviation (RSD), and with the certified metal ion concentration values were achieved. It should be mentioned that this groundwater material also contains other metal ions including cadmium, arsenic, aluminium and nickel, which do not seem to interfere in the voltammetric determination of Cu(II) and Pb(II) using Ag-nanoseeds-SPCNFE.

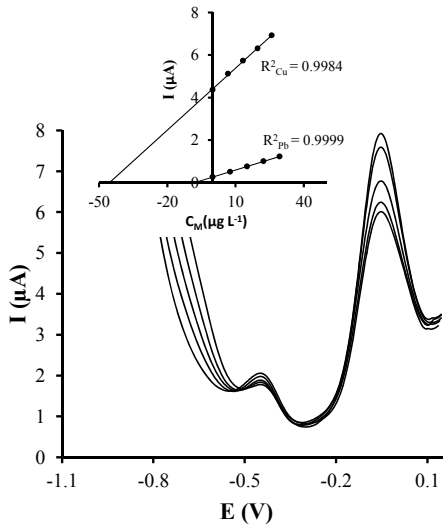

Figure 6. Stripping voltammetric measurements in groundwater samples on Ag-nanoseeds-SPCNFE at pH 4.5 using an E_d of −1.1 V during a t_d of 120 s. Inset: Pb(II) and Cu(II) standard calibration plots.

Table 2. Total concentrations of Pb(II) and Cu(II) determined in certified groundwater (BCR®-610) by stripping voltammetry on Ag-nanoseeds-SPCNFE by the standard addition calibration method applying an E_d of −1.1 V and t_d of 120 s at pH 4.5.

	Lead(II)			Copper(II)		
	c ($\mu g \cdot L^{-1}$)	RSD (%)	Relative Error (%)	c ($\mu g \cdot L^{-1}$)	RSD (%)	Relative Error (%)
Ag-nanoseeds-SPCNFE	7.83	2.94	0.64	45.6	1.2	0.2
Certified metal value	7.78	1.67	—	45.7	3.3	—

The achieved results confirm the applicability of the developed Ag-nanoseeds-SPCNFE for the simultaneous determination of Cu(II) and Pb(II) in natural samples at $\mu g \cdot L^{-1}$ levels. Therefore, Ag-nanoseeds-SPCNFE could be an interesting and valuable alternative to more conventional electrodes for the determination of metal ions, particularly in the case of Cu(II) where antimony and bismuth electrodes present some problems.

4. Conclusions

In this work, two different types of silver nanoparticles, Ag-nanoseeds and Ag-nanoprisms, were microscopically characterized and considered for the modification of carbon-based screen-printed electrodes and their application to the determination of Cu(II) and Pb(II). It should be pointed out that, in contrast to more sophisticated modification strategies, the incorporation of the silver nanoparticles to the electrode surface is based on a fast and easy procedure where silver nanoparticles solution is directly drop-casted.

The resulting sensors were microscopically and analytically characterized and compared to each other. Three different carbon substrates were tested and SPCNFE was selected because it provided better repeatability and reproducibility. Concerning the type of silver nanoparticle, both Ag-nanoseeds-SPCNFE and Ag-nanoprisms-SPCNFE provided similar repeatability, reproducibility, linear range and LODs. However, Ag-nanoseeds-SPCNFE showed higher sensitivities and their synthesis is easier.

Furthermore, Ag-nanoseeds-SPCNFE was successfully applied to the simultaneous determination of Cu(II) and Pb(II) in a groundwater certified reference material, providing good reproducibility and trueness inferred by the RSD (2.94% for Pb(II) and 1.2% for Cu(II)) and the relative error (0.64% for Pb(II) and 0.2% for Cu(II)), respectively. Therefore, these good results confirm the applicability of Ag-nanoseeds-SPCNFE for the simultaneous determination of Cu(II) and Pb(II) in natural samples.

Acknowledgments: This work is supported by the University of Barcelona, by the Spanish Ministry of Economy and Competitiveness (MINECO, Spain) for Project ENE2014-54299-C2-1-R and by the Generalitat of Catalonia (Project 2014SGR269). Clara Pérez-Ràfols acknowledges the Spanish Ministry of Economy and Competitiveness for a Ph.D. grant.

Author Contributions: Julio Bastos-Arrieta, Clara Pérez-Ràfols and Núria Serrano conceived and executed the experimental work. Julio Bastos-Arrieta carried out the synthesis and microscopic characterization of silver nanoparticles and Clara Pérez-Ràfols and Núria Serrano carried out the modification of screen-printed electrodes with nanoparticles, the voltammetric measurements and the data treatment. José Manuel Díaz-Cruz discussed the first results with them and suggested additional experiments with bare silver electrodes. The first draft of the manuscript was prepared by Julio Bastos-Arrieta, Clara Pérez-Ràfols and Núria Serrano, and it was revised and substantially improved by José Manuel Díaz-Cruz, Cristina Ariño, Joan de Pablo and Miquel Esteban.

Conflicts of Interest: The authors declare no conflict of interest.

References

1. Wang, J. *Stripping Analysis: Principles, Instrumentation and Applications*; VCH: New York, NY, USA, 1985.
2. Barek, J.; Fogg, A.G.; Muck, A.; Zima, J. Polarography and voltammetry at mercury electrodes. *Crit. Rev. Anal. Chem.* **2001**, *31*, 291–309. [CrossRef]
3. Serrano, N.; Alberich, A.; Díaz-Cruz, J.M.; Ariño, C.; Esteban, M. Coating methods, modifiers and applications of bismuth screen-printed electrodes. *Trends Anal. Chem.* **2013**, *46*, 15–29. [CrossRef]
4. Wang, J.; Lu, J.; Anik, Ü.; Hocevar, S.B.; Ogorevc, B. Insights into the anodic stripping voltammetric behavior of bismuth film electrodes. *Anal. Chim. Acta* **2001**, *434*, 29–34. [CrossRef]
5. Yang, D.; Wang, L.; Chen, Z.; Megharaj, M.; Naidu, R. Investigation of copper(II) interference on the anodic stripping voltammetry of lead(II) and cadmium(II) at bismuth film electrode. *Electroanalysis* **2013**, *25*, 2637–2644. [CrossRef]
6. Serrano, N.; Díaz-Cruz, J.M.; Ariño, C.; Esteban, M. Antimony-based electrodes for analytical determinations. *Trends Anal. Chem.* **2016**, *77*, 203–213. [CrossRef]
7. Sosa, V.; Barceló, C.; Serrano, N.; Ariño, C.; Díaz-Cruz, J.M.; Esteban, M. Antimony film screen-printed carbon electrode for stripping analysis of Cd(II), Pb(II), and Cu(II) in natural samples. *Anal. Chim. Acta* **2015**, *855*, 34–40. [CrossRef] [PubMed]
8. Uslu, B.; Ozkan, S.A. Solid electrodes in electroanalytical chemistry: Present applications and prospects for high throughput screening of drug compounds. *Comb. Chem. High Throughput Screen.* **2007**, *10*, 495–513. [CrossRef] [PubMed]
9. Herzog, G.; Arrigan, D.W. Determination of trace metals by underpotential deposition–stripping voltammetry at solid electrodes. *Trends Anal. Chem.* **2005**, *24*, 208–217. [CrossRef]
10. Aragay, G.; Merkoçi, A. Nanomaterials application in electrochemical detection of heavy metals. *Electrochim. Acta* **2012**, *84*, 49–61. [CrossRef]
11. Tukur, S.A.; Azahyusof, N. Metallic nanoparticles for modification of electrodes for heavy metals detection. *Asian J. Chem.* **2015**, *27*, 1967–1969. [CrossRef]
12. Wanekaya, A.K. Applications of nanoscale carbon-based materials in heavy metal sensing and detection. *Analyst* **2011**, *136*, 4383–4391. [CrossRef] [PubMed]
13. Arcos-Martınez, M.J.; Dominguez-Renedo, O. A novel method for the anodic stripping voltammetry determination of Sb (III) using silver nanoparticle-modified screen-printed electrodes. *Electrochem. Commun.* **2007**, *9*, 820–826. [CrossRef]
14. Xing, S.; Xu, H.; Chen, J.; Shi, G.; Jin, L. Nafion stabilized silver nanoparticles modified electrode and its application to Cr (VI) detection. *J. Electroanal. Chem.* **2011**, *652*, 60–65. [CrossRef]
15. Prakash, S.; Shahi, V.K. Improved sensitive detection of Pb^{2+} and Cd^{2+} in water samples at electrodeposited silver nanonuts on a glassy carbon electrode. *Anal. Methods* **2011**, *3*, 2134–2139. [CrossRef]

16. Barton, J.; González-García, M.B.; Hernández-Santos, D.; Fanjul-Bolado, P.; Ribotti, A.; McCaul, M.; Diamond, D.; Magni, P. Screen-printed electrodes for environmental monitoring of heavy metal ions: A review. *Microchim. Acta* **2016**, *183*, 503–517. [CrossRef]
17. Honeychurch, K.C. Screen-printed electrochemical sensors and biosensors for monitoring metal pollutants. *Insci. J.* **2012**, *2*, 1–51. [CrossRef]
18. Vogel, A.I. *Quantitative Chemical Analysis*, 5th ed.; Pearson Education Limited: Harlow, UK, 1989.
19. Aherne, D.; Ledwith, D.M.; Gara, M.; Kelly, J.M. Optical properties and growth aspects of silver nanoprisms produced by a highly reproducible and rapid synthesis at room temperature. *Adv. Funct. Mater.* **2008**, *18*, 2005–2016. [CrossRef]
20. Aherne, D.; Gara, M.; Kelly, J.M.; Gun'Ko, Y.K. From Ag Nanoprisms to Triangular AuAg Nanoboxes. *Adv. Funct. Mater.* **2010**, *20*, 1329–1338. [CrossRef]
21. Espinoza-Castañeda, M.; de la Escosura-Muñiz, A.; González-Ortiz, G.; Martín-Orúe, S.M.; Pérez, J.F.; Merkoçi, A. Casein modified gold nanoparticles for future theranostic applications. *Biosens. Bioelectron.* **2013**, *40*, 271–276. [CrossRef] [PubMed]
22. Muñoz, J.; Bastos-Arrieta, J.; Muñoz, M.; Muraviev, D.N.; Céspedes, F.; Baeza, M. CdS quantum dots as a scattering nanomaterial of carbon nanotubes in polymeric nanocomposite sensors for microelectrode array behavior. *J. Mater. Sci.* **2015**, *51*, 1610–1619. [CrossRef]
23. Nikoobakht, B.; El-Sayed, M.A. Preparation and growth mechanism of gold nanorods (NRs) using seed-mediated growth method. *Chem. Mater.* **2003**, *15*, 1957–1962. [CrossRef]
24. Pérez-Ràfols, C.; Serrano, N.; Díaz-Cruz, J.M.; Ariño, C.; Esteban, M. New approaches to antimony film screen-printed electrodes using carbon-based nanomaterials substrates. *Anal. Chim. Acta* **2016**, *916*, 17–23. [CrossRef] [PubMed]
25. Cong, H.; Yu, B.; Tang, J.; Li, Z.; Liu, X. Current status and future developments in preparation and application of colloidal crystals. *Chem. Soc. Rev.* **2013**, *42*, 7774–7800. [CrossRef] [PubMed]
26. Bonfil, Y.; Kirowa-Eisner, E. Determination of nanomolar concentrations of lead and cadmium by anodic-stripping voltammetry at the silver electrode. *Anal. Chim. Acta* **2002**, *457*, 285–296. [CrossRef]
27. Plieth, W.J. Electrochemical properties of small clusters of metal atoms and their role in the surface enhanced Raman scattering. *J. Phys. Chem.* **1982**, *86*, 3166–3170. [CrossRef]
28. Serrano, N.; González-Calabuig, A.; del Valle, M. Crown ether-modified electrodes for the simultaneous stripping voltammetric determination of Cd(II), Pb(II) and Cu(II). *Talanta* **2015**, *138*, 130–137. [CrossRef] [PubMed]
29. Liu, G.; Quynh, T.N.; Chow, E.; Böcking, T.; Hibbert, D.B.; Gooding, J.J. Study of factors affecting the performance of voltammetric copper sensors based on Gly-Gly-His modified glassy carbon and gold electrodes. *Electroanalysis* **2006**, *18*, 1141–1151. [CrossRef]
30. Bobrowski, A.; Putek, M.; Zarebski, J. Antimony film electrode prepared in situ in hydrogen potassium tartrate in anodic stripping voltammetric trace detection of Cd(II), Pb(II), Zn(II), Tl(I), In(III) and Cu(II). *Electroanalysis* **2012**, *24*, 1071–1078. [CrossRef]
31. Slavec, M.; Hocevar, S.B.; Baldrianova, L.; Tesarova, E.; Svancara, I.; Ogorevc, B.; Vytras, K. Antimony film microelectrode for anodic stripping measurement of cadmium(II), lead(II) and copper(II). *Electroanalysis* **2010**, *22*, 1617–1622. [CrossRef]
32. Sang, S.; Li, D.; Zhang, H.; Sun, Y.; Jian, A.; Zhang, Q.; Zhang, W. Facile synthesis of AgNPs on reduced graphene oxide for highly sensitive simultaneous detection of heavy metal ions. *RSC Adv.* **2017**, *7*, 21618–21624. [CrossRef]
33. Pérez-Ràfols, C.; Serrano, N.; Díaz-Cruz, J.M.; Ariño, C.; Esteban, M. Glutathione modified screen-printed carbon nanofiber electrode for the voltammetric determination of metal ions in natural samples. *Talanta* **2016**, *155*, 8–13. [CrossRef] [PubMed]
34. Pérez-Ràfols, C.; Serrano, N.; Díaz-Cruz, J.M.; Ariño, C.; Esteban, M. Penicillamine-modified sensor for the voltammetric determination of Cd(II) and Pb(II) ions in natural samples. *Talanta* **2015**, *144*, 569–573. [CrossRef] [PubMed]

Green synthesis of Ag nanoparticles using grape stalk waste extract for the modification of screen-printed electrodes.

J. Bastos-Arrieta, A. Florido, C. Pérez-Ràfols, N. Serrano, N. Fiol, J. Poch, I. Villaescusa

Nanomaterials 8 (2018) 946-959 (*Open Access*)

https://doi.org/10.3390/nano8110946

nanomaterials

MDPI

Article

Green Synthesis of Ag Nanoparticles Using Grape Stalk Waste Extract for the Modification of Screen-Printed Electrodes

Julio Bastos-Arrieta [1,2,*], Antonio Florido [1,3], Clara Pérez-Ràfols [4], Núria Serrano [4], Núria Fiol [5,*], Jordi Poch [6] and Isabel Villaescusa [5]

1 Departament d'Enginyeria Química, Escola d'Enginyeria de Barcelona Est (EEBE), Universitat Politècnica de Catalunya, BarcelonaTEch (UPC), Av. Eduard Maristany 16, 08019 Barcelona, Spain; antonio.florido@upc.edu
2 Physical Chemistry TU Dresden, Zellescher Weg 19, 01062 Dresden, Germany
3 Barcelona Research Center for Multiscale Science and Engineering, Av. Eduard Maristany 16, 08019 Barcelona, Spain
4 Departament d'Enginyeria Química i Química Analítica, Facultat de Química, Universitat de Barcelona, c/Martí i Franquès 1-11, 08028 Barcelona, Spain; claraperezrafols@ub.edu (C.P.-R.); nuria.serrano@ub.edu (N.S.)
5 Departament d'Enginyeria Química, Escola Politècnica Superior, Universitat de Girona, c/Ma Aurèlia Capmany, 61, 17071 Girona, Spain; isabel.villaescusa@udg.edu
6 Departament d'Informàtica Aplicada i Matemàtiques, Escola Politècnica Superior, Universitat de Girona, c/Ma Aurèlia Capmany, 61, 17071 Girona, Spain; jordi.poch@udg.edu
* Correspondence: julio.bastos@tu-dresden.de (J.B.-A.); nuria.fiol@udg.edu (N.F.)

Received: 20 October 2018; Accepted: 13 November 2018; Published: 17 November 2018

Abstract: The chemical synthesis of silver nanoparticles (Ag-NPs) by using an environmentally friendly methodology for their preparation is presented. Thus, considering that plants possess components that can act as reducing agents and stabilizers in nanoparticles' production, the synthesis of Ag-NPs by using an extract aqueous solution of grape stalk waste as a reducing and capping agent is studied. First, the total polyphenols and reducing sugars contained in the produced extracts at different conditions are characterized. After that, Ag-NPs are synthesized regarding the interaction of Ag ions (from silver nitrate) and the grape stalk extract. The effect of temperature, contact time, extract/metal solution volume ratio and pH solution in the synthesis of metal nanoparticles are also studied. Different sets of nanoparticle samples are characterized by means of Electron Microscopy coupled with Energy Dispersive X-Ray for qualitative chemical identification. Ag-NPs with an average diameter of 27.7 $\pm$ 0.6 nm are selected to proof their suitability for sensing purposes. Finally, screen-printed electrodes modified with Ag-NPs are tested for the simultaneous stripping voltammetric determination of Pb(II) and Cd(II). Results indicate good reproducibility, sensitivity and limits of detection around 2.7 $\mu g\ L^{-1}$ for both metal ions.

Keywords: silver nanoparticles; screen-printed electrodes; grape stalk; green synthesis; voltammetry; metal analysis

1. Introduction

Several recent publications have reviewed the greener routes to metal nanoparticles synthesis mediated by microorganisms [1], algae and waste material [2], and plant material extract [3,4]. The different routes to synthesize silver nanoparticles (Ag-NPs) have also been reviewed recently. All these routes comprise three steps: silver reduction by bioreducing agents, agglomeration and

stabilization of NPs [5]. Some authors underline the advantages of using plant derivatives extracts over microorganisms. Plant derivatives extracts have no need for cells culture maintenance nor sterile conditions [6,7]. Moreover, plant extracts provide natural capping agents for the stabilization of nanoparticles, reducing the nanoparticles synthesis process to a single step [8]. All these advantageous features of plant extracts result in less reagent consumption and, consequently, in a reduction of the cost that facilitates the development of large scale production of nanoparticles in an environmentally friendly approach. The synthesis of silver nanoparticles mediated by plant extracts, recently reviewed by Ahmed [8] and Kuppusamy [9], reveals that reduction and stabilization of the nanoparticles is performed by a combination of different biomolecules such as proteins, amino acids, enzymes, polysaccharides, alkaloids, tannins, phenolic acid, terpenoids and flavonoids. The content of these biomolecules acting as reducing and capping agents is known to be dependent on the source of the extract, providing different characteristics (i.e size, shape, stability) to the synthesized nanoparticles. In spite of the importance of the extract composition on the reduction process, few researchers reporting nanoparticles biosynthesis provide information about the main reducing components of the extract.

Grape stalks (GS) are the lignocellulosic skeleton of grape and are the main by-product after grape harvesting and wine production. The extract of some grape sub-products such as leaves, stems, seeds and dried fruit, have been used for the production of bimetallic Fe/Pd [10], Fe_3O_4-Ag [11] and silver [12] nanoparticles, respectively. Three different grape wastes (seed, skin and stalk) were used by Krishnaswamy et al. [13], for the production of gold nanoparticles. A chemical characterization of grape stalk carried out recently [14] revealed that the main components of this by-product are polar compounds soluble in hot water with a high content in tannins and other polyphenolic compounds. These results suggested that GS extract would also contain polyphenolic compounds that could act as reducing and stabilizing agents in the nanoparticles formation.

Nanoparticles (NPs) have been widely applied in different research fields due to their surface-volume ratio that provides them with unique and improved properties in comparison to the analogous bulk material. One interesting feature of NPs (e.g., Ag-NPs) is the simplicity of their application in the modification of screen-printed electrodes (SPEs). Nowadays, this results in a great platform for environmental portable electroanalysis due to their commercial availability, relatively low cost and reproducibility. Nanoparticles enhance the electron transfer among redox centers between the analyte and the electrode, decreasing the over potentials of several analytically important electrochemical reactions [15,16]. Although the use of NPs has already been successfully applied to the development of new electrochemical sensors for the determination of heavy metal ions [16–18], to the best of our knowledge, no previous research about the implementation of green-synthetized NPs has been published.

Here we report the synthesis of silver nanoparticles (Ag-NPs) mediated by the use of aqueous extract of grape stalk waste, which results in a non-reagent procedure and in the valorization of an agro-food waste. The evaluation of different factors that affect the synthesis of these Ag-NPs is also performed. Moreover, and for the first time, the feasibility of these green synthesized Ag-NPs for electrochemical assays is presented. For this purpose, screen-printed carbon nanofibers electrodes (SPCNFE), which have been demonstrated to be a suitable support for the modification of sensors [19], are modified with Ag-NPs by using the drop-casting approach. The resulting modified sensor is applied to the simultaneous determination of Cd(II) and Pb(II) ions by differential pulse anodic stripping voltammetry (DPASV) in aqueous solution as a model electrochemical metal ion system.

2. Materials and Methods

2.1. Reagents and Materials

Grape stalk waste from wine production was kindly supplied by a winemaking cooperative (Empordà-Costa Brava, Spain). The waste was rinsed abundantly with water, dried and cut to separate the pedicels from the stalk branches. The pedicels were then ground and sieved to get the

desired particle size (1–1.6 mm). Chemical reagents were acquired from Sigma Aldrich (Munich, Germany) as $AgNO_3$ for the preparation of Ag nanoparticles, $Pb(NO_3)_2 \cdot 4H_2O$ and $Cd(NO_3)_2 \cdot 4H_2O$, for the preparation of 10^{-2} mol L^{-1} Cd(II) and Pb(II) stock solutions respectively, and standardized complexometrically [20]. 0.1 mol L^{-1} acetate buffer solution (pH 4.5) was used for pH control. Ultrapure water (Milli-Q plus 185 system, Millipore, Burlington, MA, USA) was used in all experiments.

2.2. Preparation of Grape Stalk Extract

The extract was obtained by placing grape stalk waste in a 200 mL round bottom flask and adding 100 mL of Milli-Q water. A reflux condenser was placed at the top of the flask. The device was placed in a heating mantle. Extracts were obtained at different temperatures (60–100 °C) and contact times (15–120 min). After this, the extract was separated from the solid by filtration using a cellulose paper and then centrifuged for 30 min at 5000 rpm (Universal 320, Selecta). Extract samples were analyzed in order to determine their content in total polyphenols and reducing sugars. Prior to the analysis, the loss of volume of the filtrate due to possible water evaporation was compensated by adding water to a total volume of 100 mL.

Determination of Total Phenolic and Reducing Sugars

In total, 34 extracts were prepared at different experimental conditions (temperature and contact time). The total polyphenol content of the filtered extracts was analyzed by the Folin-Ciocalteu method and the reducing sugars content by reaction of the sample with Fehling's solution followed by iodimetric titration of the unreduced copper remaining in the solution. A statistical analysis of experimental data (total polyphenols and reducing sugars) was performed to determine which of the studied parameters (temperature and extraction time) had a significant influence on the concentration of total polyphenols and reducing sugars of the obtained extracts. This statistical analysis was performed using SPSS software program for Windows with a significance level of 0.05 (confidence interval 95%).

2.3. Synthesis of Silver Nanoparticles Using Grape Stalk as Reducing Agent

Synthesis of silver nanoparticles was carried out by putting into contact a certain volume of extract with a certain volume of 0.01 mol L^{-1} silver nitrate solution in sample tubes. The tubes were immersed in a thermostatic water bath (Digiterm 3000542, Selecta, Abrera, Spain) adjusting to the studied temperature (60 °C, 70 °C, 80 °C and 100 °C). The color change from pale yellow brown to reddish brown indicated the reduction of silver nitrate to metallic silver. This color change has been taken as indicative of Ag-NPs synthesis by almost all the researchers [5,21]. Once the samples were cooled down, pH of the solution was measured (pH meter Basic 20, Crison Instruments, Alella, Barcelona, Spain). Then, the samples were first filtered through Whatman No. 1 filter paper and then centrifuged at 5000 rpm for 30 min. The pellet was kept in the fridge for further analysis and the maximum absorption of the supernatant was scanned at the wavelength between 200–800 nm.

2.4. Characterization of Ag Nanoparticles

2.4.1. UV/Vis Spectroscopy

The UV/Vis spectra of the centrifugation supernatants diluted 1:10 were recorded using an UVmini-1240 spectrophotometer (Shimadzu, Kyoto, Japan). Different spectra were obtained showing the Surface Plasmon Resonance (SPR) of the prepared Ag-NPs.

2.4.2. Electron Microscopy Characterization

Spectrometer (EDX, Oxford Instrument, Oxon, United Kingdom), Zeiss® Gemini SEM/Scanning Transmission Electron (STEM) with Focus Ion Beam (FIB-SEM, Zeiss, Berlin, Germany), and High Resolution Transmission Electron Microscopy JEM 2011 with an acceleration voltage of 200 kV

(HR-TEM, JEOL, Nieuw-Vennep, The Netherlands) coupled to an EDX (Oxford Instrument, Oxon, United Kingdom) were used. Approximately 1 mL of sample was filtered and then dispersed in 5 mL of acetone as organic solvent and then placed in an ultrasound bath for 1 h. Finally, 50 µL of the solution were placed on a grid and dried before TEM analysis. For SEM analysis, 50 µL of NPs dispersion were drop-casted on a silicon wafer and then attached to a SEM sample stub with a small piece of carbon conductive tape. For STEM images, TEM grid was placed on a special sample stub holder.

The size distribution of the prepared NPs was obtained by direct observation of the TEM images and the construction of the corresponding size distribution histograms. These measurements were performed using the Image J Software, and the obtained histograms were adjusted to a three-parameter Gaussian curve (Equation (1)) where x_0 is the mean diameter (to which most nanoparticles correspond), b is the standard deviation and a is a statistical parameter related to this fitting. Histograms were calculated using the Microsoft Excel 2010, and the equation was adjusted with SigmaPlot 11.0.

$$y = ae^{[-0.5(\frac{x_0-x}{b})^2]} \quad (1)$$

2.4.3. Fourier Transformed Infrared (FTIR) Spectroscopy

To elucidate the functional groups, present in the grape stalk extract and the molecules surrounding the Ag nanoparticles, FTIR (Bruker, Ettlingen, Germany) spectra in the range of 4000–400 cm^{-1} were performed in a Platinum ATR spectrometer (Bruker, Ettlingen, Germany). Both raw extract and three times washed and centrifuged Ag-NPs (to ensure the removal of unbound molecules) were freeze dried in a lyophilizer Unitop HL (Virtis, SP Scientific, Ipswich, UK).

2.4.4. Electrochemical Characterization of Modified SPCNFE

Differential pulse anodic stripping voltammetric (DPASV) measurements were performed in an Autolab System PGSTAT12 (EcoChemie, Utrecht, The Netherlands), in a multichannel configuration, attached to a Metrohm 663 VA Stand (Metrohm, Herisau, Switzerland) and a personal computer with GPES Multichannel 4.7 software package (EcoChemie, Utrecht, The Netherlands).

The auxiliary and the reference electrode (to which all potentials are referred) were Pt wire and Ag | AgCl | KCl (3 mol L^{-1}), respectively, both purchased from Metrohm (Herisau, Switzerland). The working electrode used was a screen-printed carbon nanofiber electrode (SPCNFE) modified with silver nanoparticles (Ag-NPs-SPCNFE) and connected to the Autolab Systems by means of a flexible cable (ref. CAC, Dropsens, Oviedo, Spain). SPCNFE was a disk electrode of 4 mm diameter provided by Dropsens (ref. 110CNF, Dropsens, Oviedo, Spain).

Stripping voltammetric measurements using Ag-NPs-SPCNFE for the determination of Pb(II) and Cd(II) ions were carried out at a deposition potential (E_d) of −1.40 V applied with stirring during a deposition time (t_d) of 120 s and followed by a rest period (t_r) of 5 s. Measurements were performed by scanning the potential from −1.40 to −0.30 V, and by using pulse times of 50 ms, step potentials of 5 mV and pulse amplitudes of 50 mV. All experiments were carried out without any oxygen removal and at room temperature (20 °C).

Ag-NPs-SPCNFE working electrodes were prepared by drop-casting 40 µL of Ag-NPs solution onto the electrode surface and drying it at 50 °C for 30 min. The Ag-NPs solutions were supernatants resulting from different washings of the pellets obtained from Ag-NPs carried out at different pH values (pH 4 and 6). The corresponding pellets were suspended in 10 mL of deionized water under agitation. Then the suspension was centrifuged. The resulting supernatant (W1) was separated from the washed pellet. This washing operation was repeated three more times. The aim of these washings was to remove non-reacted ions and molecules from the silver nanoparticles suspension that could interfere on the sensor response. The obtained supernatants (W1, W2, W3 and W4, increasing regarding the number of times the pellets were washed) obtained from NPs synthesis, were drop-casted on SPCNFE to obtain 16 different modified sensors.

3. Results and Discussion

3.1. Grape Stalk Extracts

To show the effect of temperature and contact time on grape stalk extraction, box plots (BP) were used (Figure 1). The line across the box represents the median value, whereas the top and the bottom box show the location of the first and third quartiles (Q1 and Q3). The whiskers are the lines that extend from the top and bottom of the box. The box itself contains the middle 50% of the data. If the median is not equidistant from the top and the bottom of the box, then the data are skewed. BP corresponding to total polyphenol concentration values obtained at different temperatures and at different contact times are presented in Figure 1A,B, respectively.

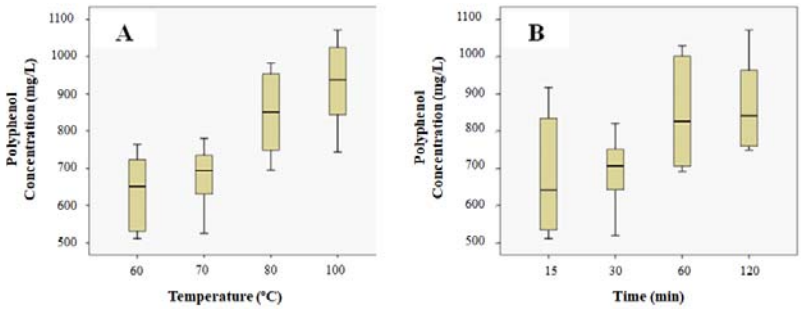

Figure 1. BP for the concentration of polyphenols at different temperatures (**A**) and contact times (**B**).

From the results of the BP, a one-way ANOVA test was performed to analyze the differences among group means and their variation, specifically for the concentration of polyphenols and reducing sugars at different temperatures and different extraction times. The results of the ANOVA test (results not presented) showed $p < 0.05$ for the concentration of polyphenols at different temperatures and contact times and also for the concentration of reducing sugars at different contact times. However, $p > 0.05$ for the concentration of reducing sugars at different temperatures was obtained. Bonferroni post hoc test was carried out to seek out the variable responsible for significant differences between the groups of data. Results indicated that temperature is a significant variable for polyphenols concentration: *p*-values for the comparison between the temperatures 60 and 70 °C and 80 and 100 °C are above 0.05. Therefore, the temperature significance lies between these two groups (70–80 °C). In the case of the variable extraction time, *p*-values were also all above 0.05 for the polyphenols and almost all below this value for the reducing sugars. These results indicate that contact time does not play a significant role in the polyphenols concentration (around 0.5 g L^{-1}) but this variable does have a significant influence in the concentration of reducing sugars (from 0.4 to 0.9 g L^{-1}).

3.2. Silver Nanoparticles Synthesis

3.2.1. FTIR Characterization of Grape Stalk

The FTIR spectra of grape stalk (GS) extract before and after the synthesis of Ag-NPs are plotted in Figure 2. The two curves present a high variation in the intensity of bands in most of the regions of the spectrum. Dried extract spectrum displays a number of adsorption peaks indicating the complex nature of this material. The broad peak in the extract spectrum at around 3328 cm^{-1} is indicative of O–H stretching vibrations. The two peaks at 2950 and 2887 cm^{-1} correspond to the asymmetric and symmetric vibration, respectively, of C-H in the olephinic chains and the peak at 1731 cm^{-1} is attributed to the carbonyl C=O in ester groups [14]. The peaks at 1602 and 1524 cm^{-1} are due to vibration of benzene and the peaks at 1132, 1106, 1067 and 1048 can be due to C–O stretching of alcohols and phenols [22].

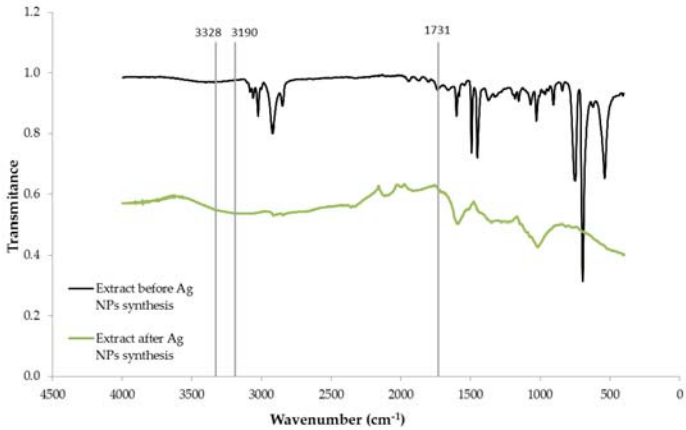

Figure 2. FTIR spectrum of dried grape stalks extract before and after the synthesis of Ag-NPs.

Dried extract spectrum after the synthesis of Ag-NPs shows a broad band in the region of OH-stretching vibrations around 3190 cm^{-1}. The shift from 3328 to 3190 cm^{-1} must be attributed to the formation of Ag-NPs. The observed broadening of the band is characteristic of hydrogen bonding (intra and inter molecular bonds). Free hydroxyl groups might interact with silver to stabilize Ag-NPs. The functional groups p-OH, m-OH and COOH of phenolic groups have been reported to act as hydrogen donors/acceptors [23,24]. A cooperative association between phenolic compounds and other components of the extract may contribute to the stabilization of the nanoparticles [25]. The band at 1731 cm^{-1} attributed to C=O stretching mode has disappeared, indicating that this group is involved in silver reduction and/or NPs stabilization. The bands corresponding to alcohol and phenol stretching shifted to lower wavenumbers and showed a very weak intensity.

3.2.2. Study of Factors Affecting Ag-NPs Synthesis

Some physical and chemical parameters such as pH, contact time between extract and metal solution, temperature, extract/metal solution (v/v) ratio and metal salt concentration largely affect the synthesis process and the characteristics (size, shape and morphology) of the synthetized NPs [5]. Therefore, the influence of these parameters on Ag-NPs synthesis mediated by GS extract was investigated. Visual observation of color, changes in the pH and spectra of UV-Vis were useful tools to monitoring Ag-NPs formation.

Effect of pH

The influence of pH on Ag-NPs was investigated adjusting the pH of the extract at different pH within 2.0–9.0, meanwhile the pH of 0.01 mol L^{-1} $AgNO_3$ solution was kept unaltered. In these experiments, the volume of extract and Ag solutions was 4 and 6 mL, respectively, the temperature 80 °C and the contact time 2 h.

The nanoparticles suspension obtained from rinsing the pellet up to three times with Milli-Q water, showed maximum absorbance at around 450 nm, indicating the presence of Ag nanoparticles. It has been reported that silver colloids exhibit maximum absorbance within the range 400–500 nm due to Surface Plasmon Resonance (SPR) [26–28].

As can be seen in Figure 3A, a peak at 307 nm was observed. This peak must be attributed to the organic matter of the GS extract. This peak presents the higher absorbance value in the solution at pH 2, when no other peak was clearly observed. In the case of pH 4 and 6, a peak around 450 nm was observed. This peak can be attributed to the SPR of silver nanoparticles as mentioned in Section 2.4.1. It must be remarked that the peak absorbance from solution at pH 6 was higher than at pH 4. As peak

intensity could be related to Ag-NPs concentration, the increase on peak intensity of solution at pH 6 compared to pH 4 could indicate higher nanoparticles presence in solution. Two peaks were observed in the UV-Vis plot of pH 8 solution and both peaks are in the Ag-NP SPR range. The wavelength of the band shifted to 470 nm when the reaction pH was 4 and 6. The shift towards larger wavelengths (red shift) indicates an increase in the mean diameter of Ag-NPs [29,30].

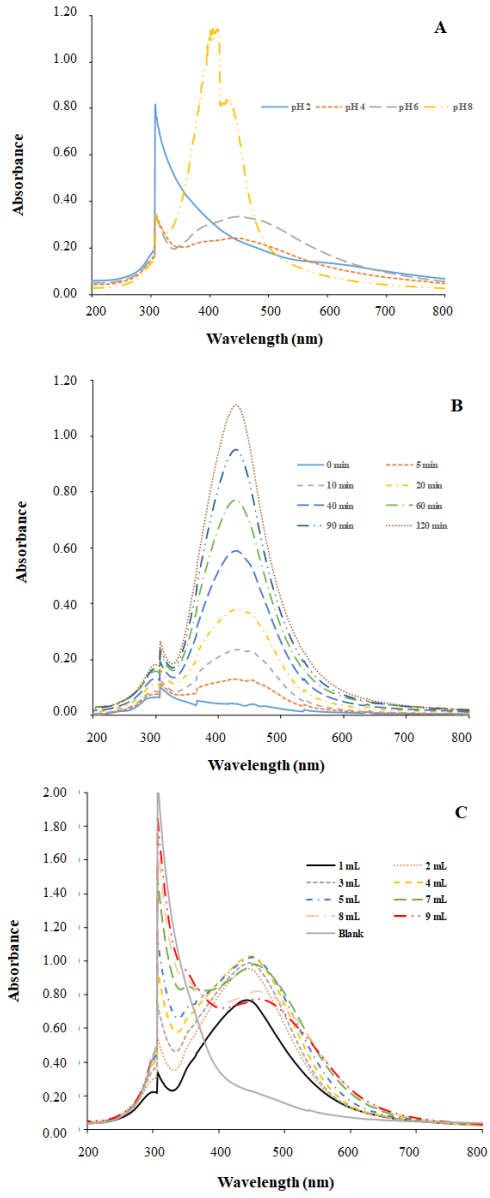

Figure 3. UV/Vis Spectra showing the influence of different parameters in the synthesis of Ag-NPs with the GS extract: (**A**) pH, (**B**) contact time and (**C**) extract addition.

The high band observed at 440 nm seems to indicate a great number of Ag-NPs. Additionally, the shift towards lower wavelengths indicates a decrease in the mean diameter of Ag NPs [25,26]. Thus, SPR seems to indicate a great number of smaller diameter Ag-NPs when synthesis takes place at pH 8. Nevertheless, the additional peak observed at 415 nm indicates the presence of other compounds in solution that could affect Ag-NPs quality.

Effect of Contact Time

In order to ascertain the time required for the completion of the reduction reaction, several tubes containing 4 mL of extract and 6 mL of 0.01 mol L^{-1} $AgNO_3$ were heated at 80 °C. The tubes were removed from the thermostatic bath at different times ranging from 5 min to 8 h.

The UV-Vis spectra of Ag-NPs solution obtained at different reaction times are depicted in Figure 3B. In the experimental conditions used (4 mL extract, 6 mL 0.01 M $AgNO_3$, 80 °C, pH 4) the Ag-NPs SPR band is noticeable after 5 min of reaction. Up to this reaction time the absorbance intensity increased with time, suggesting a great number of nanoparticles in the solution.

The pH of the reaction mixture was measured before and after the reduction reaction. The initial pH (4.01) increased in the first 5 min to 4.15 and then progressively diminished with time and reached the pH value of 3.02 after 8 h. The pH change might be related to the involvement of some compounds in the reduction or capping processes leading to Ag-NPs formation.

Effect of Extract/Silver Solution (v/v) Ratio

Different volumes of extract and silver solution ratios were investigated in order to determine the effect of silver addition and the effect of extract addition, respectively. The first one consisted in fixing the volume of extract (4 mL) and adding different volumes (1–6 mL) of 0.01 mol L^{-1} $AgNO_3$. In the second one, the volume of silver solution was fixed (1 mL) and the volume of the extract was varied (1–9 mL). For both sets of experiments, the total volume in the tubes was adjusted to 10 mL by adding Milli-Q water. Heating temperature of 80 °C and contact time of 2 h were kept as before.

The plot of the obtained spectra at increasing volumes of extract is presented in Figure 3C. The reacted solutions exhibited an intense dark reddish-brown color with independence of the volume of extract added to 1 mL 0.01 mol L^{-1} $AgNO_3$. The increasing sharp peak at 307 nm refers to light absorption of extract components at this wavelength. As expected, absorbance intensity at this wavelength increases with the addition of more volume of extract. Maximum absorbance intensity of the SPR band increased with the addition of 1 to 5 mL of extract. Higher volumes of extract led to the opposite trend as absorbance values decreased with the extra extract addition. The decrease of absorbance could be due to the deficiency of silver ions with respect to the amount of biomolecules that could provoke the agglomeration of smaller particles to form larger Ag-NPs that would absorb light to a lower extent [29]. SPR band values shifted from 447.5 to 459.0 nm with the addition of extract volume from 1 to 9 mL, indicating the effect of extract concentration in the mean diameter of Ag-NPs. López-Carrillo et al. [31] reported, that in general, particle size can be controlled by changing the volume of the reducing agent.

3.2.3. Electron Microscopy Characterization

The suitability of the GS extract in the synthesis of Ag-NPs was proved by direct observation of SEM and TEM images. As an example, Figure 4 shows the electron microscopy characterization of a sample solution of Ag-NPs synthetized at pH 4. Results reveal that Ag-NPs obtained through this methodology presented an average diameter of (27.7 $\pm$ 0.6) nm. Moreover, the chemical identity of the Ag-NPs was proved by EDX spectra as it is shown in Figure 4B,D.

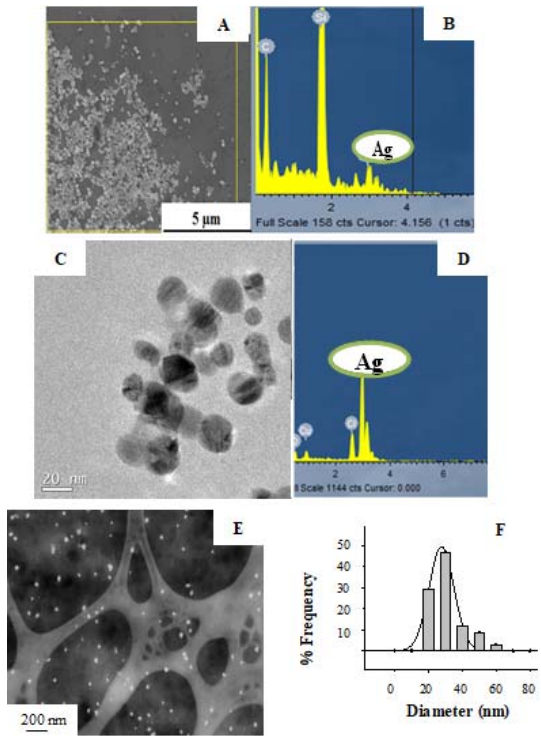

Figure 4. Electron Microscopy micrographs for Ag-NPs synthesized at pH 4 using the GS extract as reducing agent. SEM micrograph (**A**), corresponding EDX spectra (**B**) and TEM micrograph (**C**) with corresponding EDX spectra (**D**) showing the presence of silver. STEM image of Ag-NPs (**E**) with size distribution histogram (**F**).

The size distribution analysis for the different Ag-NPs synthetized at different pH and measured by TEM images was determined and it is summarized in Table 1. Due to the higher surface-to-volume ratio, these Ag-NPs can present higher electrocatalytical activity. In consequence, they could be suitable for the modification of electrodes, and will be addressed in the following section.

Table 1. Diameter measurements of the Ag-NPs prepared at different pH obtained from TEM micrographs.

Sample Preparation pH	Diameter (nm)
2	55.4 ± 0.3
4	27.7 ± 0.6
6	54.3 ± 0.1
8	9.0 ± 0.2

As can be seen, the smaller particles size of Ag-NPs was obtained when synthesis was carried out at pH 8. This confirms the result of the pH effect on Ag-NPs synthesis analyzed by UV-VIS spectra (see above). Similar nanoparticle diameters were obtained when synthesis was carried out at pH 2 and pH 6. Thus, TEM results ratify the effect of the pH on nanoparticle size. Nevertheless, other aspects related to size stabilization (Ag^+ ion concentration as NP precursor, concentration of reducing-stabilizing agent, temperature of reaction) seem to have a greater influence than pH on particle size, as no clear trend between pH and size was observed.

Figure 5 presents SEM images of the non-modified (Figure 5A) and Ag-NPs-modified (Figure 5B,C) SPCNFEs. One can observe that the drop-casting strategy does not alter the morphology of the electrode, but leads to the incorporation of the green synthesized Ag-NPs, distributing all over the surface (Figure 5C). This fact is relevant for the enhancement of the electroanalytical features of the SPCNFE.

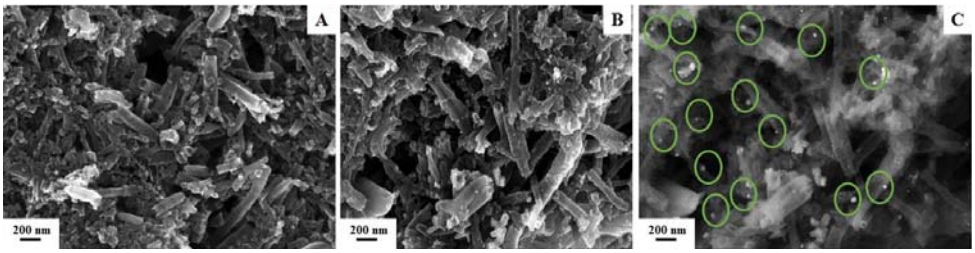

Figure 5. SEM InLens images of raw SPCNFE (**A**) and SPCNFE after the drop casting of Ag-NPs (**B**). SEM Secondary Lens of SPCNFE highlighting the location of the drop-casted Ag-NPs (**C**).

3.2.4. Electrochemical Characterization

The selected E_d, t_d and t_r were firstly optimized to ensure the simultaneous determination of Cd(II) and Pb(II) at each Ag-NPs-SPCNFE in the selected concentration range (data not shown), being for all cases an E_d of -1.40 V applied with stirring during a t_d of 120 s and followed by a t_r of 5 s.

The comparison of the analytical performance of the SPCNFE modified with Ag-nanoparticles obtained from different synthesis pH conditions and after two or three additional rinsing suspensions (W3 and W4) is shown in Figure 6. In order to study the effect of the NP size on the electrochemical behavior and to avoid the presence of other compounds in solution, Ag-NPs obtained at pH 4 and 6 were chosen to prepare SPCNFE. The aim of the modified Ag-NPs-SPCNFE is the simultaneous determination of a solution containing Pb(II) and Cd(II). Well-defined peaks can be observed for both Pb(II) and Cd(II) ions at -0.42 and -0.55 V, respectively, with all electrodes. However, more intense peaks are obtained using the SPCNFE modified with Ag-NPs prepared at pH 4, supernatant W3 (SPCNFE—pH4.W3), particularly in the case of Cd(II).

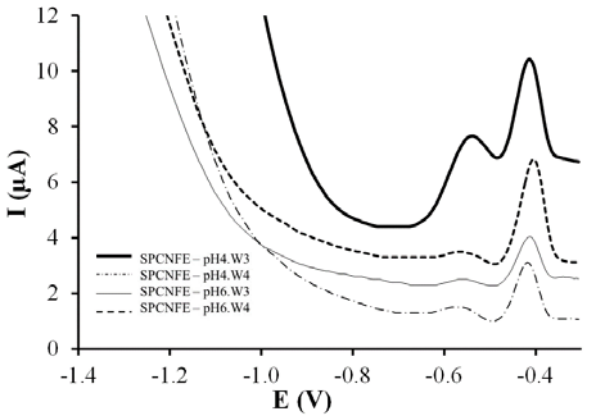

Figure 6. Stripping voltammetric measurements of the SPCNFE modified with Ag-NPs obtained from different synthesis pH conditions and washing suspensions for the simultaneous detection of Cd(II) and Pb(II) at 77 µg L^{-1} and pH 4.5.

Simultaneous calibration of Pb(II) and Cd(II) ions by DPASV were carried out on each Ag-NPs-SPCNFE. For this purpose, nine increasing concentrations of Pb(II) and Cd(II) ranging from 1.1 to 100.4 and from 1.1 to 100.1 μg L^{-1}, respectively, were used as calibration samples. Figure 7 shows, as an example, the evolution of the DPASV signals of both metal ions using SPCNFE modified with silver nanoparticles obtained from SPCNFE—pH4.W3 when their concentrations increase (the other three Ag-NPs-SPCNFE present equivalent behaviors). The obtained calibration data on each Ag-NPs-SPCNFE are summarized in Table 2. The limit of detection (LOD) was calculated as three times the standard deviation of the intercept over the slope of the calibration curve of the target ions. The limit of quantification (LOQ) was evaluated by considering 10 times the previous ratio. The lowest value of the linear concentration range was established from the corresponding LOQ. As shown in Table 2, linear calibration curves were obtained for Pb(II) and Cd(II) up to a maximum concentration level of 100.4 and 27.5–39.7 μg L^{-1}, respectively, depending on the considered Ag-NPs-SPCNFE. Regarding sensitivities (nA μg^{-1} L), obtained from the slope of the calibration curves, they varied from 21.2 to 62 for Pb(II) and from 5.1 to 46 for Cd(II) depending on the Ag-NPs-SPCNFE (Table 2). The LOD of the determination of the two metals in the four considered Ag-NPs-SPCNFEs ranged from 2.7 to 4.9 for Pb(II) and from 2.8 to 8.1 for Cd(II) according to the considered Ag-NPs-SPCNFE, whereas the LOQ varied from 8.9 to 16.2 for Pb(II) and from 9.5 to 26.9 for Cd(II) (as seen in Table 2). It should be mentioned that no previous LOD and LOQ data for SPCNFEs modified with Ag-NPs from natural sources are available in the literature. Nevertheless, as compared to previous results reported using other electrodes, e.g., synthetic Ag-NPs-based electrodes [16,32], bismuth film electrodes [33], antimony film electrodes [34], chemically modified electrodes [35–38], the LOD and LOQ achieved in this work for Cd(II) and Pb(II) are similar or even lower depending on the considered modified electrode.

Therefore, the reported calibration data suggests that all the considered Ag-NPs-SPCNFEs could be suitable and a valuable option for more conventional electrodes for the simultaneous determination of Pb(II) and Cd(II) at trace levels in natural samples. However, the best results (higher sensitivities, lower LODs and wider linear ranges) were obtained with SPCNFE-pH4.W3.

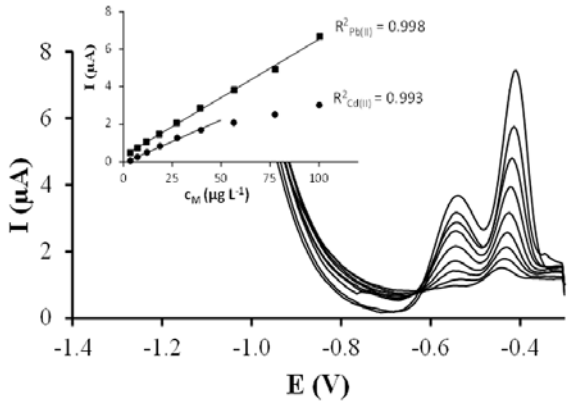

Figure 7. DPASV measurements and calibration curves (insets) obtained for the simultaneous calibration of Pb(II) and Cd(II) in acetate buffer pH 4.5 using an Ag-NPs modified -SPCNFE at an E_d of −1.4 V and a t_d of 120 s.

Table 2. Calibration data for the simultaneous determination of Pb(II) and Cd(II) at each Ag-NPs-SPCNFE at E_d of −1.4 V, t_d of 120 s and pH 4.5. Standard deviations are denoted by parenthesis.

Sample	Analytical Parameter	DPASV Calibration	
		Pb(II)	Cd(II)
SPCNFE—pH4.W3	Sensitivity (nA μg^{-1} L)	62 (1)	46 (2)
	R^2	0.998	0.993
	Linear range [a] ($\mu g\ L^{-1}$)	8.9–100.4	9.5–39.7
	LOD ($\mu g\ L^{-1}$)	2.7	2.8
SPCNFE—pH4.W4	Sensitivity (nA μg^{-1} L)	26.0 (0.7)	8.5 (0.5)
	R^2	0.996	0.993
	Linear range [a] ($\mu g\ L^{-1}$)	13.3–100.4	16.0–39.7
	LOD ($\mu g\ L^{-1}$)	4.0	4.8
SPCNFE—pH6.W3	Sensitivity (nA μg^{-1} L)	21.2 (0.5)	5.1 (0.5)
	R^2	0.996	0.980
	Linear range [a] ($\mu g\ L^{-1}$)	12.3–100.4	26.9–39.7
	LOD ($\mu g\ L^{-1}$)	3.7	8.1
SPCNFE—pH6.W4	Sensitivity (nA μg^{-1} L)	43 (1)	13.8 (0.8)
	R^2	0.993	0.989
	Linear range [a] ($\mu g\ L^{-1}$)	16.2–100.4	10.0–27.5
	LOD ($\mu g\ L^{-1}$)	4.9	3.0

[a] The lowest value of the linear range was considered from the LOQ.

4. Conclusions

An environmentally friendly preparation of Ag-NPs by using non-toxic reducing chemicals has been developed. Thus, total polyphenols and reducing sugars present in plant extracts from grape stalk wastes were used as reducing agents and stabilizers in the nanoparticles production. The extract and the Ag-NPs generation have been studied and optimized considering several parameters and have been characterized in detail by different spectroscopic and electron microscopy techniques. Finally, these Ag-NPs were drop-casted on the SPCNFE and the resulting sensors were analytically characterized to proof their suitability for sensing purposes. These modified Ag-NPs-SPCNFE were tested for the simultaneous stripping voltammetric determinations of Pb(II) and Cd(II), providing appropriate reproducibility, sensitivity, linear range and LODs at $\mu g\ L^{-1}$ range; more precisely, $LOD_{Pb(II)}$ 2.7 $\mu g\ L^{-1}$ and $LOD_{Cd(II)}$ 2.8 $\mu g\ L^{-1}$, evidencing the enhancement of the SPCNFE electrodes by adding the above mentioned Ag-NPs.

Author Contributions: J.B.-A. and A.F. carried out the analysis data obtained from the synthesis and microscopic characterization of silver nanoparticles. C.P.-R. and N.S. carried out the modification of screen-printed electrodes with nanoparticles, the voltammetric measurements and the data treatment. N.F., J.P. and I.V. carried out the preparation and characterization of the grape stalk, besides the green synthesis of the Ag NPs. All authors contributed to the writing, revision and critical discussion of the results presented in the final version of the manuscript.

Funding: This research has been supported by Ministerio de Economia y Competitividad (MINECO) and Fondo Europeo de Desarrollo Regional (FEDER), projects CTM2015-68859-C2-1-R and C2-2-R, and by the Generalitat de Catalunya (Projects 2017SGR311 and 2017SGR312).

Acknowledgments: Clara Pérez-Ràfols also acknowledges the Ministerio de Educación, Cultura y Deporte (MECD) for a Ph.D. grant. Special thanks to Nathalie Gerits, Jeongeun Kim and Pau-Isai Jaile for helping in part of the experimental work.

Conflicts of Interest: The authors declare no conflict of interest.

References

1. Zhang, X.; Yan, S.; Tyagi, R.D.; Surampalli, R.Y. Synthesis of nanoparticles by microorganisms and their application in enhancing microbiological reaction rates. *Chemosphere* **2011**, *82*, 489–494. [CrossRef] [PubMed]
2. Sharma, D.; Kanchi, S.; Bisetty, K. Biogenic synthesis of nanoparticles: A review. *Arab. J. Chem.* **2015**. [CrossRef]
3. Kuppusamy, P.; Yusoff, M.M.; Maniam, G.P.; Govindan, N. Biosynthesis of metallic nanoparticles using plant derivatives and their new avenues in pharmacological applications—An updated report. *Saudi Pharm. J.* **2016**, *24*, 473–484. [CrossRef] [PubMed]
4. Mittal, A.K.; Chisti, Y.; Banerjee, U.C. Synthesis of metallic nanoparticles using plant extracts. *Biotechnol. Adv.* **2013**, *31*, 346–356. [CrossRef] [PubMed]
5. Srikar, S.K.; Giri, D.D.; Pal, D.B.; Mishra, P.K.; Upadhyay, S.N. Green synthesis of silver nanoparticles: A review. *Green Sustain. Chem.* **2016**, *6*, 34–56. [CrossRef]
6. He, Y.; Du, Z.; Lv, H.; Jia, Q.; Tang, Z.; Zheng, X.; Zhang, K.; Zhao, F. Green synthesis of silver nanoparticles by Chrysanthemum morifolium Ramat. extract and their application in clinical ultrasound gel. *Int. J. Nanomed.* **2013**, *8*, 1809–1815. [CrossRef] [PubMed]
7. Ravichandran, V.; Vasanthi, S.; Shalini, S.; Ali Shah, S.A.; Harish, R. Green synthesis of silver nanoparticles using Atrocarpus altilis leaf extract and the study of their antimicrobial and antioxidant activity. *Mater. Lett.* **2016**, *180*, 264–267. [CrossRef]
8. Ahmed, S.; Ahmad, M.; Swami, B.L.; Ikram, S. A review on plants extract mediated synthesis of silver nanoparticles for antimicrobial applications: A green expertise. *J. Adv. Res.* **2016**, *7*, 17–28. [CrossRef] [PubMed]
9. Kuppusamy, P.; Ichwan, S.J.A.; Parine, N.R.; Yusoff, M.M.; Maniam, G.P.; Govindan, N. Intracellular biosynthesis of Au and Ag nanoparticles using ethanolic extract of Brassica oleracea L. and studies on their physicochemical and biological properties. *J. Environ. Sci. (China)* **2015**, *29*, 151–157. [CrossRef] [PubMed]
10. Luo, F.; Yang, D.; Chen, Z.; Megharaj, M.; Naidu, R. Characterization of bimetallic Fe/Pd nanoparticles by grape leaf aqueous extract and identification of active biomolecules involved in the synthesis. *Sci. Total Environ.* **2016**, *562*, 526–532. [CrossRef] [PubMed]
11. Venkateswarlu, S.; Natesh Kumar, B.; Prathima, B.; Anitha, K.; Jyothi, N.V. V A novel green synthesis of Fe_3O_4-Ag core shell recyclable nanoparticles using Vitis vinifera stem extract and its enhanced antibacterial performance. *Phys. B Condens. Matter* **2015**, *457*, 30–35. [CrossRef]
12. Dziwoń, K.; Pulit-Prociak, J.; Banach, M. Green technologies in obtaining nanomaterials–using white grapes (Vitis vinifera) in the processes for the preparation of silver nanoparticles. *Chemik* **2015**, *69*, 33–38.
13. Krishnaswamy, K.; Vali, H.; Orsat, V. Value-adding to grape waste: Green synthesis of gold nanoparticles. *J. Food Eng.* **2014**, *142*, 210–220. [CrossRef]
14. Pujol, D.; Liu, C.; Fiol, N.; Olivella, M.À.; Gominho, J.; Villaescusa, I.; Pereira, H. Chemical characterization of different granulometric fractions of grape stalks waste. *Ind. Crops Prod.* **2013**, *50*, 494–500. [CrossRef]
15. Muñoz, J.; Bastos-Arrieta, J.; Muñoz, M.; Muraviev, D.N.; Céspedes, F.; Baeza, M. Simple green routes for the customized preparation of sensitive carbon nanotubes/epoxy nanocomposite electrodes with functional metal nanoparticles. *RSC Adv.* **2014**, *4*, 44517–44524. [CrossRef]
16. Pérez-Ràfols, C.; Bastos-Arrieta, J.; Serrano, N.; Díaz-Cruz, J.M.; Ariño, C.; de Pablo, J.; Esteban, M. Ag nanoparticles drop-casting modification of screen-printed electrodes for the simultaneous voltammetric determination of Cu(II) and Pb(II). *Sensors* **2017**, *17*, 1458. [CrossRef] [PubMed]
17. Lu, Y.; Liang, X.; Niyungeko, C.; Zhou, J.; Xu, J.; Tian, G. A review of the identification and detection of heavy metal ions in the environment by voltammetry. *Talanta* **2018**, *178*, 324–338. [CrossRef] [PubMed]
18. Economou, A. Screen-printed electrodes modified with "green" metals for electrochemical stripping analysis of toxic elements. *Sensors* **2018**, *18*, 1032. [CrossRef] [PubMed]
19. Pérez-Ràfols, C.; Serrano, N.; Díaz-cruz, J.M.; Ariño, C.; Esteban, M. New approaches to antimony film screen-printed electrodes using carbon-based nanomaterials substrates. *Anal. Chim. Acta* **2016**, *916*, 17–23. [CrossRef] [PubMed]
20. Vogel, A.I. *Textbook of Quantitative Chemical Analysis*, 5th ed.; Pearson Education Limited: Harlow, UK, 1989.

21. Ramteke, C.; Chakrabarti, T.; Sarangi, B.K.; Pandey, R. Synthesis of silver nanoparticles from the aqueous extract of leaves of ocimum sanctum for enhanced antibacterial activity. *Hindawi Publ. Corp. J. Chem.* **2013**, *2013*, 278925. [CrossRef]
22. Xu, H.; Wang, L.; Su, H.; Gu, L.; Han, T.; Meng, F.; Liu, C. Making good use of food wastes: green synthesis of highly stabilized silver nanoparticles from grape seed extract and their antimicrobial activity. *Food Biophys.* **2015**, *10*, 12–18. [CrossRef]
23. Tchaikovskaya, O.N.; Basyl', O.K.; Sultimova, N.B. Proton-acceptor and proton-donor properties of phenol and its substitutes. *Russ. Phys. J.* **2005**, *48*, 1245–1250. [CrossRef]
24. Lerma-garcía, M.; Ávila, M.; Simó-alfonso, E.F.; Ríos, Á.; Zougagh, M. Synthesis of gold nanoparticles using phenolic acids and its application in catalysis. *J. Mater. Environ. Sci.* **2014**, *5*, 1919–1926.
25. Mehanna, N.S.; Hassan, Z.M.R.; El-Din, H.M.F.; Ali, A.A.-E.; Amarowicz, R.; El-Messery, T.M. Effect of interaction phenolic compounds with milk proteins on cell line. *Food Nutr. Sci.* **2014**, *5*, 2130–2146. [CrossRef]
26. François, E.M.; Marcelle, L.S.; Cecile, O.E.; Agnes, A.N.; Djiopang, Y.S.; Fanny, A.E.M.; Lidwine, N.; Harouna, M.; Emmanuel, M.M. Unexplored vegetal green synthesis of silver nanoparticles: A preliminary study with Corchorus olitorus Linn and Ipomea batatas (L.) Lam. *African J. Biotechnol.* **2016**, *15*, 341–349. [CrossRef]
27. Demirbas, A.; Welt, B.A.; Ocsoy, I. Biosynthesis of red cabbage extract directed Ag NPs and their effect on the loss of antioxidant activity. *Mater. Lett.* **2016**, *179*, 20–23. [CrossRef]
28. Velgosová, O.; Mražíková, A.; Marcinčáková, R. Influence of pH on green synthesis of Ag nanoparticles. *Mater. Lett.* **2016**, *180*, 336–339. [CrossRef]
29. Ajitha, B.; Kumar Reddy, Y.A.; Reddy, P.S.; Jeon, H.-J.; Ahn, C.W. Role of capping agents in controlling silver nanoparticles size, antibacterial activity and potential application as optical hydrogen peroxide sensor. *RSC Adv.* **2016**, *6*, 36171–36179. [CrossRef]
30. Khalil, M.M.H.; Ismail, E.H.; El-Baghdady, K.Z.; Mohamed, D. Green synthesis of silver nanoparticles using olive leaf extract and its antibacterial activity. *Arab. J. Chem.* **2014**, *7*, 1131–1139. [CrossRef]
31. Carrillo-López, L.M.; Morgado-González, A.; Morgado-González, A. Biosynthesized silver nanoparticles used in preservative solutions for Chrysanthemum cv. Puma. *J. Nanomater.* **2016**, *2016*. [CrossRef]
32. Prakash, S.; Shahi, V.K. Inproved sensitive detection of Pb^{2+} and Cd^{2+} in water samples at electrodeposited silver nanonuts on a glassy carbon electrode. *Anal. Methods* **2011**, *3*, 2134–2139. [CrossRef]
33. Serrano, N.; Alberich, A.; Díaz-Cruz, J.M.; Ariño, C.; Esteban, M. Coating methods, modifiers and applications of bismuth screen-printed electrodes. *Trends Anal. Chem.* **2013**, *46*, 15–29. [CrossRef]
34. Serrano, N.; Díaz-Cruz, J.M.; Ariño, C.; Esteban, M. Antimony- based electrodes for analytical determinations. *Trends Anal. Chem.* **2016**, *77*, 203–213. [CrossRef]
35. Pérez-Ràfols, C.; Serrano, N.; Díaz-Cruz, J.M.; Ariño, C.; Esteban, M. Glutathione modified screen-printed carbon nanofiber electrode for the voltammetric determination of metal ions in natural samples. *Talanta* **2016**, *155*, 8–13. [CrossRef] [PubMed]
36. Serrano, N.; González-Calabuig, A.; del Valle, M. Crown ether-modified electrodes for the simultaneous stripping voltammetric determination of Cd(II), Pb(II) and Cu(II). *Talanta* **2015**, *138*, 130–137. [CrossRef] [PubMed]
37. Serrano, N.; Prieto-Simón, B.; Cetó, X.; del Valle, M. Array of peptide-modified electrodes for the simultaneous determination of Pb(II), Cd(II) and Zn(II). *Talanta* **2014**, *125*, 159–166. [CrossRef] [PubMed]
38. Pérez-Ràfols, C.; Serrano, N.; Manuel Díaz-Cruz, J.; Ariño, C.; Esteban, M. Penicillamine-modified sensor for the voltammetric determination of Cd(II) and Pb(II) ions in natural samples. *Talanta* **2015**, *144*, 569–573. [CrossRef] [PubMed]

Carbon-stabilized porous silicon as novel voltammetric sensor platforms.

C. Pérez-Ràfols, K. Guo, N. H. Voelcker, B. Prieto-Simon

Article

Carbon-stabilized porous silicon as novel voltammetric sensor platforms

Clara Pérez-Ràfols [1], Keying Guo [2], Nicolas H. Voelcker[2], and Beatriz Prieto-Simón [2,*]

[1] Department of Chemical Engineering and Analytical Chemistry, Universitat de Barcelona, Martí i Franquès 1-11, E–08028 Barcelona (Spain).
[2] Disposition and Dynamics, Monash Institute of Pharmaceutical Sciences, Monash University, Parkville, 3052 Victoria (Australia).
* Correspondence: beatriz.prietosimon@monash.edu;

Abstract: The applicability of carbon-stabilized porous silicon (pSi) as a voltammetric sensor platform is demonstrated for the first time. For this purpose, the voltammetric response of hydroquinone, catechol and resorcinol was studied at thermally hydrocarbonized pSi (THCpSi) and at thermally carbonized pSi (TCpSi) and compared to glassy carbon electrode (GCE). The highest currents and most reversible signals were achieved with TCpSi, which also allowed the simultaneous voltammetric determination of the three isomers. Furthermore, the analytical performance of TCpSi was also studied, reveling good reproducibility, sensitivity and limits of detections, which were below 5 μmol L^{-1} in all cases.

Keywords: Porous silicon; thermal carbonization; electrochemical sensor; voltammetry; hydroquinone; catechol; resorcinol

1. Introduction

Porous silicon (pSi) is a very versatile porous nanomaterial that has attracted attention in a wide range of fields with applications as diverse as drug delivery, energy conversion and sensors among others. This wide interest is due to some of the unique features of porous silicon such as availability, biocompatibility, fast and simple fabrication process, large surface area, adjustable pore size and thickness and a convenient surface chemistry that allows different routes for surface functionalization [1–3].

In particular, the possibility to control pore morphology of pSi and its versatile surface chemistry provides a wide range of possibilities in the design of chemical sensors and biosensors. In fact, pSi has been successfully applied to the development of optical and electrical chemical sensors. Optical sensors are commonly based on the monitoring of the shift in the fringe pattern caused by changes in the average refractive index [4,5] whereas electrical sensors are usually based on the monitoring of either conductance or capacitance changes [4]. However, little research has been done in the development of electrochemical sensors based on pSi, which present some interesting features including high sensitivity, low cost, relatively simple instrumentation, easy miniaturization processes and portability [6,7].

One of the main challenges that needs to be overcome in order to use pSi as an electrochemical transducer is the low chemical stability of freshly etched pSi resulting from the presence of highly reactive silicon hydride species, which can be easily oxidized in both water and air and lead to the formation of an insulating SiO_2 surface. Therefore, the most common stabilization methods based on pSi oxidation through thermal or chemical treatments or anodic oxidation are not ideal in this case.

Other approaches that have been explored in order to both stabilize and increase the conductivity of pSi, making it more fit for electrochemical sensing, include different thin film coating methods based on metals or conductive polymers [4,5].

Another possibility that allows the stabilization of pSi is based on the creation of an ultrathin carbon layer by thermal decomposition of acetylene. This method was first introduced by Salonen *et al.* [6] and has already found many applications in the fields of drug delivery, optical and electrical sensors, batteries and electrochemical supercapacitors [7,8]. However, it was only recently that this stabilization method was explored for the development of electrochemical sensors. In this sense, Guo *et al.* [9] studied the electrochemical performance of thermally hydrocarbonized pSi (THCpSi) and thermally carbonized pSi (TCpSi) and demonstrated that carbon-stabilized pSi present a large effective surface area and a fast electron transfer kinetics while maintaining the unique features of pSi (large surface are, adjustable pore morphology, versatile surface chemistry…), rendering it suitable to perform as electrochemical platforms. Its applicability was tested by the development of an impedimetric immunosensor for the detection of MS2 batcteriphage, highlighting the potential of carbon-stabilized pSi for biosensing applications.

However, carbon-stabilized pSi also presents some interesting features derived from the ultrathin carbon layer formed during the thermal decomposition of acetylene. It has been shown that the coupling of carbon-based nanomaterials with electrochemical sensors not only increases their sensitivity but can also provide a better selectivity towards some analytes [10,11]. Therefore, carbon-stabilized pSi is not just appealing to biosensing applications; it can also be a good electrochemical platform as a bare substrate, without the need of further modification.

Thus, in this work we report for the first time the application of carbon-stabilized pSi without any further surface functionalization in electrochemical sensing. For this purpose, the electrochemical performance of both THCpSi and TCpSi was investigated and their applicability to differential pulse voltammetric (DPV) measurements was evaluated through the voltammetric determination of the three isomers of dihydroxybenzene (catechol, hydroquinone and resorcinol), commonly used as chemicals in several products (cosmetics, dyes, pesticides, medicines,…) and considered environmental pollutants due to their high toxicity and low degradability [12,13].

2. Materials and Methods

2.1. Materials

6 inch, boron doped (p-type) Si wafers with 0.00055-0.001 Ω cm resistivity, (100)-oriented were purchased from Siltronix (France). Hydrofluoric acid (48%, AR grade) was purchased from Scharlau (Australia). The acetylene gas cylinder (1 m^3 industrial grade, dissolved) was purchased from BOC (Australia). Potassium ferricyanide $K_3[Fe(CN)_6]$, potassium ferrocyanide $K_4[Fe(CN)_6]$, hydroquinone (HQ), catechol (CC), resorcinol (RC) and phosphate buffered saline (PBS) tablets were provided by Sigma-Aldrich (Australia).

2.2. Instrumentation

Scanning electron microscopy (SEM) images were obtained with a FEI NovaNano SEM 430 at an accelerating voltage of 10 kV. Attenuated total reflectance Fourier transform infrared (ATR-FTIR) spectroscopy was performed with a Thermo Scientific Nicolet 6700 FTIR spectrometer.

Voltammetric measurements were performed on a CH Instrument model 600D Series (CH Instruments, USA) controlled with the provided software package. A homemade three-electrode Teflon cell, placed in a Faraday cage and containing the THCpSi or TCpSi substrate as the working electrode was used. The working electrode area was delimited to 7.5 mm diameter by an o-ring.

Ag/AgCl/NaCl (3 mol L^{-1}) provided by BAS Inc (West Lafayette, IN, USA) and platinium wire were used as reference and counter electrodes respectively. All the potentials are referred to Ag/AgCl. Glassy carbon electrodes (GCE) with 3 mm diameter used for comparison purposes were provided by CH Instruments.

2.3. Fabrication of THCpSi and TCpSi

2.3.1. Fabrication of pSi

A 6 inch Si wafer was anodically etched in an electrolyte solution containing 1:1 (v:v) HF/ethanol to produce pSi, using a MPSB wet etching system (A.M.M.T GmbH, Germany), which can load a 6 inch Si wafer with an exposed etching area of 132 cm^2 (https://www.ammt.com/products/porous-silicon-etching/mpsb/). A sacrificial layer produced with a current density of 61 mA cm^{-2} for 30 s was removed with 1 mol L^{-1} sodium hydroxide [14]. Then the etching cell was rinsed with water, absolute ethanol and dried with N_2 gas. Next, a current density of 53 mA cm^{-2} was applied to the etching cell for 20 s to form pores of 72 ± 15 nm in diameter with a thickness of 500 nm. The freshly etched pSi was finally rinsed with ethanol and kept in a desiccator.

2.3.2. Carbon stabilization of pSi by acetylene gas

Thermal Hydrocarbonization of freshly etched pSi (THCpSi) was carried out at 525 ºC under a 1:1 N_2:acetylene mixture flow whereas Thermal Carbonization of freshly etched pSi (TCpSi) consisted on a two-step carbonization process, where THC treatment was followed by annealing at 800 ºC. More detailed experimental information can be found elsewhere [9].

2.4. Electrochemical measurements

Electrochemical characterization was performed by cyclic voltammetry (CV) using 2 mmol L^{-1} ferrocyanide/ ferricyanide in 10 mmol L^{-1} PBS buffer (pH 7.4) as redox probe. CV measurements were performed from -0.2 V to 0.8 V at a scan rate of 100 mV s^{-1}.

For the study of the three dihydroxybenzene isomers, CC, HQ and RC solutions were prepared daily in deaerated 10 mmol L^{-1} PBS buffer (pH 7.4) and kept in the dark to prevent oxidation. CV measurements were performed between -0.3 V and 1 V at a scan rate of 50 mV s^{-1} and DPV measurements were performed after 30 s stirring by scanning the potential from -0.2 V to 0.9 V using step potentials of 5 mV, pulse amplitudes of 50 mV and pulse times of 50 ms.

3. Results and discussion

3.1. THCpSi and TCpSi fabrication and characterization

Thermal carbonization and thermal hydrocarbonization by acetylene were used to stabilize pSi samples. As it was previously reported by Guo *et al* [9], these procedures allow the stabilization of pSi without altering its dimensions or nanostructured morphology, which can be controlled by adjusting the anodization conditions. Figure 1 shows the SEM images obtained for TCpSi single layers nanostructures, with an average porous diameter of 72 ± 15 nm and a 500 nm thickness layer.

The changes in chemical stability caused by TC and THC were studied by ATR-FTIR. As it can be seen in Figure 2, after both thermal treatments, the characteristic bands of freshly etched pSi at 2087, 2114 and 905 cm^{-1}, corresponding to the stretching vibrations of Si-H and Si-H_2 and the Si-H deformation mode respectively, completely disappeared and were substituted by new bands associated to saturated C-H and unsaturated C=C stretching vibrations and the CH_3 symmetric deformation mode of Si-CH_3 [15].

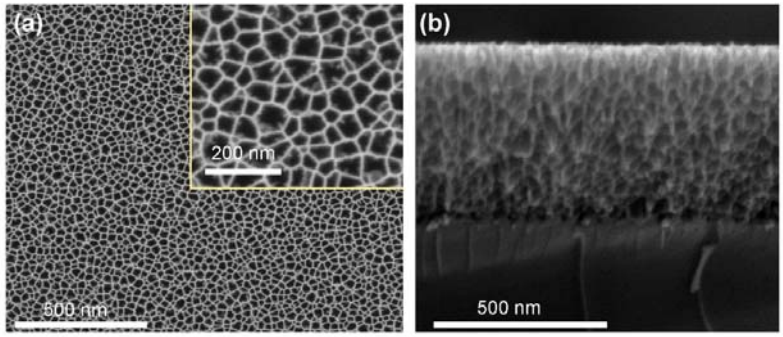

Figure 1. SEM images of TCpSi single layer nanostructures at (**a**) top and (**b**) cross-sectional view. The pSi layer was electrochemically etched in a 1:1 (v:v) HF/ethanol solution by applying a current density of 53 mA cm^{-2} for 20 s in a MPSB wet etching system.

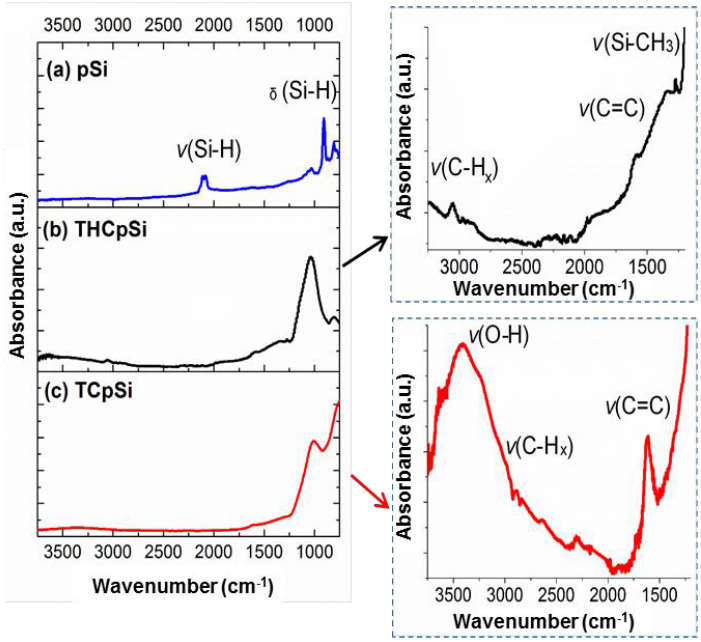

Figure 2. ATR-FTIR spectra of the single layer of (**a**) freshly etched pSi, (**b**) THCpSi and (**c**) TCpSi.

The electrochemical performance of both THCpSi and TCpSi was evaluated by CV in the presence of ferrocyanide/ ferricyanide in 10 mmol L^{-1} PBS buffer (pH 7.4) as redox probe. Figure 3 shows the CV measurements of 20 consecutive cycles for both THCpSi and TCpSi. On the first cycles both materials present well-defined peaks corresponding to the oxidation and reduction of $[Fe(CN)_6]^{3-/4-}$, although a superior electrochemical performance, inferred by larger anodic currents and smaller peak to peak potential difference, was achieved with TCpSi. Furthermore, TCpSi response is stable along the 20 repetitive measurements, with a relative standard deviation (RSD) of the anodic current of 2.2 %, whereas TCHpSi response decreases and loses reversibility with each consecutive cycle, with a total signal loss over 35% after 20 measurements. This better electrochemical performance observed for TCpSi could be explained by its higher chemical stability coupled with a larger carbon surface coverage [9].

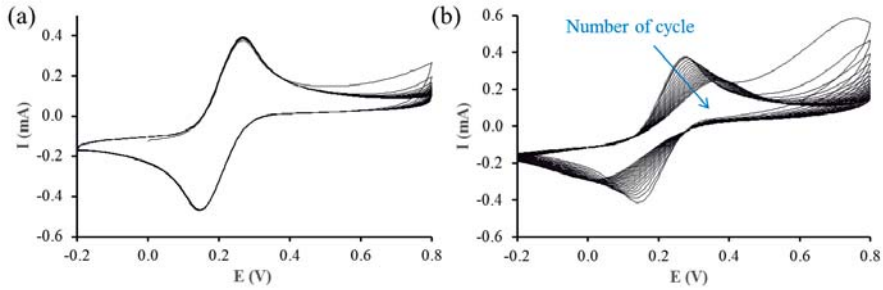

Figure 3. CV measurements of 20 consecutive cycles in a 2 mmol L^{-1} ferrocyanide/ ferricyanide solution in 10 mmol L^{-1} PBS buffer pH 7.4 using (**a**) TCpSi and (**b**) THCpSi.

3.2. Electrochemical behaviour of HQ, CC and RC

Initially the electrochemical behavior of HQ, CC and RC at PBS pH 7.4 was studied at both TCpSi and THCpSi by CV and compared to the behavior observed at a glassy carbon electrode (GCE). Figure 4 shows the CV measurements carried out in a solution containing 30 µmol L^{-1} of either HQ, CC or RC with each sensor.

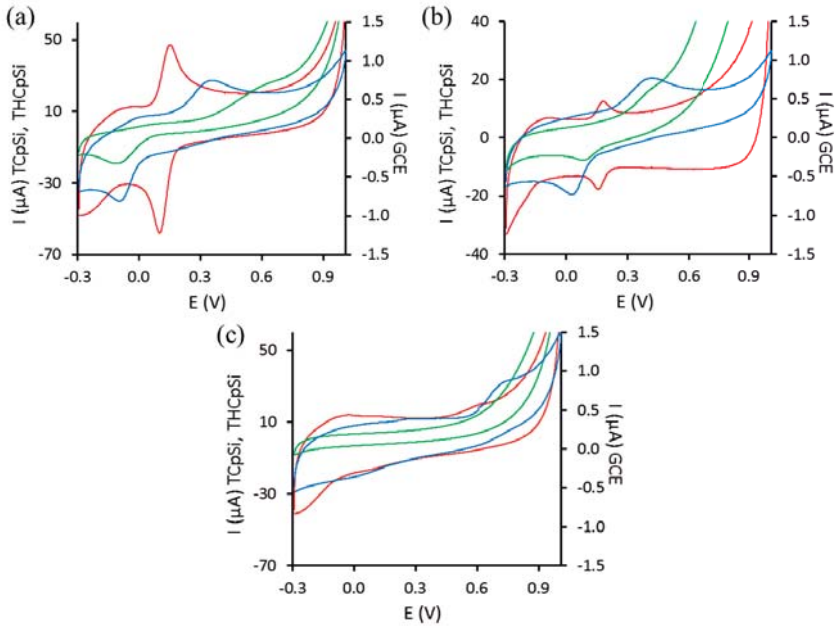

Figure 4. CV measurements of 30 µmol L^{-1} HQ (**a**), CC (**b**) or RC (**c**) solution in 10 mmol L^{-1} PBS buffer pH 7.4 using GCE (blue line), TCpSi (red line) and THCpSi (green line). GCE currents are referred to the right axis whereas TCpSi and THCpSi currents are referred to the left axis.

As it can be seen, both HQ (Figure 4a) and CC (Figure 4b) present a similar behavior, with an anodic and a cathodic peak, respectively, at 341 mV and -103 mV for HQ and at 403 mV and 19 mV for CC using GCE. This corresponds to a peak potential separation (ΔE_P) of 444 mV and 384 mV for HQ and CC respectively, which differs significantly from the 29.5 mV characteristic of the two-electron reactions expected in this case (Scheme 1), indicating that both HQ and CC present an

irreversible electrochemical behavior at GCE. On the other hand, much higher currents were achieved with both TCpSi and THCpSi, which can be attributed to their larger surface area. However, in terms of reversibility TCpSi showed a much better behavior, reducing the ΔE_P to 47 mV and 18 mV for HQ and CC respectively, which is probably due to an increase of the electron transfer kinetics provided by the nanostructure of pSi. The lack of improvement in reversibility observed in the case of THCpSi (ΔE_P for HQ and CC are 650 mV and 341 mV respectively) could be explained by its hydrophobic nature.

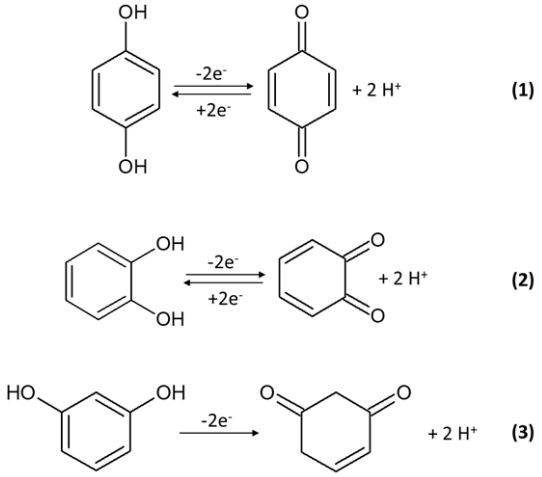

Scheme 1. Redox reactions of (**1**) HQ, (**2**) CC and (**3**) RC.

The electrochemical behavior of RC (Figure 4c) is completely different from that shown by HQ and CC. No cathodic peak was observed at GCE and the anodic current was much smaller than those of HQ and CC. These facts could be explained by the low thermodynamic stability of the RC quinonic form and the lack of aromatic ring activation due to the OH groups meta- position [16]. Regarding the carbon-stabilized pSi substrates, the RC anodic peak was only observed in the case of TCpSi, where it was shifted to less positive potentials.

At the view of this results and considering both the better stability shown in the CV characterization with $[Fe(CN)_6]^{3-/4-}$ and the increase of electron transfer kinetics that gives rise to a more reversible behavior of HQ, CC and RC, TCpSi was selected as the best carbon-stabilized pSi substrate and considered for further studies.

In this sense, its applicability to the simultaneous determination of HQ, CC and RC was also evaluated by DPV. Figure 5 shows the voltammograms obtained for a solution containing 30 µmol L^{-1} of HQ, CC and RC in 10 mmol L^{-1} PBS buffer (pH 7.4) for TCpSi and GCE. It can be observed that in the case of GCE only RC can be correctly determined since HQ and CC are completely overlapped, whereas in the case of TCpSi three separate peaks corresponding to HQ, CC and RC are obtained, allowing the simultaneous determination of the three isomers.

3.3. Analytical performance of TCpSi

The analytical performance of TCpSi for the voltammetric determination of HQ, CC and RC was evaluated. First of all, some experimental parameters such as pH and accumulation time (t_{acc}) were optimized. The voltammetric signals are highly influenced by pH due to the two protons involved in the oxidation processes, which results in a considerable shift to more negative potentials at higher pHs. However, from pH 4 to 8 the separation between HQ and CC peaks could not be improved because the shift rate is almost identical for the two isomers. In terms of current, the signal

increased from pH 4 to 7.5 and slightly decreased at pH 8. Thus, the physiological pH (7.4) was selected as the optimal pH value.

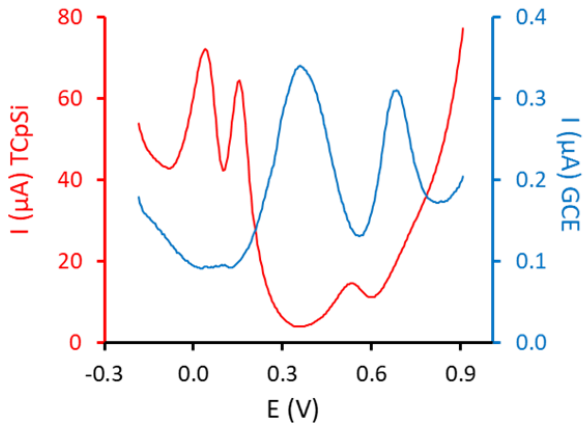

Figure 5. DPV measurements of a solution containing 30 µmol L^{-1} HQ, CC and RC in PBS 10 mmol L^{-1} pH 7.4 at TCpSi (red lines) and GCE (blue lines). GCE currents are referred to the right axis whereas TCpSi currents are referred to the left axis.

Regarding t_{acc}, different voltammetric measurements were performed from 0 to 240 s in a solution containing 30 µmol L^{-1} of HQ, CC and RC in 10 mmol L^{-1} PBS buffer (pH 7.4). For all three isomers, the current slightly increased after 30 s of t_{acc} but no further increase was observed for longer t_{acc}. Therefore, a t_{acc} of 30 s was selected as the optimal value.

Once the experimental conditions were optimized, the analytical performance of TCpSi was studied considering repeatability, reproducibility, sensitivity, linear range and limits of detection (LOD) and quantification (LOQ). All these values are summarized in Table 1.

Table 1. Calibration parameters, reproducibility and repeatability for the separate determination of HQ, CC and RC on TCpSi at PBS 10 mmol L^{-1} pH 7.4 after 30 s of accumulation. Standard deviations are denoted by parenthesis.

	HQ	CC	RC
Sensitivity (a.u. µmol^{-1} L)	1.20 (0.04)	1.19 (0.03)	0.30 (0.01)
R^2	0.994	0.998	0.991
Linear range (µmol L^{-1}) [1]	5.6 – 35.2	3.4 – 25.4	14.2 – 50.0
LOD (µmol L^{-1})	1.67	1.01	4.25
Reproducibility (%)	2.79	7.56	0.39
Repeatability (%)	5.10	3.51	5.79

[1] The lowest value of the linear range was considered from the LOQ.

Repeatability was calculated from 5 repetitive measurements of a solution containing 30 µmol L^{-1} of HQ, CC and RC in 10 mmol L^{-1} PBS buffer (pH 7.4) using the same electrode whereas reproducibility was computed from the slope of two independent and individual calibration curves carried out from 0.5 to 50 µmol L^{-1} and using different sensors. For all three isomers, a repeatability and reproducibility lower than 6% and 8 % respectively was achieved. These values are similar to those reported in the literature for GCE modified with different nanomaterials [11,17,18].

In terms of sensitivity, calculated as the slope of the calibration curve, HQ and CC showed similar sensitivities and significantly higher than RC, which is in agreement with the more intensive peaks observed for HQ and CC. On the other hand, LODs and LOQs were calculated as three and

ten times, respectively, the standard deviation of the intercept over the slope of the calibration curve. In all cases LOQs were at the level of few μmol L^{-1}, achieving the lowest value for CC and the highest for RC. However, it should also be pointed out that only RC shows a linear response up to 50 μmol L^{-1}. The LODs and LOQs achieved are only slightly higher than those reported literature for GCE modified with different nanomaterials [11,17,18] and similar to those reported for a commercial graphene screen-printed electrode [19], with the additional advantages provided by pSi (versatility, biocompatibility, fast and simple fabrication process, adjustable morphology…). Therefore, the fast electron transfer kinetics and the good analytical performance of TCpSi highlight its potential to act as a new substrate for electrochemical sensors.

5. Conclusions

The potential application of carbon-stabilized pSi as voltammetric sensor platform has been successfully demonstrated. First of all TCpSi and THCpSi were compared in terms of electrochemical reproducibility and its response to HQ, CC and RC, concluding that TCpSi is a much more reproducible substrate with a faster electron transfer kinetics that results in more reversible signals. Furthermore, TCpSi presented a better electrochemical response to HQ, CC and RC than GCE, not only inferred by the higher reversibility but also by the possibility to simultaneously determine HQ and CC. A good analytical performance was also achieved by TCpSi, with repeatability, reproducibility and LODs similar to those reported for GCE modified with different nanomaterials or commercial screen-printed electrodes. Finally, it should also be highlighted that TCpSi retains all the advantages provided by pSi: versatility, biocompatibility, fast and simple fabrication process, adjustable morphology…

Acknowledgments: Authors acknowledge financial support from the Australian Research Council's Discovery and Linkage Project Schemes (DP160104362 and LP160101050). Clara Pérez-Ràfols acknowledges the Spanish Ministry of Education, Culture and Sports for a Ph.D grant (reference FPU15/02140).

References

1. Canham, L. *Handbook of porous silicon*; 2nd ed.; Springer: Birmingham, UK, 2017.
2. Sailor, M.J. Fundamentals of porous silicon preparation. In *Porous silicon in practice: Preparation, characterization and applications*; Wiley-VCH Verlag GmbH & Co. KGaA: Weinheim, Germany, 2012; pp. 1–42.
3. Stewart, M.P.; Buriak, J.M. Chemical and biological applications of porous silicon technology. *Adv. Mater.* **2000**, *12*, 859–869.
4. Salis, A.; Setzu, S.; Monduzzi, M.; Mula, G.; Chimiche, S.; Csgi, C.; Fisica, D.; Cagliari, U. Porous silicon-based electrochemical biosensors. In *Biosensors-Emerging materials and applications*; InTech: London, UK, 2011.
5. Roychaudhuri, C. A review on porous silicon based electrochemical biosensors: Beyond surface area enhancement factor. *Sensors Actuators B. Chem.* **2015**, *210*, 310–323.
6. Salonen, J.; Lehto, V.-P.; Björkqvist, M.; Laine, E.; Niinistö, L. Studies of thermally-carbonized porous silicon surfaces. *Phys. Status Solidi A* **2002**, *182*, 123–126.
7. Salonen, J.; Mäkilä, E. Thermally carbonized porous silicon and its recent applications. *Adv. Mater.* **2018**, *30*, 1703819–1703837.
8. Salonen, J.; Kaasalainen, M.; Rauhala, O.-P.; Lassila, L.; Hakamies, M.; Jalkanen, T.; Hahn, R.; Schmuki, P.; Mäkilä, E. Thermal carbonization of porous silicon: the current status and recent applications. *ECS Trans.* **2015**, *69*, 167–176.
9. Guo, K.; Sharma, A.; Toh, R.J.; Alvárez de Eulate, E.; Gengenbach, T.R.; Cetó, X.; Voelcker, N.H.; Prieto-Simón, B. Porous silicon nanostructures as effective faradaic electrochemical sensing platforms.

Adv. Funct. Mater. **2019**, *29*, 1809206–1809217.

10. Pérez-Ràfols, C.; Serrano, N.; Díaz-Cruz, J.M.; Ariño, C.; Esteban, M. New approaches to antimony film screen-printed electrodes using carbon-based nanomaterials substrates. *Anal. Chim. Acta* **2016**, *916*, 17–23.
11. Qi, H.; Zhang, C. Simultaneous determination of hydroquinone and catechol at a glassy carbon electrode modified with multiwall carbon nanotubes. *Electroanalysis* **2005**, *17*, 832–838.
12. *EEC Directive 80/77/CEE 15-7-1990. Off. J. Eur. Communities (30/08/1990)*; European Community: Bruselles, 1990.
13. *Límites de exposición profesional para agentes químicos en España*; Instituto Nacional de Seguridad e Higiene en el Trabajo (INSHT), 2014.
14. Sciacca, B.; Secret, E.; Pace, S.; Gonzalez, P.; Geobaldo, F.; Quignard, F.; Cunin, F. Chitosan-functionalized porous silicon optical transducer for the detection of carboxylic acid-containing drugs in water. *J. Mater. Chem.* **2011**, *21*, 2294–2302.
15. Sciacca, B.; Alvarez, S.D.; Geobaldo, F.; Sailor, M.J. Bioconjugate functionalization of thermally carbonized porous silicon using a radical coupling reaction. *Dalt. Trans.* **2010**, *39*, 10847–10853.
16. Nasr, B.; Abdellatif, G.; Cañizares, P.; Sáez, C.; Lobato, J.; Rodrigo, M.A. Electrochemical oxidation of hydroquinone, resorcinol, and catechol on boron-doped diamond anodes. *Environ. Sci. Technol.* **2005**, *39*, 7234–7239.
17. Du, H.; Ye, J.; Zhang, J.; Huang, X.; Yu, C. A voltammetric sensor based on graphene-modified electrode for simultaneous determination of catechol and hydroquinone. *J. Electroanal. Chem.* **2011**, *650*, 209–213.
18. Yu, J.; Du, W.; Zhao, F.; Zeng, B. High sensitive simultaneous determination of catechol and hydroquinone at mesoporous carbon CMK-3 electrode in comparison with multi-walled carbon nanotubes and Vulcan XC-72 carbon electrodes. *Electrochim. Acta* **2009**, *54*, 984–988.
19. Aragó, M.; Ariño, C.; Dago, À.; Díaz-Cruz, J.M.; Esteban, M. Simultaneous determination of hydroquinone, catechol and resorcinol by voltammetry using graphene screen-printed electrodes and partial least squares calibration. *Talanta* **2016**, *160*, 138–143.

8.1 Elèctrodes modificats químicament

En aquest primer apartat es presenten i discuteixen els diferents elèctrodes modificats químicament desenvolupats al llarg d'aquesta tesi doctoral. Majoritàriament, el desenvolupament d'aquests elèctrodes es troba recollit als següents articles:

- C. Pérez-Ràfols, N. Serrano, J. M. Díaz-Cruz, C. Ariño, M. Esteban, Glutathione modified screen-printed carbon nanofiber electrode for the voltammetric determination of metal ions in natural samples, Talanta 155 (2016) 8-13.

- C. Pérez-Ràfols, N. Serrano, J. M. Díaz-Cruz, C. Ariño, M. Esteban, A chemically-bound glutathione sensor bioinspired by the defense of organisms against heavy metal contamination: optimization of the immobilization conditions, Chemosensors 5 (2017) 12-20.

- J. Puy-Llovera, C. Pérez-Ràfols, N. Serrano, J. M. Díaz-Cruz, C. Ariño, M. Esteban, Selenocystine modified screen-printed electrode as an alternative sensor for the voltammetric determination of metal ions, Talanta 175 (2017) 501-506.

- C. Pérez-Ràfols, M. Rosal, N. Serrano, C. Ariño, M. Esteban, J. M. Díaz-Cruz, Expanding the possibilities of electrografting modification of voltammetric sensors through two complementary strategies, Electrochimica Acta, 319 (2019) 878-884

Cal mencionar que, a més, en aquest apartat també s'introduirà el sensor crown-6-SPCNFE, el desenvolupament del qual es troba recollit en un apartat de l'article Sensors and Actuators B 245 (2017) 18-24 que s'introduirà al capítol 9.

Els elèctrodes recollits en aquest apartat es mostren a la figura 8.1, on també s'esquematitzen les etapes de les modificacions corresponents.

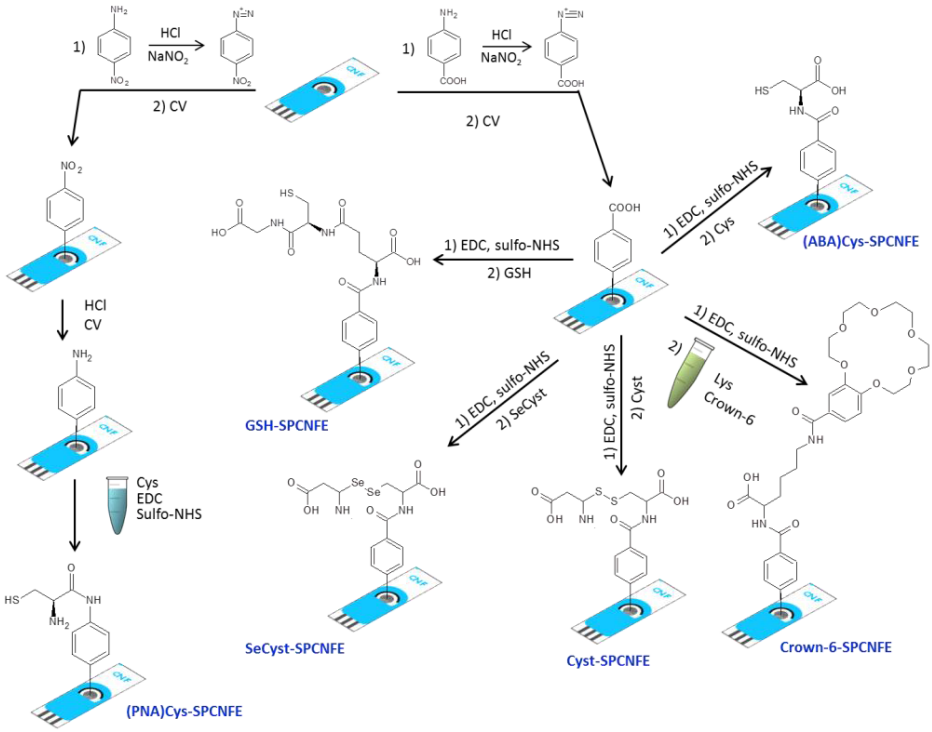

Figura 8.1. Elèctrodes modificats químicament desenvolupats al llarg d'aquesta tesi doctoral.

8.1.1 Caracterització

El seguiment del correcte desenvolupament de les diferents etapes dels processos de modificació química s'ha realitzat per CV. En les dues estratègies emprades, l'etapa d'*electrografting* dóna lloc a un pic ample i irreversible, corresponent a la reducció de la sal de diazoni, que va disminuint a mesura que s'apliquen més cicles ja que es forma una capa orgànica a la superfície de l'elèctrode que dificulta l'aproximació de nous cations diazoni (figura 8.2a i 8.2b) [45]. D'altra banda, la reducció dels grups nitro a grups amino també dóna lloc a un pic de reducció ample i irreversible que desapareix al cap de 5 cicles, fet que indica que la reducció dels grups nitro ha sigut completa (figura 8.2c) [99].

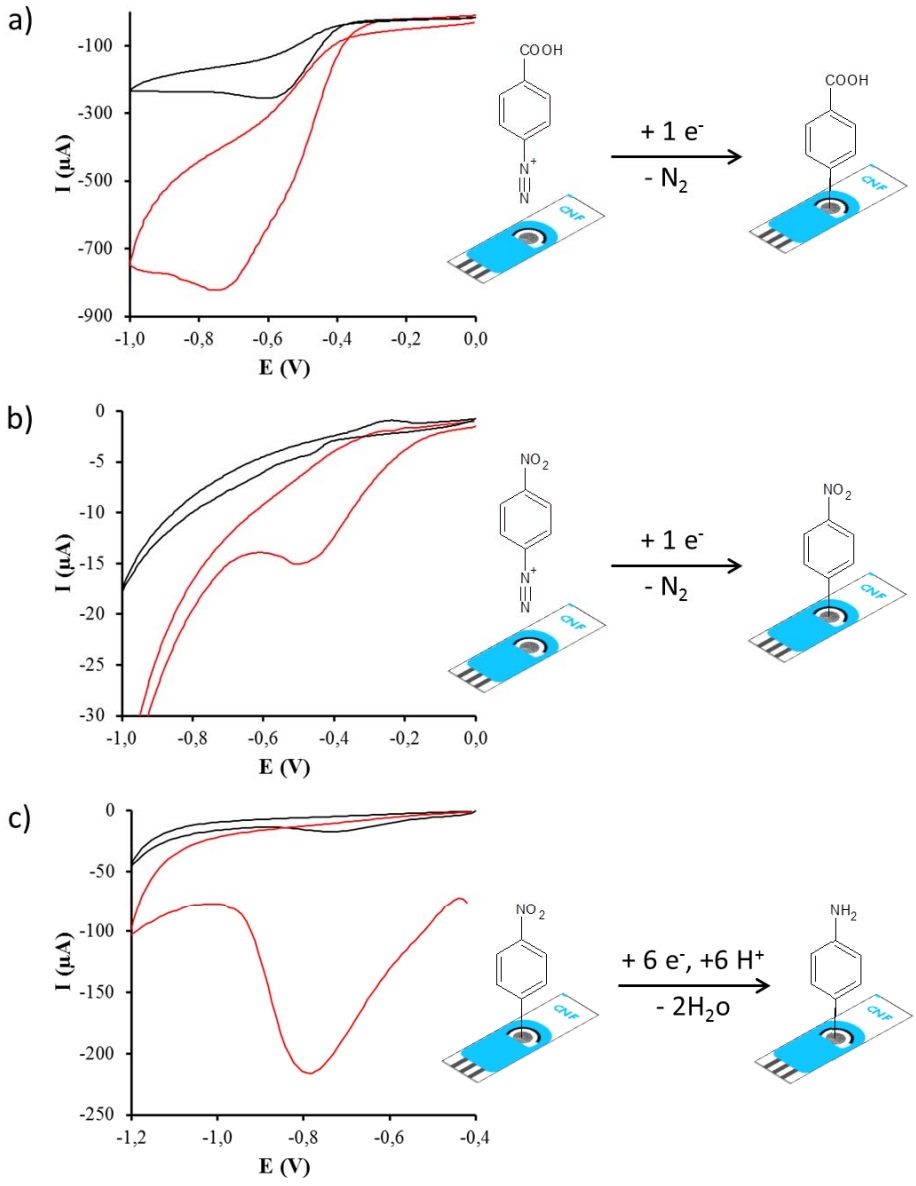

Figura 8.2. Voltamperogrames cíclics característics de l'etapa d'*electrografting* partint d'ABA (a) i PNA (b) i de la reducció del grup nitro (c). El primer i últim cicle es representen en vermell i negre respectivament.

D'altra banda, la caracterització de l'elèctrode per CV en presència del sistema redox model $[Fe(CN)_6]^{3-/4-}$ també ens permet comprovar que les diferents etapes de modificació s'estan produint correctament. Així, tal i com es pot veure a la

figura 8.3, la funcionalització de la superfície de l'elèctrode amb grups carboxílic, nitro o amino dóna lloc a una disminució del senyal electroquímic ja que la capa orgànica formada actua com a barrera, dificultant l'aproximació dels ions $[Fe(CN)_6]^{3-/4-}$. La disminució del senyal és més pronunciada en el cas de la funcionalització amb grups carboxílics ja que, a més de l'efecte barrera, a pH 7,4 també es genera una repulsió electrostàtica entre les càrregues negatives del grups carboxilats i els ions $[Fe(CN)_6]^{3-/4-}$. En el cas de les superfícies modificades amb grups nitro i amino s'observa també l'aparició d'un pic d'oxidació i un pic de reducció a -0,18 V i -0,24 V respectivament, que corresponen al sistema reversible NO/NHOH [100,101]. Finalment, la immobilització del modificador també dóna lloc a una variació del senyal que, tot i que depèn del modificador específic, en tots els casos estudiats augmenta respecte al senyal obtingut just després de l'*electrografting*, arribant en molts casos a donar més senyal que el sensor no modificat.

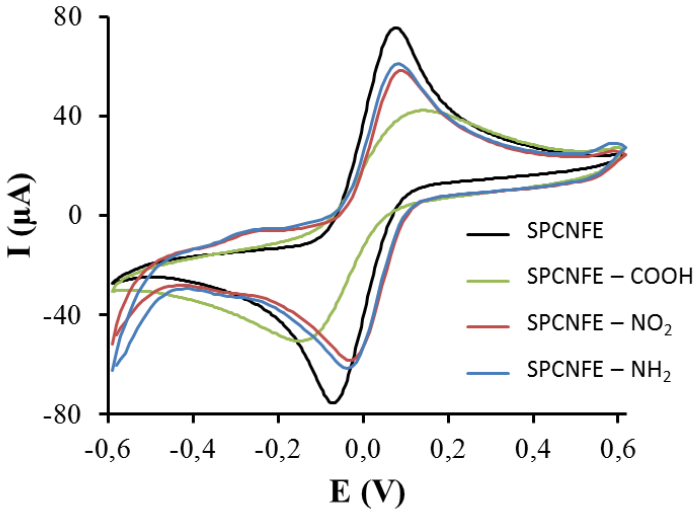

Figura 8.3. Caracterització per CV del SPCNFE sense modificar (negre) i funcionalitzat amb grups carboxílic (verd), nitro (vermell) o amino (blau). Les mesures estan fetes en una solució 2 mmol L^{-1} de $[Fe(CN)_6]^{3-/4-}$ en tampó de fosfats pH 7,4 i a 100 mV s^{-1}.

La caracterització de l'elèctrode per CV en presència del sistema redox model $[Fe(CN)_6]^{3-/4-}$, aquest cop a diferents pHs, també permet estudiar el comportament àcid-base de l'elèctrode ja que, al ser un sistema redox no dependent del pH, les variacions del senyal es poden atribuir a la variació de la

càrrega de la superfície, que afecta a les interaccions electrostàtiques amb els ions $[Fe(CN)_6]^{3-/4-}$. Aquest estudi, que s'inclou a l'article Electrochimica Acta, 319 (2019) 878-884 per a les dues variants d'*electrografting*, mostra un pK_a experimental al voltant de pH 4,5 corresponent a la desprotonació dels àcids benzoics o anilines que no han reaccionat amb la Cys i un segon pK_a experimental al voltant de 8 o 9 corresponent a la desprotonació del grup tiol i/o amino de la Cys.

8.1.2 Aplicació a la determinació d'ions metàl·lics

Els diferents sensors modificats desenvolupats s'han estudiat per a la determinació d'ions metàl·lics. En general, per al desenvolupament de nous elèctrodes s'ha emprat el sistema model Cd(II) i Pb(II) ja que es tracta d'una parella de metalls àmpliament estudiada que dóna lloc a dos pics ben definits i permet atribuir les diferències observades en la resposta al sensor desenvolupat. Posteriorment, els sensors que han donat millors resultats s'han aplicat també a la determinació d'altres ions metàl·lics com el Zn(II), el Tl(I), l'In(III) i el Bi(III). A la taula 8.1 es recullen els paràmetres analítics obtinguts per als diferents sensors i metalls estudiats.

A partir d'aquests resultats es pot observar que quan es desenvolupa un nou elèctrode modificat químicament cal tenir en compte principalment tres aspectes: el suport sobre el qual es realitza la modificació, la tria del modificador a immobilitzar i el grup funcional a través del qual s'immobilitza el modificador.

L'efecte del suport es pot veure a partir de la determinació de Cd(II) i Pb(II) amb els elèctrodes modificats amb glutatió, un d'ells emprant un suport de carboni (SPCE) i l'altre emprant un suport de CNF (SPCNFE). S'observa que el SPCNFE ofereix millors prestacions, particularment en termes de reproductibilitat entre elèctrodes. Aquesta millora en la reproductibilitat es deu a la capacitat d'aquest suport per mantenir les gotes de reactius sobre la superfície de l'elèctrode de treball, que és especialment important en l'última etapa del procés de modificació on s'incorpora el GSH. A diferència del SPCNFE, el SPCE no és capaç de sostenir adequadament la gota, que s'estén pels tres elèctrodes i, per tant, no es garanteix que s'introdueixi sempre la mateixa quantitat de GSH sobre l'elèctrode de treball, fet que es tradueix en una manca de reproductibilitat

entre elèctrodes. D'altra banda, l'ús del SPCNFE també permet augmentar la sensibilitat per al Pb(II) i disminuir significativament el LOD per al Cd(II), tot i que en aquest cas la sensibilitat és menor.

El segon aspecte que cal tenir en compte és la tria del modificador a immobilitzar, que pot implicar variacions en l'última etapa del procés de modificació en funció de la seva solubilitat. Aquesta etapa és òptima quan el modificador es troba totalment dissolt i en la seva forma zwiteriònica, fet que no suposa cap problema en el cas del GSH i la Cys ja que, en els nivells de concentració necessaris, són solubles en tampó MES a pH 4,5. No obstant, en el cas de la Cyst, la SeCyst i el crown-6 es fa necessari dissoldre'ls total o parcialment en etanol i mantenir-los tapats per evitar que s'evapori abans que es produeixi la reacció. Aquest fet pot afectar la repetitivitat i reproductibilitat del sensor, com és el cas del Cyst-SPCNFE.

D'altra banda, si es comparen les sensibilitats obtingudes per als diferents metalls, s'observa que, a excepció del GSH-SPCNFE on la sensibilitat per al Cd(II) és més baixa de l'esperada, tots els sensors basats en molècules tiòliques presenten la mateixa sensibilitat relativa als diversos metalls, sent l'ordre de preferència Cd(II) > Pb(II) > Zn(II) > Tl(I) > In(III) > Bi(III). En termes absoluts, petites variacions en l'estructura del modificador poden implicar importants canvis en la sensibilitat dels sensors tal com es pot veure al comparar el SeCyst-SPCNFE amb el Cyst-SPCNFE. L'intercanvi dels sofres per selenis permet duplicar la sensibilitat del sensor i disminuir els LODs, fet que es pot explicar a partir de la teoria de Pearson d'àcid-base tou-dur on el seleni, al ser una base més tova que el sofre, presenta més afinitat pel Cd(II) i el Pb(II) que són àcids tous i frontera respectivament. D'altra banda, l'ús del crown-6, que presenta un mecanisme d'interacció completament diferent amb els metalls, basat en aquest cas en la mida de l'ió metàl·lic i de la cavitat de l'èter corona, permet invertir l'ordre de sensibilitats per a l'In(III) i el Tl(I) fet que, com es veurà més endavant, és important per obtenir sensibilitats creuades en les llengües electròniques.

Finalment, el tercer factor que cal tenir en compte és el grup funcional a través del qual s'immobilitza el modificador. Així, tot i que el procediment més habitual per a la immobilització de lligands peptídics és a través del seu grup amino, també existeix la possibilitat d'immobilitzar-lo a través del seu grup carboxílic.

Taula 8.1. Resum dels paràmetres analítics obtinguts per a la determinació de metalls amb els diferents elèctrodes modificats químicament. Si no s'indica el contrari, les mesures s'han realitzat per a cada metall individual, a pH 4,5, amb un E_d de -1,4 V i amb un t_d de 120 s. Les desviacions estàndards s'indiquen entre parèntesis.

	Zn(II)	Cd(II)	Pb(II)	Bi(III)	In(III)	Tl(I)
GSH-SPCE						
Sensibilitat (u.a. μg^{-1} L)	--	1,22 (0,05)	1,07 (0,02)	--	--	--
Interval de linealitat ($\mu g\ L^{-1}$)[a]	--	43,8 – 153,0	11,7 – 153,0	--	--	--
LOD ($\mu g\ L^{-1}$)	--	13,2	3,5	--	--	--
Repetitivitat (%)	--	8,2	8,3	--	--	--
Reproductibilitat (%)	--	> 20[b]	> 20[b]	--	--	--
GSH-SPCNFE						
Sensibilitat (u.a. μg^{-1} L)	1,71 (0,04)	0,63 (0,01)	3,02 (0,04)	0,240 (0,005)	0,47 (0,01)	0,97 (0,02)
Interval de linealitat ($\mu g\ L^{-1}$)[a]	24,5 – 198,3	10,8 – 150,1	10,1 – 150,1	29,1 – 200,7	26,4 – 200,4	41,8 – 274,9
LOD ($\mu g\ L^{-1}$)	7,4	3,2	3,0	8,7	7,9	12,5
Repetitivitat (%)	--	5,1	7,6	--	--	--
Reproductibilitat (%)	--	6,8[b]	8,9[b]	--	--	--

Taula 8.1 (continuació) Resum dels paràmetres analítics obtinguts per a la determinació de metalls amb els diferents elèctrodes modificats químicament. Si no s'indica el contrari, les mesures s'han realitzat per a cada metall individual, a pH 4,5, amb un E_d de -1,4 V i amb un t_d de 120 s. Les desviacions estàndards s'indiquen entre parèntesis.

	Zn(II)	Cd(II)	Pb(II)	Bi(III)	In(III)	Tl(I)
SeCyst-SPCNFE[g]						
Sensibilitat (nA μg^{-1} L)	--	32,4 (0,4)	14,3 (0,2)	--	2,11 (0,03)[d]	3,02 (0,05)[d]
Interval de linealitat ($\mu g\ L^{-1}$)[a]	--	10,7 – 150,0	10,8 – 150,0	--	14,1 – 200,0[d]	14,8 – 200,0[d]
LOD ($\mu g\ L^{-1}$)	--	3,2	3,2	--	4,2[d]	4,5[d]
Repetitivitat (%)	--	6,5	9,4	--	--	--
Reproductibilitat (%)	--	11,1[b]	9,1[b]	--	--	--
Cyst-SPCNFE[g]						
Sensibilitat (nA μg^{-1} L)	--	14,2 (0,3)	7,6 (0,1)	--	--	--
Interval de linealitat ($\mu g\ L^{-1}$)[a]	--	19,1 – 150,0	15,1 – 150,0	--	--	--
LOD ($\mu g\ L^{-1}$)	--	5,7	4,5	--	--	--
Repetitivitat (%)	--	27,4	34,9	--	--	--
Reproductibilitat (%)	--	28,5[b]	34,1[b]	--	--	--

Taula 8.1 (continuació) Resum dels paràmetres analítics obtinguts per a la determinació de metalls amb els diferents elèctrodes modificats químicament. Si no s'indica el contrari, les mesures s'han realitzat per a cada metall individual, a pH 4,5, amb un E_d de -1,4 V i amb un t_d de 120 s. Les desviacions estàndards s'indiquen entre parèntesis.

	Zn(II)	Cd(II)	Pb(II)	Bi(III)	In(III)	Tl(I)
(ABA)Cys-SPCNFE[g]						
Sensibilitat (u.a. μg^{-1} L)	2,19 (0,05)	5,39 (0,05)[e,f]	2,75 (0,01)[e,f]	0,196 (0,005)	0,277 (0,004)	1,08 (0,03)
Interval de linealitat ($\mu g\ L^{-1}$)[a]	26,3 – 198,3	7,3 – 153,9[e,f]	3,7 – 153,9[e,f]	38,0 – 200,7	18,2 (200,4)	57,8 – 274,9
LOD ($\mu g\ L^{-1}$)	7,9	2,2[e,f]	1,1[e,f]	11,4	5,5	17,4
Repetitivitat (%)	--	1,5[e,f]	1,6[e,f]	--	--	--
Reproductibilitat (%)	--	1,3[c,e,f]	1,2[c,e,f]	--	--	--
(PNA)Cys-SPCNFE[g]						
Sensibilitat (u.a. μg^{-1} L)	--	4,63 (0,03)[e]	3,44 (0,01)[e]	--	--	--
Interval de linealitat ($\mu g\ L^{-1}$)[a]	--	4,6 – 153,9[e]	3,4 – 153,9[e]	--	--	--
LOD ($\mu g\ L^{-1}$)	--	1,4[e]	1,0[e]	--	--	--
Repetitivitat (%)	--	1,4[e]	1,3[e]	--	--	--
Reproductibilitat (%)	--	0,8[c,e]	0,9[c,e]	--	--	--

Taula 8.1 (continuació) Resum dels paràmetres analítics obtinguts per a la determinació de metalls amb els diferents elèctrodes modificats químicament. Si no s'indica el contrari, les mesures s'han realitzat per a cada metall individual, a pH 4,5, amb un E_d de -1,4 V i amb un t_d de 120 s. Les desviacions estàndards s'indiquen entre parèntesis.

	Zn(II)	Cd(II)	Pb(II)	Bi(III)	In(III)	Tl(I)
Crown-6-SPCNFE						
Sensibilitat (u.a. μg^{-1} L)	--	--	--	--	0,57 (0,01)	0,30 (0,01)
Interval de linealitat ($\mu g\ L^{-1}$)[a]	--	--	--	--	45,8 – 300,4	36,4 – 270,2
LOD ($\mu g\ L^{-1}$)	--	--	--	--	13,7	10,9
Repetitivitat (%)	--	--	--	--	--	--
Reproductibilitat (%)	--	--	--	--	--	--

[a]El LOQ s'ha considerat com a valor inferior de l'interval linealitat.

[b]Reproductibilitat calculada per a un únic nivell de concentració.

[c]Reproductibilitat calculada per a diferents nivells de concentració, a partir dels pendents de les rectes de calibratge.

[d]Mesures realitzades amb un E_d de -1,3 V.

[e]Mesures realitzades amb un E_d de -1,0 V.

[f]Mesures realitzades a pH 5.

[g]Els valors de Cd(II) i Pb(II) corresponen a la determinació simultània dels dos metalls.

Tot i que aquest segon procediment implica una etapa extra en el procés de modificació ja que no es pot funcionalitzar la superfície directament amb grups amino sinó que cal funcionalitzar-la primer amb grups nitro i posteriorment reduir-los, el temps de modificació és semblant ja que l'activació dels grups carboxílics amb EDC i sulfo-NHS es pot realitzar paral·lelament a la funcionalització de la superfície. Aquestes dues variants de modificació s'han comparat per a la immobilització de la Cys i s'observa que el (PNA)Cys-SPCNFE, on la Cys s'ha immobilitzat a través del grup carboxílic, proporciona un pic més gaussià i una major sensibilitat per al Pb(II) alhora que permet disminuir el LOQ del Cd(II), sent així l'únic dels elèctrodes desenvolupat que, a més de detectar, també permet quantificar el Cd(II) per sota els límits legals establerts a la directiva marc de l'aigua (2000/60/EC).

8.2 Pel·lícules metàl·liques

En aquest segon apartat es presenten i discuteixen els diferents elèctrodes basats en pel·lícules metàl·liques amb què s'ha treballat al llarg d'aquesta tesi doctoral. Majoritàriament, el desenvolupament d'aquests elèctrodes es troba recollit als següents articles:

- C. Pérez-Ràfols, N. Serrano, J. M. Díaz-Cruz, C. Ariño, M. Esteban, New approaches to antimony film screen-printed electrodes using carbon-based nanomaterials substrates, Analytica Chimica Acta 916 (2016) 17-23.

- C. Pérez-Ràfols, P. Trechera, N. Serrano, J. M. Díaz-Cruz, C. Ariño, M. Esteban, Determination of Pd(II) using an antimoni film coated on a screen-printed elèctrode by adsorptive stripping voltammetry, Talanta 167 (2017) 1-7.

A més, en aquest apartat també s'introduiran el sensor *ex-situ*-BiSPCE, el desenvolupament dels quals es troba recollit en un apartat de l'article Talanta 192 (2019) 147-153, que s'introduirà al capítol 9.

Els elèctrodes recollits en aquest apartat es mostren a la figura 8.4.

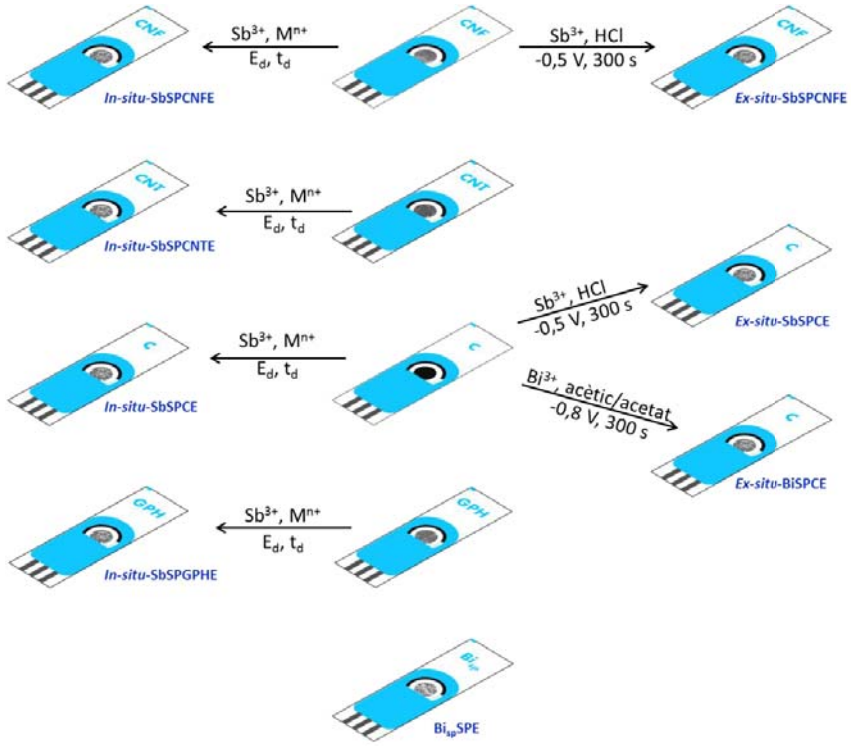

Figura 8.4. Elèctrodes de pel·lícules metàl·liques amb què s'ha treballat al llarg d'aquesta tesi doctoral.

8.2.1 Caracterització

La tècnica emprada per a la caracterització dels elèctrodes basats en pel·lícules metàl·liques ha sigut la SEM ja que permet obtenir informació morfològica de la superfície de l'elèctrode. Inicialment es van adquirir imatges SEM dels elèctrodes no modificats que s'han emprat com a suports per a la formació de les pel·lícules metàl·liques. En aquestes imatges, que es mostren a la figura 8.5, es poden observar les morfologies característiques de cadascun dels nanoal·lòtrops de carboni. Així, el SPCE mostra una superfície rugosa força uniforme que contrasta amb l'aspecte de cintes tubulars agrupades en petits feixos del SPCNFE, l'aparença a espaguetis recargolats del SPCNTE o la disposició hexagonal característica del SPGPHE. Es pot observar també que en aquests

últims tres casos l'àrea superficial real de l'elèctrode és molt major que en el cas del SPCE.

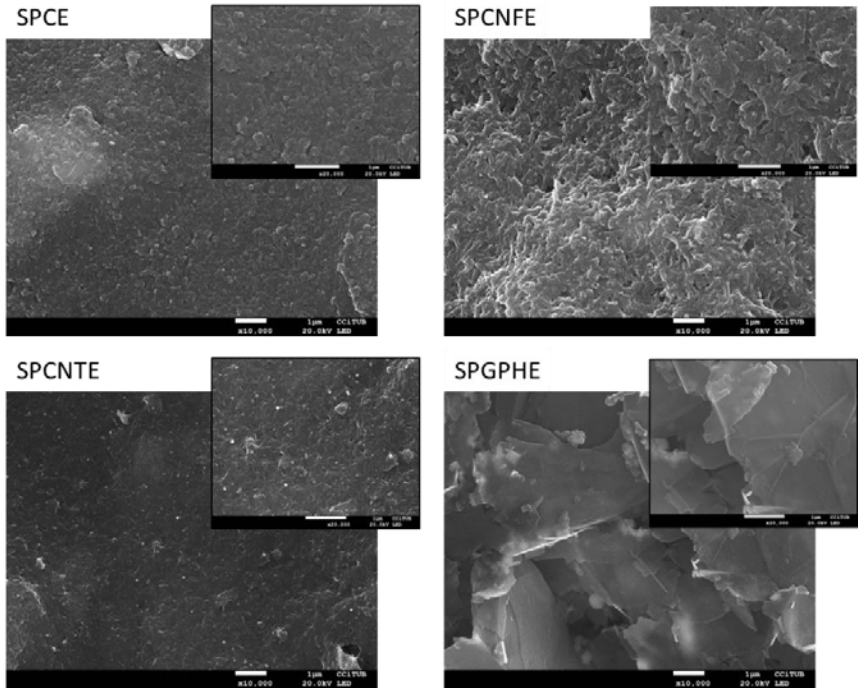

Figura 8.5. Imatges SEM a 10.000 i 20.000 (*insets*) augments dels elèctrodes SPCE, SPCNFE, SPCNTE i SPGPHE no modificats.

Aquests quatre SPEs es van emprar com a suports per depositar pel·lícules *in-situ* i/o *ex-situ* d'antimoni o de bismut. A la figura 8.6 es mostren, a tall d'exemple, les imatges SEM corresponents a l'*in-situ*-SbSPCNFE, l'*ex-situ*-BiSPCE i el Bi_{sp}SPE. En el cas de les pel·lícules *in-situ* i *ex-situ* es pot observar l'antimoni o el bismut depositat que, tot i no recobrir completament tota la superfície de l'elèctrode, es troba distribuït aleatòriament al llarg de tota ella donant lloc a pel·lícules relativament uniformes. D'altra banda, la morfologia del Bi_{sp}SPE és completament diferent ja que en aquest cas es tracta d'un suport ceràmic sobre el qual s'ha depositat bismut per deposició física en fase vapor.

En el cas dels elèctrodes basats en pel·lícules metàl·liques també es pot comprovar que la pel·lícula s'ha format correctament amb una mesura voltamperomètrica ja que, tal com es pot observar a la figura 8.7, l'oxidació de l'antimoni i el bismut donen lloc a pics molt intensos al voltant de -0,2 V i -0,4 V

respectivament. Aquests mateixos pics són els que, en el cas de les pel·lícules *ex-situ*, limiten la finestra de potencials anòdics ja que suposen l'oxidació de la pel·lícula.

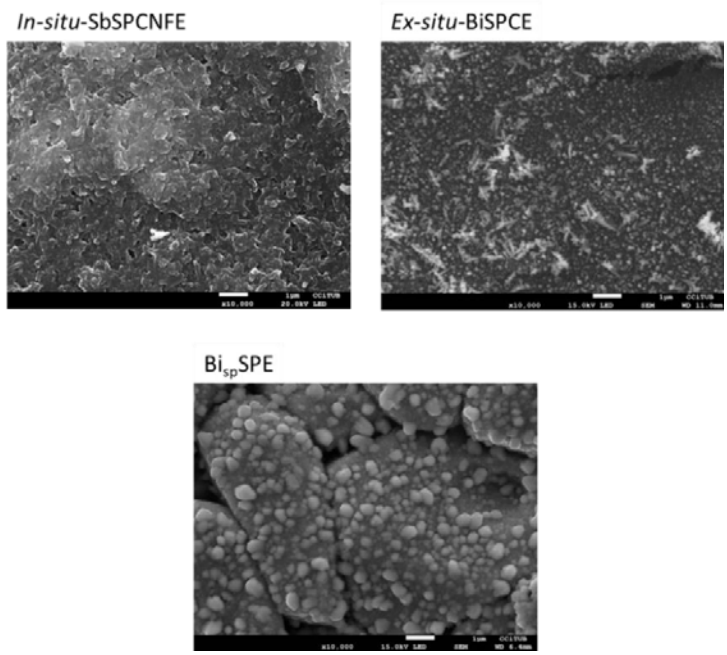

Figura 8.6. Imatges SEM a 10.000 augments dels elèctrodes *in-situ*-SbSPCNFE, *ex-situ*-BiSPCE i Bi_{sp}SPE

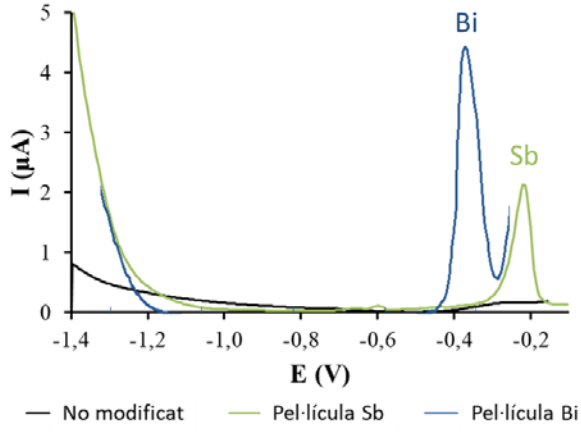

Figura 8.7. Voltamperogrames característics de l'oxidació de les pel·lícules d'antimoni (verd) i de bismut (blau) en comparació a un elèctrode de carboni no modificat (negre).

8.2.2 Aplicació a la determinació d'ions metàl·lics

Els diversos elèctrodes basats en pel·lícules de bismut o d'antimoni anteriorment mencionats s'han estudiat per a la determinació d'ions metàl·lics, concretament els ions Cd(II), Pb(II), Zn(II), Tl(I), In(III), Bi(III) i Pd(II). A la taula 8.2 es recullen els paràmetres analítics obtinguts per als diferents sensors i metalls estudiats.

A partir d'aquests resultats, es pot observar que per a la determinació de metalls amb elèctrodes basats en pel·lícules de bismut o d'antimoni cal tenir en compte principalment quatre aspectes: el suport sobre el qual es depositarà la pel·lícula, el metall que formarà la pel·lícula (Bi o Sb), el tipus de pel·lícula que s'emprarà (*in-situ* / *ex-situ* / *sputtered*) i la tècnica voltamperomètrica de redissolució (ASV o AdSV) que estarà relacionada amb el metall a estudiar.

L'efecte del suport es va avaluar a partir de la determinació simultània de Cd(II) i Pb(II) amb elèctrodes basats en pel·lícules *in-situ* d'antimoni. En principi, la major àrea superficial real de l'elèctrode proporcionada pels diferents nanoal·lòtrops de carboni hauria de traduir-se en un augment de la sensibilitat i una disminució dels LODs i LOQs. Aquestes millores s'observen amb les CNF tant per al Cd(II) com per al Pb(II) i amb els CNT per al Cd(II). En el cas del Pb(II) amb CNT s'observa un doble pic, probablement degut a una deposició no uniforme de l'antimoni sobre els CNTs, que impedeix obtenir una millora en la sensibilitat. D'altra banda, en el cas del grafè s'observa una disminució de la sensibilitat i un augment dels LODs i LOQs que, juntament amb la manca de reproductibilitat entre elèctrodes, fa pensar que les unitats comercials de SPGPHE encara no estan prou ben desenvolupades. Aquesta manca de reproductibilitat entre unitats sensores també s'observa, tot i que en menor grau, en el cas del SPCNTE. Per tant, només l'ús del SPCNFE com a suport millora prou les prestacions analítiques dels elèctrodes basats en pel·lícules *in-situ* d'antimoni com per justificar el major cost econòmic associat a l'ús de suports constituïts per nanoal·lòtrops de carboni.

D'altra banda, si considerem el metall emprat per a la formació de les pel·lícules, s'observa que l'ordre de preferència de l'antimoni pels diferents ions metàl·lics que es determinen per ASV seria Cd(II) > Zn(II) > Pb(II) > Tl(I) > In(III) > Bi(III). Aquest ordre és molt semblant a l'observat a l'apartat anterior en el cas dels elèctrodes modificats químicament amb molècules tiòliques, a excepció del

Taula 8.2. Resum dels paràmetres analítics obtinguts per a la determinació de metalls amb les diferents pel·lícules metàl·liques. Si no s'indica el contrari, les mesures s'han realitzat per a cada metall individual. Les desviacions estàndards s'indiquen entre parèntesis.

	Zn(II)	Cd(II)	Pb(II)	Pd(II)	In(III)	Tl(I)
***In-situ*-SbSPCE[c]**						
Sensibilitat (u.a. μg^{-1} L)	--	3,24 (0,05)	0,87 (0,03)	--	--	--
Interval de linealitat ($\mu g\ L^{-1}$)[a]	--	9,4 – 100,3	17,5 – 100,9	--	--	--
LOD ($\mu g\ L^{-1}$)	--	2,8	5,3	--	--	--
Repetitivitat (%)	--	2,6	3,5	--	--	--
Reproductibilitat (%)	--	2,8[b]	4,5[b]	--	--	--
***In-situ*-SbSPGPHE[c]**						
Sensibilitat (u.a. μg^{-1} L)	--	1,37 (0,03)	0,48 (0,02)	--	--	--
Interval de linealitat ($\mu g\ L^{-1}$)[a]	--	13,2 – 100,3	28,8 – 100,9	--	--	--
LOD ($\mu g\ L^{-1}$)	--	4,0	8,6	--	--	--
Repetitivitat (%)	--	2,8	2,9	--	--	--
Reproductibilitat (%)	--	18,0[b]	17,2[b]	--	--	--

Taula 8.2 (continuació). Resum dels paràmetres analítics obtinguts per a la determinació de metalls amb les diferents pel·lícules metàl·liques. Si no s'indica el contrari, les mesures s'han realitzat per a cada metall individual. Les desviacions estàndards s'indiquen entre parèntesis.

	Zn(II)	Cd(II)	Pb(II)	Pd(II)	In(III)	Tl(I)
***In-situ*-SbSPCNTE**[c]						
Sensibilitat (u.a. μg^{-1} L)	--	4,33 (0,06)	0,49 (0,01)	--	--	--
Interval de linealitat ($\mu g\ L^{-1}$)[a]	--	8,6 – 100,3	14,7 – 100,9	--	--	--
LOD ($\mu g\ L^{-1}$)	--	2,6	4,4	--	--	--
Repetitivitat (%)	--	1,5	1,3	--	--	--
Reproductibilitat (%)	--	11,4[b]	11,3[b]	--	--	--
***In-situ*-SbSPCNFE**[c]						
Sensibilitat (u.a. μg^{-1} L)	--	4,74 (0,03)	1,36 (0,01)	--	--	--
Interval de linealitat ($\mu g\ L^{-1}$)[a]	--	3,7 – 100,3	6,9 – 100,9	--	--	--
LOD ($\mu g\ L^{-1}$)	--	1,1	2,1	--	--	--
Repetitivitat (%)	--	1,0	1,1	--	--	--
Reproductibilitat (%)	--	1,2[b]	4,4[b]	--	--	--

Taula 8.2 (continuació). Resum dels paràmetres analítics obtinguts per a la determinació de metalls amb les diferents pel·lícules metàl·liques. Si no s'indica el contrari, les mesures s'han realitzat per a cada metall individual. Les desviacions estàndards s'indiquen entre parèntesis.

	Zn(II)	Cd(II)	Pb(II)	Pd(II)	In(III)	Tl(I)
***Ex-situ*-SbSPCE[d]**						
Sensibilitat (u.a. μg^{-1} L)	--	--	--	2,25 (0,03)	--	--
Interval de linealitat ($\mu g\ L^{-1}$)[a]	--	--	--	9,0 – 100,2	--	--
LOD ($\mu g\ L^{-1}$)	--	--	--	2,7	--	--
Repetitivitat (%)	--	--	--	0,5	--	--
Reproductibilitat (%)	--	--	--	1,6[b]	--	--
Bi_{sp}SPE[d]						
Sensibilitat (u.a. μg^{-1} L)	--	--	--	1,84 (0,05)	--	--
Interval de linealitat ($\mu g\ L^{-1}$)[a]	--	--	--	17,9 – 100,2	--	--
LOD ($\mu g\ L^{-1}$)	--	--	--	5,4	--	--
Repetitivitat (%)	--	--	--	1,3	--	--
Reproductibilitat (%)	--	--	--	5,0[b]	--	--

Taula 8.2 (continuació). Resum dels paràmetres analítics obtinguts per a la determinació de metalls amb les diferents pel·lícules metàl·liques. Si no s'indica el contrari, les mesures s'han realitzat per a cada metall individual. Les desviacions estàndards s'indiquen entre parèntesis.

	Zn(II)	Cd(II)	Pb(II)	Bi(III)	In(III)	Tl(I)
***Ex-situ*-SbSPCNFE**[e]						
Sensibilitat (u.a. μg^{-1} L)	2,26 (0,03)	2,42 (0,02)	0,85 (0,01)	0,157 (0,002)	0,75 (0,01)	1,10 (0,02)
Interval de linealitat ($\mu g\ L^{-1}$)[a]	14,9 – 198,3	10,7 – 200,0	13,2 – 200,8	17,2 – 200,7	21,0 – 200,4	28,5 – 274,9
LOD ($\mu g\ L^{-1}$)	4,5	3,2	4,0	5,2	6,3	8,6
***Ex-situ*-BiSPCE**[f]						
Sensibilitat (nA μg^{-1} L)	--	--	--	--	8,40 (0,07)	3,91 (0,03)
Interval de linealitat ($\mu g\ L^{-1}$)[a]	--	--	--	--	8,0 – 200,0	7,0 – 200,0
LOD ($\mu g\ L^{-1}$)	--	--	--	--	2,4	2,1

[a]El LOQ s'ha considerat com a valor inferior de l'interval linealitat.

[b]Reproductibilitat calculada per a un únic nivell de concentració.

[c]Determinació simultània de Cd(II) i Pb(II). Mesures per ASV a pH 2 i amb E_d=-1,5 V i t_d=120 s.

[d]Mesures per AdSV a pH 4,5 i amb E_{acc}=-0,6 V i t_{acc}=180 s.

[e]Mesures per ASV a pH 4,5 i amb E_d=-1,4 V i t_d=120 s.

[f]Mesures per ASV a pH 4,5 i amb E_d=-1,3 V i t_d=120 s.

Zn(II), que presenta més afinitat que el Pb(II) per les pel·lícules d'antimoni. Al comparar-lo amb els elèctrodes basats en pel·lícules de bismut, altra vegada s'observa una inversió de l'ordre de sensibilitats entre el Tl(I) i l'In(III), fet que permetrà obtenir sensibilitats creuades en el desenvolupament de llengües electròniques.

En el cas de la determinació de Pd(II), que es realitza per AdSV emprant DMG com a agent complexant, s'observa que l'*ex-situ*-SbSPCE dóna lloc a pics de Pd(II) molt més definits i simètrics que el Bi_{sp}SPE, alhora que proporciona una major sensibilitat i un LOD i LOQ inferior.

Finalment, en termes del mètode de formació de la pel·lícula cal mencionar que, tot i que a la taula 8.2 es mostren els paràmetres analítics obtinguts per a la determinació de Cd(II) i Pb(II) tant per a l'*in-situ*-SbSPCNFE com per a l'*ex-situ*-SbSPCNFE, els valors mostrats no són comparables ja que les condicions de mesura són molt diferents. No obstant, la tria entre pel·lícules *in-situ* o *ex-situ* sol realitzar-se en funció del tipus de mesura. En general, i sempre que les condicions de mesura ho permetin, les pel·lícules *in-situ* són l'opció preferible ja que no impliquen una etapa de formació de la pel·lícula prèvia a la mesura. Les pel·lícules *ex-situ*, per contra, són més versàtils ja que eviten possibles interferències causades per l'addició d'un excés de bismut o d'antimoni a la solució de mesura que conté la mostra i permeten realitzar mesures també per AdSV, on els potencials de mesura difereixen molt dels potencials necessaris per a la formació de la pel·lícula.

8.3 Nanopartícules metàl·liques

En aquest tercer apartat es presenten i discuteixen els diferents elèctrodes de NPs metàl·liques amb què s'ha treballat al llarg d'aquesta tesi doctoral. Totes elles són NPs de plata i s'han sintetitzat amb la col·laboració del grup de Recuperació de Recursos i Gestió Ambiental de la Universitat Politècnica de Catalunya o del grup de Metalls i Mediambient de la Universitat de Girona. El desenvolupament d'aquests elèctrodes es troba recollit als següents articles:

- C. Pérez-Ràfols, J. Bastos-Arrieta, N. Serrano, J. M. Díaz-Cruz, C. Ariño, J. de Pablo, M. Esteban, Ag nanoparticles drop-casting modification of screen-printed electrodes for the simultaneous voltammetric determination of Cu(II) and Pb(II), Sensors 17 (2017) 1458-1469.
- J. Bastos-Arrieta, A. Florido, C. Pérez-Ràfols, N. Serrano, N. Fiol, J. Poch, I. Villaescusa, Green synthesis of Ag nanoparticles using grape stalk waste extract for the modification of screen-printed electrodes, Nanomaterials 8 (2018) 946-959.

Els elèctrodes recollits en aquest apartat es mostren a la figura 8.8.

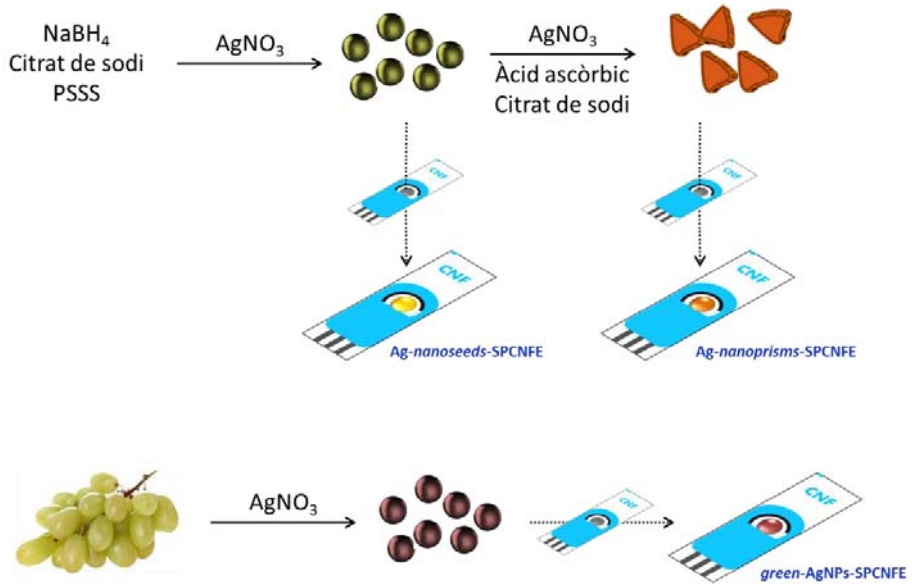

Figura 8.8. Elèctrodes de NPs metàl·liques amb què s'ha treballat al llarg d'aquesta tesi doctoral.

8.3.1 Caracterització

Al treballar amb NPs el més habitual és caracteritzar tant la solució de NPs per comprovar que la síntesi s'ha produït correctament com els SPEs modificats amb NPs per assegurar que les NPs s'han adherit a la superfície.

La tècnica emprada per a la caracterització de la solució de NPs és la TEM ja que proporciona major resolució que la SEM i, al tractar-se d'una solució, és possible aconseguir una mostra prou fina. En aquest cas la TEM permet obtenir informació sobre la mida i la forma de les NPs sintetitzades. A la figura 8.9, on es mostren les imatges TEM dels tres tipus de NPs amb què s'ha treballat al llarg d'aquesta tesi doctoral, es pot observar que tant les Ag-*nanoseeds* com les NPs sintetitzades per una ruta verda tenen una forma esfèrica que contrasta amb la forma prismàtica de les Ag-*nanoprisms.* D'altra banda, també s'observa que les Ag-*nanoseeds* (9,1 ± 0,4 nm) són més petites que les Ag-*nanoprisms* (14,0 ± 0,9 nm) i que la ruta de síntesi verda dóna lloc a les NPs de plata més grans (27,7 ± 0,6 nm).

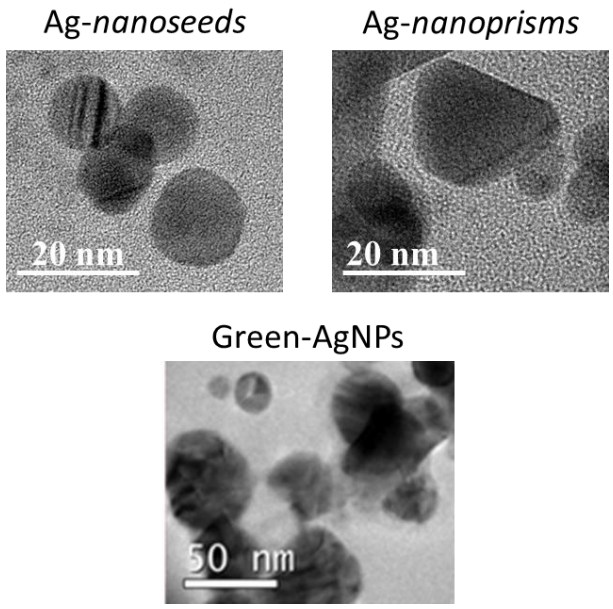

Figura 8.9. Imatges TEM de les Ag-*nanoseeds*, Ag-*nanoprisms* i les *green*-AgNPs.

D'altra banda, per caracteritzar les superfícies dels elèctrodes s'utilitza la tècnica del SEM. Les imatges SEM de la superfícies del SPCNFE un cop ja s'han dipositat les NPs per *dropcasting* permet observar la seva distribució aleatòria al llarg de tota la superfície electròdica. A la figura 8.10 es mostra, a tall d'exemple, la imatge SEM del *green*-AgNPs-SPCNFE, on s'han ressaltat les NPs de plata.

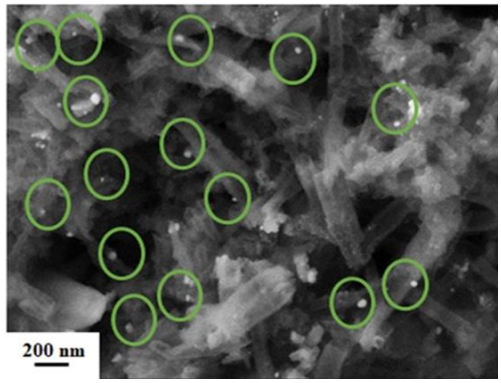

Figura 8.10. Imatge SEM del *green*-AgNPs-SPCNFE ressaltant la localització de les NPs de plata dipositades.

Finalment, tal com s'ha vist per a les pel·lícules metàl·liques, en el cas de les NPs de plata també es pot comprovar que s'han adherit a la superfície de l'elèctrode amb una mesura voltamperomètrica ja que l'oxidació de la plata dóna lloc a un pic intens al voltant de 0,2 V, fet que limita la finestra de potencials anòdic.

8.3.2 Aplicació a la determinació d'ions metàl·lics

Els diversos sensors modificats amb NPs de plata s'han estudiat per a la determinació d'ions metàl·lics, concretament els ions Cd(II), Pb(II) i Cu(II). A la taula 8.3 es recullen els paràmetres analítics obtinguts per als diferents sensors i metalls estudiats.

A partir dels resultats obtinguts, s'ha observat que per a la determinació de metalls amb sensors modificats amb NPs de plata cal considerar tant el suport on es dipositen les NPs com el tipus de NPs (mida i forma).

L'efecte del suport es va estudiar a l'article Sensors 17 (2017) 1458-1469 amb les Ag-*nanoseeds* fent especial èmfasi en la repetitivitat i la reproductibilitat. Així, es va observar que la major àrea superficial i rugositat proporcionada tant per les CNF com pel grafè permeten un millor ancoratge de les NPs a la superfície de l'elèctrode, fet que es tradueix en una millora de la repetitivitat del sensor. No obstant, només el SPCNFE proporciona la reproductibilitat entre diferents elèctrodes desitjada.

Taula 8.3. Resum dels paràmetres analítics obtinguts per a la determinació simultània de metalls amb els diferents sensors modificats amb NPs metàl·liques. Les desviacions estàndards s'indiquen entre parèntesis.

	Cd(II)	Pb(II)	Cu(II)
Ag-*nanoseeds*-SPCNFE[c]			
Sensibilitat (nA μg^{-1} L)	--	43 (1)	73 (2)
Interval de linealitat ($\mu g\ L^{-1}$)[a]	--	6,6 – 53,5	10,0 – 77,0
LOD ($\mu g\ L^{-1}$)	--	1,98	2,99
Repetitivitat (%)	--	5,5	3,6
Reproductibilitat (%)	--	8,1[b]	5,2[b]
Ag-*nanoprisms*-SPCNFE[c]			
Sensibilitat (nA μg^{-1} L)	--	25,9 (0,7)	34,4 (0,5)
Interval de linealitat ($\mu g\ L^{-1}$)[a]	--	7,8 – 53,5	8,3 – 100,7
LOD ($\mu g\ L^{-1}$)	--	2,35	2,49
Repetitivitat (%)	--	5,1	3,6
Reproductibilitat (%)	--	9,3[b]	6,3[b]
Green-AgNPs-SPCNFE[d]			
Sensibilitat (nA μg^{-1} L)	46 (2)	62 (1)	--
Interval de linealitat ($\mu g\ L^{-1}$)[a]	9,5 – 39,7	8,9 – 100,4	--
LOD ($\mu g\ L^{-1}$)	2,8	2,7	--

[a]El LOQ s'ha considerat com a valor inferior de l'interval linealitat.
[b]Reproductibilitat calculada per a un únic nivell de concentració.
[c]Mesures a pH 4,5 i amb E_d=-1,1 V i t_d=120 s.
[d]Mesures a pH 4,5 i amb E_d=-1,4 V i t_d=120 s.

D'altra banda, comparant les dues NPs sintètiques es pot observar que, tot i que tots dos elèctrodes permeten assolir LODs i LOQs inferiors als límits legals establerts a la directiva marc de l'aigua (2000/60/EC) amb repetitivitats i

reproductibilitats semblants, l'Ag-*nanoseeds*-SPCNFE proporciona una major sensibilitat pel Pb(II) i el Cu(II) que l'Ag-*nanoprisms*-SPCNFE. Aquesta major sensibilitat pot ser deguda a la forma esfèrica de les NPs, que li proporciona una major àrea superficial per unitat de volum, i a la major mullabilitat de la solució d'Ag-*nanoseeds,* que facilita una distribució més homogènia de les NPs al llarg de la superfície de l'elèctrode. Aquesta major sensibilitat, juntament amb la seva síntesi més senzilla, fa que l'Ag-*nanoseeds*-SPCNFE sigui un millor candidat per a la determinació d'ions metàl·lics a nivell traça que l'Ag-*nanoprisms*-SPCNFE.

Finalment, les NPs de plata sintetitzades a partir d'una ruta verda també permeten obtenir sensors adequats per a la determinació de metalls a nivell traça, permetent detectar el Cd(II) i quantificar el Pb(II) per sota els límits legals establerts a la directiva marc de l'aigua (2000/60/EC). En aquest punt cal mencionar que, tot i que aparentment sembli que el *green*-AgNPs-SPCNFE és més sensible al Pb(II) que l'Ag-*nanoseeds*-SPCNFE, aquests valors no es poden comparar donat que les mesures estan realitzades a diferents E_d per permetre la detecció amb Cd(II) o Cu(II) en funció del cas.

8.4 Silici porós

En aquest quart apartat es presenten i discuteixen els estudis realitzats amb elèctrodes de silici porós estabilitzats tèrmicament amb acetilè. Aquests estudis es van realitzar durant l'estada predoctoral al Monash Institute of Pharmaceutical Sciences (MIPS) i els resultats es troben recollits al següent manuscrit:

- C. Pérez-Ràfols, K Guo, N. H. Voelcker, B. Prieto-Simón. Carbon-stabilized porous silicon as novel voltammetric sensor platforms, En preparació.

Els elèctrodes recollits en aquest apartat es mostren a la figura 8.11.

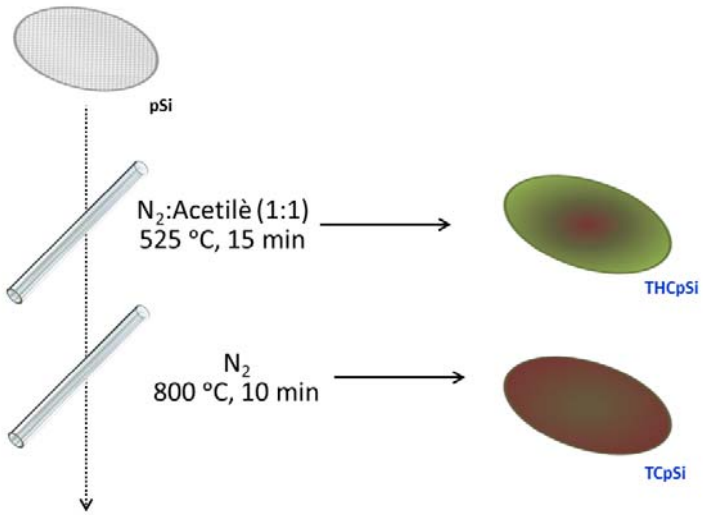

Figura 8.11. Elèctrodes de silici porós amb què s'ha treballat al llarg d'aquesta tesi doctoral.

8.4.1 Caracterització

La tècnica emprada per a la caracterització morfològica dels elèctrodes de pSi desenvolupats ha estat la SEM. Donat que cap dels dos tractaments tèrmics considerats per a l'estabilització del pSi altera la morfologia o les dimensions del pSi, les imatges SEM dels elèctrodes TCpSi i THCpSi són pràcticament idèntiques. A la figura 8.12, on es mostra la imatge SEM d'un elèctrode de TCpSi, es poden observar els nanoporus formats mitjançant l'anodització d'oblees de silici, que presenten un diàmetre mitjà de 72 ± 15 nm i una profunditat de 500 nm.

D'altra banda, es pot confirmar que el tractament tèrmic s'ha produït correctament mitjançant els espectres infrarojos de transformada de Fourier amb reflectància total atenuada (ATR-FTIR, *attenuated total reflectance Fourier transform infrared*). Tal com es pot veure a la figura 8.13, el pSi sense estabilitzar mostra bandes característiques de l'estirament (υ) i la deformació (δ) dels enllaços Si-H a 2087 i 905 cm^{-1} respectivament mentre que tant en el cas del TCpSi com el THCpSi, aquestes bandes han sigut substituïdes per bandes associades a l'estirament d'enllaços C-H (3047 cm^{-1}), C=C (1600 cm^{-1}) i Si-CH_3 (1250-1260 cm^{-1}) [102].

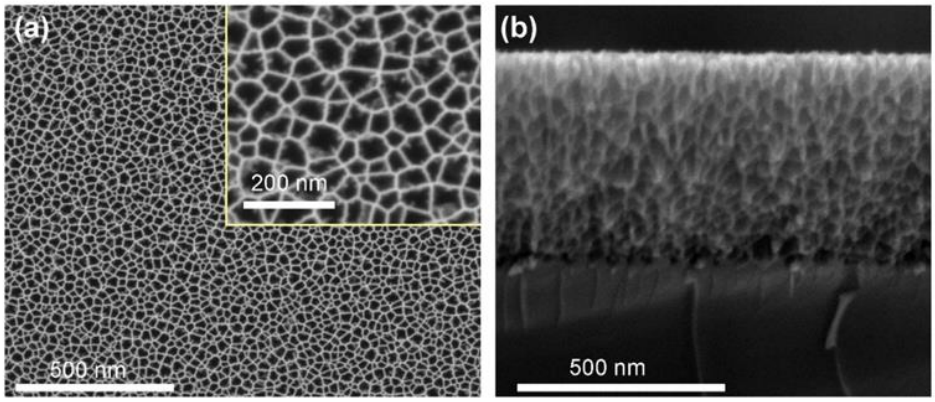

Figura 8.12. Imatges SEM amb una visió superior (a) i transversal (b) del TCpSi.

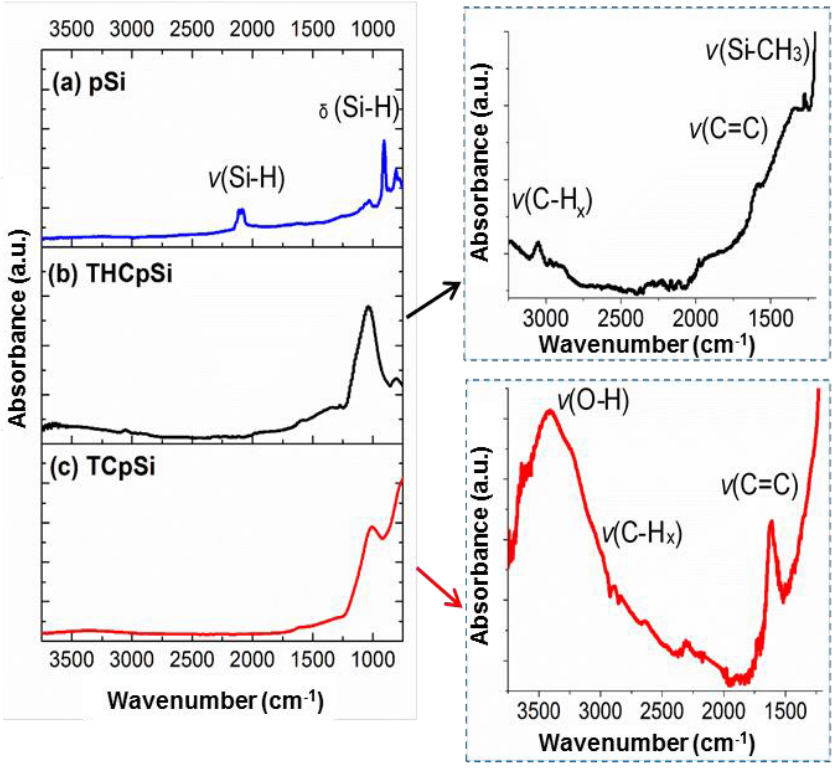

Figura 8.13. Espectre ATR-FTIR del pSi no estabilitzat (a), el THCpSi (b) i el TCpsi (c).

Finalment, els dos pSi estabilitzats tèrmicament també s'han caracteritzat electroquímicament per CV. Inicialment, tal com es pot veure a la figura 8.14, s'observa que tots dos substrats donen lloc a pics ben definits per a l'oxidació i reducció dels ions $[Fe(CN)_6]^{3-/4-}$ però el comportament electroquímic és millor en el cas del TCpSi ja que els pics són més intensos i la separació de pics (ΔE_p) és menor (115 mV per al TCpSi i 145 mV per al THCpSi). A més, el TCpSi és un substrat més reproduïble ja que al realitzar 20 cicles consecutius el senyal es manté mentre que el senyal del TCHpSi decau i perd reversibilitat. Aquest millor comportament electroquímic pot ser degut a la major estabilitat química i cobertura de carboni del TCpSi [79].

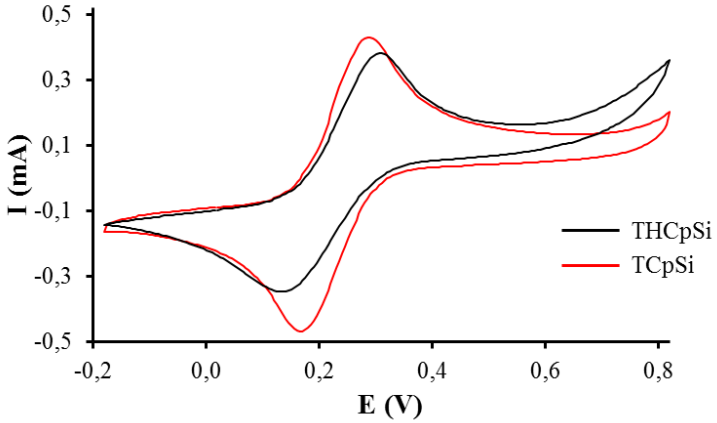

Figura 8.14. Voltamperogrames cíclics d'una solució 2 mmol L^{-1} $[Fe(CN)_6]^{3-/4-}$ en tampó fosfats 10 mmol L^{-1} (pH 7,4) emprant THCpSi i TCpSi.

8.4.2 Aplicació a la determinació d'isòmers del dihidroxibenzè

En primer lloc, cal mencionar que inicialment es van considerar els elèctrodes de pSi per a la determinació d'ions metàl·lics però es va observar que aquests materials no permeten treballar a potencials tan negatius ja que el silici es redueix durant l'etapa de preconcentració i posteriorment, durant l'escombratge de potencials, dóna lloc a pics d'oxidació a la zona de potencials característica dels ions metàl·lics.

És per això que es va optar per anàlits orgànics que no requereixen potencials tan negatius, com és el cas de la hidroquinona (HQ), el catecol (CC) i el resorcinol (RC). Es tracta dels tres isòmers del dihridròxibenzè i són substàncies que s'empren en una gran varietat de productes (cosmètics, tints, fàrmacs, pesticides…). Electroquímicament es poden determinar ja que s'oxiden a la forma quinònica (figura 8.15) però presenten la dificultat que la HQ i el CC tenen potencials d'oxidació molt semblants i els seus pics solen solapar-se.

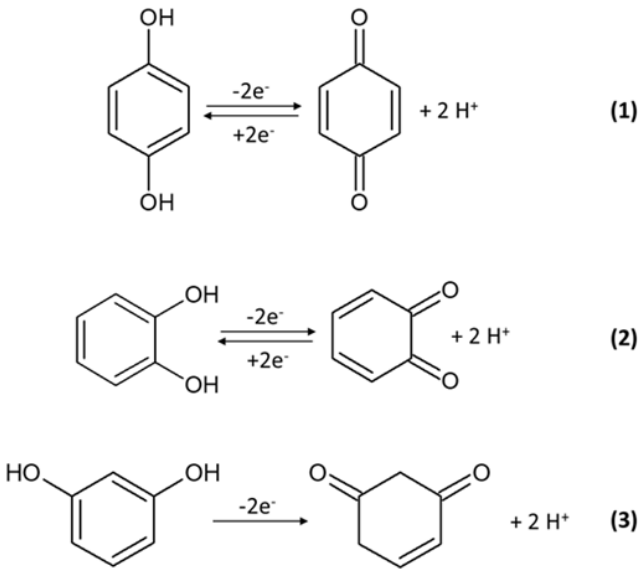

Figura 8.15. Reaccions redox de la HQ (1), CC (2) i RC (3).

Inicialment es va estudiar el comportament electroquímic dels tres isòmers en TCpSi i THCpSi per CV i en tots dos casos es va observar un important augment de la intensitat respecte el GCE, que es pot atribuir a la major àrea superficial proporcionada per l'estructura de pSi. No obstant, el caràcter hidròfil del TCpSi permet obtenir senyals molt més reversibles que el THCpSi, de naturalesa hidrofòbica. A més, el TCpSi també permet diferenciar clarament entre els pics de la HQ i el CC.

A la taula 8.4 es recullen els paràmetres analítics obtinguts per a la determinació de HQ, CC i RC en TCpSi. Es pot observar que el TCpSi proporciona bona repetitivitat i reproductibilitat en tots els casos però que en termes de sensibilitat i LOD la determinació de HQ i CC és molt més favorable que la del RC. Cal remarcar però, que l'interval de linealitat del RC és bastant més ampli.

Taula 8.4. Resum dels paràmetres analítics obtinguts per a la determinació de HQ, CC i RC amb TCpSi en tampó fosfats 10 mmol L^{-1} pH 7,4. Les desviacions estàndards s'indiquen entre parèntesis.

	HQ	CC	RC
TCpSi			
Sensibilitat (a.u. µmol^{-1} L)	1,20 (0,04)	1,19 (0,03)	0,30 (0,01)
Interval de linealitat (µmol L^{-1})[a]	5,6 – 35,2	3,4 – 25,4	14,2 – 50,0
LOD (µmol L^{-1})	1,67	1,01	4,25
Repetitivitat (%)	5,1	3,5	5,8
Reproductibilitat (%)	2,8[b]	7,6[b]	0,4[b]

[a]El LOQ s'ha considerat com a valor inferior de l'interval linealitat.

[b]Reproductibilitat calculada per a diferents nivells de concentració, a partir dels pendents de les rectes de calibratge.

9

Desenvolupament de llengües voltamperomètriques

Aquest capítol engloba tres treballs centrats en el desenvolupament de noves llengües voltamperomètriques per a la determinació de mostres complexes d'ions metàl·lics i la seva aplicació a mostres reals. Concretament, en el primer i en el tercer treball s'ha estudiat el sistema Tl(I) i In(III) i en el segon treball el sistema Cd(II), Pb(II), Tl(I) i Bi(III) en presència de Zn(II) i In(III).

En aquest cas, la discussió de resultats està dividida en tres apartats que corresponen a la selecció dels sensors que formaran la llengua electrònica, al disseny experimental emprat i al tractament quimiomètric de les dades. A més, en aquest capítol també s'avalua l'aplicació de dos mètodes de calibratge multivariant diferents: el calibratge extern, que s'ha estudiat en els tres treballs, i l'addició estàndard multivariant, que s'ha estudiat només en l'últim treball.

Simultaneous determination of Tl(I) and In(III) using a voltammetric sensor array.

C. Pérez-Ràfols, N. Serrano, J. M. Díaz-Cruz, C. Ariño, M. Esteban

Sensors and Actuators B 245 **(2017)** 18-24

https://doi.org/10.1016/j.snb.2017.01.089

Sensors and Actuators B 245 (2017) 18–24

Contents lists available at ScienceDirect

Sensors and Actuators B: Chemical

journal homepage: www.elsevier.com/locate/snb

Simultaneous determination of Tl(I) and In(III) using a voltammetric sensor array

Clara Pérez-Ràfols, Núria Serrano*, José Manuel Díaz-Cruz, Cristina Ariño, Miquel Esteban

Departament d'Enginyeria Química i Química Analítica, Facultat de Química, Universitat de Barcelona, Martí i Franquès 1-11, E-08028 Barcelona, Spain

ARTICLE INFO

Article history:
Received 5 September 2016
Received in revised form 9 January 2017
Accepted 12 January 2017
Available online 17 January 2017

Keywords:
Sensor array
Metal ions
Stripping voltammetry
Screen-printed electrodes
Modified electrodes
Partial least squares

ABSTRACT

A sensor array consisting of a chemically modified sensor in which 4-carboxybenzo-18-crown-6 was immobilized onto a screen-printed carbon nanofiber-modified electrode (crown-6-SPCNFE) and an *ex-situ* antimony film deposited on a screen-printed carbon nanofiber-modified electrode (*ex-situ*-SbSPCNFE) was applied for the resolution of the strong overlapped signals resulting from the simultaneous determination of Tl(I) and In(III) by stripping voltammetry. A Partial Least Squares model was constructed and good calibration curves of predicted *vs.* expected concentrations of the considered metal ions, with correlation coefficients higher than 0.98 for both training and test sets, were obtained. These results provided by the sensor array were compared with those obtained by a single electrode. Moreover, this sensor array was successfully applied for the voltammetric determination of both Tl(I) and In(III) in tap water, providing comparable results to those obtained by ICP-MS measurements.

1. Introduction

Thallium and indium are relatively rare metals that do not have any essential biological role but have been shown to be highly toxic. Due to their unique chemical properties, the use of these metals has increased in the last years. Indium is mostly used for alloys and solders whereas thallium is used for switches and closures. In addition, the use of both indium and thallium has recently been expanded in medical procedures and electronics industry [1,2].

Different techniques such as inductively coupled plasma mass spectrometry (ICP-MS) or inductively coupled plasma atomic emission spectroscopy (ICP-OES) have been used for the analysis of thallium and indium [3,4]. Electroanalytical techniques, and voltammetric stripping techniques in particular, can also be a good alternative, since they are low cost, highly reproducible, selective and sensitive, and they present capability to multielement analysis and excellent detection and quantification limits [5]. However, when traditional working electrodes like mercury are used, the simultaneous determination of indium and thallium is problematic because of their overlapping stripping signals. More promising results regarding the separation of thallium and indium peaks were achieved using alternative working electrodes such as an *in-situ* antimony film deposited onto a glassy carbon electrode [6]. Classical solid electrodes though, require continuous and tedious cleaning processes that can be avoided by using screen-printed electrodes (SPE). In fact, SPEs have recently undergone great advances, allowing the mass production of reproducible and low-cost devices. In addition, SPEs usually incorporate the whole electrode system (working, reference and auxiliary) which, coupled with their miniaturized size and their ability to be connected to portable instrumentation, makes them more suitable for *on-site* analysis. [7–10].

SPEs can also be further modified following different strategies such as electrodeposition of metal films or covalent modification through electrografting using aryl diazonium salts [11]. Particularly for metal ion determination, in the first case, good results have been reported for both bismuth film electrodes [12] and antimony film electrodes [13] whereas in the second case different ligands can be immobilized onto the electrode surface, *i.e.* good results have been reported using peptide related structures [14–18] or crown ethers [19,20] as ligands.

In both strategies of modification, the substrate is also an important aspect that has to be taken into account during the preparation of these modified sensors. It is well-known that the use of carbon- based nanomaterials such as carbon nanotubes (CNT), carbon nanofibers (CNF) or graphene (GPH) enhance the effective surface and improve the electron-transfer kinetics. In particular, it has been reported that sensors with better analytical performance

* Corresponding author.
E-mail address: nuria.serrano@ub.edu (N. Serrano).

http://dx.doi.org/10.1016/j.snb.2017.01.089
0925-4005/

can be obtained if a carbon nanofiber modified screen-printed electrode (SPCE-CNF) is used as electrode substrate [15,21], since CNFs are easier to functionalize and simultaneously provide mechanical and electrical property enhancements.

These chemical sensors can be used as single-electrode sensors for the voltammetric determination of metal ions in samples of biological, food and environmental origin but for some analytes it is difficult to obtain sensors with appropriate selectivity and sensitivity. In some cases, the analysis of unresolved signals obtained by electroanalytical techniques has been successfully carried out using different chemometric tools such as partial least squares (PLS) or multivariate curve resolution by alternating least squares (MCR-ALS) [22]. However, in the event of a strong signal overlapping or interactions between different analytes, better results can be achieved by combining the signals obtained from different sensors grouped in a sensor array. In this array approach each electrode is modified with different compounds in search for a multivariate response. Although a sensor array requires longer manufacturing time, a multichannel potentiostat to control the potential and the use of chemometric tools to process the more complex data, the information obtained by the sensor array is much better than that provided from a single sensor [23,24]. Therefore, this sensor array allows the combination of several less specific sensors with cross-selectivity to obtain multivariate data sets that can be further analysed by chemometric methods.

Thus, in this study a sensor array formed by the combination of an *ex-situ* antimony film deposited on a screen-printed carbon nanofiber-modified electrode (*ex-situ*-SbSPCNFE) and a chemically modified sensor in which 4-carboxybenzo-18-crown-6 was immobilized onto a screen-printed carbon nanofiber-modified electrode (crown-6-SPCNFE) is presented. The obtained data-set was further analysed using PLS, which successfully allowed the simultaneous voltammetric determination of thallium and indium ions in water samples.

2. Experimental section

2.1. Chemicals and solutions

All chemicals used were of analytical grade. Sb(III) 1000 mg L^{-1} atomic absorption standard solution, 2-(*N*-morpholino)-ethanesulfonic acid (MES), potassium ferrocyanide $K_4[Fe(CN)_6]\cdot 3H_2O$, hydrochloric acid, nitric acid, acetic acid, and sodium acetate were supplied by Merck (Darmstadt, Germany). Sodium nitrite, *N*-hydroxysulfosuccinimide (sulfo-NHS), 4-aminobenzoic acid (ABA), *N*-(3-dimethylaminopropyl)-*N*′-ethylcarbodiimide hydrochloride (EDC), perchloric acid, methanol, potassium dihydrogen phosphate, and sodium monophosphate were purchased from Sigma-Aldrich (St. Louis, MO, USA). Potassium ferricyanide $K_3[Fe(CN)_6]$ and 4-carboxybenzo-18-crown-6 were provided by Panreac (Barcelona, Spain) and Acros (Geel, Belgium) respectively.

In(III) and Tl(I) stock solutions 10^{-3} mol L^{-1} were prepared from $In_2(SO_4)_3\cdot 5H_2O$ and TlCl respectively, supplied by Sigma-Aldrich. Stock solution concentrations were determined by ICP-MS. Ultrapure water (Milli-Q plus 185 system, Millipore) was used in all experiments.

Tap water sample was collected in the laboratory from the local water distribution network, managed by Agbar Company (Barcelona; http://www.agbar.es/eng/home.asp) and mostly using water coming from Llobregat River.

2.2. Instrumentation

Differential pulse anodic stripping voltammetric (DPASV) measurements were performed in an Autolab System PGSTAT12 (EcoChemie, The Netherlands), in its multichannel configuration and using GPES Multichannel 4.7 software package (EcoChemie).

Ag|AgCl|KCl (3 mol L^{-1}) supplied by Metrohm (Switzerland) was used as reference electrode and an *ex-situ* antimony film and a 4-carboxybenzo-18-crown-6 modified electrode, both prepared using a commercial carbon nanofiber modified screen-printed disk electrode (ref. 110CNF, DS SPCE) of 4 mm diameter provided by DropSens (Oviedo, Spain) as substrate, were used as working electrodes. The carbon counter electrode from one of the SPEs was used as counter electrode and two flexible cables (ref. CAC, DropSens) were used to connect the SPEs to the Autolab System.

A Crison micro pH 2000 pH-meter was used for pH measurements.

All measurements were carried out at room temperature (20 °C) and a purified nitrogen atmosphere (Linde N50) was used for the antimony film preparation.

Inductively coupled plasma mass spectrometry Perkin-Elmer model NexIon 350 D with a collision cell (helium) (USA) was used for ICP-MS measurements.

2.3. Preparation of modified SPEs

2.3.1. Crown-6 modified electrode (Crown-6-SPCNFE)

The immobilization of 4-carboxybenzo-18-crown-6 on the surface of SPCE-CNF was based on a procedure previously reported [19], with slight modifications. Briefly, the aryl diazonium salt was generated *in-situ* by adding 4 mmol L^{-1} of $NaNO_2$ to a cooled solution of 146 mmol L^{-1} of ABA in 1 mol L^{-1} HCl. This solution was mixed in an ice bath for 30 min before the electrochemical grafting process was conducted. For this purpose, the SPCE-CNF was immersed in the diazonium salt solution and 30 cyclic voltammetry (CV) cycles from 0 V to −1 V at 0.2 V s^{-1} were applied. The electrodes were rinsed with water and ethanol and the carboxylic groups were activated by dropping 10 μL of a 35 mmol L^{-1} sulfo-NHS and 26 mmol L^{-1} EDC solution in 0.1 mol L^{-1} MES buffer (pH 4.5) onto the electrode surface and leaving it for 1 h. In order to conjugate the activated carboxylic groups with the carboxy-modified ligand, a lysine spacer was intercalated in between them by incubating 2.9 mg of 4-carboxybenzo-18-crown-6 with 100 μL 5 mmol L^{-1} lysine in 0.1 mol L^{-1} MES buffer/ethanol (10%) for 3 h at 4 °C. Then 10 μL of this solution were dropped onto the functionalized electrode surface and left to react overnight at 4 °C.

The electrochemical characterisation of the crown-6-SPCNFE was carried out using 2 mmol L^{-1} ferrocyanide/ferricyanide as redox probe in 100 mmol L^{-1} phosphate buffer (pH 7.4) at each functionalization step by cyclic voltammetry (CV) leading voltammograms that confirm the modifications taking place on the electrode surface (Figure not shown).

2.3.2. Ex-situ *antimony film electrode (*ex-situ-*SbSPCNFE)*

The SPCE-CNF was immersed, together with the reference and auxiliary electrodes, into a 0.01 mol L^{-1} HCl solution containing 50 mg L^{-1} of Sb(III). This solution was dearated for 10 min and an E_d of −0.5 V was applied with stirring for 300 s, followed by a rest period of 20 s, without stirring. Finally, the electrode was rinsed with water. This methodology was previously tested, showing a very high repeatability and reproducibility [25].

2.4. Voltammetric measurements

DPASV determinations of Tl(I) and In(III) using crown-6-SPCNFE and *ex-situ*-SbSPCNFE were performed at a deposition potential (E_d) of −1.4 V, applied with stirring, during a deposition time (t_s) of 120 s and followed by a rest period (t_r) of 5 s. Determinations were done by scanning the potential from −1.4 to −0.5 V, using pulse

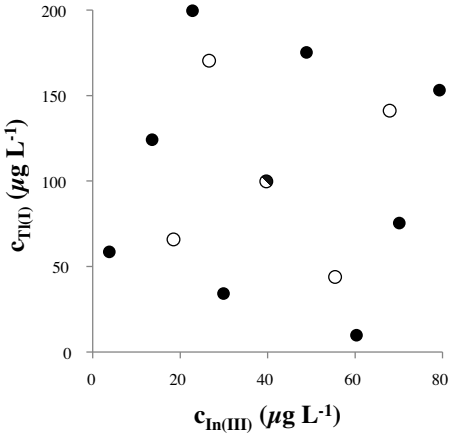

Fig. 1. Experimental design used for training (●) and testing (○) subsets. Central point is included in both training and testing subset.

amplitudes of 100 mV, a step potential of 5 mV, and pulse times of 50 ms.

The remaining bound metals from both working electrodes were eliminated through a cleaning step, which consisted in applying a conditioning potential (E_{cond}) of −0.3 V for 15 s in 0.1 mol L^{-1} $HClO_4$ after each measurement.

In order to obtain the linear calibration plots for the separate determination of Tl(I) and In(III), metal ion concentrations were increased in 0.1 mol L^{-1} acetate buffer solution at pH 4.5.

For the simultaneous determination of Tl(I) and In(III) a total set of 14 samples, distributed among training (9) and test (5) subsets, were prepared from appropriate dilution of stock solutions. Training samples were distributed in a square design and test samples where distributed along the experimental domain (Fig. 1). It should be noted that central point is included in both training and testing subsets.

In addition, the suitability of the sensor array for the simultaneous determination of In(III) and Tl(I) in natural samples was tested by measuring 3 replicates of a spiked tap water sample with Tl(I) and In(III) concentrations distributed in the range of the calibration curves.

2.5. Sample preparation

Water samples collected from the local water distribution network were spiked with 225 μg L^{-1} of Tl(I) and 75 μg L^{-1} of In(III). These values were further determined by ICP-MS. For voltammetric determinations, an aliquot of spiked water sample was diluted with acetate buffer to pH 4.5 resulting in solution concentrations of 145.5 μg L^{-1} of Tl(I) and 48.5 μg L^{-1} of In(III).

2.6. Data processing

Data matrices were built from stripping voltammograms measured for all samples with crown-6-SPCNFE as a single-sensor or with the sensor array consisting of an *ex-situ*-SbSPCNFE and a crown-6-SPCNFE. Prior to building the PLS model different pre-processing steps were applied, including baseline correction, smoothing Savitzky-Golay, 1st derivative Savitzky-Golay, reference correction and autoscale.

Table 1
Calibration data for the separate determination of In(III) and Tl(I) on crown-6-SPCNFE and *ex-situ*-SbSPCNFE modified electrodes at E_d of −1.4 V using a t_d of 120 s at acetate buffer pH 4.5. The standard deviations are denoted by parenthesis.

	In(III)	Tl(I)
Crown-6-SPCNFE		
Sensitivity (a.u. μg^{-1} L)	0.57 (0.01)	0.30 (0.01)
R^2	0.998	0.998
LOD (μg L^{-1})	13.7	10.9
***Ex-situ*-SbSPCNFE**		
Sensitivity (a.u. μg^{-1} L)	0.75 (0.01)	1.10 (0.02)
R^2	0.999	0.999
LOD (μg L^{-1})	6.3	8.6

Pre-processing of the data matrices, variable selection and construction of PLS model were made using Matlab® [26] with PLS-toolbox [27].

3. Results and discussion

As the most novel aspect of the present work is the part concerning Tl(I) and In(III) sensing using the crown-6-SPCNFE this was studied in detail. Once stablished the working conditions, the crown-6-SPCNFE was analytically characterized for the determination of Tl(I) and In(III) given that there are no previous studies in this regard. *Ex-situ*-SbSPCNFE response towards Tl(I) and In(III) was already studied in a previous work, involving the simultaneous voltammetric determination of Cd(II), Pb(II), Tl(I), In(III), Zn(II), and Bi(III) [28]. Table 1 summarizes the calibration data of both crown-6-SPCNFE and *ex-situ*-SbSPCNFE for the analysis of Tl(I) and In(III).

3.1. Analytical performance of crown-6-SPCNFE

The effect of deposition potential was firstly tested in order to ensure the maximum separation between Tl(I) and In(III) peaks. For this purpose, voltammetric measurements applying different E_d ranging from −1.6 V to −1.3 V for 120 s were performed in a solution containing 100 μg L^{-1} Tl(I) and In(III) at acetate buffer pH 4.5 on crown-6-SPCNFE (Fig. 2A). As it can be observed, the best separation is obtained at −1.4 V. More negative potentials result in a decrease of In(III) peak in comparison to Tl(I) peak whereas more positive potentials results in smaller peaks for both Tl(I) and In(III) ions.

Individual calibrations of Tl(I) and In(III) by stripping voltammetry applying the optimized potential of −1.4 V and a t_d of 120 s were then carried out. For this purpose, thirteen standard solutions with increasing concentrations of Tl(I) or In(III) within the range 1.2–270.3 and 1.8–300.4 μg L^{-1} respectively were measured, obtaining comparable responses that allowed the determination of both metal ions in the considered concentration ranges. Calibration data are summarized in Table 1. Both In(III) and Tl(I) showed good linear responses of peak area *vs* metal ion concentration and the sensitivity, obtained from the slope of the calibration curve, was higher in the case of indium(III). Regarding the limits of detection (LOD), calculated as 3 times the standard deviation of the intercept over the slope of the calibration curve of each metal, were at the level of μg L^{-1} for both metal ions, being slightly better in the case of thallium(I).

The effect of having Tl(I) and In(III) in different proportion was also evaluated. Fig. 2B shows the stripping measurements obtained by applying an E_d of −1.4 V during 120 s for several solutions containing different concentrations of Tl(I) and In(III) at acetate buffer pH 4.5. A high interaction between both metal ions can be observed. The best peak separation is achieved when similar concentrations of Tl(I) and In(III) are considered whereas a strong overlapping can

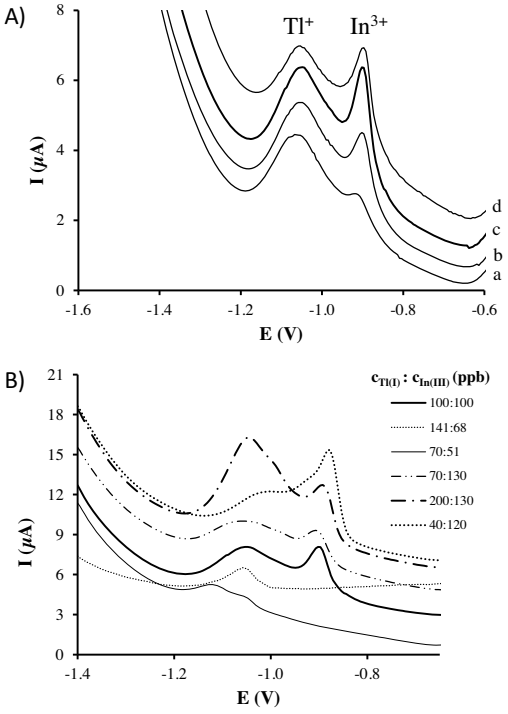

Fig. 2. DPASV voltammograms on crown-6-SPCNFE at acetate buffer pH 4.5 (A) of a solution containing 100 μg L^{-1} Tl(I) and In(III) and applying a t_d of 120 s and an E_d of −1.6 V (a), −1.5 V (b), −1.4 V (c) and −1.3 V(d) and (B) of solutions containing different concentrations of Tl(I) and In(III) applying and E_d of −1.4 V.

be observed when one metal ion concentration is much higher than the other. This is especially problematic because different environmental studies carried out in the Antarctica, Sweden and Japan have reported that usually thallium(I) is found at higher concentrations than indium(III) [3,29,30]. The strong overlapping observed at these metal ion proportions prevents the use of univariate calibration for the determination of Tl(I) and In(III) on crown-6-SPCNFE. Therefore, a multivariate calibration approach was considered.

3.2. Multivariate calibration studies

For the simultaneous voltammetric determination of Tl(I) and In(III) on crown-6-SPCNFE, a PLS model was constructed. For this purpose, calibration and validation sets constituted by 9 (64%) and 5 (36%) samples respectively (Fig. 1) were considered. Taking into account that in real samples thallium(I) is usually found at higher concentrations than indium(III), the experimental design was conceived so that most samples contained more Tl(I) than In(III). More specifically, Tl(I) concentration ranged from 9.7 to 199.5 μg L^{-1} whereas In(III) concentration ranged from 3.8 to 79.3 μg L^{-1}.

A key step in the construction of PLS models is data pretreatment. In this sense, baseline was firstly corrected by fitting a polynomial curve to points which were known to be part of the baseline. Following baseline correction, smoothing and first derivative Savitzky-Golay were applied and data were autoscaled. Pretreated data were studied by PCA and one outlier was detected and therefore removed from the training set. Then, PLS-1 models

Table 2
Main parameters of the regression lines obtained in the comparison between predicted *vs.* expected values of the training and test subsets for In(III) and Tl(I) (ranges calculated at the 95% confidence level) for crown-6-SPCNFE. The standard deviations are denoted by parenthesis.

	In(III)	Tl(I)
Training set		
Slope	1.000 (0.002)	1.00 (0.02)
Intercept (μg L^{-1})	0.0 (0.1)	0 (2)
R^2	1.000	0.999
RMSE[a] (μg L^{-1})	0.11	2.44
Test set		
Slope	0.2 (0.4)	0.84 (0.07)
Intercept (μg L^{-1})	32 (20)	10 (6)
R^2	0.123	0.980
RMSE[a] (μg L^{-1})	15.96	11.52

[a] RMSE: root mean square error.

were built for the determination of both Tl(I) and In(III). The number of latent variables (LVs), selected by the results provided by both training and test subsets, was 3 for both Tl(I) and In(III). Comparison graphs of obtained *vs* expected concentrations for In(III) and Tl(I) are shown in Fig. 3A and B respectively, whereas Table 2 shows the main parameters of the regression lines, as well as the root mean square error (RMSE) obtained for calibration and validation. Good results were obtained in the calibration of both In(III) and Tl(I), with slopes and correlation coefficients close to 1, intercepts close to 0 and really small RMSE values. Validation for thallium(I) was also quite good, although in this case higher prediction errors were obtained. Validation for indium(III) however, was not successful since a linear response could not be obtained, which suggest that the calibration model was overadjusted. It should also be pointed out that the sample containing the lowest concentration of In(III) could not be fitted by the model. Therefore, although quite good results were obtained for Tl(I), the simultaneous determination of Tl(I) and In(III) could not be successfully carried out using only crown-6-SPCNFE as working electrode.

3.3. Sensor array

As it was mentioned above the use of crown-6-SPCNFE as working electrode is not good enough for the simultaneous determination of In(III) and Tl(I). However, in these cases much better results can be obtained if two sensors with different responses are combined in a sensor array [23,24]. In this sense, an *ex-situ* antimony film was selected as a second working electrode. This electrode was previously characterized for the determination of both In(III) and Tl(I) [28] and it showed a distinctive (cross)response from crown-6-SPCNFE, with sensitivities of 0.75 and 1.10 a.u. μg^{-1} L for In(III) and Tl(I) respectively (Table 1). The voltammetric performance of *ex-situ*-SbSPCNFE for the simultaneous determination of Tl(I) and In(III) in the selected concentration range provides even more highly overlapped signals than crown-6-SPCNFE (Fig. 4), that make not possible neither the univariate calibration nor the achievement of satisfactory results by means of a multivariate calibration. However, the cross-selectivity observed for crown-6-SPCNFE and *ex-situ*-SbSPCNFE makes them good candidates for the sensor array. Thus, a new PLS model was constructed following the same steps as before for the crown-6-SPCNFE but this time a matrix containing the responses of both sensors was used as input. In this case the LVs used were 3 for Tl(I) and 5 for In (III). The comparison graphs of obtained *vs.* expected concentrations for In(III) and Tl(I) using the sensor array constituted by crown-6-SPCNFE and *ex-situ*-SbSPCNFE are shown in Fig. 5A and B respectively and the main parameters of the regression lines are summarized in Table 3. Good calibration models are still obtained for both In(III) and Tl(I) and predictions are much better than the ones obtained with only

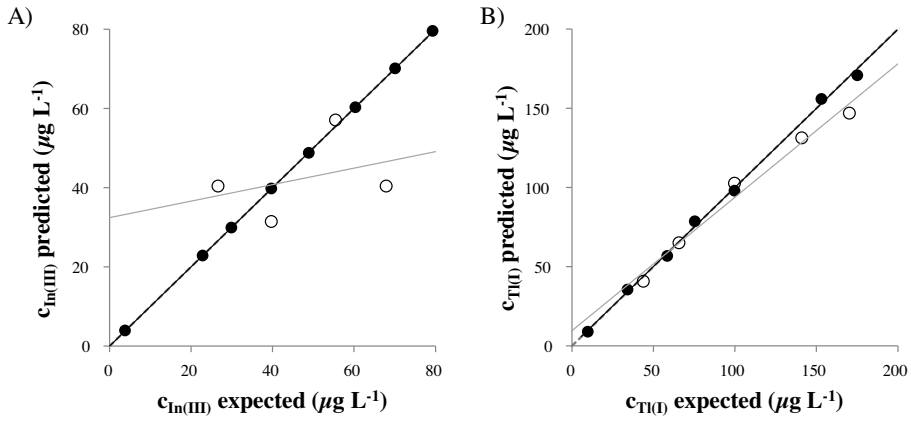

Fig. 3. Comparison graphs of predicted *vs.* expected concentrations obtained on crown-6-SPCNFE for In(III) (A) and Tl(I) (B) for training set (●) and test set (○). Dashed line represents theoretical diagonal line (y = x).

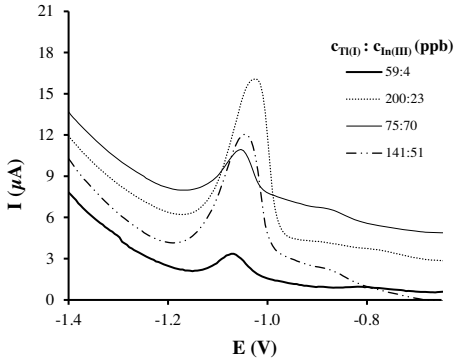

Fig. 4. DPASV voltammograms on *ex-situ*-SbSPCNFE at acetate buffer pH 4.5 of solutions containing different concentrations of Tl(I) and In(III) applying and E_d of −1.4 V.

Table 3
Main parameters of the regression lines obtained in the comparison between predicted *vs.* expected values of the training and test subsets for In(III) and Tl(I) (ranges calculated at the 95% confidence level) for the sensor array. The standard deviations are denoted by parenthesis.

	In(III)	Tl(I)
Training set		
Slope	1.00 (0.02)	1.000 (0.003)
Intercept (μg L^{-1})	0 (1)	0.0 (0.4)
R^2	0.997	0.999
RMSE[a] (μg L^{-1})	1.20	0.49
Test set		
Slope	1.07 (0.10)	1.00 (0.08)
Intercept (μg L^{-1})	−5 (5)	0 (9)
R^2	0.984	0.981
RMSE[a] (μg L^{-1})	2.60	6.55

[a] RMSE: root mean square error.

crown-6-SPCNFE although, in the case of the In(III) model the sample containing the lowest concentration could not either be fitted by the model. Using the sensor array good linear responses are achieved for obtained *vs.* predicted concentrations, with slopes and intercepts close to 1 and 0 respectively. Furthermore, much lower RMSEs are obtained for both metal ions. Therefore, the sensor array constituted by crown-6-SPCNFE and *ex-situ*-SbSPCNFE can successfully be applied for the simultaneous determination of In(III) and Tl(I). These results suggest that this sensor array could also be successfully applied to the simultaneous determination of these metal ions in natural waters.

Table 4
Total concentrations of Tl(I) and In(III) determined in tap water samples by DPASV on the multisensor array formed by Crown-6-SPCNFE/*Ex-situ*-SbSPCNFE modified electrodes and by ICP-MS.

		Tl(I)	In(III)
DPASV	c (μg L^{-1})	219.4	80.5
	RSD (%)	2.8	9.2
ICP-MS	c (μg L^{-1})	223.5	74.7
	RSD (%)	0.8	1.8

n = 3 for RSD (%).

3.4. Real sample analysis

At the view of the previous results, the sensor array formed by crown-6-SPCNFE and *ex-situ*-SbSPCNFE was considered for the simultaneous determination of Tl(I) and In(III) in natural waters and its applicability was tested on a spiked tap water. In this sense, three replicates of the tap water were analysed by voltammetric stripping voltammetry with the sensor array, using the same experimental conditions and obtaining voltammetric signals that behave in a similar way to those from training and test sets.

The previously calibrated PLS model was employed to calculate Tl(I) and In(III) concentrations. A good concordance of metal ions concentration, inferred by the obtained RSD%, was achieved between the different replicates, especially in the case of Tl(I) (Table 4). In order to test the accuracy of the proposed method the sample was also analysed by ICP-MS, a well-established technique for the determination of metals, and the results obtained from both techniques were statistically compared. In this sense, a two-tailed *t*-test (equal variances) was performed and it was concluded that the sensor array and ICP-MS provide statistically similar results for a confidence level of 95%.

Therefore, these results confirm that the combination of crown-6-SPCNFE and *ex-situ*-SbSPCNFE in a sensor array coupled with an appropriate PLS model is successfully capable for the simultaneous

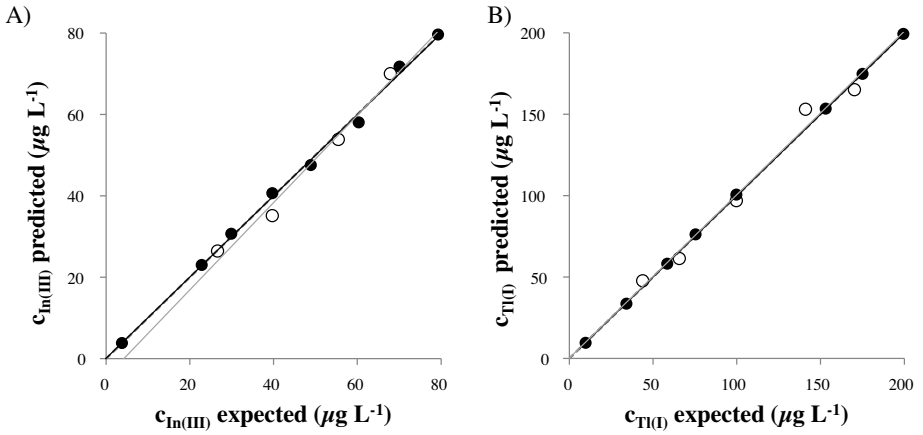

Fig. 5. Comparison graphs of predicted *vs.* expected concentrations obtained on the sensor array for In(III) (A) and Tl(I) (B) for training set (●) and test set (○). Dashed line represents theoretical diagonal line (y = x).

determination of Tl(I) and In(III) in real samples. Furthermore, this sensor array is proposed as an interesting and cheaper alternative to more conventional techniques such as ICP-MS.

4. Conclusions

Taking advantage of the good characteristic of the nanomaterial modified screen-printed electrodes, in this paper the immobilization of 4-carboxybenzo-18-crown-6 assisted by lysine on aryl diazonium salt monolayers anchored to the surface of a screen-printed carbon nanofiber-modified electrode (crown-6-SPCNFE) was applied for the determination of Tl(I) and In(III). The individual analytical characterization provided detection limits at levels of $\mu g\,L^{-1}$ for both metal ions and wide linear ranges. However, the overlapped character of the voltammetric signals obtained in the simultaneous determination of both metal ions hinders the univariate calibration and also, in the case of In(III), the multivariate calibration.

Taking into account the complementary response provided by *ex-situ*-SbSPCNFE for these metal ions, this sensor was considered for the combination with crown-6-SPCNFE in a sensor array approach. The data provided by the sensor array were treated by a PLS model and successful results were obtained for both training and testing, with predicted *vs.* expected concentrations calibration curves with slopes and correlation coefficients close to 1 and intercepts close to 0. This study confirms that the use of a sensor array approach represents a great improvement of the results (specially for In(III)) with respect to a single-electrode, in the fact that it allows the resolution of these strongly overlapped signals with a good prediction of both metal ion concentrations. Moreover, the simultaneous determination of Tl(I) and In(III) in a spiked tap water was also satisfactorily achieved, providing comparable results to those obtained by ICP-MS measurements.

Acknowledgments

This work is supported by the Ministry of Economy and Competitiveness (Project CTQ2012–32863) and the Generalitat of Catalonia (Project 2014SGR269). Clara Pérez-Ràfols acknowledges the Generalitat of Catalonia for a Ph.D. grant.

References

[1] B. Fowler, Indium and thallium in health, in: Trace Elem Heal. A Rev. Curr. Issues, Butterworth & Co, London, UK, 1983.
[2] Agency for Toxic Substances and Disease Registry (ATSDR), (n.d.). http://www.atsdr.cdc.gov/.
[3] S. Grahn, U. Karlsson, A. Düker, Historical pollution of seldom monitored trace elements in Sweden–part B: sediment analysis of silver, antimony, thallium and indium, J. Environ. Monit. 8 (2006) 732–744, http://dx.doi.org/10.1039/b601948j.
[4] H. Sereshti, Y. Entezari Heravi, S. Samadi, Optimized ultrasound-assisted emulsification microextraction for simultaneous trace multielement determination of heavy metals in real water samples by ICP-OES, Talanta 97 (2012) 235–241, http://dx.doi.org/10.1016/j.talanta.2012.04.024.
[5] J. Wang, Stripping Analysis: Principles, Instrumentation and Applications, VCH, Deerfield Beach, FL, 1985.
[6] J. Zhang, Y. Shan, J. Ma, L. Xie, X. Du, Simultaneous determination of indium and thallium ions by anodic stripping voltammetry using antimony film electrode, Sens. Lett. 7 (2009) 605–608, http://dx.doi.org/10.1166/sl.2009.1117.
[7] Z. Taleat, A. Khoshroo, M. Mazloum-Ardakani, Screen-printed electrodes for biosensing: a review (2008–2013), Microchim. Acta 181 (2014) 865–891, http://dx.doi.org/10.1007/s00604-014-1181-1.
[8] J. Barton, M.B.G. García, D.H. Santos, P. Fanjul-Bolado, A. Ribotti, M. McCaul, et al., Screen-printed electrodes for environmental monitoring of heavy metal ions: a review, Microchim. Acta 183 (2016) 503–517, http://dx.doi.org/10.1007/s00604-015-1651-0.
[9] A. Hayat, J.L. Marty, Disposable screen printed electrochemical sensors: tools for environmental monitoring, Sensors 14 (2014) 10432–10453, http://dx.doi.org/10.3390/s140610432.
[10] O.D. Renedo, M.A. Alonso-Lomillo, M.J.A. Martínez, Recent developments in the field of screen-printed electrodes and their related applications, Talanta 73 (2007) 202–219, http://dx.doi.org/10.1016/j.talanta.2007.03.050.
[11] D. Bélanger, J. Pinson, Electrografting: a powerful method for surface modification, Chem. Soc. Rev. 40 (2011) 3995–4048, http://dx.doi.org/10.1039/c0cs00149j.
[12] N. Serrano, A. Alberich, J.M. Díaz-Cruz, C. Ariño, M. Esteban, Coating methods, modifiers and applications of bismuth screen-printed electrodes, Trends Anal. Chem. 46 (2013) 15–29, http://dx.doi.org/10.1016/j.trac.2013.01.012.
[13] N. Serrano, J.M. Díaz-Cruz, C. Ariño, M. Esteban, Antimony- based electrodes for analytical determinations, Trends Anal. Chem. 77 (2016) 203–213, http://dx.doi.org/10.1016/j.trac.2016.01.011.
[14] C. Pérez-Ràfols, N. Serrano, J. Manuel Díaz-Cruz, C. Ariño, M. Esteban, Penicillamine-modified sensor for the voltammetric determination of Cd(II) and Pb(II) ions in natural samples, Talanta 144 (2015) 569–573, http://dx.doi.org/10.1016/j.talanta.2015.06.083.
[15] C. Pérez-Ràfols, N. Serrano, J.M. Díaz-Cruz, C. Ariño, M. Esteban, Glutathione modified screen-printed carbon nanofiber electrode for the voltammetric determination of metal ions in natural samples, Talanta 155 (2016) 8–13, http://dx.doi.org/10.1016/j.talanta.2016.04.011.
[16] N. Serrano, B. Prieto-Simón, X. Cetó, M. del Valle, Array of peptide-modified electrodes for the simultaneous determination of Pb(II), Cd(II) and Zn(II), Talanta 125 (2014) 159–166, http://dx.doi.org/10.1016/j.talanta.2014.02.052.

[17] E. Chow, J.J. Gooding, Peptide modified electrodes as electrochemical metal ion sensors, Electroanalysis 18 (2006) 1437–1448, http://dx.doi.org/10.1002/elan.200603558.
[18] J.J. Gooding, Peptide-modified electrodes for detecting metal ions, in: Alegret, Merkoçi (Eds.), Electrochem. Sens. Anal., Elsevier, Amsterdam, 2007, pp. 189–210, http://dx.doi.org/10.1016/S0166-526X(06)49010-3.
[19] N. Serrano, A. González-Calabuig, M. del Valle, Crown ether-modified electrodes for the simultaneous stripping voltammetric determination of Cd(II), Pb(II) and Cu(II), Talanta 138 (2015) 130–137, http://dx.doi.org/10.1016/j.talanta.2015.01.044.
[20] A. González-Calabuig, D. Guerrero, N. Serrano, M. del Valle, Simultaneous voltammetric determination of heavy metals by use of crown ether-modified electrodes and chemometrics, Electroanalysis 28 (2016) 663–670, http://dx.doi.org/10.1002/elan.201500512.
[21] C. Pérez-Ràfols, N. Serrano, J.M. Díaz-cruz, C. Ariño, M. Esteban, New approaches to antimony film screen-printed electrodes using carbon-based nanomaterials substrates, Anal. Chim. Acta 916 (2016) 17–23, http://dx.doi.org/10.1016/j.aca.2016.03.003.
[22] M. Esteban, C. Ariño, J.M. Díaz-Cruz, Chemometrics for the analysis of voltammetric data, Trends Anal. Chem. 25 (2006) 86–92, http://dx.doi.org/10.1016/j.trac.2005.07.009.
[23] M. del Valle, Sensor arrays and electronic tongue systems, Int. J. Electrochem. 2012 (2012) 1–12, http://dx.doi.org/10.1155/2012/986025.
[24] M. del Valle, Electronic tongues employing electrochemical sensors, Electroanalysis 22 (2010) 1539–1555, http://dx.doi.org/10.1002/elan.201000013.
[25] C. Barceló, N. Serrano, C. Ariño, J.M. Díaz-Cruz, M. Esteban, Ex-situ antimony screen-printed carbon electrode for voltammetric determination of Ni(II)-ions in wastewater, Electroanalysis 28 (2016) 640–644, http://dx.doi.org/10.1002/elan.201500511.
[26] Matlab, Version R2008b Ed., Mathworks Inc., Natick, MA, USA, 2008.
[27] PLS-toolbox version 7 8.2 (Eigenvector Research Inc., Wenatchee, USA), (n.d.).
[28] C. Pérez-Ràfols, N. Serrano, J.M. Díaz-Cruz, C. Ariño, M. Esteban, A screen-printed voltammetric electronic tongue for the analysis of complex mixtures of metal ions, Sens. Actuat. B-Chem. (2016) (Submitted for publication).
[29] A. Matsumoto, T.K. Hinkley, Determination of lead cadmium, indium, thallium and silver in ancient ices from Antarctica by isotope dilution-thermal ionization mass spectrometry, Geochem. J. 31 (1997) 175–181.
[30] A. Miyazaki, A. Kimura, H. Tao, Distribution of indium, thallium and bismuth in the environmental water of Japan, Bull. Environ. Contam. Toxicol. 89 (2012) 1211–1215, http://dx.doi.org/10.1007/s00128-012-0851-0.

Biographies

Clara Pérez-Ràfols graduated in Chemistry with highest honors at the University of Barcelona (UB) in 2014 and received her Master's degree in Analytical Chemistry in 2015, also from the University of Barcelona. She is currently doing her Ph.D. in the area of Analytical Chemistry and Environment in the UB, focusing on the development of sensors and voltammetric electronic tongues for the simultaneous determination of several metal ions. She has published 6 research works in indexed journals.

Núria Serrano was born in 1977. She is acting Senior Lecturer at the Department of Chemical Engineering and Analytical Chemistry, University of Barcelona (UB), Spain. In 2007 she completed the Ph.D. at the same University. As a postdoctoral researcher, she worked for one year at the Department of Chemistry (Masaryk University, Brno) in 2010; and she spent nine months at the Sensors and Biosensors group (Autonomous University of Barcelona, Bellaterra) in 2013. Her research is mainly focussed on the development of sensors and voltammetric electronic tongues, based on screen-printed electrodes, for the determination of heavy metals. She has participated in 9 competitive research projects, has supervised 2 Ph.D. Theses and has published more than 40 research works in indexed journals.

José Manuel Díaz Cruz was born in 1965. Since 1995 he is Associate Professor of the Department of Chemical Engineering and Analytical Chemistry of the University of Barcelona (UB), Spain, where he had obtained the Ph.D. degree in 1992. In 1993 worked for one year in the Department of Physical and Colloid Chemistry (Wageningen University, The Netherlands). His main research contributions have been in the field of electroanalytical chemistry, studying: i) the interactions of metal ions with macromolecular ligands, colloidal particles and sulphur-containing compounds; ii) the influence of adsorption phenomena in voltammetric measurements; iii) the application of chemometric methods to electroanalytical data and iv) the development of sensors based on screen-printed electrodes. He has participated in 22 competitive research projects, has supervised 8 Ph.D. Theses and has published more than 120 research works in indexed journals.

Cristina Ariño was born in 1956. Nowadays, she is Associate Professor of the Department of Chemical Engineering and Analytical Chemistry at the University of Barcelona (UB), Spain. She obtained the Ph.D. degree in 1986 and was appointed Associate Professor in 1987. She has participated in more than 20 competitive research projects, has supervised 8 Ph.D. Theses and has published more than 120 research works in indexed journals. Being her research contributions in the field of electroanalytical chemistry, studying: (i) the interactions of metal ions with macromolecular ligands, particles, and sulphur-containing compounds; (ii) the influence of adsorption phenomena in voltammetric measurements; (iii) the application of chemometric methods to voltammetric data concerning solution equilibria; (iv) development and applications of sensors based in screen-printed technology and (v) the possibilities of screen printed electrodes in amperometric detection. She has also contributed in teaching electroanalytical courses in different master programs from the Faculty of Pharmacy of the University of Concepción (Chile), from the Faculty of Chemistry of the University of Santiago de Chile (Chile) and in different editions of an European Joint Master in Quality in Analytical Laboratories.

Miquel Esteban (1955) is Professor at the Department of Chemical Engineering and Analytical Chemistry, University of Barcelona (UB), Spain. He obtained the Ph.D. at UB, and was appointed Associate Professor in 1984 and Full Professor in 1993. Stays abroad: Institut für Angewandte Physikalische Chemie (Kernforschungsanlage, KFA, Jülich, Germany) in 1986; Department of Physical and Colloid Chemistry (Wageningen Agricultural University, Wageningen, Netherlands) in 1987; EC Scientific Visitor at the Institute for Reference Materials and Measurements (IRMM) in the Joint Research Centre (Geel, Belgium) in 1994 and 1997; European Synchroton Radiation Facility (ESRF, Grenoble, France) in 1999. Academic responsibilities: Secretary of the Faculty of Chemistry (1987–1991), Vice-President of the Division of Experimental Sciences and Mathematics (2000–2003), Head of the Department of Analytical Chemistry (2004–2008) and of Chemical Engineering and Analytical Chemistry (2016-) and member of UB government council (2004–2008). His main research contributions have been in the field of electroanalytical chemistry, studying: i) the interactions of metal ions with macromolecular ligands and sulphur-containing compounds; ii) the influence of adsorption phenomena in voltammetric measurements; iii) the application of chemometric methods to voltammetric data concerning solution equilibria and iv) development and applications of sensors based in screen-printed technology. He has participated in more than 20 competitive research projects, has supervised 5 Ph.D. Theses and has published more than 160 research works in indexed journals.

A screen-printed voltammetric electronic tongue for the analysis of complex mixtures of metal ions.

C. Pérez-Ràfols, N. Serrano, J. M. Díaz-Cruz, C. Ariño, M. Esteban

Sensors and Actuators B 250 **(2017)** 393-401

https://doi.org/10.1016/j.snb.2017.04.165

Sensors and Actuators B 250 (2017) 393–401

Contents lists available at ScienceDirect

Sensors and Actuators B: Chemical

journal homepage: www.elsevier.com/locate/snb

A screen-printed voltammetric electronic tongue for the analysis of complex mixtures of metal ions

Clara Pérez-Ràfols, Núria Serrano*, José Manuel Díaz-Cruz, Cristina Ariño, Miquel Esteban

Departament d'Enginyeria Química i Química Analítica, Facultat de Química, Universitat de Barcelona, Martí i Franquès 1-11, E-08028 Barcelona, Spain

ARTICLE INFO

Article history:
Received 1 December 2016
Received in revised form 25 April 2017
Accepted 26 April 2017
Available online 27 April 2017

Keywords:
Voltammetric electronic tongue
Screen-printed electrodes
Modified electrodes
Metal determination
Stripping voltammetry
Partial least squares regression

ABSTRACT

A voltammetric electronic tongue was constituted by four screen-printed modified electrodes: a carbon nanofiber modified electrode, an *ex-situ* antimony film electrode prepared from carbon nanofiber modified electrode, and two carbon nanofiber electrodes chemically modified with Cys and GSH. The tongue was successfully applied to the analysis of a complex mixture of metal ions (4 analytes and 2 interferences) by differential pulse anodic stripping voltammetry. Each sensor was firstly studied for the determination of each metal separately confirming that all electrodes showed differentiated response for the metals. The obtained voltammetric signals provided by the sensor array were processed by Partial Least Squares regression (PLS) to resolve the overlapped nature of the obtained multimetal stripping measurements. This PLS model was built considering a hierarchical model in order to reduce the large amount of data. The method was applied to synthetic mixtures of Cd(II), Pb(II), Tl(I), and Bi(III) in the presence of Zn(II) and In(III) at the levels of μg L^{-1} and successfully validated with correlation coefficients of both calibration and prediction higher than 0.9 obtained from predicted *vs.* expected concentration graphs. Moreover, the simultaneous determination of Cd(II), Pb(II), Tl(I), and Bi(III) in the presence of Zn(II) and In(III) in a spiked tap water was also satisfactory achieved, providing comparable results to those obtained by ICP-MS.

1. Introduction

Heavy metals are natural components of the earth crust and can be released to the environment from both natural and anthropogenic sources such as forest fires, volcanic eruptions, sea spray, biogenic aerosols, mineral extraction, metal processing and incineration of pharmaceutical products, batteries, plastics and electrical goods among others [1,2]. In contrast to other toxic substances, heavy metals are non-biodegradable. This fact increases the risk to human health that represent human or anthropogenic contributions to air, water, soil and food by modifying their speciation [3]. This risk is even higher due to heavy metals tend to bioaccumulate and biomagnificate [4,5]. Some heavy metals are essential for the human life in small concentrations. However, most of these metals are harmful when they are found at higher concentrations, being lead, cadmium, arsenic and mercury the most toxic. Heavy metals can be incorporated to the human body through the air, water, food or skin adsorption [4]. Therefore, monitoring heavy metals is very important both for human health and environment. In the last years different techniques were applied for the determination of heavy metals, being atomic absorption spectroscopy, inductively coupled plasma mass spectrometry or inductively coupled plasma atomic emission spectroscopy the most representative ones [6–8]. Nevertheless, these techniques require long times of analysis, expensive instruments and trained personal. A faster and cheaper alternative that requires simple and portable instrumentation is given by electroanalytical techniques, which present excellent detection limits, sensitivity to the presence of different metal species and ability to multielement determination [9].

In voltammetric measurements of metal ions the electrode usually works as a single-electrode sensor which allows the simultaneous determination of several metal ions when non-overlapped peaks are obtained, i.e. the determination of Zn(II), Cd(II), Pb(II) and Cu(II) with the classical hanging mercury drop electrode [10,11]. However, when the solution contains a complex mixture of metal ions with intricate voltammetric responses (overlapped peaks, different interactions between metals. . .) the use of a single- electrode sensor does not allow its resolution. To solve these more complex systems a good strategy can be the use of several electrodes grouped in arrays of sensors with low selectivity that present a

* Corresponding author.
E-mail address: nuria.serrano@ub.edu (N. Serrano).

http://dx.doi.org/10.1016/j.snb.2017.04.165
0925-4005/

cross-response performance, giving rise to a multi-sensor array or (bio)electronic tongue, in which each electrode is different searching for a multivariate response [12–15]. Although the use of voltammetric tongues for electroanalytical purposes requires a larger amount of samples for calibration and the use of a multichannel potentiostat, these disadvantatges can be overcome if the achieved information is better than that provided by a single sensor.

An essential aspect of any electronic tongue is data analysis. In particular, voltammetric tongues generate large amounts of data, which makes necessary a first step in order to preprocess and compress them prior to building the chemometric model. This preprocessment usually focuses on making data independent from units, removing redundant information or enhancing signal-to-noise ratio. In order to build the model different multivariate chemometric tools such as principal component analysis (PCA), partial least squares regression (PLS) or artificial neural network (ANN) have been used to maximize the information achieved from the voltammetric data set using the sensor array, that a priori are difficult to analyse [12,16,17].

The use of arrays of voltammetric sensors has recently enabled an application very much desirable from the industrial sector, which is the use of electronic tongue systems to monitor and to detect defects during production of beverages and food [12]. In addition, sensor arrays are also useful in other research fields such as environmental analysis or bioanalysis [14,18–21]. In particular, voltammetric electronic tongues have been recently applied for metal ion determination in simple metal mixtures [22–25]. Nevertheless, to the best of our knowledge no more than 3 different metals were considered.

To ensure the desired cross-response of the electrode array the combination of different sensors modified following different strategies can be useful. In this sense, electrodeposition of metal films onto electrode surfaces [26,27] or chemical modification by electrografting with aryl diazonium salts [28] are two modification processes well known that can lead to sensors presenting a very different voltammetric response.

Nowadays, the screen-printing technology is well established for the production of sensors for electrochemical purposes. This technology allows the mass production of quite reproducible single-use devices with accessible and low cost character that usually incorporate a three-electrode configuration (working, reference and counter) on the same strip. Moreover, recent advances in this technology also allow the production of devices with different designs and the use of different inks (carbon, gold, silver, platinum. . .) that can include nanomaterials too [26,29–33]. In fact, the use of carbon- based nanomaterials, and in particular carbon nanofiber (CNF), as substrates for electrode modifications has been reported to provide sensors with a better analytical performance due to their enhanced real surface area [34,35].

Thus, the coupling of SPEs with a voltammetric electronic tongue presents an attractive option for the determination of complex mixtures of heavy metal ions.

In this respect, this study presents a voltammetric electronic tongue which employs an array of sensors constituted by a carbon nanofiber modified screen-printed electrode (SPCE-CNF), an *ex-situ* antimony film electrode prepared from carbon nanofiber modified screen-printed electrode (SbSPCE-CNF), and two chemically modified sensors in which Cys and GSH were immobilized on aryl diazonium salt monolayers anchored to the surface of a carbon nanofiber modified screen-printed electrode (Cys-SPCE-CNF and GSH-SPCE-CNF, respectively) to consider for the first time the multivariate analysis of a really complex metal ion mixture including Cd(II), Pb(II), Tl(I), In(III), Zn(II), and Bi(III) in natural water samples. The electrochemical responses obtained from anodic stripping voltammetry (ASV) were used as departure information and the data treatment was performed with appropriate PLS model.

2. Experimental section

2.1. Chemicals and solutions

All chemicals were of analytical grade and used without additional purification. Sb(III) 1.000 mg L^{-1} atomic absorption standard solution was provided from Merck (Darmstadt, Germany). Potassium ferrocyanide $K_4[Fe(CN)_6]\cdot 3H_2O$, 2-(N-morpholino)-ethanesulfonic acid (MES), nitric acid, hydrochloric acid, sodium acetate, acetic acid and glutathione (GSH), in the reduced form, with purity greater than 99% were purchased from Merck. *N*-hydroxysulfosuccinimide (sulfo-NHS), *N*-(3-dimethylaminopropyl)-*N'*-ethylcarbodiimide hydrochloride (EDC), 4-aminobenzoic acid (ABA), sodium nitrite, methanol, perchloric acid, sodium monophosphate, potassium dihydrogen phosphate, and L-cysteine (Cys) with purity greater than 99% were provided by Sigma-Aldrich (St. Louis, MO, USA). Potassium ferricyanide $K_3[Fe(CN)_6]$ was supplied by Panreac (Barcelona, Spain). Zn(II), Cd(II), Pb(II), Tl(I), In(III) and Bi(III) stock solutions 10^{-2} mol L^{-1} were prepared from $Pb(NO_3)_2\cdot 4H_2O$, $Cd(NO_3)_2\cdot 4H_2O$, $Zn(NO_3)_2\cdot 4H_2O$, TlCl, $In_2(SO_4)_3\cdot 5H_2O$ and Bi(III) 1000 mg L^{-1} atomic absorption standard solution respectively supplied by Sigma-Aldrich. Ultrapure water (Milli-Q plus 185 system, Millipore) was used in all experiments.

Tap water sample was collected in the laboratory from the local water distribution network, managed by Agbar Company (Barcelona; http://www.agbar.es/eng/home.asp) and mostly using water coming from Llobregat River.

2.2. Instrumentation

An Autolab System PGSTAT12 (EcoChemie, The Netherlands), in a multichannel configuration, using GPES Multichannel 4.7 software package (EcoChemie) was used to perform differential pulse anodic stripping voltammetric (DPASV) measurements. The voltammetric cell was constituted by an Ag|AgCl|KCl (3 mol L^{-1}) reference electrode (to which all potentials are referred) provided by Metrohm (Switzerland), the four working screen-printed electrodes (SPEs) modified with CNF, Sb film, Cys and GSH respectively, and a carbon counter electrode from one of the SPEs as a common counter electrode. The working SPEs were prepared from commercial carbon nanofiber modified screen-printed disk electrodes (ref. 110CNT, DS SPCE) of 4 mm diameter supplied by Dropsens (Oviedo, Spain). Four flexible cables ref. (CAC, DropSens) were used to connect the SPEs to the Autolab System (Fig. 1).

For pH measurements, a Crison micro pH 2000 pH-meter was used.

All measurements were carried out without oxygen removal and at room temperature (20 °C).

Inductively coupled plasma mass spectrometry Perkin-Elmer model Elan 6000 (USA) was used for ICP-MS measurements.

2.3. Preparation of modified SPEs

2.3.1. Carbon nanofiber modified screen-printed electrode (SPCE-CNF)

SPCE-CNF can be used as it is commercially acquired without any previous treatment before measurements.

2.3.2. Ex-situ antimony film electrode (ex-situ-SbSPCE-CNF)

The SPCE-CNF, the auxiliary and the reference electrodes were immersed into a plating solution containing 0.01 mol L^{-1} HCl and 50 mg L^{-1} of Sb(III). An $E_d = -0.50$ V was applied during 300 s with

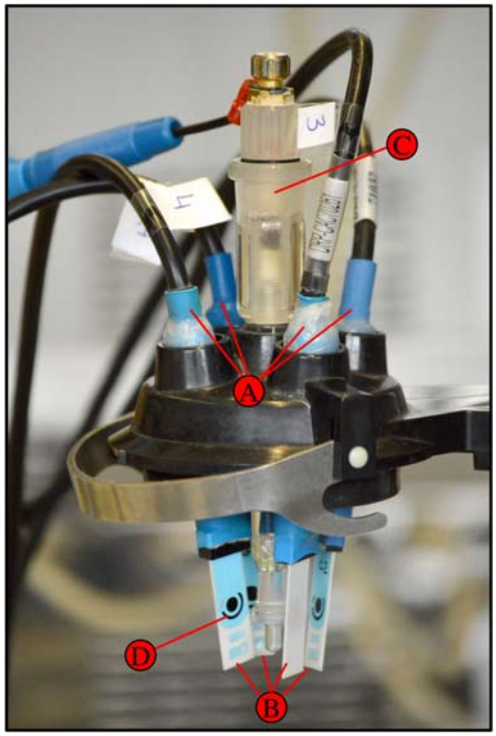

Fig. 1. Experimental setup for simultaneous stripping voltammetric measurements with four different screen-printed electrodes. A) DRP-CAC connectors. B) Screen-printed electrodes. C) Ag/AgCl reference electrode. D) Carbon auxiliary electrode.

solution stirring, followed by a rest period (without stirring) of 20 s. This methodology was previously tested showing a very high repeatability and reproducibility [36].

2.3.3. Glutathione modified electrode (GSH-SPCE-CNF)

GSH was immobilized on aryl diazonium salt monolayers anchored to the surface of SPCE-CNF [35]. Briefly, firstly the aryl diazonium salt is generated by adding 2 mmol L^{-1} of $NaNO_2$ to a cooled solution of 73 mmol L^{-1} of ABA in 1 mol L^{-1} HCl. After mixing for 30 min in an ice bath, the electrochemical grafting process was conducted by the application of 15 cycles of cyclic voltammetry from 0 V to −1 V at 0.2 V s^{-1}. For the covalent immobilization of GSH via carbodiimide coupling, 10 μL of a 35 mmol L^{-1} sulfo-NHS and 26 mmol L^{-1} EDC solution in 0.1 mol L^{-1} MES buffer (pH 4.5) were dropped onto the functionalized SPE and left for 1 h. Finally, the activated carboxyl groups reacted overnight with the amine terminal groups of GSH (2.9 mg/100 μL GSH solution in MES buffer) at 4 °C.

This methodology was previously tested showing a very high repeatability and reproducibility[35].

2.3.4. Cysteine modified electrode (Cys-SPCE-CNF)

Cys was immobilized on aryl diazonium salt monolayers anchored to the surface of SPCE-CNF. For the preparation of the Cys-SPCE-CNF the GSH-SPCE-CNF above mentioned procedure was implemented, using Cys instead of GSH.

2.4. Voltammetric measurements

Stripping voltammetric (DPASV) measurements using SPCE-CNF, *ex-situ*-SbSPCE-CNF, GSH-SPCE-CNF and Cys-SPCE-CNF were performed by applying with stirring a deposition potential (E_d) of −1.4 V during a deposition time (t_d) of 120 s followed by a rest period (t_r) of 5 s. Voltammograms were obtained by scanning the potential from −1.4 to −0.3 V, using a step potential of 5 mV, pulse amplitudes of 50 mV and pulse times of 50 ms.

In order to eliminate the remaining bound metals from the electrodes a cleaning step was performed between measurements by applying a conditioning potential (E_{cond}) of −0.3 V for 15 s in 0.1 mol L^{-1} $HClO_4$ for *ex-situ*-SbSPCE-CNF, GSH-SPCE-CNF and Cys-SPCE-CNF electrodes and 0 V for 15 s in 0.1 mol L^{-1} HNO_3 for SPCE-CNF electrode. On the other hand, the array of electrodes was completely replaced by a new set every 20 measurements to ensure their optimal performance.

Linear calibration plots for the separate determination of considered metal ions were obtained by increasing metal ion concentrations in 0.1 mol L^{-1} acetate buffer solution at pH 4.5.

In order to allow the simultaneous analysis of Zn(II), Cd(II), Pb(II), Tl(I), In(III) and Bi(III) a total set of 57 samples ranging from 0 to 200 μg L^{-1} were prepared from appropriate dilution of stock solutions. The total set of samples was distributed among training and test subsets. The training subset was formed by 45 samples (79%) distributed in a 6 factor central composite design whereas the test subset was formed by 12 samples (21%) located in the centre of the cubes faces (Fig. 2a). In addition, control samples (replicates of the central point of the experimental design) were inserted every 10 measurements.

Furthermore, 3 replicates of a spiked tap water sample with the six considered metal ions distributed in the range of the calibration curve were employed to test the suitability of the four-sensor array for the analysis of Zn(II), Cd(II), Pb(II), Tl(I), In(III) and Bi(III) in natural samples.

2.5. Sample preparation

Water samples collected from the local water distribution network were firstly acidified (pH 4.5) and then spiked with 70 μg L^{-1} of Zn(II), In(III) and Bi(III), 80 μg L^{-1} of Cd(II) and Tl(III) and 90 μg L^{-1} of Pb(II). Total metal ion concentrations were further determined by ICP-MS.

2.6. Data processing

Prior to building the PLS model a preprocessing step was performed on each voltammogram. With this purpose, an orthogonal signal correction (OSC) [37] was performed in order to remove variations to the data that are not relevant to the model (noise, baseline…). OSC was performed on calibration data and then applied to the validation data and natural samples data.

In order to reduce the large amount of data generated for each sample (4 sensors x 555 current values) a hierarchical model was considered [38]. In this sense, the data set was separated in 4 blocks corresponding to the 4 sensors and PLS was performed on each block. Scores values obtained for each block were used as new descriptors and PLS was performed again (Fig. 2b).

Pre-processing of the data matrices, variable selection and construction of PLS model were made using Matlab® [39] with PLS-toolbox [40].

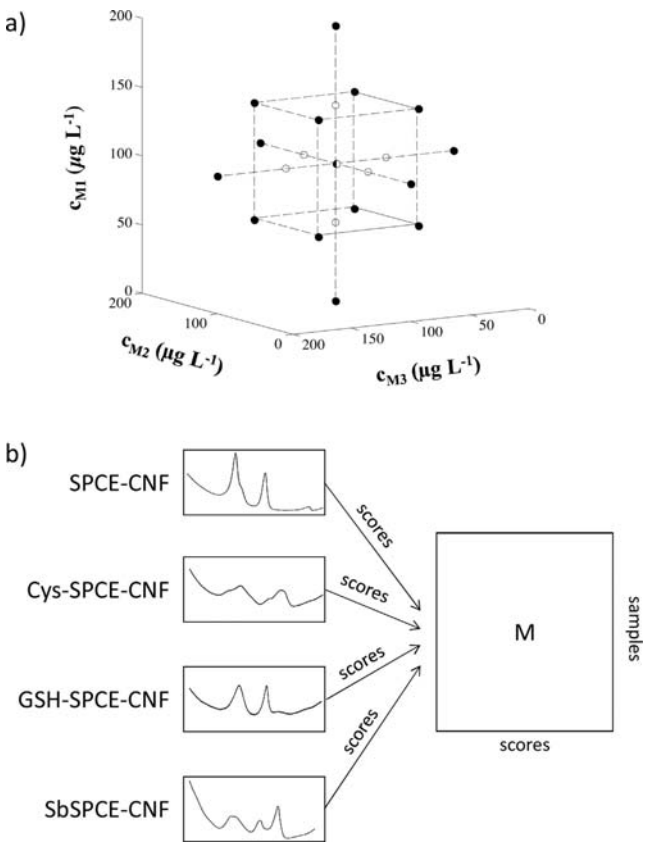

Fig. 2. a) Experimental design used for training (●) and testing (○) subsets. M_1, M_2 and M_3 represent any possible combination of 3 metals among Zn(II), Cd(II), Tl(I), Pb(II), In(III) and Bi(III). b) Hierarchical PLS model performed on the data set obtained with the voltammetric electronic tongue. Scores values from each sensor are used as descriptors in a new data matrix, M.

Table 1
Calibration data for the separate determination of Zn(II), Cd(II), Pb(II), Bi(III), In(III) and Tl(I) on the multisensor array formed by SPCE-CNF/GSH-SPCE-CNF/Cys-SPCE-CNF/*Ex-situ*-SbSPCE-CNF modified electrodes at E_d of −1.4 V using a t_d of 120 s at pH 4.5.

	Zn(II)	Cd(II)	Pb(II)	Bi(III)	In(III)	Tl(I)
SPCE-CNF						
Sensitivity (a.u. μg^{-1} L)	3.75 (0.06)	5.45 (0.05)	4.59 (0.03)	0.40 (0.01)	2.80 (0.03)	2.73 (0.03)
R^2	0.999	0.999	0.999	0.996	0.999	0.999
Linear range[a] (μg L^{-1})	16.9–198.3	11.3–200.0	8.7–200.8	56.1–200.7	10.0–200.4	21.7–274.9
LOD (μg L^{-1})	5.1	3.4	2.6	16.8	3.0	6.5
GSH-SPCE-CNF						
Sensitivity (a.u. μg^{-1} L)	1.71 (0.04)	0.62 (0.01)	3.27 (0.03)	0.240 (0.005)	0.47 (0.01)	0.97 (0.02)
R^2	0.998	0.999	0.999	0.998	0.998	0.998
Linear range[a] (μg L^{-1})	24.5–198.3	11.6–200.0	10.8–200.8	29.1–200.7	26.4–200.4	41.8–274.9
LOD (μg L^{-1})	7.4	3.5	3.2	8.7	7.9	12.5
Cys-SPCE-CNF						
Sensitivity (a.u. μg^{-1} L)	2.19 (0.05)	1.43 (0.01)	3.48 (0.03)	0.196 (0.005)	0.277 (0.004)	1.08 (0.03)
R^2	0.997	0.999	0.999	0.998	0.999	0.998
Linear range[a] (μg L^{-1})	26.3–198.3	10.9–200.0	10.3–200.8	38.0–200.7	18.2–200.4	57.8–274.9
LOD (μg L^{-1})	7.9	3.3	3.1	11.4	5.5	17.4
***Ex-situ*-SbSPCE-CNF**						
Sensitivity (a.u. μg^{-1} L)	2.26 (0.03)	2.42 (0.02)	0.85 (0.01)	0.157 (0.002)	0.75 (0.01)	1.10 (0.02)
R^2	0.999	0.999	0.999	0.999	0.999	0.999
Linear range[a] (μg L^{-1})	14.9–198.3	10.7–200.0	13.2–200.8	17.2–200.7	21.0–200.4	28.5–274.9
LOD (μg L^{-1})	4.5	3.2	4.0	5.2	6.3	8.6

[a] The lowest value of the linear range was considered from LOQ.

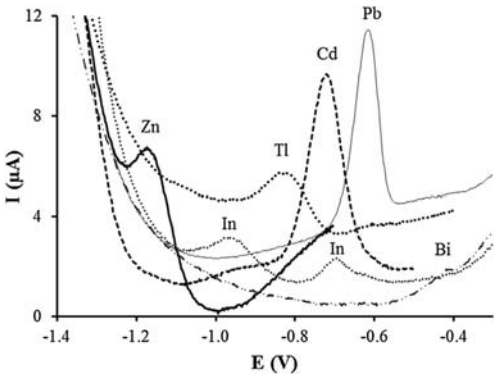

Fig. 3. Individual DPASV voltammograms of a solution containing 120 μg L^{-1} of Pb(II), Zn(II), Cd(II), Tl(I), In(III) and Bi(III) recorded on SPCE-CNF applying an E_d of -1,4 V during 120 s at acetate buffer pH 4.5.

3. Results and discussion

3.1. Voltammetric calibration data

Firstly, individual calibration of Zn(II), Cd(II), Pb(II), Tl(I), In(III) and Bi(III) ions by DPASV was carried out on each SPCE-CNF, *ex-situ*-SbSPCE-CNF, GSH-SPCE-CNF and Cys-SPCE-CNF respectively. The optimized application [25,34,35] of an E_d of −1.4 V with stirring during a t_d of 120 s followed by a t_r of 5 s without stirring allows, at each of the four electrodes, the determination of all metal ions in the considered concentration range. In order to build the calibration curves, ten standard concentrations of the considered metal ions were used. Comparable voltammetric responses for Zn(II), Cd(II), Pb(II), Tl(I), In(III) and Bi(III) were obtained using SPCE-CNF, *ex-situ*-SbSPCE-CNF, GSH-SPCE-CNF and Cys-SPCE-CNF at identical experimental conditions. Fig. 3 shows, as an example, the individual voltammetric responses obtained for each metal ion on SPCE-CNF. The individual responses on the other electrodes can be found in the supplementary material (Fig. S1). Table 1 summarizes the sensitivities calculated from the slope of the calibration lines of each metal ion at the four modified SPEs and the correlation coefficients, as well as the limits of detection (LOD) considered as 3 times the standard deviation of the intercept over the slope of the calibration curve of the target ions, and the limits of quantification (LOQ) calculated as 10 times the previous ratio for all six metals. It should be pointed out that LOQ was designed as the lowest value of the linear concentration range. Very good linear responses of the peak area *vs.* concentration were achieved for Zn(II), Cd(II), Pb(II), Tl(I), In(III) and Bi(III) until a concentration level close to 200 μg L^{-1} for all considered metal ions at the four modified SPEs. Regarding the obtained sensitivities it can be stated that: i) using SPCE-CNF, Cd(II) was the metal ion presenting better sensitivity; ii) Pb(II) was the most sensitive metal using both GSH-SPCE-CNF and Cys-SPCE-CNF; iii) using *ex-situ*-SbSPCE-CNF, Cd(II) and also Zn(II) showed better sensitivity; and iv) the best sensitivity for In(III) and Bi(III) were achieved on SPCE-CNF. The LODs of the six metal ions in the four modified SPEs ranged from 2.6 to 16.8 μg L^{-1} depending on both the metal ion and the modified SPE (Table 1) and the LOQ varied from 8.7 to 56.1 μg L^{-1} depending again on both the metal ion and the modified SPE (Table 1). These LODs and LOQs values are on the same order than previous reported modified electrodes [26,27,29,35].

Moreover, taking into account the guidelines for drinking water quality [41], the proposed sensors seem to be perfectly suitable for the detection of heavy metals ions in environmental water.

Therefore, the obtained calibration data indicate that the four modified SPEs could be completely appropriate for the analysis of Zn(II), Cd(II), Pb(II), Tl(I), In(III) and Bi(III) at trace levels in environmental samples. Moreover, the cross-response of the selected sensors was stated. Thus, the use of the four modified SPEs as an electrode array configuration instead of as single sensors could introduce some discrimination power to elucidate a mixture of the different metal ions.

3.2. Multimetal stripping voltammetric measurements

The stripping voltammetric performance of several mixtures of Zn(II), Cd(II), Pb(II), Tl(I), In(III) and Bi(III) was studied using SPCE-CNF, *ex-situ*-SbSPCE-CNF, GSH-SPCE-CNF and Cys-SPCE-CNF working as an electrode array inside the concentration range 0–200 μg L^{-1} to identify potential interactions between the considered metal ions. As an example, Fig. 4a shows four stripping voltammograms recorded using *ex-situ*-SbSPCE-CNF (random concentrations). Complex voltammograms with an important overlapping effect were observed hindering not only the straight determination of the different metals of the mixture but also the direct assignment of the oxidation peak potential of each considered metal in the intricate voltammograms. Nevertheless, from separate metal stripping measurements and in general terms, the overlapped peaks from −1.4 V to −0.9 V could be attributed to Zn(II), Cd(II) and Tl(I) whereas the peaks related to Pb(II) and In(III) would be those shown from −0.9 V to −0.55 V and finally the peak close to −0.4 V would be assigned to Bi(III). Fig. 4b shows, as an example, a comparison of the stripping voltammograms of 100 μg L^{-1} Zn(II), Cd(II), Tl(I), Pb(II), In(III) and Bi(III) provided by Cys-SPCE-CNF (thin line), *ex-situ*-SbSPCE-CNF (dashed thin line), GSH-SPCE-CNF (dashed thick line) and SPCE-CNF (thick line). Some significant differences in metal peak potentials and shapes can be clearly perceived in the stripping voltammetric response of the sensor array depending on both the metal ion and the modified SPE used. This fact confirms that the information provided by the electrode array is significantly better than that obtained from a single electrode. Thus, despite the intricate signal origin, in a next step, the voltammetric data set of metal ion mixtures provided by the sensor array will be proposed to be used to calibrate Zn(II), Cd(II), Tl(I), Pb(II), In(III) and Bi(III) with a suitable PLS model that may consider any overlapping to assist us in the better determination of the studied metal ions.

3.3. Calibration and validation of PLS model in metal mixtures

For the voltammetric electronic tongue study a total set of 57 metal mixtures samples (45 corresponding to the training set and 12 to the test set) with concentrations ranging from 0 to 200 μg L^{-1} were prepared and voltammetric stripping measurements were performed simultaneously on SPCE-CNF, *ex-situ*-SbSPCE-CNF, GSH-SPCE-CNF and Cys-SPCE-CNF. It should be pointed out that, although it has already been proven that these electrodes can be used for a large set of measurements [35,36], to ensure the optimal performance of the sensor array, all the electrodes were replaced every 20 measurements. In addition, due to the large amount of samples considered, the measurements were carried out in two consecutive days. However, control samples inserted between measurements corroborate the use of different electrode units in different days does not affect the voltammetric stripping response.

Prior to building the PLS models, each sensor signal was processed by OSC (1 component determined by the amount of Y block

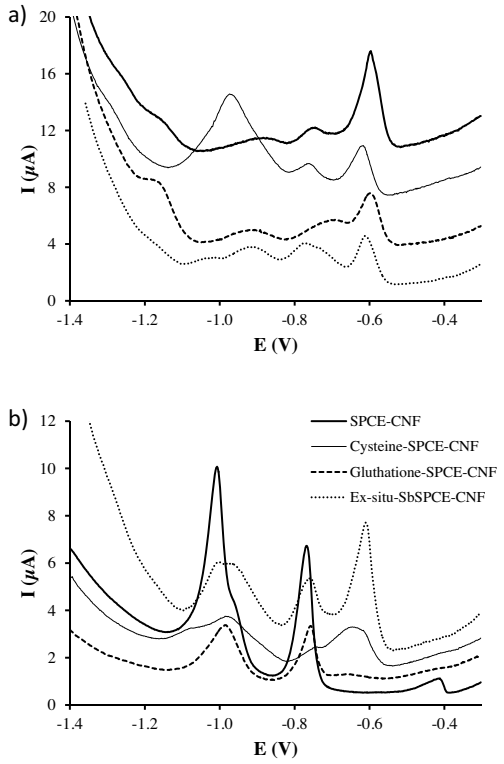

Fig. 4. a) DPASV voltammograms on *ex-situ*-SbSPCE-CNF and applying a E_d of -1,4 V during 120 s at acetate buffer pH 4.5 of a solution containing 142 μg L^{-1} Zn(II), Pb(II), In(III) and Bi(III) and 58 μg L^{-1} Cd(II) and Tl(I) (thick line), 142 μg L^{-1} Cd(II), Tl(I), In(III) and Bi(III) and 58 μg L^{-1} Zn(II) and Pb(II) (thin line), 142 μg L^{-1} Zn(II), In(III) and 58 μg L^{-1} Cd(II), Pb(II), Bi(III) and Tl(I) (dashed thick line), 142 μg L^{-1} Tl(I) and In(III) and 58 μg L^{-1} Zn(II), Cd(II), Pb(II) and Bi(III) (dashed thin line). b) DPASV voltammograms of 100 μg L^{-1} Zn(II), Cd(II), Tl(I), Pb(II), In(III) and Bi(III) on Cys-SPCE-CNF (thin line), *ex-situ*-SbSPCE-CNF (dashed thin line), GSH-SPCE-CNF (dashed thick line) and SPCE-CNF (thick line) applying an E_d of −1,4 V during 120 s at acetate buffer pH 4.5.

variance explained by the first latent variable) and the resulting data were mean centred. The effect of OSC is that undesired variations of experimental data (eg, noise, baseline) are removed from the signal whereas variance attributed to target ions is retained. Because of the large amount of information generated (4 voltammograms for each sample), a hierarchical model was considered. In this sense, PLS-2 was performed on each working electrode processed signal, score values were combined in a new data matrix and PLS was performed again, but now in the modality of PLS-1 (Fig. 2b).

As it was previously mentioned, Zn(II), Cd(II) and Tl(I) peaks are overlapped in the left side of the voltammogram (from −1.4 V to −0.9 V) whereas Pb(II) and In(III) peaks appear from −0.9 V to −0.55 V and Bi(III) corresponds to the peak near −0.4 V. For this reason, although individual models were performed for each metal, PLS-2 models considering only Zn(II), Cd(II) and Tl(I), only Pb(II) and In(III) or only Bi(III) were performed on each sensor. The number of latent variables, pre-established by cross-validation (venetian blinds method), was selected considering the predictive ability for each metal ion separately and varied from 1 to 6 in the hierarchical step and from 2 to 3 in the final step depending on the considered metal.

Table 2
Selection of sensors used in the PLS model for each metal.

	Cd(II)	Pb(II)	Tl(I)	Bi(III)
SPCE-CNF	x	x	x	x
GSH-SPCE-CNF	x		x	x
Cys-SPCE-CNF	x	x		
Ex-situ-SbSPCE-CNF	x	x		

Table 3
Main parameters obtained for the fitted regression lines for the comparison between predicted *vs.* expected values for the training subset of samples and the different metal ions (ranges calculated at the 95% confidence level).

Metal	Slope	Intercept (μg L^{-1})	Correlation	RMSE (μg L^{-1})
Cd(II)	0.90 (0.05)	10 (5)	0.951	12.1
Pb(II)	0.93 (0.04)	8 (4)	0.931	10.7
Tl(I)	0.90 (0.05)	10 (5)	0.927	12.3
Bi(III)	0.92 (0.04)	8 (4)	0.949	11.8

RMSE: root mean square error.

Another important aspect to be considered is the number of electrodes to be used in each PLS model. In this sense, it was observed that adding two electrodes with similar sensitivities to the model increases the number of variables, and therefore the complexity of the model, but does not improve its performance. The electrodes used in the PLS model built for each metal are shown in Table 2. It should be pointed out that the inclusion of samples measured in different days on different units does not influence the building of the PLS model.

Good PLS models were obtained for Pb(II), Cd(II), Tl(I) and Bi(III) but not for In(III) and Zn(II). However, the presence of these metals in the sample does not hinder the calibration of PLS models for Pb(II), Cd(II), Tl(I) and Bi(III). The global performance of the models built is shown in Fig. 5 and Table 3. As it can be seen, calibration curves are close to the ideal one, with slopes and correlation values close to 1 and intercept values close to 0. Root mean square errors (RMSE) for calibration were also calculated and are shown in Table 3.

The predictive ability of each model was evaluated with the test subset. As it can be seen in the comparison graphs of predicted *vs.* expected concentration (Fig. 5), test samples (white symbols) are always in the variation range defined by the training set (black symbols). RMSE for prediction, 6.64 for Pb(II), 11.01 for Cd(II), 8.71 for Tl(I) and 14.8 for Bi(III), were all comparable to those obtained for calibration. It should be pointed out that, despite of the increased complexity of the considered system (4 analytes and 2 interferences), the obtained RMSEs values for prediction are similar to those reported by previous voltammetric electronic tongues for metal ions determination [22–25].

These results suggest that the combination of SPCE-CNF, *ex-situ*-SbSPCE-CNF, GSH-SPCE-CNF and Cys-SPCE-CNF as a sensor array could be used for the simultaneous determination of Cd(II), Pb(II), Tl(I) and Bi(III) in the presence of Zn(II) and In(III) in natural samples.

3.4. Application to the analysis of real samples

At the view of the above results, a sensor array formed by SPCE-CNF, *ex-situ*-SbSPCE-CNF, GSH-SPCE-CNF and Cys-SPCE-CNF was considered for the determination of Cd(II), Pb(II), Tl(I) and Bi(III) in the presence of Zn(II) and In(III) in real samples and its applicability was tested on a spiked tap water. Then, voltammetric stripping measurements of three replicates of the determination of the tap

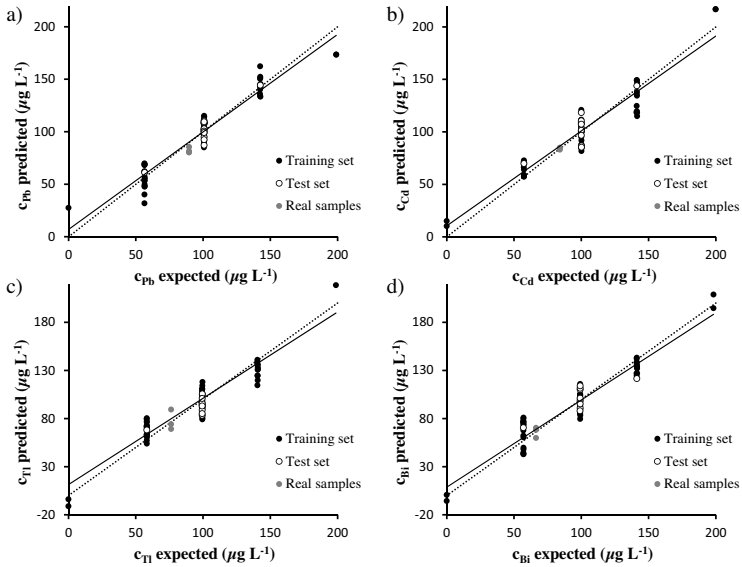

Fig. 5. Comparison graphs of predicted *vs.* expected concentrations for a) Pb(II), b) Cd(II), c) Tl(I) and d) Bi(III) for training set (●), test set (○) and real samples (●). Dashed line represents theoretical diagonal line (y = x).

Table 4
Total concentrations of Cd(II), Pb(II), Tl(I) and Bi(III) determined in tap water samples by DPASV on the multisensor array formed by SPCE-CNF/GSH-SPCE-CNF/Cys-SPCE-CNF/*Ex-situ*-SbSPCE-CNF modified electrodes and by ICP-MS.

		Cd(II)	Pb(II)	Tl(I)	Bi(III)
DPASV	c (μg L^{-1})	84.1	83.4	77.6	66.1
	RSD (%)	1.1	3.6	13.6	8.4
ICP-MS	c (μg L^{-1})	84.2	89.6	76.3	66.4
	RSD (%)	0.6	0.6	0.6	0.4

n = 3 for RSD (%).

water by means of the electronic tongue were carried out in the above mentioned conditions and voltammetric signals that behave equally to the training and test sets were obtained.

Cd(II), Pb(II), Tl(I) and Bi(III) concentrations were calculated from the previously calibrated PLS models. A good concordance of all metal ion concentrations between all replicates inferred by the obtained RSD(%) (Table 4) was achieved, especially in the case of Cd(II) and Pb(II). The obtained results, shown in Table 4, were also compared to those obtained by ICP-MS. In order to evaluate the agreement between each metal ion concentration obtained from both techniques, a two-tailed *t*-test (equal variances) was performed for each sample and it was concluded that the results obtained by the electronic tongue and ICP-MS were statistically similar for a confidence level of 95%.

Therefore, these good results confirm the applicability of the combination of SPCE-CNF, e*x-situ*-SbSPCE-CNF, GSH-SPCE-CNF and Cys-SPCE-CNF in a sensor array with a suitable PLS model for the simultaneous determination of Cd(II), Pb(II), Tl(I) and Bi(III) in the presence of Zn(II) and In(III) in real samples, being an interesting and cheaper alternative to more conventional techniques such as ICP-MS.

4. Conclusions

In this work, a voltammetric electronic tongue based completely on screen-printed electrodes has been successfully applied for the first time for the analysis of a complex mixture of metal ions in natural samples (4 analytes in the presence of 2 interferences). This electronic tongue was constituted by four sensors that have been modified following different strategies: SPCE-CNF, e*x-situ*-SbSPCE-CNF, GSH-SPCE-CNF and Cys-SPCE-CNF.

Firstly, the voltammetric performance of each metal on each electrode was studied and a cross-response between them was stated. Although the voltammetric response of the metal mixture of each sensor is very complex due to the presence of overlapped signals, the combination of the four modified SPEs as an electrode array configuration instead of as single sensors introduces some discrimination power that allows to elucidate the mixture of the considered metal ions. In this sense, in the present study, the simultaneous quantification of Cd(II), Pb(II), Tl(I) and Bi(III) in the presence of Zn(II) and In(III) was successfully carried out by combining the voltammetric responses from the four electrodes with chemometric tools. Hence, obtained DPASV data were processed by a PLS model that was built considering a hierarchical model in order to reduce the large amount of data. Good results, both for training and testing, inferred by correlation coefficients evaluated from pre-

dicted *vs.* expected concentrations were obtained. Moreover, the simultaneous determination of Cd(II), Pb(II), Tl(I) and Bi(III) in the presence of Zn(II) and In(III) in a spiked tap water was also satisfactory achieved, providing comparable results to those obtained by ICP-MS.

The reported results demonstrate that the use of the presented sensor array combined with the construction of an appropriate PLS model is suitable for the simultaneous quantification of Cd(II), Pb(II), Tl(I) and Bi(III) in the presence of Zn(II) and In(III) in environmental samples.

Acknowledgments

This work is supported by the Generalitat of Catalonia (Project 2014SGR269). Clara Pérez-Ràfols acknowledges the Spanish Ministry of Economy and Competitiveness for a Ph.D grant.

Appendix A. Supplementary data

Supplementary data associated with this article can be found, in the online version, at http://dx.doi.org/10.1016/j.snb.2017.04.165.

References

[1] I.D.L. Foster, S.M. Charlesworth, Heavy metals in the hydrological cycle: trends and explanation, Hydrol. Process. 10 (1996) 227–261.
[2] J. Barek, J. Zima, Eighty years of polarography-history and future, Electroanalysis 15 (2003) 467–472, http://dx.doi.org/10.1002/elan.200390055 http://onlinelibrary.wiley.com///abstract.
[3] M.I. Castro-González, M. Méndez-Armenta, Heavy metals: implications associated to fish consumption, Environ. Toxicol. Pharmacol. 26 (2008) 263–271, http://dx.doi.org/10.1016/j.etap.2008.06.001.
[4] J. Baby, J.S. Raj, E.T. Biby, P. Sankarganesh, M.V. Jeevitha, S.U. Ajisha, et al., Toxic effect of heavy metals on aquatic environment, Int. J. Biol. Chem. Sci. 4 (2010) 939–952, http://dx.doi.org/10.1111/j.1439-0507.2010.01876.x.
[5] S.E. Jorgensen, B. Fath, Encyclopedia of Ecology, vol. 1, Newnes, 2008.
[6] D. Mendil, Ö.F. Ünal, M. Tüzen, M. Soylak, Determination of trace metals in different fish species and sediments from the River Yeşilirmak in Tokat, Turkey, Food Chem. Toxicol. 48 (2010) 1383–1392, http://dx.doi.org/10.1016/j.fct.2010.03.006.
[7] H. Sereshti, Y. Entezari Heravi, S. Samadi, Optimized ultrasound-assisted emulsification microextraction for simultaneous trace multielement determination of heavy metals in real water samples by ICP-OES, Talanta 97 (2012) 235–241, http://dx.doi.org/10.1016/j.talanta.2012.04.024.
[8] B. Dai, M. Cao, G. Fang, B. Liu, X. Dong, M. Pan, et al., Schiff base-chitosan grafted multiwal led carbon nanotubes as a novel solid-phase extraction adsorbent for determination of heavy metal by ICP-MS, J. Hazard. Mater. 219–220 (2012) 103–110, http://dx.doi.org/10.1016/j.jhazmat.2012.03.065.
[9] J. Wang, Stripping Analysis: Principles, Instrumentation and Applications, VCH, Deerfield Beach, FL, 1985.
[10] I. Šinko, J. Doleal, Simultaneous determination of copper cadmium, lead and zinc in water by anodic stripping polarography, J. Electroanal. Chem. Interfacial Electrochem. 25 (1970) 299–306.
[11] S. Das, V. Kumar, M. Gupta, N. Singh, S.S. Assistant, N. Delhi, Simultaneous determination of zinc (Zn), cadmium (Cd) lead (Pb) and copper (Cu) in blood using differential- pulse anodic-stripping voltammetry, Int. J. Eng. Res. 4 (2015) 235–239.
[12] M. del Valle, Sensor arrays and electronic tongue systems, Int. J. Electrochem. 2012 (2012) 1–12, http://dx.doi.org/10.1155/2012/986025.
[13] J. Zeravik, A. Hlavacek, K. Lacina, P. Skládal, State of the art in the field of electronic and bioelectronic tongues – towards the analysis of wines, Electroanalysis 21 (2009) 2509–2520, http://dx.doi.org/10.1002/elan.200900285.
[14] P. Ciosek, W. Wróblewski, Sensor arrays for liquid sensing-electronic tongue systems, Analyst 132 (2007) 963–978, http://dx.doi.org/10.1039/b705107g.
[15] X. Cetó, N.H. Voelcker, B. Prieto-Simón, Bioelectronic tongues: new trends and applications in water and food analysis, Biosens. Bioelectron. 79 (2016) 608–626, http://dx.doi.org/10.1016/j.bios.2015.12.075.
[16] M. Esteban, C. Ariño, J.M. Díaz-Cruz, Chemometrics for the analysis of voltammetric data, TrAC—Trends Anal. Chem. 25 (2006) 86–92, http://dx.doi.org/10.1016/j.trac.2005.07.009.
[17] X. Cetó, F. Céspedes, M. del Valle, Comparison of methods for the processing of voltammetric electronic tongues data, Microchim. Acta. 180 (2013) 319–330, http://dx.doi.org/10.1007/s00604-012-0938-7.
[18] Y. Tahara, K. Toko, Electronic tongues –a review, IEEE Sens. J. 13 (2013) 3001–3011.
[19] M. del Valle, Electronic tongues employing electrochemical sensors, Electroanalysis 22 (2010) 1539–1555, http://dx.doi.org/10.1002/elan.201000013.
[20] F. Winquist, Voltammetric electronic tongues – Basic principles and applications, Microchim. Acta 163 (2008) 3–10, http://dx.doi.org/10.1007/s00604-007-0929-2.
[21] A. Gutés, F. Céspedes, M. del Valle, Electronic tongues in flow analysis, Anal. Chim. Acta 600 (2007) 90–96, http://dx.doi.org/10.1016/j.aca.2007.03.039.
[22] N. Serrano, B. Prieto-Simón, X. Cetó, M. del Valle, Array of peptide-modified electrodes for the simultaneous determination of Pb(II), Cd(II) and Zn(II), Talanta 125 (2014) 159–166, http://dx.doi.org/10.1016/j.talanta.2014.02.052.
[23] N. Serrano, A. González-Calabuig, M. del Valle, Crown ether-modified electrodes for the simultaneous stripping voltammetric determination of Cd(II), Pb(II) and Cu(II), Talanta 138 (2015) 130–137, http://dx.doi.org/10.1016/j.talanta.2015.01.044.
[24] A. González-Calabuig, D. Guerrero, N. Serrano, M. del Valle, Simultaneous voltammetric determination of heavy metals by use of crown ether-modified electrodes and chemometrics, Electroanalysis 28 (2016) 663–670, http://dx.doi.org/10.1002/elan.201500512.
[25] C. Pérez-Ràfols, N. Serrano, J.M. Díaz-Cruz, C. Ariño, M. Esteban, Simultaneous determination of Tl(I) and In(III) using a voltammetric sensor array, Sens. Actuators B Chem. 245 (2017) 18–24, http://dx.doi.org/10.1016/j.snb.2017.01.089.
[26] N. Serrano, A. Alberich, J.M. Díaz-Cruz, C. Ariño, M. Esteban, Coating methods, modifiers and applications of bismuth screen-printed electrodes, TrAC—Trends Anal. Chem. 46 (2013) 15–29, http://dx.doi.org/10.1016/j.trac.2013.01.012.
[27] N. Serrano, J.M. Díaz-Cruz, C. Ariño, M. Esteban, Antimony- based electrodes for analytical determinations, TrAC—Trends Anal. Chem. 77 (2016) 203–213, http://dx.doi.org/10.1016/j.trac.2016.01.011.
[28] D. Bélanger, J. Pinson, Electrografting: a powerful method for surface modification, Chem. Soc. Rev. 40 (2011) 3995–4048, http://dx.doi.org/10.1039/c0cs00149j.
[29] J. Barton, M.B.G. García, D.H. Santos, P. Fanjul-Bolado, A. Ribotti, M. McCaul, et al., Screen-printed electrodes for environmental monitoring of heavy metal ions: a review, Microchim. Acta. 183 (2016) 503–517, http://dx.doi.org/10.1007/s00604-015-1651-0.
[30] M. Li, Y.T. Li, D.W. Li, Y.T. Long, Recent developments and applications of screen-printed electrodes in environmental assays-a review, Anal. Chim. Acta 734 (2012) 31–44, http://dx.doi.org/10.1016/j.aca.2012.05.018.
[31] J.P. Metters, R.O. Kadara, C.E. Banks, New directions in screen printed electroanalytical sensors: an overview of recent developments, Analyst 136 (2011) 1067–1076, http://dx.doi.org/10.1039/c0an00894j.
[32] O.D. Renedo, M.A. Alonso-Lomillo, M.J.A. Martínez, Recent developments in the field of screen-printed electrodes and their related applications, Talanta 73 (2007) 202–219, http://dx.doi.org/10.1016/j.talanta.2007.03.050.
[33] K. Duarte, C.I.L. Justino, A.C. Freitas, A.M.P. Gomes, A.C. Duarte, T.A.P. Rocha-Santos, Disposable sensors for environmental monitoring of lead, cadmium and mercury, TrAC—Trends Anal. Chem. 64 (2015) 183–190, http://dx.doi.org/10.1016/j.trac.2014.07.006.
[34] C. Pérez-Ràfols, N. Serrano, J.M. Díaz-Cruz, C. Ariño, M. Esteban, New approaches to antimony film screen-printed electrodes using carbon-based nanomaterials substrates, Anal. Chim. Acta 916 (2016) 17–23, http://dx.doi.org/10.1016/j.aca.2016.03.003.
[35] C. Pérez-Ràfols, N. Serrano, J.M. Díaz-Cruz, C. Ariño, M. Esteban, Glutathione modified screen-printed carbon nanofiber electrode for the voltammetric determination of metal ions in natural samples, Talanta 155 (2016) 8–13, http://dx.doi.org/10.1016/j.talanta.2016.04.011.
[36] C. Barceló, N. Serrano, C. Ariño, J.M. Díaz-Cruz, M. Esteban, Ex-situ antimony screen-printed carbon electrode for voltammetric determination of Ni(II)-ions in wastewater, Electroanalysis 28 (2016) 640–644, http://dx.doi.org/10.1002/elan.201500511.
[37] S. Wold, H. Antti, F. Lindgren, J. Öhman, Orthogonal signal correction of near-infrared spectra, Chemom. Intell. Lab. Syst. 44 (1998) 175–185.
[38] S. Wold, J. Trygg, A. Berglund, H. Antti, Some recent developments in PLS modeling, Chemom. Intell. Lab. Syst. 51 (2001) 131–150.
[39] Matlab, Version, r2008b ed., Mathworks Inc., Natick, MA, USA, 2008.
[40] PLS-toolbox Version 7.8.2, Eigenvector Research Inc., Wenatchee, USA, 2017.
[41] Guidelines for Drinking-water Quality, 4th ed., World Health Organization, Geneva, Switzerland, 2011.

Biographies

Clara Pérez-Ràfols was born 1992. She graduated in Chemistry with highest honors at the University of Barcelona (UB) in 2014 and received her Master's degree in Analytical Chemistry in 2015, also from the University of Barcelona. She is currently doing her Ph.D. in the area of Analytical Chemistry and Environment in the UB, focusing on the development of sensors and voltammetric electronic tongues for the simultaneous determination of several metal ions. She has published 11 research works in indexed journals.

Núria Serrano was born in 1977. She is temporary Senior Lecturer at the Department of Chemical Engineering and Analytical Chemistry, University of Barcelona (UB), Spain. In 2007 she completed the Ph.D. at the same University. As a postdoc-

toral researcher, she worked for one year at the Department of Chemistry (Masaryk University, Brno) in 2010; and she spent nine months at the Sensors and Biosensors group (Autonomous University of Barcelona, Bellaterra) in 2013. Her research is mainly focussed on the development of sensors and voltammetric electronic tongues, based on screen-printed electrodes, for the determination of heavy metals. She has participated in 9 competitive research projects, has supervised 2 Ph.D. Theses and has published more than 45 research works in indexed journals.

José Manuel Díaz Cruz was born in 1965. Since 1995 he is Associate Professor of the Department of Chemical Engineering and Analytical Chemistry of the University of Barcelona (UB), Spain, where he had obtained the Ph.D. degree in 1992. In 1993 worked for one year in the Department of Physical and Colloid Chemistry (Wageningen University, The Netherlands). His main research contributions have been in the field of electroanalytical chemistry, studying: i) the interactions of metal ions with macromolecular ligands, colloidal particles and sulphur-containing compounds; ii) the influence of adsorption phenomena in voltammetric measurements; iii) the application of chemometric methods to electroanalytical data and iv) the development of sensors based on screen-printed electrodes. He has participated in 22 competitive research projects, has supervised 8 Ph.D. Theses and has published more than 130 research works in indexed journals.

Cristina Ariño was born in 1956. Nowadays, she is Associate Professor of the Department of Chemical Engineering and Analytical Chemistry at the University of Barcelona (UB), Spain. She obtained the Ph.D. degree in 1986 and was appointed Associate Professor in 1987. She has participated in more than 20 competitive research projects, has supervised 8 Ph.D. Theses and has published more than 130 research works in indexed journals. Being her research contributions in the field of electroanalytical chemistry, studying: (i) the interactions of metal ions with macromolecular ligands, particles, and sulfur-containing compounds; (ii) the influence of adsorption phenomena in voltammetric measurements; (iii) the application of chemometric methods to voltammetric data concerning solution equilibria; (iv) development and applications of sensors based in screen-printed technology; and (v) the possibilities of screen printed electrodes in amperometric detection. She has also contributed in teaching electroanalytical courses in different master programs from the Faculty of Pharmacy of the University of Concepción (Chile), from the Faculty of Chemistry of the University of Santiago de Chile (Chile) and in different editions of an European Joint Master in Quality in Analytical Laboratories.

Miquel Esteban was born in 1955. He is Professor at the Department of Chemical Engineering and Analytical Chemistry, University of Barcelona (UB), Spain. He obtained the Ph.D. at UB, and was appointed Associate Professor in 1984 and Full Professor in 1993. Stays abroad: Institut für Angewandte Physikalische Chemie (Kernforschungsanlage, KFA, Jülich, Germany) in 1986; Department of Physical and Colloid Chemistry (Wageningen Agricultural University, Wageningen, Netherlands) in 1987; EC Scientific Visitor at the Institute for Reference Materials and Measurements (IRMM) in the Joint Research Centre (Geel, Belgium) in 1994 and 1997; European Synchroton Radiation Facility (ESRF, Grenoble, France) in 1999. Academic responsibilities: Secretary of the Faculty of Chemistry (1987–1991), Vice-President of the Division of Experimental Sciences and Mathematics (2000–2003), Head of the Department of Analytical Chemistry (2004–2008) and of Chemical Engineering and Analytical Chemistry (2016-) and member of UB government council (2004–2008). His main research contributions have been in the field of electroanalytical chemistry, studying: i) the interactions of metal ions with macromolecular ligands and sulphur-containing compounds; ii) the influence of adsorption phenomena in voltammetric measurements; and iii) the application of chemometric methods to voltammetric data concerning solution equilibria; iv) development and applications of sensors based in screen-printed technology. He has participated in more than 20 competitive research projects, has supervised 5 Ph.D. Theses and has published more than 170 research works in indexed journals.

A new multivariate standard addition strategy for stripping voltammetric electronic tongues: Application to the determination of Tl(I) and In(III) in samples with complex matrices.

C. Pérez-Ràfols, J. Puy-Llovera, N. Serrano, C. Ariño, M. Esteban, J. M. Díaz-Cruz

Talanta 192 **(2019)** 147-153

https://doi.org/10.1016/j.talanta.2018.09.035

Talanta 192 (2019) 147–153

Contents lists available at ScienceDirect

Talanta

journal homepage: www.elsevier.com/locate/talanta

A new multivariate standard addition strategy for stripping voltammetric electronic tongues: Application to the determination of Tl(I) and In(III) in samples with complex matrices

Clara Pérez-Ràfols, Jaume Puy-Llovera, Núria Serrano*, Cristina Ariño, Miquel Esteban, José Manuel Díaz-Cruz

Departament d'Enginyeria Química i Química Analítica, Facultat de Química, Universitat de Barcelona, Martí i Franquès 1-11, E–08028 Barcelona, Spain

ARTICLE INFO

Keywords:
Sensor array
Multivariate standard addition
Partial least squares (PLS) calibration
Matrix effect
Anodic striping voltammetry

ABSTRACT

A new multivariate standard addition strategy applicable to stripping methods was proposed as an extention of the classical univariate standard addition method for the resolution of complex samples involving overlapped peaks and complex matrices. The proposed strategy consists in alternate additions of the considered analytes and the further extrapolation to a simulated blank solution measured by skipping the preconcentration step (deposition time = 0). This calibration approach was successfully tested in tonic water samples spiked with Tl(I) and In(III) using a sensor array based on a SeCyst-SPCNFE and an *ex-situ*-BiSPCE, providing good concordance between replicates and much better accuracy than the usual multivariate external calibration method.

1. Introduction

Analytical determinations based on instrumental analysis require the use of calibration methods. When univariate instrumental responses are involved, three well-known calibration methods can be used [1,2]: external standard, standard addition and internal standard.

All these methods can be easily applied in samples involving one analyte or several analytes as far as they do not interfere with each other. However, when there are interactions between species and/or overlapped signals the application of these univariate methodologies is hindered and it is necessary to use multivariate strategies that include a data treatment based on chemometric techniques such as Partial Least Squares (PLS) [3].

Regarding voltammetric measurements, in the last two decades the use of sensor arrays or electronic tongues has been popularized for the resolution of complex samples [4,5]. These devices are based on the use of sensors with reduced selectivity, grouped in arrays with cross-response characteristics. This strategy is usually coupled to an external calibration that involves an experimental design with both a set of training samples to build a calibration model and a set of test samples to validate such calibration model. Once the model has been validated, it can be later applied to predict the concentration of the analytes in unknown samples, essentially by interpolation. This strategy would be the multivariate analog to the external standard univariate method and has been extensively applied in numerous works [6–10]. It usually provides good results for calibration, validation and prediction of unknown samples, which share the same matrix, but presents problems when complex samples are analysed. In these cases, the use of matrix matched standard, where the matrix sample is simulated, can be useful [11]. However, the reconstruction of the matrix sample is not always straightforward and obtaining a blank sample (without analytes) is not possible. Therefore the application of matrix matching methods cannot be easily generalized. In voltammetric univariate measurements matrix problems are solved by the use of the standard addition method. Since the early years of Chemometrics, several approaches have been proposed to attempt the extrapolation of the standard addition method to the multivariate analysis. Kowalski and coworkers [12–14] developed the generalized standard addition method (GSAM) based on the classical least-squares calibration (CLS) of a 'signal increase' matrix where the spectra of the sample was subtracted from the original spectra of the successive standard additions [15–18]. An improved PLS version of GSAM was later proposed [19]. However, the use of the GSAM decayed along the 1990's when the study of second order data grabbed the attention of multivariate standard addition strategies [20–23]. Another approach proposed by Melucci and Locatelli [24] was based on the direct application of PLS to the sample voltammograms before and after the additions, the construction of a calibration model related to added concentrations and the extrapolation to a blank voltammogram for the

* Corresponding author.
E-mail address: nuria.serrano@ub.edu (N. Serrano).

https://doi.org/10.1016/j.talanta.2018.09.035
Received 13 July 2018; Received in revised form 5 September 2018; Accepted 11 September 2018
Available online 12 September 2018
0039-9140/

prediction of the concentration of the target analyte. However, this method was never applied to the determination of more than one analyte. More recently, our group extended this approach to multicomponent analysis [25]. It should be pointed out that this method requires the extrapolation to the voltammogram of a blank solution. However, obtaining this 'true blank solution' is not so easy in real complex samples already containing the analyte, since it is really difficult, if not impossible, to remove analytes from such real samples without altering their matrix. In techniques like differential pulse voltammetry (DPV), there are not many solutions available for that. A compromise strategy would be to find unpolluted samples of similar matrix to these under study. In contrast, techniques involving the preconcentration of the analyte such as anodic stripping voltammetry (ASV) present much more possibilities in this sense, since the deposition time is a key parameter, which can help to simulate the voltammogram of a hypothetic "true blank" solution (that is not possible to obtain or prepare) from the measurement of the real sample at deposition time zero. This idea is based on the fact that the overall stripping signal is essentially the sum of a first component consisting in the capacitive currents caused by the scan and a second one including the faradaic currents of the analytes that are accumulated on and stripped from the electrode. Eventually, the first component can also include some faradaic currents from oxidations and reductions of the matrix not involved in accumulation/stripping processes. From this fact, a hypothesis is made assuming that a decrease in the deposition time practically does not affect the first component but it causes a decrease in the second component comparable to the effect of a decrease in the concentration of the analytes in the solution. In the limiting case of deposition time tending to zero, the voltammogram would consist only on the first component and, hence, should be very similar to that obtained at non-zero deposition time in the absence of analytes in the solution, *i.e.*, in the measurement of a blank.

Thus, in the present paper we propose a methodology where, in order to simulate this 'true blank solution' in ASV measurements, the deposition step is skipped (deposition time, $t_d = 0$) to avoid the accumulation of the target analytes on the electrode surface. For this purpose, we have chosen typical analytes usually determined by ASV, *i.e.* trace metal ions. Specifically we have considered the simultaneous determination of Tl(I) and In(III) in a spiked tonic water solution (as an example of a complex food matrix sample) using a sensor array based on a bismuth film screen-printed carbon electrode (BiSPCE) and a selenocystine modified screen-printed carbon nanofiber electrode (SeCyst-SPCNFE). These sensors, which have been proved to provide good results for metal ion determination [26,27], were chosen for this array due to their cross-response. This experimental system was selected to compare this novel multivariate standard addition calibration method with the more common multivariate external calibration used for electronic tongues (Fig. 1).

2. Experimental section

2.1. Chemicals and solutions

4-aminobenzoic acid (ABA), selenocystine, N-hydroxysulfosuccinimide (sulfo-NHS) and sodium nitrite were supplied by Sigma-Aldrich (St. Louis, MO, USA). 2-(N-morpholino)-ethanesulfonic (MES), potassium ferrocyanide $K_4[Fe(CN)_6]\cdot 3H_2O$, sodium acetate and acetic acid were obtained from Merck (Darmstadt, Germany). Potassium ferricyanide $K_3[Fe(CN)_6]$ and ethanol were provided by Panreac (Barcelona, Spain). N-(3-dimethylaminopropyl)-N′-ethylcarbodiimide hydrochloride (EDC) was purchased from AppliChem (Darmstadt, Germany). All reagents were of analytical grade and ultrapure water (Milli-Q plus 185 system, Millipore) was used in all experiments.

Bi(III) and In(III) 1.000 g L^{-1} atomic absorption standard solutions were supplied by Fluka. Tl(I) stock solutions 10^{-3} mol L^{-1} were prepared from TlCl, supplied by Sigma-Aldrich, and stock solution concentrations were determined by ICP-MS.

Tonic water samples were purchased in local supermarkets.

2.2. Instrumentation

An Autolab System PGSTAT12 (EcoChemie, The Netherlands), in its multichannel configuration and using GPES Multichannel 4.7 software package (EcoChemie) was used to perform differential pulse anodic stripping voltammetric (DPASV) measurements.

Ag|AgCl|KCl (3 mol L^{-1}) and Pt wire were used as reference and auxiliary electrodes respectively. A selenocystine modified electrode prepared from a commercial carbon nanofiber modified screen-printed electrode (SeCyst-SPCNFE) and an *ex-situ* bismuth film prepared from a commercial carbon screen-printed electrode (*ex-situ*-BiSPCE) were used as working electrodes. Both carbon and carbon nanofiber screen-printed electrodes (ref. 110, DS SPCE and ref. 110CNF, DS SPCE respectively) were of 4 mm diameter and were purchased from DropSens (Oviedo, Spain). These screen-printed electrodes were connected to the Autolab System by means of flexible cables (ref. CAC, DropSens).

pH measurements were performed using a Crison micro pH 2000 pH-meter.

All measurements were carried out at room temperature (20 °C) and a purified nitrogen atmosphere (Linde N50) was used for the bismuth film preparation.

2.3. Preparation of modified SPEs

2.3.1. Selenocystine modified electrode (SeCyst-SPCNFE)

Selenocystine was immobilized on the surface of a SPCNFE following a procedure previously reported [26]. Briefly, $NaNO_2$ 0.2 mmol L^{-1} was added to a cooled solution of ABA 73 mmol L^{-1} in HCl 1 mol L^{-1} for the *in-situ* generation of the aryl diazonium salt. After 5 min of stirring in an ice bath, 10 µL of the resulting solution were dropped onto the electrode surface and the electrochemical grafting process was performed by applying 10 cyclic voltammetric cycles from 0 V to −1 V at 0.2 V s^{-1}. Then, to activate the generated carboxylic groups, the electrodes were incubated for 1 h with 10 µL of a 26 mmol L^{-1} EDC and 35 mmol L^{-1} sulfo-NHS solution in 100 mmol L^{-1} MES buffer (pH 4.5). Finally, the activated groups reacted over night with the amine terminal groups of selenocystine (94 mmol L^{-1} in ethanol absolute) at 4 °C.

2.3.2. Ex-situ bismuth film electrode (ex-situ-BiSPCE)

The deposition of the bismuth film was based on a procedure previously reported [28]. The SPCE, the auxiliary and the reference electrodes were immersed in a solution of 0.2 mol L^{-1} acetate buffer (pH 4.5) containing 100 mg L^{-1} Bi(III). After 10 min of deaeration, a deposition potential (E_d) of −0.80 V was applied with stirring for 300 s, followed by a rest period of 20 s, without stirring.

2.4. Voltammetric measurements

DPASV measurements of Tl(I) and In(III) using a sensor array based on SeCyst-SPCNFE and *ex-situ*-BiSPCE were carried out applying a deposition potential (E_d) of −1.30 V during a deposition time (t_d) of 120 s with stirring, followed by a rest period (t_r) of 5 s, and scanning the potential from −1.30 V to −0.65 V, using a step potential of 5 mV, pulse times of 50 ms, pulse amplitudes of 100 mV and a scan rate of 10 mV s^{-1}.

Individual calibration plots were obtained increasing Tl(I) or In(III) concentrations in 0.1 mol L^{-1} acetate buffer solution (pH 4.5).

For tonic water samples determinations, two different calibration strategies, multivariate external calibration and multivariate standard addition, were explored (Fig. 1).

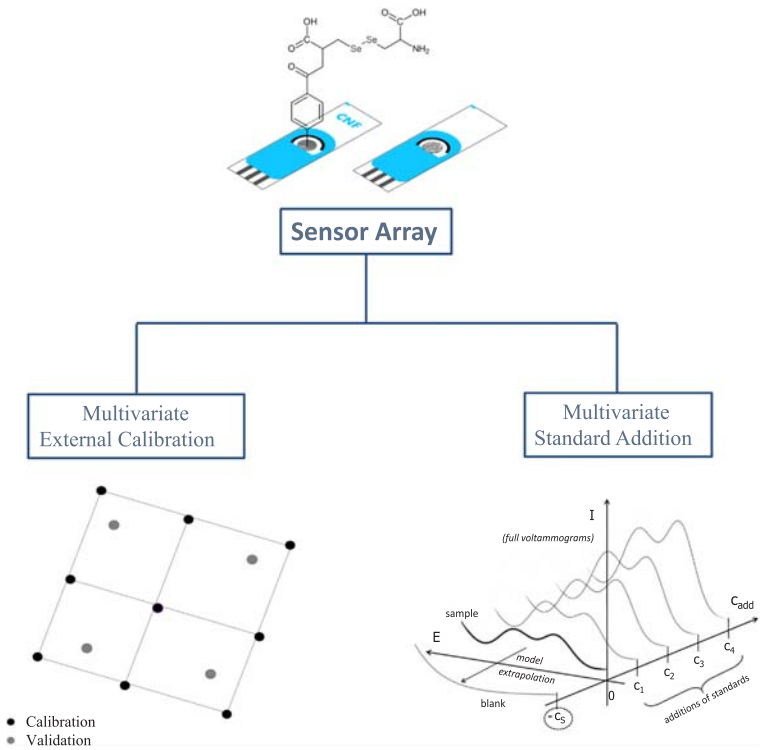

Fig. 1. Scheme of the different multivariate calibration strategies used.

2.4.1. Multivariate external calibration

For the multivariate external calibration a set of 9 training samples and 5 validation samples was used in which training samples were distributed in a square design and validation samples along the experimental domain (Table 1). These samples were prepared in acetate buffer (pH 4.5) by appropriate dilution of stock solutions. For the determination of Tl(I) and In(III) in spiked tonic water samples three replicates were considered.

Table 1
Concentration values, in $\mu g\,L^{-1}$, for the samples included in the training and test subsets.

Tl(I)	In(III)
Training subset	
19.9	58.9
38.9	112.0
59.0	174.9
73.1	38.9
93.1	93.1
112.2	156.0
136.0	20.2
156.0	73.1
174.9	135.9
Test subset	
51.1	67.0
115.9	82.0
82.2	129.2
129.0	35.9
144.0	144.0

In order to eliminate the remaining bound metals, both working electrodes were cleaned by applying a cleaning potential of −0.30 V during 15 s in 0.1 mol L^{-1} $HClO_4$ after each measurement. This potential was selected as the highest potential that can be used without oxidising the bismuth film.

2.4.2. Multivariate standard addition

For the multivariate standard addition the spiked tonic water diluted with acetate buffer (pH 4.5) was placed in the cell. Prior to starting the calibration curves, blank measurements were simulated by scanning twice the sample without the application of a deposition time (t_d = 0).

The calibration curves were performed using the above-mentioned DPASV conditions (E_d = −1.30 V, t_d = 120 s). Firstly, three replicates of the initial sample were measured and then alternate additions of Tl(I) and In(III) solutions were carried out.

Three replicates of this calibration strategy were performed for the spiked tonic water sample, using a new set of electrodes for each replicate.

2.5. Sample preparation

Tonic water samples were spiked with 100 $\mu g\,L^{-1}$ of Tl(I) and 225 $\mu g\,L^{-1}$ of In(III). Voltammetric measurements were carried out after dilution of the spiked tonic water sample with acetate buffer at pH 4.5 (dilution factor 1:2).

2.6. Data processing

In order to build data matrices, DPASV measurements using both SeCyst-SPCNFE and *ex-situ*-BiSPCE were considered. Firstly, different pre-processing steps were performed, including baseline correction, derivative gap-segment (the derivative is calculated using multiple points instead of two adjacent points) and autoscale. These pre-processed data were used for the PLS models built in both calibration methods.

For the multivariate external calibration, PLS1 models were constructed using Tl(I) or In(III) concentrations present on each calibration sample. For both Tl(I) and In(III) models 4 latent variables (LV) were selected.

For the multivariate standard addition, PLS1 models were constructed using Tl(I) and In(III) standard added concentrations. 5 and 3 LVs were selected for Tl(I) and In(III) PLS1 models respectively.

Data pre-processment, variable selection and construction of PLS model were performed using Matlab® [29] with PLS-toolbox [30].

3. Results and discussion

It is well-known that the voltammetric simultaneous determination of Tl(I) and In(III) is problematic due to their overlapped stripping signals. In a previous study [9], it was concluded that one working electrode was not enough for the resolution of this system whereas the use of a sensor array based on two electrodes with cross-response provided much better results, allowing the simultaneous determination of both metal ions in synthetic and spiked tap water samples.

In this work a sensor array based on a SeCyst-SPCNFE and an *ex-situ*-BiSPCE was selected to study the resolution of this system in samples with stronger matrix effect. In order to study the cross-response between these two sensors, individual calibrations of Tl(I) and In(III) were carried out for each sensor. Firstly, the E_d was optimized to -1.30 V to ensure the best separation between Tl(I) and In(III) peaks. Then, twelve standard solutions of increasing concentration ranging from 1.1 to 200.0 $\mu g\,L^{-1}$ of either Tl(I) or In(III) were measured, obtaining well-defined peaks in all cases (data not shown). Calibration data for both sensors are reported in Table 2. As it can be observed, good linear responses were achieved for both sensors in all the concentration range considered, with limits of detection (LOD), calculated as 3 times the standard deviation of the intercept over the slope of the calibration curve, at the level of a few $\mu g\,L^{-1}$ and slightly lower in the case of *ex-situ*-BiSPCE. Regarding sensitivities, which were obtained from the slopes of the calibration curves, higher sensitivities were achieved with *ex-situ*-BiSPCE, especially for In(III), and a cross-selectivity was obtained between both sensors since SeCyst-SPCNFE is more sensitive to Tl(I) than In(III) and *ex-situ*-BiSPCE is more sensitive to In(III) than Tl(I). Therefore, the sensor array based on SeCyst-SPCNFE and *ex-situ*-BiSPCE presents the cross-response required for the simultaneous determination of Tl(I) and In(III).

Table 2
Calibration data for the individual determination of Tl(I) and In(III) on SeCyst-SPCNFE and *ex-situ*-BiSPCE at E_d of -1.30 V, t_d of 120 s and pH 4.5. The standard deviations are denoted by parenthesis.

	SeCyst-SPCNFE		*Ex-situ*-BiSPCE	
	Tl(I)	In(III)	Tl(I)	In(III)
Sensitivity (nA μg^{-1} L)	3.02 (0.05)	2.11 (0.03)	3.91 (0.03)	8.40 (0.07)
R^2	0.999	0.999	0.999	0.999
Linear range ($\mu g\,L^{-1}$)[a]	14.8–200.0	14.1–200.0	7.0–200.0	8.0–200.0
LOD ($\mu g\,L^{-1}$)	4.5	4.2	2.1	2.4

[a] The lowest value of the linear range was considered from the LOQ.

3.1. Multivariate external calibration

A PLS model was built in order to simultaneously determine Tl(I) and In(III) using the considered sensor array. With this aim, the above mentioned training and test subsets were taken into account (Table 1). The concentration range considered was 19.9–174.9 $\mu g\,L^{-1}$ for Tl(I) and 20.2–174.9 $\mu g\,L^{-1}$ for In(III).

Considering that data pretreatment plays a key role in the building of a PLS model, voltammograms were firstly smoothed and baseline corrected with automatic weighted least squares (AWLS). The resulting voltammograms for SeCyst-SPCNFE and *ex-situ*-BiSPCE are shown in Figs. 2A and 2B respectively. Then the data were derived using gap-segment function and autoscaled. PLS1 models for the determination of Tl(I) and In(III) were built from these pretreated data. Figs. 3A and 3B show the comparison graphs between predicted *vs* expected concentration of Tl(I) and In(III) respectively and general parameters of the regression lines including slopes, intercepts, correlation coefficients and the root mean square errors (RMSE) for both training and test subsets are summarized in Table 3. Good results were achieved for target metal ions for both training and test subsets, with intercepts close to 0, slopes and correlation coefficients close to one and small RMSE values.

After the successful calibration and validation of the system, these models were applied for the simultaneous determination of Tl(I) and In (III) in spiked tonic water samples. As it can be observed in Fig. 3 and Table 4, the concordance between samples, inferred by the provided RSD (%), was good for both studied metal ions. However, the accuracy of the results, inferred by the relative error (%), is very poor, particularly in the case of In(III). This lack of accuracy could be attributed to the sample matrix effect. As it can be seen in Fig. 2, the tonic water voltammograms (thick lines) present a different behaviour than calibration or validation samples prepared in acetate buffer (thin lines), *i.e.* lower signals for similar concentrations and shifted potentials, which cause different overlapping of peaks (higher overlapping in the case of SeCyst-SCPNFE and lower overlapping for *ex-situ*-BiSPCE).

These results differ from previously reported studies [9], where the use of a sensor array coupled to PLS models could successfully predict Tl(I) and In(III) concentrations in tap water. This fact could be attributed to the higher complexity of the matrix in the sample here considered. Hence, this external calibration strategy provides successful results when simple real samples, where analytes behave similar to calibration and validation samples, are studied; whereas more complex matrix samples, which affect the analytes behaviour, lead to poor results.

3.2. Multivariate standard addition

As it was mentioned above, the use of multivariate external calibration does not allow the simultaneous determination of Tl(I) and In (III) in samples with complex matrices. Therefore in this work a novel calibration strategy, multivariate standard addition, was pioneeringly applied for the resolution of this system by stripping voltammetry. Figs. 4A and 4B show the DPASV measurements resulting from the application of this calibration approach on both SeCyst-SPCNFE and *ex-situ*-BiSPCE respectively.

The proposed strategy requires the measurement of a “true blank” solution, which usually is difficult to obtain in samples that already contain the target analytes but, as discussed before, can be simulated in accumulation methods like stripping voltammetry, by measuring at zero deposition time. In this sense, a blank voltammogram was firstly simulated using the considered sensor array by scanning the spiked tonic water sample from -1.30 V to -0.65 V without any deposition step ($t_d = 0$) (grey lines in Fig. 4). With the removal of the deposition step, the deposition of Tl(I) and In(III) on the electrode surface is avoided but the matrix sample effect is still considered. It should be pointed out the importance of this simulated blank voltammogram since it will be used as target of the subsequent PLS model. For this

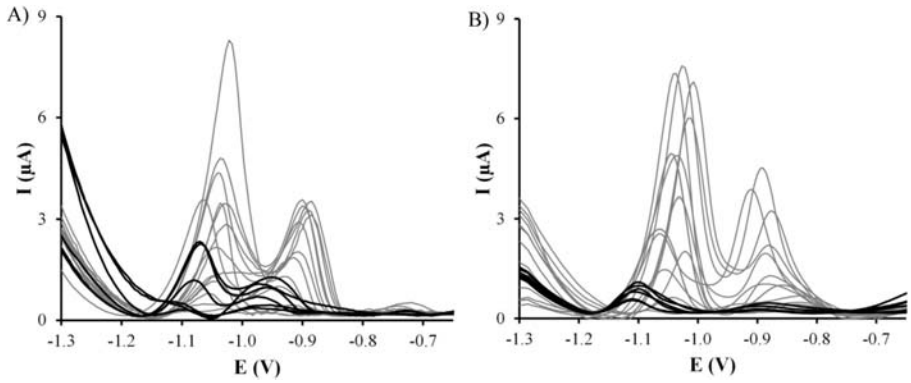

Fig. 2. DPASV voltammograms on SeCyst-SPCNFE (A) and *ex-situ*-BiSPCE (B) in acetate buffer at pH 4.5, t_d of 120 s and an E_d of − 1.30 V of the calibration and validation samples used for the multivariate external calibration (thin lines) of Tl(I) and In(III) and tonic water samples spiked with different concentrations of these metal ions (thick lines).

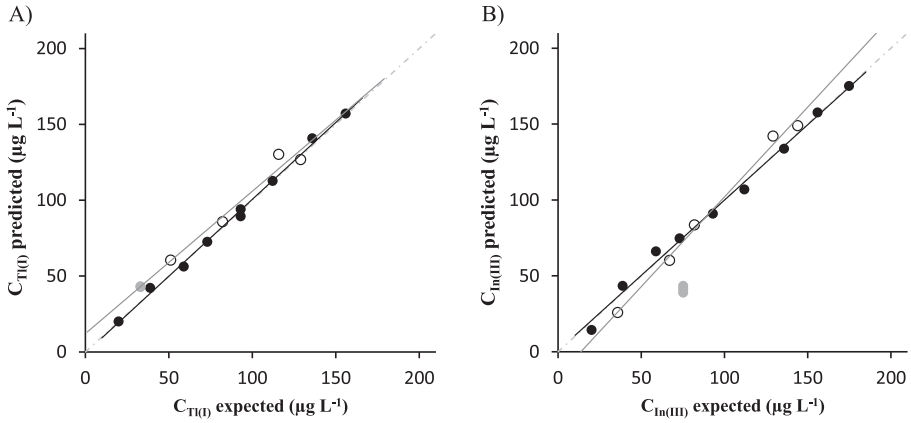

Fig. 3. Comparison graphs of predicted vs. expected concentrations obtained with the sensor array for Tl(I) (A) and In(III) (B) for training set (●,——), test set (○,——) and spiked tonic water samples (●). Dashed line represents theoretical diagonal line (y = x).

Table 3
Main parameters of the regression lines obtained in the comparison between predicted vs. expected values of the training and test subsets for In(III) and Tl(I) (ranges calculated at the 95% confidence level) for the sensor array. The standard deviations are denoted by parenthesis.

	In(III)	Tl(I)
Training set		
Slope	0.99 (0.03)	1.00 (0.02)
Intercept (μg L^{-1})	1 (3)	0 (2)
R^2	0.993	0.997
RMSE[a] (μg L^{-1})	4.05	2.62
Test set		
Slope	1.18 (0.06)	0.9 (0.1)
Intercept (μg L^{-1})	−16 (6)	12 (14)
R^2	0.993	0.959
RMSE[a] (μg L^{-1})	8.25	8.81

[a] RMSE: root mean square error.

Table 4
Total concentrations of Tl(I) and In(III) determined in tonic water samples by DPASV on the multisensor array formed by SeCyst-SPCNFE / *ex-situ*-BiSPCE modified electrodes using the multivariate external calibration and the multivariate standard addition method.

	Expected	Multivariate external calibration	Multivariate standard addition
Thallium(I)			
c (μg L^{-1})	33.1	43.0	33.0
RSD (%)	–	0.3	7.1
Relative error (%)	–	29.7	0.5
Indium(III)			
c (μg L^{-1})	75.1	41.1	73.4
RSD (%)	–	3.2	1.7
Relative error (%)	–	45.3	2.3

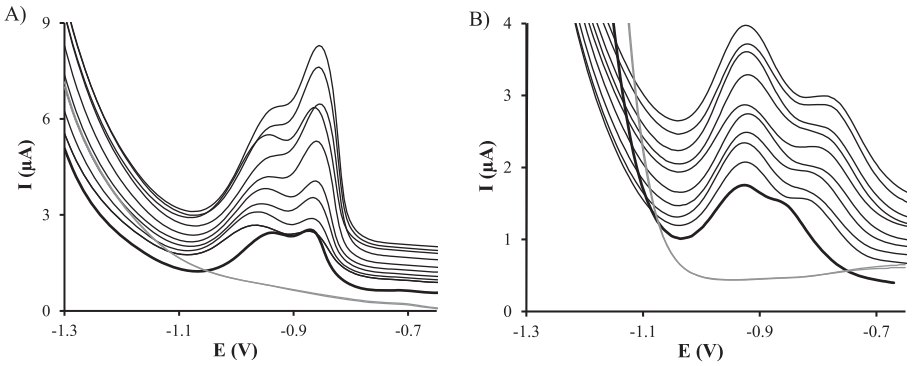

Fig. 4. DPASV voltammograms on SeCyst-SPCNFE (A) and *ex-situ*-BiSPCE (B) applying a t_d of 120 s and an E_d of − 1.30 V of the spiked tonic water sample (thick line), the subsequent alternate Tl(I) and In(III) additions (thin lines) and the simulated blank at t_d = 0 (grey line).

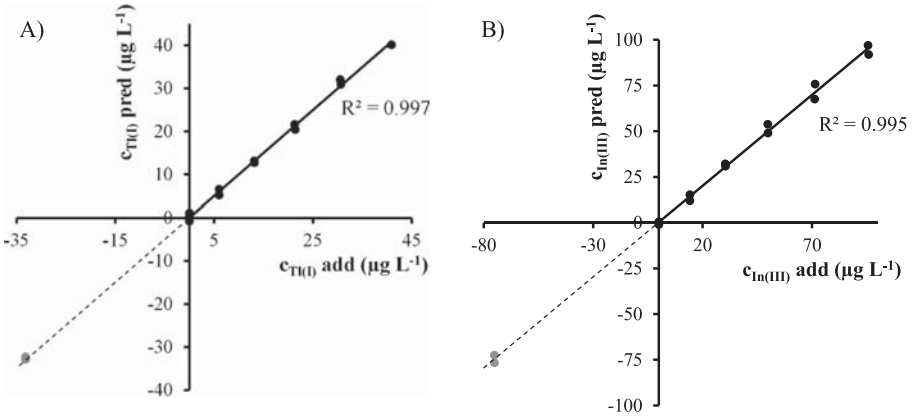

Fig. 5. Comparison graphs of predicted *vs.* expected added concentrations obtained with the sensor array for Tl(I) (A) and In(III) (B) for the spiked tonic water and the subsequent alternate additions (•) and for the extrapolation of the concentration in the simulated blank (●).

reason, this simulated blank was recorded twice. After that, the spiked tonic water sample was measured with the optimized stripping conditions (E_d = − 1.30 V and t_d = 120 s) (thick lines in Fig. 4) and finally the voltammograms after successive alternate additions of both metal ions were also recorded (thin lines in Fig. 4).

As in the case of multivariate external calibration, a data pretreatment is required prior to the construction of PLS1 models. In this sense, the data were derived using gap-segment function and autoscaled. In this case PLS1 models were calibrated using the obtained signals of the initial sample and the subsequent additions as X variable and the added concentrations of Tl(I) or In(III) as Y variable. Then this model was applied to determine Tl(I) or In(III) concentrations in the spiked tonic water sample by the extrapolation of these concentrations to the simulated blank voltammogram. Figs. 5A and 5B show a representative comparison graph of predicted *vs.* expected added concentrations for both Tl(I) and In(III) respectively.

Three replicates of the spiked tonic water sample were analysed using the proposed multivariate standard addition methodology and the mean of the concentrations obtained for both target metal ions are shown in Table 4. As it can be observed, good concordance between replicates was obtained even though the presence of deposited Tl(I) and In(III) change the hydrogen evolution potential, as seen by the change of the background current at low potentials. In comparison to the multivariate external calibration a much better accuracy, inferred by the relative error (%), was achieved for both Tl(I) and In(III). These results suggest that the multivariate standard addition calibration method is a more suitable strategy than the multivariate external calibration for the measurement of overlapped analytes in samples with complex matrices. This improvement could be also attributed to the fact that in the multivariate standard addition approach only a few Tl/In concentration ratios are involved whereas in the multivariate external calibration the Tl/In concentration ratios vary significantly along the experimental design, causing higher potential shifts as it can be seen comparing Figs. 2 and 4. Therefore, the loss of linearity caused by this potential shift makes it more difficult to model this system by PLS.

4. Conclusions

In this work the simultaneous voltammetric determination of Tl(I) and In(III) in tonic water using a sensor array based on a SeCyst-SPCNFE and an *ex-situ*-BiSPCE was studied as a model system of overlapped peaks present in samples with complex matrices. Firstly the resolution of this system was attempted using the more classical multivariate external calibration but, although this system was successfully

calibrated and validated for both metal ions using synthetic samples, the complexity of the tonic water matrix did not allow the accurate determination of Tl(I) and In(III).

Taking into account that in the case of univariate analysis these problems related to matrix complexity can be overcome by the application of the standard addition method, a newly proposed multivariate standard addition strategy was tested for the resolution of this system. Taking advantage of the presence of an accumulation step in anodic stripping techniques, a new approach was postulated based on the removal of this accumulation step ($t_d = 0$) to simulate a true blank solution. This strategy was successfully applied allowing the simultaneous determination of Tl(I) and In(III) in the spiked tonic water sample, inferred from the good accuracy and low RSD (%).

Thus, this proposed multivariate standard addition calibration method is postulated as an alternative calibration strategy for the resolution of complex systems involving overlapped peaks and complex matrices that cannot be neither solved by the multivariate external calibration nor simulated to allow the application of matrix matching strategies. In particular, the proposed methodology can be a powerful incentive for the development of stripping voltammetric electronic tongues able to work in really complicate media.

Aknowledgment

This work is supported by the Generalitat of Catalonia (Project 2017SGR311). Clara Pérez-Ràfols acknowledges the Spanish Ministry of Education, Culture and Sports for a Ph.D grant (reference FPU15/02140) and the Water Research Institute (IdRA) of the University of Barcelona for its support.

References

[1] D.C. Harris, Quantitative Chemical Analysis, 7th ed, W.H. Freeman and Company, New York, USA, 2007.
[2] J.N. Miller, J.C. Miller, Statistics and Chemometrics for Analtical Chemistry, 6th ed, Pearson, Essex, UK, 2010.
[3] S.D. Brown, R. Tauler, B. Walczak (Eds.), Comprehensive Chemometrics, Elsevier Science, Amsterdam, The Netherlands, 2009.
[4] M. del Valle, Electronic tongues employing electrochemical sensors, Electroanalysis 22 (2010) 1539–1555, https://doi.org/10.1002/elan.201000013.
[5] M. del Valle, Sensor arrays and electronic tongue systems, Int. J. Electrochem. 2012 (2012) 1–12, https://doi.org/10.1155/2012/986025.
[6] N. Serrano, B. Prieto-Simón, X. Cetó, M. del Valle, Array of peptide-modified electrodes for the simultaneous determination of Pb(II), Cd(II) and Zn(II), Talanta 125 (2014) 159–166, https://doi.org/10.1016/j.talanta.2014.02.052.
[7] A. González-Calabuig, D. Guerrero, N. Serrano, M. del Valle, Simultaneous voltammetric determination of heavy metals by use of crown ether-modified electrodes and chemometrics, Electroanalysis 28 (2016) 663–670, https://doi.org/10.1002/elan.201500512.
[8] N. Serrano, A. González-Calabuig, M. del Valle, Crown ether-modified electrodes for the simultaneous stripping voltammetric determination of Cd(II), Pb(II) and Cu(II), Talanta 138 (2015) 130–137, https://doi.org/10.1016/j.talanta.2015.01.044.
[9] C. Pérez-Ràfols, N. Serrano, J.M. Díaz-Cruz, C. Ariño, M. Esteban, Simultaneous determination of Tl(I) and In(III) using a voltammetric sensor array, Sens. Actuators B Chem. 245 (2017) 18–24, https://doi.org/10.1016/j.snb.2017.01.089.
[10] C. Pérez-Ràfols, N. Serrano, J.M. Díaz-Cruz, C. Ariño, M. Esteban, A screen-printed voltammetric electronic tongue for the analysis of complex mixtures of metal ions, Sens. Actuators B Chem. 250 (2017) 393–401, https://doi.org/10.1016/j.snb.2017.04.165.
[11] R.H. Labrador, J. Olsson, F. Winquist, R. Martínez-Máñez, J. Soto, Determination of bisulfites in wines with an electronic tongue based on pulse voltammetry, Electroanalysis 21 (2009) 612–617, https://doi.org/10.1002/elan.200804457.
[12] B.E. Saxberg, B.R. Kowalski, Generalized standard addition method, Anal. Chem. 51 (1979) 1031–1038.
[13] C. Jochum, P. Jochum, B.R. Kowalski, Error propagation and optimal performance in multicomponent Analysis, Anal. Chem. 53 (1981) 85–92, https://doi.org/10.1021/ac00224a023.
[14] J.H. Kalivas, Precision and stability for the generalized standard addition method, Anal. Chem. 55 (1983) 565–567, https://doi.org/10.1021/ac00254a033.
[15] J.H. Kalivas, B.R. Kowalski, Automated multicomponent analysis with corrections for interferences and matrix effects, Anal. Chem. 55 (1983) 532–535.
[16] R.W. Gerlach, B.R. Kowalski, The generalized standard addition method: intermetallic interferences in anodic stripping voltammetry, Anal. Chim. Acta 134 (1982) 119–127.
[17] E.A.G. Zagatto, A.O. Jacintho, F.J. Krug, B.F. Reis, Flow injection systems with inductively-coupled argon plasma atomic emission spectrometry: part 2. The generalized standard addition method, Anal. Chim. Acta 145 (1983) 169–178.
[18] J.H. Kalivas, B.R. Kowalski, Generalized standard addition method for multicomponent instrument characterization and elimination of interferences in inductively coupled plasma spectrometry, Anal. Chem. 53 (1981) 2207–2212.
[19] I.E. Frank, J.H. Kalivas, B.R. Kowalski, Partial least squares solutions for multicomponent analysis, Anal. Chem. 55 (1983) 1800–1804.
[20] V.A. Lozano, R. Tauler, G.A. Ibañez, A.C. Olivieri, Standard addition analysis of fluoroquinolones in human serum in the presence of the interferent salicylate using lanthanide-sensitized excitation-time decay luminescence data and multivariate curve resolution, Talanta 77 (2009) 1715–1723, https://doi.org/10.1016/j.talanta.2008.10.020.
[21] E. Peré-Trepat, S. Lacorte, R. Tauler, Alternative calibration approaches for LC – MS quantitative determination of coeluted compounds in complex environmental mixtures using multivariate curve resolution, Anal. Chim. Acta 595 (2007) 228–237, https://doi.org/10.1016/j.aca.2007.04.011.
[22] V.A. Lozano, G. Ibañez, A.C. Olivieri, A novel second-order standard addition analytical method based on data processing with multidimensional partial least-squares and residual bilinearization, Anal. Chim. Acta 651 (2009) 165–172, https://doi.org/10.1016/j.aca.2009.08.027.
[23] A. Afkhami, M. Abbasi-Tarighat, M. Bahram, H. Abdollahi, A new strategy for solving matrix effect in multivariate calibration standard addition data using combination of H-point curve isolation and H-point standard addition methods, Anal. Chim. Acta 613 (2008) 144–151, https://doi.org/10.1016/j.aca.2008.02.056.
[24] D. Melucci, C. Locatelli, Multivariate calibration in differential pulse stripping voltammetry using a home-made carbon-nanotubes paste electrode, J. Electroanal. Chem. 675 (2012) 25–31, https://doi.org/10.1016/j.jelechem.2012.04.020.
[25] K. Martínez, C. Ariño, J.M. Díaz-Cruz, N. Serrano, M. Esteban, Multivariate standard addition for the analysis of overlapping voltammetric signals in the presence of matrix effects: application to the simultaneous determination of hydroquinone and catechol, Chemom. Intell. Lab. Syst. 178 (2018) 32–38, https://doi.org/10.1016/j.chemolab.2018.05.002.
[26] J. Puy-Llovera, C. Pérez-Ràfols, N. Serrano, J.M. Díaz-Cruz, C. Ariño, M. Esteban, Selenocystine modified screen-printed electrode as an alternative sensor for the voltammetric determination of metal ions, Talanta 175 (2017) 501–506, https://doi.org/10.1016/j.talanta.2017.07.089.
[27] N. Serrano, A. Alberich, J.M. Díaz-Cruz, C. Ariño, M. Esteban, Coating methods, modifiers and applications of bismuth screen-printed electrodes, Trends Anal. Chem. 46 (2013) 15–29, https://doi.org/10.1016/j.trac.2013.01.012.
[28] N. Serrano, J.M. Díaz-Cruz, C. Ariño, M. Esteban, *Ex-situ* deposited bismuth film on screen-printed carbon electrode: a disposable device for stripping voltammetry of heavy metal ions, Electroanalysis (2010) 1460–1467, https://doi.org/10.1002/elan.200900183.
[29] Matlab, version R 2008b ed., Mathworks Inc., : Natick, MA, USA, 2008.
[30] PLS-toolbox version 7.8.2 (Eigenvector Research Inc., Wenatchee, USA), (n.d.).

9.1 Selecció i disposició dels sensors

Al llarg del capítol 8 s'ha discutit l'aplicació dels diversos sensors desenvolupats a la determinació d'ions metàl·lics. En tots els casos estudiats s'ha treballat individualment amb cada metall o simultàniament amb parelles de metalls amb potencials de reducció força diferents com és el cas del sistema model Pb(II) i Cd(II) o del sistema Pb(II) i Cu(II). Aquesta diferència de potencials permet resoldre el sistema amb un sol sensor ja que s'obtenen pics totalment separats que es poden tractar independentment amb mètodes de calibratge univariant. No obstant, existeixen sistemes de metalls més complexes en què els diferents ions interfereixen entre ells o presenten senyals solapats. En aquests casos cal recórrer a l'ús de llengües voltamperomètriques, on es combinen diversos sensors no específics amb un tractament de dades multivariant per resoldre el sistema. Al llarg d'aquesta tesi doctoral s'han estudiat dos d'aquests sistemes complexes, que es caracteritzen per la presència d'un elevat nombre de metalls (sistema Cd(II), Pb(II), Tl(I) i Bi(III) en presència de Zn(II) i In(III)) o per la presència de dos metalls que donen lloc a senyals fortament solapats (sistema Tl(I) i In(III)).

En el desenvolupament d'una llengua electrònica és especialment important seleccionar correctament els sensors i la seva disposició. Pel que fa a la tria dels sensors, tal com s'ha explicat a l'apartat 3.1, l'ideal és tenir un conjunt de sensors que presentin una resposta creuada de manera que tots ells responguin a tots els anàlits però amb una sensibilitat diferent. Així, per a una mateixa mostra cada sensor proporcionarà una resposta diferent i la baixa selectivitat dels sensors es podrà compensar amb el tractament de dades.

En els tres treballs, la resposta creuada dels sensors s'ha estudiat a través de la resposta independent de cada sensor per a cada anàlit. A la taula 9.1 es mostren les sensibilitats obtingudes per a cada sensor i metall considerats, que s'han obtingut a partir dels pendents de la respectives rectes de calibratge per a cada metall individual. En el cas de les dues llengües voltamperomètriques desenvolupades per al sistema Tl(I) i In(III) es pot observar clarament la resposta creuada ja que en els dos casos un dels sensors és més sensible al Tl(I) i l'altre a l'In(III), fet que posteriorment es tradueix en senyals voltamperomètrics invertits (figura 9.1).

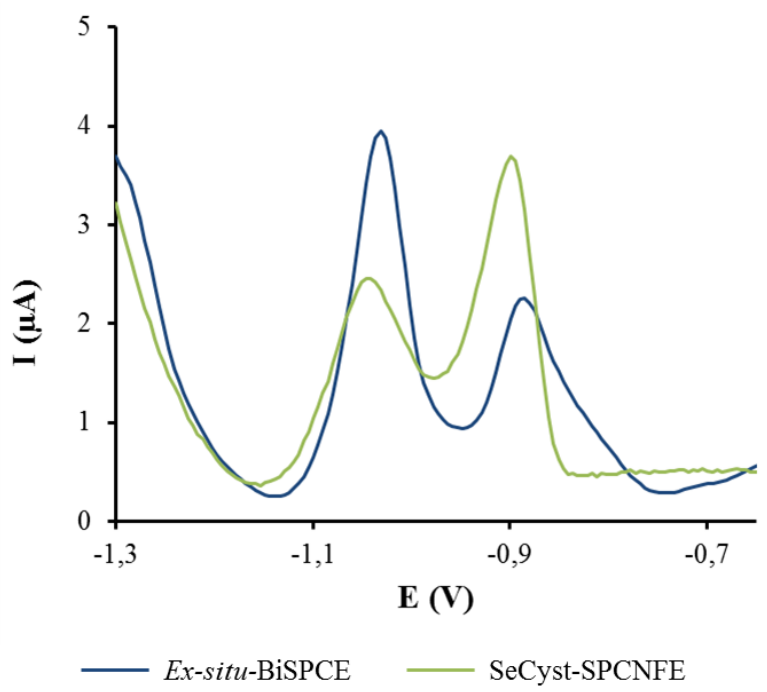

Figura 9.1. Voltamperogrames obtinguts per a una mescla de 82 i 129 µg L^{-1} de Tl(I) i In(III) respectivament a pH 4,5, amb un E_d de -1,3 V, un t_d de 120 s i emprant l'*ex-situ*-BiSPCE (blau) o el SeCyst-SPCNFE (verd).

En el cas del sistema Cd(II), Pb(II), Tl(I) i Bi(III) en presència de Zn(II) i In(III) es pot observar també que cadascun dels quatre sensors inclosos a la llengua voltamperomètrica presenta un ordre de sensibilitats diferent. Cal mencionar també que els dos elèctrodes que presenten un ordre de sensibilitats més semblants són els dos elèctrodes modificats químicament, que només difereixen en què el GSH-SPCNFE és més sensible al Tl(I) que al Cd(II) i el Cys-SPCNFE a l'inrevés. No obstant, aquesta inversió d'ordre és important ja que el Cd(II) i Tl(I) s'oxiden a la mateixa zona de potencials, fet que justifica la inclusió dels dos sensors a la llengua voltamperomètrica.

Pel que fa a la disposició dels elèctrodes, d'entre les diferents disposicions mostrades a la figura 3.2, en tots tres treballs s'ha emprat la segona disposició (figura 3.2b), és a dir, aquella en què tots els elèctrodes de treball estan referits a un mateix elèctrode de referència extern i a un mateix elèctrode auxiliar, que pot ser l'elèctrode auxiliar intern d'un dels SPEs o un elèctrode de platí extern

Taula 9.1 Sensibilitats obtingudes per als diferents sensors i metalls considerats en les tres llengües voltamperomètriques. Si no s'indica el contrari, les mesures s'han realitzat a pH 4,5, amb un E_d de -1,4 V i amb un t_d de 120 s. Les desviacions estàndards s'indiquen entre parèntesis.

	Zn(II)	Cd(II)	Pb(II)	Bi(III)	In(III)	Tl(I)
Sistema Tl(I) i In(III)[a] (Sensors and Actuators B 245 (2017) 18-24)						
Ex-situ-SbSPCNFE	--	--	--	--	0,75 (0,01)	1,10 (0,02)
Crown-6-SPCNFE	--	--	--	--	0,57 (0,01)	0,30 (0,01)
Sistema Cd(II), Pb(II), Tl(I) i Bi(III) en presència de Zn(II) i In(III)[a] (Sensors and Actuators B 250 (2017) 393-401)						
SPCNFE	3,75 (0,06)	5,45 (0,05)	4,59 (0,03)	0,40 (0,01)	2,80 (0,03)	2,73 (0,03)
GSH-SPCNFE	1,71 (0,04)	0,62 (0,01)	3,27 (0,03)	0,240 (0,005)	0,47 (0,01)	0,97 (0,02)
Cys-SPCNFE	2,19 (0,05)	1,43 (0,01)	3,48 (0,03)	0,196 (0,005)	0,277 (0,004)	1,08 (0,03)
Ex-situ-SbSPCNFE	2,26 (0,03)	2,42 (0,02)	0,85 (0,01)	0,157 (0,002)	0,75 (0,01)	1,10 (0,02)
Sistema Tl(I) i In(III)[b] (Talanta 192 (2019) 147-153)						
SeCyst-SPCNFE	--	--	--	--	2,11 (0,03	3,02 (0,05)
Ex-situ-BiSPCE	--	--	--	--	8,40 (0,07)	3,91 (0,03)

[a]Sensibilitats expressades com a u.a. μg^{-1} L.

[b]Sensibilitats expressades com a nA. μg^{-1} L. Mesures realitzades amb un E_d de -1,3 V.

en funció del treball considerat. D'altra banda, cal mencionar que s'ha optat per aquesta disposició enlloc de la seva versió miniaturitzada compacte (figura 3.2c) perquè en tots els treballs s'han combinat elèctrodes de treball modificats seguint diferents estratègies (principalment pel·lícules metàl·liques i modificacions químiques) i el fet de tenir SPEs independents permet controlar millor que els diferents processos de modificació no s'interfereixin entre si.

Finalment, donat l'elevat volum de dades proporcionat per cada sensor, és convenient emprar sempre el mínim nombre de sensors possibles i evitar incloure a la llengua sensors redundats per tal de facilitar el posterior tractament de dades. A priori és difícil determinar el nombre de sensors necessaris però, en general, no se sol emprar un nombre de sensors superior al nombre d'anàlits.

En el cas del sistema Tl(I) i In(III) l'estudi del nombre de sensors s'inclou a l'article Sensors and Actuators B 245 (2017) 18-24, on es va observar que l'ús d'un sol sensor, el crown-6-SPCNFE en aquest cas, no proporciona prou informació per resoldre satisfactòriament la mescla. En aquest cas, l'ús d'un sol sensor només permet determinar correctament el Tl(I), que és l'ió amb major sensibilitat per a aquest elèctrode, mentre que la introducció d'un segon sensor amb resposta creuada (*Ex-situ*-SbSPCNFE) permet la determinació simultània dels dos metalls tot i el seu fort solapament.

D'altra banda, en el cas del sistema Cd(II), Pb(II), Tl(I) i Bi(III) en presència de Zn(II) i In(III), el nombre de sensors es va avaluar per a cada ió metàl·lic en concret. Només en el cas del Cd(II) és necessari emprar les dades provinents dels quatre sensors ja que en el cas del Pb(II) és suficient amb tres sensors i en el cas del Tl(I) i el Bi(III) dos sensors ja proporcionen prou informació. Cal mencionar que en el cas del Zn(II) i l'In(III) no es va obtenir una bona capacitat de predicció independentment del nombre de sensors considerat.

9.2 Disseny experimental

Juntament amb la selecció dels sensors, una altra etapa crucial que pot afectar al desenvolupament d'una llengua electrònica és el disseny experimental

seleccionat, que dependrà del nombre d'ions metàl·lics i del sistema de calibratge multivariant emprat.

Tal com s'ha explicat anteriorment, l'ús de sistemes de calibratge multivariants externs requereix d'un set de mostres de calibratge i d'un set de mostres de validació. El nombre de mostres de calibratge ve determinat pel nombre d'ions metàl·lics a determinar o presents a la mostra mentre que la composició d'aquestes mostres depèn de l'interval de concentracions de treball. Aquest interval no té perquè ser igual per a tots els metalls i ve definit per l'interval de linealitat dels sensors emprats i la concentració de les mostres a analitzar.

A partir d'aquí, es poden distribuir les mostres de calibratge seguint diferents dissenys experimentals. En els treballs realitzats al llarg d'aquesta tesi doctoral s'ha emprat un disseny central compost de 6 factors per al sistema Cd(II), Pb(II), Tl(I) i Bi(III) en presència de Zn(II) i In(III) i una variació del disseny factorial amb 2 factors i 3 nivells, on hi ha hagut una rotació dels eixos, per al sistema Tl(I) i In(III) (figura 7.4). El disseny central compost de 6 factors és especialment útil en el sistema Cd(II), Pb(II), Tl(I) i Bi(III) en presència de Zn(II) i In(III) ja que permet considerar un elevat nombre d'ions metàl·lics però presenta l'inconvenient de considerar només 5 nivells de concentració per a cada metall, fet que després dificulta el tractament de dades. Aquest inconvenient s'ha solucionat en el cas del sistema Tl(I) i In(III) realitzant una rotació dels eixos del disseny factorial, permetent considerar així múltiples nivells de concentració (figura 9.2). Finalment, un cop establert el disseny experimental per a les mostres de calibratge, es distribueixen les mostres de validació al llarg del domini experimental.

D'altra banda, quan es treballa amb mostres amb matrius complexes i no és possible simular la matriu per aplicar el *matrix matching,* és necessari recórrer a altres mètodes de calibratge com l'addició estàndard multivariant per minimitzar els efectes matriu. Tal com s'ha explicat a l'apartat 5.2, l'addició estàndard és un mètode de calibratge molt ben establert per a sistemes univariants però que encara no disposa d'una estratègia consensuada per a l'anàlisi multivariant. En aquesta tesi doctoral s'ha emprat una estratègia basada en PLS on es construeix el model amb els voltamperogrames de la mostra i de les successives addicions i posteriorment s'extrapola al voltamperograma simulat del blanc per calcular la concentració dels metalls. En aquest cas és

important definir bé tant l'ordre de les addicions com la manera de simular el blanc de la mostra al qual després s'extrapolarà el model.

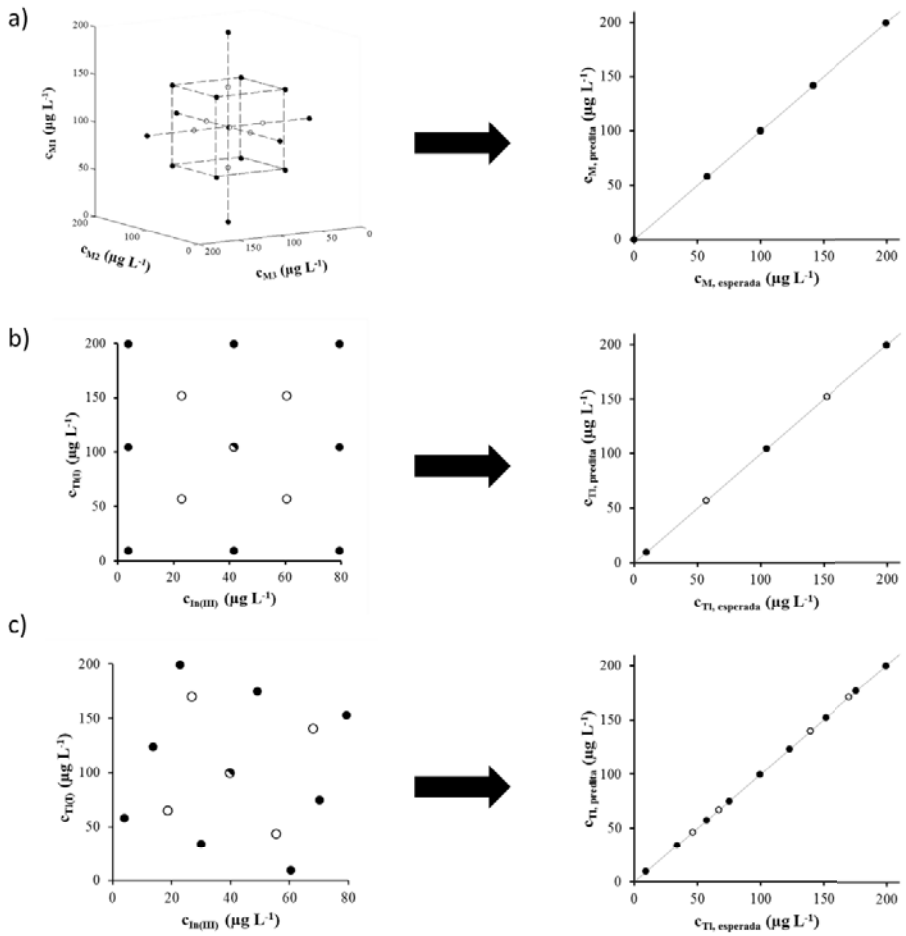

Figura 9.2. Efecte del disseny sobre els nivells de concentració considerats per a un disseny central compost de 6 factor (a) i un disseny factorial amb 2 factors i 3 nivells sense rotació (b) i amb rotació (c). Mostres de calibratge (●) i de validació (○).

En termes d'addicions, en sistemes simples amb pics separats que permeten aplicar l'addició estàndard univariant de manera independent a cada un dels metalls, el més habitual és realitzar addicions simultànies de tots els metalls. No obstant, aquesta opció no és aplicable a l'addició estàndard multivariant ja que el model PLS no seria capaç de distingir la contribució al senyal de cada ió metàl·lic. Així, en aquest cas és preferible afegir cada metall de manera

individual per tal que el model PLS pugui associar les variacions dels senyals amb els metalls. A més, d'entre tots els possibles dissenys experimentals s'ha observat també que l'addició alterna dels metalls millora els resultats obtinguts ja que es mantenen ràtios de concentracions similars al llarg de tota la valoració i, per tant, el grau de solapament entre els dos pics no varia tant i es més fàcil d'ajustar amb el model PLS [98].

Finalment, en aquesta estratègia de calibratge multivariant és especialment important simular correctament el blanc ja que és el senyal on s'extrapolarà el model PLS per tal de calcular la concentració dels metalls a la mostra. En el cas concret de les tècniques voltamperomètriques de redissolució aquesta simulació es pot realitzar si es mesura la mostra sense aplicar l'etapa de deposició. Així, es mantenen els corrents capacitatius i la contribució de qualsevol espècie present a la mostra que no s'acumuli però, al no haver-hi etapa de deposició, s'evita l'acumulació dels metalls i la seva posterior contribució al senyal voltamperomètric. A la figura 9.3 es pot observar que aquest mètode de simulació permet obtenir blancs simulats d'una mostra fortificada amb Tl(I) i In(III) pràcticament idèntics als blancs obtinguts en una mostra sense fortificar.

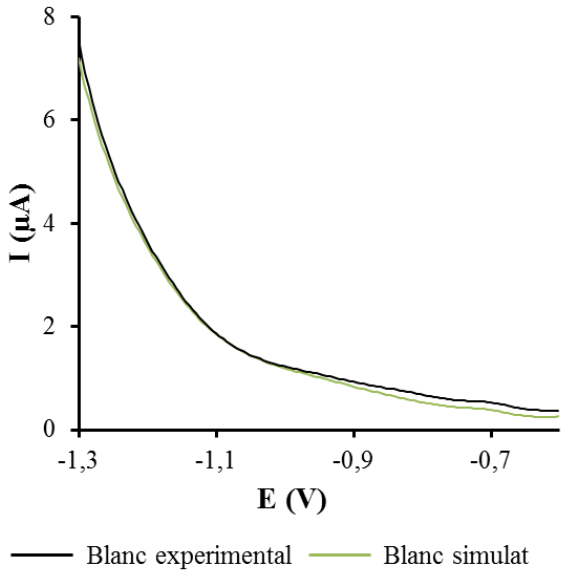

Figura 9.3. Blanc experimental (negre) i simulat sense aplicar l'etapa de deposició (verd) per a una mostra d'aigua de tònica emprant l'elèctrode SeCyst-SPCNFE.

9.3 Tractament quimiomètric de les dades

Tal com s'ha explicat al capítol 3, una llengua voltamperomètrica està formada tant per un conjunt de sensors com per un model quimiomètric, que és el que permet compensar la baixa selectivitat dels sensors i poder identificar el tipus de mostra o quantificar algun dels seus paràmetres o anàlits. La construcció d'aquest model quimiomètric està fortament condicionada pel pretractament de les dades, que en el cas de les mesures voltamperomètriques sol estar enfocat a disminuir el soroll o corregir derives de la línia base.

A tall d'exemple, a la figura 9.4 es mostra l'efecte del pretractament. En el cas del sistema Tl(I) i In(III) (figura 9.4a), on s'observa fàcilment la zona del voltamperograma on es localitzen els pics, inicialment es corregeix la deriva de la línia base i després s'aplica la derivada per tal d'accentuar les diferències a la zona de solapament entre els dos pics. D'altra banda, en el cas del sistema Cd(II), Pb(II), Tl(I) i Bi(III) en presència de Zn(II) i In(III) (figura 9.4b), on es contemplen moltes més mostres i la zona on apareixen els pics no està tan ben definida, s'ha utilitzat l'OSC per tal d'eliminar variàncies dels voltamperogrames no relacionades amb la concentració dels metalls.

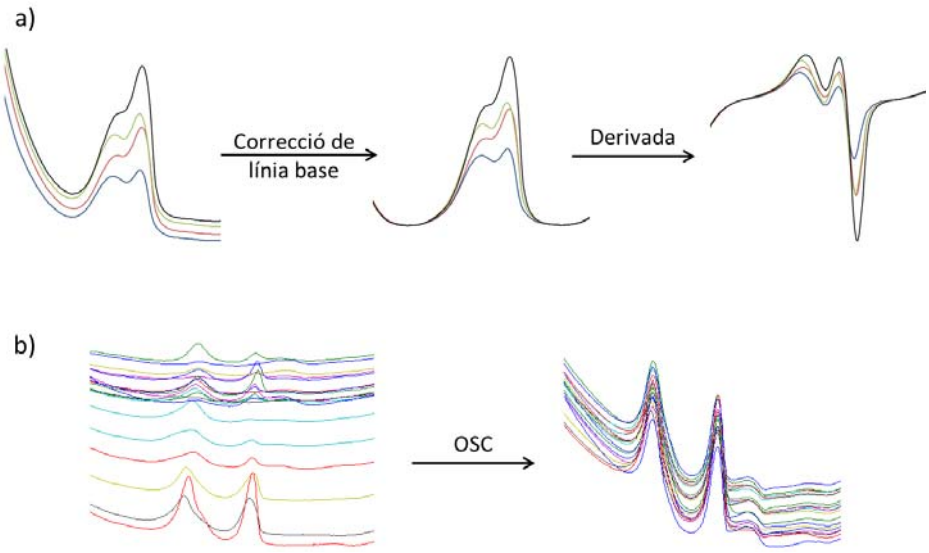

Figura 9.4. Efecte del pretractament de les dades (a) en el sistema Tl(I) i In(III) i (b) en el sistema Cd(II), Pb(II), Tl(I) i Bi(III) en presència de Zn(II) i In(III).

Un altre aspecte que cal considerar al llarg del pretractament de les dades és la quantitat d'informació amb què es treballarà ja que, en el cas de ser molt elevada, cal considerar una compressió de les dades prèvia a la construcció del model quimiomètric. Aquest ha sigut el cas del sistema Cd(II), Pb(II), Tl(I) i Bi(III) en presència de Zn(II) i In(III) ja que s'empren quatre sensors i amb un interval de potencials molt ampli, fet que resulta en 2220 valors d'intensitat per a cada mostra (4 sensors x 555 valors d'intensitat). En aquest cas s'ha optat per emprar un model jeràrquic on inicialment s'aplica un model PLS-2 considerant tots els metalls que se solapen en una mateix zona de potencials i els *scores* obtinguts s'empren com a nous descriptors per a construir un nou model PLS-1 (figura 9.5).

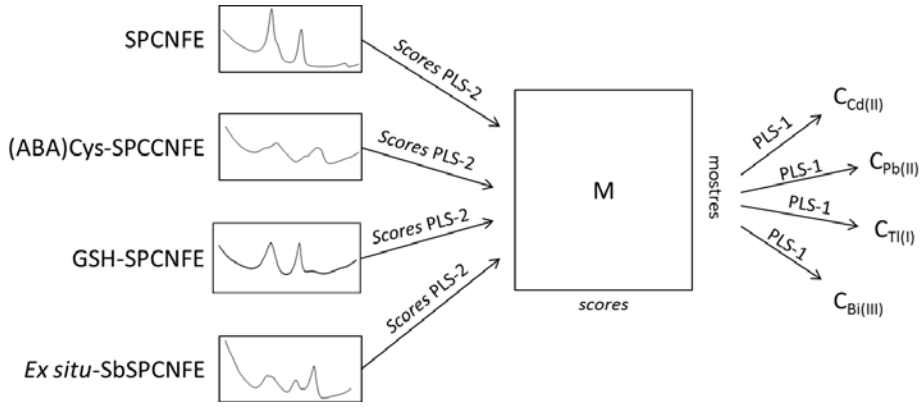

Figura 9.5. Esquematització del model jeràrquic emprat per al sistema Cd(II), Pb(II), Tl(I) i Bi(III) en presència de Zn(II) i In(III).

9.3.1 Calibratge multivariant extern

Per al calibratge multivariant extern s'han construït models PLS-1 amb les mostres de calibratge. El nombre de LVs s'ha determinat a partir de la validació creuada en el cas del sistema Cd(II), Pb(II), Tl(I) i Bi(III) en presència de Zn(II) i In(III) i tenint en compte la capacitat predictiva del model en el cas del sistema Tl(I) i In(III) ja que el nombre de mostres no és prou elevat per obtenir resultats fiables a la validació creuada.

La bondat dels models PLS-1 s'ha avaluat en primera instància tenint en compte la predicció de les pròpies mostres de calibratge i posteriorment considerant les mostres de validació, que no han intervingut en la construcció dels models PLS-1. Els paràmetres considerats en tots dos casos, que es mostren a la taula 9.2, han sigut el RMSE i la regressió lineal obtinguda al comparar els valors predits i esperats, que idealment hauria de tenir un pendent de 1, una ordenada de 0 i una R^2 de 1. En tots els casos s'han obtingut valors satisfactoris de RMSE i una bona correlació entre els valors de concentració predits i esperats. A més, s'obtenen valors similars per al calibratge i la validació, fet que confirma que en cap cas s'ha sobreajustat el model. Cal mencionar que en el cas del sistema Cd(II), Pb(II), Tl(I) i Bi(III) en presència de Zn(II) i In(III) no es mostren els valors corresponents a la regressió de les mostres de validació ja que amb el disseny experimental emprat només es consideren 3 nivells de concentració i la majoria de les mostres es trobava al nivell central, fet que fa que la recta obtinguda no avaluï bé la capacitat predictiva del model.

Un cop calibrats i validats els models PLS-1, s'ha avaluat l'aplicabilitat de les llengües voltamperomètriques desenvolupades en mostres reals. Les dues primeres llengües electròniques desenvolupades (Sensors and Actuators B 245 (2017) 18-24 i Sensors and Actuators B 250 (2017) 393-401) s'han aplicat a l'anàlisi de mostres d'aigua de l'aixeta fortificada, que s'han analitzat per triplicat. En tots els casos s'han obtingut resultats amb bona precisió, amb un RSD inferior al 14%, i els resultats s'han comparat amb els resultats proporcionats per ICP-MS amb un test t de dues cues (variàncies iguals), concloent que les dues tècniques donen lloc a resultats estadísticament iguals amb un 95% de confiança. No obstant, a l'aplicar la tercera llengua voltamperomètrica (Talanta 192 (2019) 147-153) a l'anàlisi de mostres d'aigua de tònica fortificades amb Tl(I) i In(III) s'observa que, tot i seguir obtenint una bona precisió amb un RSD inferior al 4% en tots els casos, els resultats proporcionats per la llengua voltamperomètrica difereixen molt dels valors esperats. Aquest fet és degut al fort efecte matriu de l'aigua de tònica, que afecta a la forma, a la posició i al solapament dels pics voltamperomètrics i impedeix la correcta aplicació dels models PLS-1.

Taula 9.2 Nombre de LVs emprades per a la construcció dels models PLS-1 i RMSE i principals paràmetres de la regressió lineal obtinguda al comparar els valors predits i esperats per al calibratge i la validació d'aquests models. Les desviacions estàndards s'indiquen entre parèntesis.

	Cd(II)	Pb(II)	Bi(III)	Tl(I)	In(III)
Sensors and Actuators B 245 (2017) 18-24					
Nombre de LVs				3	5
Calibratge					
Pendent	--	--	--	1,000 (0,003)	1,00 (0,02)
Ordenada	--	--	--	0,0 (0,4)	0 (1)
R^2	--	--	--	0,999	0,997
RMSE	--	--	--	0,49	1,20
Validació					
Pendent	--	--	--	1,00 (0,08)	1,07 (0,10)
Ordenada	--	--	--	0 (9)	-5 (5)
R^2	--	--	--	0,981	0,984
RMSE	--	--	--	6,55	2,60

Taula 9.2 (continuació) Nombre de LVs emprades per a la construcció dels models PLS-1 i RMSE i principals paràmetres de la regressió lineal obtinguda al comparar els valors predits i esperats per al calibratge i la validació d'aquests models. Les desviacions estàndards s'indiquen entre parèntesis.

	Cd(II)	Pb(II)	Bi(III)	Tl(I)	In(III)
Sensors and Actuators B 250 (2017) 393-401					
Nombre de LVs	2	3	2	2	--
Calibratge					
Pendent	0,90 (0,05)	0,93 (0,04)	0,92 (0,04)	0,90 (0,05)	--
Ordenada	10 (5)	8 (4)	8 (4)	10 (5)	--
R	0,951	0,931	0,949	0,927	--
RMSE	12,06	10,68	11,78	12,26	--
Validació					
Pendent	--	--	--	--	--
Ordenada	--	--	--	--	--
R	--	--	--	--	--
RMSE	11,01	6,64	14,83	8,71	--

Taula 9.2 (continuació) Nombre de LVs emprades per a la construcció dels models PLS-1 i RMSE i principals paràmetres de la regressió lineal obtinguda al comparar els valors predits i esperats per al calibratge i la validació d'aquests models. Les desviacions estàndards s'indiquen entre parèntesis.

	Cd(II)	Pb(II)	Bi(III)	Tl(I)	In(III)
Talanta 192 (2019) 147-153					
Nombre de LVs				4	4
Calibratge					
Pendent	--	--	--	1,00 (0,02)	0,99 (0,03)
Ordenada	--	--	--	0 (2)	1 (3)
R^2	--	--	--	0,997	0,993
RMSE	--	--	--	2,62	4,05
Validació					
Pendent	--	--	--	0,9 (0,1)	1,18 (0,06)
Ordenada	--	--	--	12 (14)	-16 (6)
R^2	--	--	--	0,959	0,993
RMSE	--	--	--	8,81	8,25

9.3.2 Addició estàndard multivariant

L'addició estàndard multivariant s'ha aplicat a la determinació de Tl(I) i In(III) en aigua de tònica ja que, tal com s'ha vist a l'apartat anterior, es tracta d'una mostra amb un fort efecte matriu que no permet determinar correctament aquests dos metalls amb un calibratge multivariant extern. Aquest estudi s'inclou a l'article Talanta 192 (2019) 147-153.

En aquest cas, la determinació de la mostra d'aigua de tònica s'ha realitzat també per triplicat i els models PLS-1 s'han construït emprant els voltamperogrames dels dos sensors corresponents a la mostra i a les successives addicions alternes de Tl(I) i In(III). Per a aquests models s'han emprat 5 LV pel Tl(I) i 3 LVs per l'In(III), que s'han seleccionat tenint en compte el RMSE i la regressió lineal obtinguda al comparar els valors predits i esperats. Els valors d'aquests paràmetres obtinguts en cada una de les tres rèpliques es mostren a la taula 9.3.

Les concentracions d'aquests ions metàl·lics a l'aigua de tònica fortificada s'han calculat per extrapolació d'aquests models al senyal d'un blanc que s'ha simulat a l'inici de cada valoració realitzant la mateixa mesura d'ASV però sense aplicar l'etapa de deposició. Els resultats obtinguts mantenen una precisió similar als proporcionats pel calibratge multivariant extern i, a més, permeten una determinació molt més acurada de les concentracions, amb un error relatiu respecte al valor teòric inferior al 3% en els dos casos. Així, l'addició estàndard multivariant proporciona millors resultats que el calibratge multivariant extern en aquelles mostres on la matriu afecta a la forma, la mida, la posició o el solapament dels pics ja que en aquest cas es considera en el calibratge del model PLS-1.

Taula 9.3. RMSE i principals paràmetres de la regressió lineal obtinguda al comparar els valors predits i esperats per al calibratge dels models PLS-1. Les desviacions estàndard s'indiquen entre parèntesi

	Rèplica 1	**Rèplica 2**	**Rèplica 3**
Tal·li, 5LVs			
Pendent	1,00 (0,02)	1,00 (0,02)	1,00 (0,02)
Ordenada	0,0 (0,3)	0,0 (0,3)	0,1 (0,4)
R^2	0,997	0,997	0,996
RMSE	0,739	0,773	0,811
Indi, 3LV			
Pendent	0,98 (0,04)	0,98 (0,04)	0,99 (0,02)
Ordenada	1 (2)	1 (2)	0 (1)
R^2	0,983	0,979	0,995
RMSE	4,330	4,964	2,435

PART V
Conclusions

The results presented throughout this Doctoral Thesis can lead to the following conclusions:

1. Several new voltammetric sensors based on different modification strategies (chemical modification, metal films, metal NPs and carbon nanoallotropes) have been developed for the determination of trace metal ions as alternatives to the more toxic HMDE. A good analytical performance was achieved in all cases, with high sensitivity, linearity, repeatability and reproductibility and LODs and LOQs at the level of low μg L^{-1}. Furthermore, all the developed sensors are based on the use of SPEs, which can overcome some of the main limitations of HMDE such as the difficulty of implementing it to *on-site* or *on-line* analysis and its limited modification possibilities.

2. The successful modification of SPEs following different modification strategies has been proved by a step-by-step characterization in all cases. In this sense, useful information can be provided by both electrochemical and electron microscopy techniques depending on the chosen modification strategy.

3. SPEs modified with carbon nanoallotopes and CNF in particular have been demonstrated to be a more suitable SPE substrate for the development of trace metal voltammetric sensors based on the considered modification strategies. In general, the use of SPCNFE provides sensors with a better analytical performance, especially in terms of repeatability and reproducibility but also in terms of sensitivity or LODs and LOQs.

4. The known affinity of thiol-rich peptides for metal ions can be successfully applied to the development of more sensitive and/or selective chemically modified voltammetric sensors. The performance of these sensors can be improved selecting a peptide with higher affinity for the target metal ion or using different strategies that allow the immobilization of the same peptide onto the electrode surface through different functional groups. Furthermore, the use of modifiers with a different type of interaction with metal ions like crown ethers can lead to sensors with much different selectivity.

5. Both bismuth and antimony are greener alternatives to mercury for the development of metal film modified SPEs for the voltammetric determination of trace metal ions. Although Sb-SPEs present a wider

potential window and can be used in more acidic media, Bi-SPEs are less toxic and can provide interesting changes in metal ion selectivity. In both cases, the *ex-situ* modification is a more suitable strategy than the *in-situ* modification for the AdSV determination of metals or the development of voltammetric electronic tongues.

6. Several types of AgNPs have been tested for the development of screen-printed -based voltammetric sensors. The performance of the resulting sensors is influenced by the shape and size of the metal NP, obtaining better results with smaller and spherical NPs. Furthermore, trace metal voltammetric sensors can also be developed through the modification of SPEs with AgNPs synthesized using a green strategy based on the use of grape stalk waste extract.

7. Carbon stabilized pSi has been introduced as a new voltammetric sensor substrate. Although this material is not stable at the cathodic potentials required for metal ion determination, the suitability of this material has been demonstrated for the simultaneous determination of HQ, CC and RC, allowing the separation of HQ and CC and providing a good analytical performance.

8. The different strategies considered for the modification of SPEs allow the development of voltammetric sensors with different sensitivity and selectivity towards metal ions and, therefore, provide the necessary cross-response for the development of voltammetric electronic tongues to resolve complex mixtures of metal ions.

9. The development of voltammetric electronic tongues based on screen-printed modified electrodes allows the analysis of complex mixtures of metal ions. In this sense, two complex systems based on the combination of a large number of metal ions (Cd(II), Pb(II), Tl(I) and Bi(III) in the presence of Zn(II) and In(III)) and two metals with overlapping peaks (Tl(I) and In(III)) have been successfully resolved. The developed voltammetric tongues have been validated through the determination of a test set, showing a good prediction capability inferred by low RMSEs and a good correlation between expected and predicted concentration values.

10. Multivariate external calibration has been proved to provide good predictions for synthetic samples and real samples were the target metal ions behave in a similar way, without significant changes in peak shape, position or overlapping. However, one of the major limitations of multivariate external calibration is its inability to successfully predict metal concentrations in more complex samples with a strong matrix effect. For these cases, a new multivariate standard addition method that simulates the blank signal by skipping the deposition step of ASV has been developed and successfully applied to the determination of Tl(I) and In(III) in spiked tonic water samples.

PART VI
Referències

[1] N. Bjerrum, Bjerrum's Inorganic Chemistry, 3rd Danish, Heinemann, London, UK, 1936.

[2] J.H. Duffus, "Heavy metals"— A meaningless term? (IUPAC Technical Report), Pure Appl. Chem. 74 (2002) 793–807. doi:10.1351/pac200274050793.

[3] O. Pourret, J.C. Bollinger, "Heavy metal" - What to do now: To use or not to use?, Sci. Total Environ. 610–611 (2018) 419–420. doi:10.1016/j.scitotenv.2017.08.043.

[4] O. Pourret, On the necessity of banning the term "heavy metal" from the scientific literature, Sustainability. 10 (2018) 2879–2880. doi:10.3390/su10082879.

[5] M.E. Hodson, Heavy metals - Geochemical bogey men?, Environ. Pollut. 129 (2004) 341–343. doi:10.1016/j.envpol.2003.11.003.

[6] L. Madrid, "Heavy metals": Reminding a long-standing and sometimes forgotten controversy, Geoderma. 155 (2010) 128–129. doi:10.1016/j.geoderma.2009.11.031.

[7] U.N. Bhat, A.B. Khan, Heavy metals: an ambiguous category of inorganic contaminants, nutrients and toxins, Res. J. Environ. Sci. 5 (2011) 682–690. doi:10.1111/ijfs.12122.

[8] H. Ali, E. Khan, What are heavy metals? Long-standing controversy over the scientific use of the term "heavy metals" – proposal of a comprehensive definition, Toxicol. Environ. Chem. 100 (2018) 6–19. doi:10.1080/02772248.2017.1413652.

[9] G.E. Batley, "Heavy metal" – A useful term, Integr. Environ. Assess. Manag. 8 (2012) 215–215. doi:10.1002/ieam.1290.

[10] R. Hübner, K.B. Astin, R.J.H. Herbert, "Heavy metal" - Time to move on from semantics to pragmatics?, J. Environ. Monit. 12 (2010) 1511–1514. doi:10.1039/c0em00056f.

[11] J.E. Fergusson, The heavy elements: chemistry, environmental impact, and health effects, Pergamon Press, Oxford, 1991.

[12] E. Callender, Heavy metals in the environment-historical trends, in: Environmental Geochemistry, vol. 9, Elsevier Science, Oxford, 2005. doi:10.2134/jeq1993.00472425002200010029x.

[13] L. Landner, R. Reuther, Metals in society and in the environment: a critical review of current knowledge on fluxes, speciation, bioavailability and risk for adverse effects of copper, chromium, nickel and zinc, Kluwer Academic Publishers, New York, Boston, Dordrecht, London, Moscow, 2004. doi:10.1007/1-4020-2742-7.

[14] J.O. Nriagu, A history of global metal pollution, Science. 272 (1996) 223–224. doi:10.1126/science.272.5259.223.

[15] I.D.L. Foster, S.M. Charlesworth, Heavy metals in the hydrological cycle: trends and explanation, Hydrol. Process. 10 (1996) 227–261. doi:10.1002/(SICI)1099-1085(199602)10:2<227::AID-HYP357>3.0.CO;2-X.

[16] J.O. Nriagu, J.M. Pacyna, Quantitative assessment of worldwide contamination of air, water and soils by trace metals, Nature. 333 (1988) 134–139. doi:doi-org.sire.ub.edu/10.1038/333134a0.

[17] J. Baby, J.S. Raj, E.T. Biby, P. Sankarganesh, M. V. Jeevitha, S.U. Ajisha, S.S. Rajan, Toxic effect of heavy metals on aquatic environment, Int. J. Biol. Chem. Sci. 4 (2010) 939–952. doi:10.1111/j.1439-0507.2010.01876.x.

[18] K.J. Appenroth, Definition of “heavy metals” and their role in biological systems, in: Soil heavy metals, vol. 19, Springer-Verlag, Jena, Germany, 2010. doi:10.1007/978-3-642-02436-8.

[19] A. Violante, V. Cozzolino, L. Perelomov, A.G. Caporale, M. Pigna, Mobility and bioavailability of heavy metals and metalloids in soil environments, J. Soil Sci. Plant Nutr. 10 (2010) 268–292. doi:10.4067/s0718-95162010000100005.

[20] J.S. Rieuwerts, I. Thornton, M.E. Farago, M.R. Ashmore, Factors influencing metal bioavailability in soils: Preliminary investigations for the development of a critical loads approach for metals, Chem. Speciat. Bioavailab. 10 (1998) 61–75. doi:10.3184/095422998782775835.

[21] G.F. Nordberg, B.A. Fowler, M. Nordberg, Toxicology of metals: Overview, definitions, concepts and trends, in: Handbook of the toxicology of metals, 4th ed., Elsevier, London, UK, 2015. doi:10.1016/B978-0-444-59453-2.00001-9.

[22] A. Radu, D. Diamond, Ion-selective electrodes in trace level analysis of heavy metals: Potentiometry for the XXI century, in: Comprehensive analytical chemistry, vol. 49, Elsevier Science, Amsterdam, The Netherlands, 2007. doi:10.1016/S0166-526X(06)49002-4.

[23] F. Arduini, G. Palleschi, Screening and confirmatory methods for the detection of heavy metals in foods, in: Persistent organic pollutants and toxic metals in foods, Woodhead Publishing Limited, Cambridge, UK, 2013. doi:10.1533/9780857098917.1.81.

[24] G. Aragay, A. Merkoçi, Nanomaterials application in electrochemical detection of heavy metals, Electrochim. Acta. 84 (2012) 49–61. doi:10.1016/j.electacta.2012.04.044.

[25] J. Barek, J. Zima, Eighty years of polarography–history and future, Electroanalysis. 15 (2003) 467–472. doi:10.1002/elan.200390055.

[26] J. Barek, A.G. Fogg, A. Muck, J. Zima, Polarography and voltammetry at mercury electrodes, Crit. Rev. Anal. Chem. 31 (2001) 291–309. doi:10.1080/20014091076776.

[27] J. Barek, J. Moreira, J. Zima, Modern electrochemical methods for monitoring of chemical carcinogens, Sensors. 5 (2005) 148–158. doi:10.3390/S5040148.

[28] A. Economou, P.R. Fielden, Mercury film electrodes: developments, trends and potentialities for electroanalysis, Analyst. 128 (2003) 205–212. doi:10.1039/b201130c.

[29] B. Uslu, S.A. Ozkan, Solid electrodes in electroanalytical chemistry: present applications and prospects for high throughput screening of drug compounds, Comb. Chem. High Throughput Screen. 10 (2007) 495–513. doi:10.2174/138620707782152425.

[30] G. Hanrahan, D.G. Patil, J. Wang, Electrochemical sensors for environmental monitoring: Design, development and applications, J. Environ. Monit. 6 (2004) 657–664. doi:10.1039/b403975k.

[31] M. Li, Y.T. Li, D.W. Li, Y.T. Long, Recent developments and applications of screen-printed electrodes in environmental assays-A review, Anal. Chim. Acta. 734 (2012) 31–44. doi:10.1016/j.aca.2012.05.018.

[32] J. Barton, M.B.G. García, D.H. Santos, P. Fanjul-Bolado, A. Ribotti, M. McCaul, D. Diamond, P. Magni, Screen-printed electrodes for environmental monitoring of heavy metal ions: a review, Microchim. Acta. 183 (2016) 503–517. doi:10.1007/s00604-015-1651-0.

[33] O.D. Renedo, M.A. Alonso-Lomillo, M.J.A. Martínez, Recent developments in the field of screen-printed electrodes and their related applications, Talanta. 73 (2007) 202–219. doi:10.1016/j.talanta.2007.03.050.

[34] G.M.S. Alves, L.S. Rocha, H.M.V.M. Soares, Multi-element determination of metals and metalloids in waters and wastewaters, at trace concentration level, using electroanalytical stripping methods with environmentally friendly mercury free-electrodes: A review, Talanta. 175 (2017) 53–68. doi:10.1016/j.talanta.2017.06.077.

[35] Dropsens, screen printed electrodes, http://www.dropsens.com/en/screen_printed_electrodes_pag.html#customized_spes (accessed April 20, 2019).

[36] S. Alegret, M. del Valle, A. Merkoçi, Sensores electroquímicos, Universitat Autònoma de Barcelona, Barcelona, Spain, 2004.

[37] C. Ariño, N. Serrano, J.M. Díaz-Cruz, M. Esteban, Voltammetric determination of metal ions beyond mercury electrodes. A review, Anal. Chim. Acta. 990 (2017) 11–53. doi:10.1016/j.aca.2017.07.069.

[38] E. Chow, J.J. Gooding, Peptide modified electrodes as electrochemical metal ion sensors, Electroanalysis. 18 (2006) 1437–1448. doi:10.1002/elan.200603558.

[39] J.J. Gooding, Peptide-modified electrodes for detecting metal ions, in: Electrochemical sensor analysis, vol. 49, Elsevier Science, Amsterdam, The Netherlands, 2007. doi:10.1016/S0166-526X(06)49010-3.

[40] N. Serrano, A. González-Calabuig, M. del Valle, Crown ether-modified electrodes for the simultaneous stripping voltammetric determination of Cd(II), Pb(II) and Cu(II), Talanta. 138 (2015) 130–137. doi:10.1016/j.talanta.2015.01.044.

[41] J.J. Gooding, S. Ciampi, The molecular level modification of surfaces: from self-assembled monolayers to complex molecular assemblies, Chem. Soc. Rev. 40 (2011) 2704–2718. doi:10.1039/c0cs00139b.

[42] U.E. Wawrzyniak, P. Ciosek, M. Zaborowski, G. Liu, J.J. Gooding, Gly-Gly-His immobilized on monolayer modified back-side contact miniaturized sensors for complexation of copper ions, Electroanalysis. 25 (2013) 1461–1471. doi:10.1002/elan.201200667.

[43] G. Liu, T.N. Quynh, E. Chow, T. Böcking, D.B. Hibbert, J.J. Gooding, Study of factors affecting the performance of voltammetric copper sensors based on Gly-Gly-His modified glassy carbon and gold electrodes, Electroanalysis. 18 (2006) 1141–1151. doi:10.1002/elan.200603546.

[44] M. Delamar, R. Hitmi, J. Pinson, J.M. Savéant, Covalent modification of carbon surfaces by grafting of functionalized aryl radicals produced from electrochemical reduction of diazonium salts, J. Am. Chem. Soc. 114 (1992) 5883–5884. doi:doi.org/10.1021/ja00040a074.

[45] D. Bélanger, J. Pinson, Electrografting: a powerful method for surface modification, Chem. Soc. Rev. 40 (2011) 3995–4048. doi:10.1039/c0cs00149j.

[46] S. Baranton, D. Bélanger, Electrochemical derivatization of carbon surface by reduction of in situ generated diazonium cations, J. Phys. Chem. B. 109 (2005) 24401–24410. doi:10.1021/jp054513+.

[47] J.J. Gooding, Advances in interfacial design for electrochemical biosensors and sensors: Aryl diazonium salts for modifying carbon and metal electrodes, Electroanalysis. 20 (2008) 573–582. doi:10.1002/elan.200704124.

[48] A.J. Downard, Electrochemically assisted covalent modification of carbon electrodes, Electroanalysis. 12 (2000) 1085–1096. doi:10.1002/1521-4109(200010)12:14<1085::AID-ELAN1085>3.0.CO;2-A.

[49] J. Wang, J. Lu, S.B. Hocevar, P.A.M. Farias, B. Ogorevc, Bismuth-coated carbon electrodes for anodic stripping voltammetry, Anal. Chem. 72 (2000) 3218–3222. doi:10.1021/ac000108x.

[50] C. Kokkinos, A. Economou, Stripping analysis at bismuth-based electrodes, Curr. Anal. Chem. 4 (2008) 183–190. doi:10.2174/157341108784911352.

[51] V. Jovanovski, S.B. Hočevar, B. Ogorevc, Bismuth electrodes in contemporary electroanalysis, Curr. Opin. Electrochem. 3 (2017) 114–122. doi:10.1016/j.coelec.2017.07.008.

[52] J. Wang, Stripping analysis at bismuth electrodes: A review, Electroanalysis. 17 (2005) 1341–1346. doi:10.1002/elan.200403270.

[53] S.B. Hocevar, I. Svancara, B. Ogorevc, K. Vytras, Antimony film electrode for electrochemical stripping analysis, Anal. Chem. 79 (2007) 8639–8643. doi:10.1021/ac070478m.

[54] N. Serrano, J.M. Díaz-Cruz, C. Ariño, M. Esteban, Antimony- based electrodes for analytical determinations, TrAC Trends Anal. Chem. 77 (2016) 203–213. doi:10.1016/j.trac.2016.01.011.

[55] W.W. Zhu, N.B. Li, H.Q. Luo, Simultaneous determination of chromium(III) and cadmium(II) by differential pulse anodic stripping voltammetry on a stannum film electrode, Talanta. 72 (2007) 1733–1737. doi:10.1016/j.talanta.2007.04.055.

[56] V. Jovanovski, N.I. Hrastnik, S.B. Hočevar, Copper film electrode for anodic stripping voltammetric determination of trace mercury and lead, Electrochem. Commun. 57 (2015) 1–4. doi:10.1016/j.elecom.2015.04.018.

[57] M. Korolczuk, K. Tyszczuk, M. Grabarczyk, Adsorptive stripping voltammetry of nickel and cobalt at in situ plated lead film electrode, Electrochem. Commun. 7 (2005) 1185–1189. doi:10.1016/j.elecom.2005.08.022.

[58] N. Serrano, A. Alberich, J.M. Díaz-Cruz, C. Ariño, M. Esteban, Coating methods, modifiers and applications of bismuth screen-printed electrodes, TrAC - Trends Anal. Chem. 46 (2013) 15–29. doi:10.1016/j.trac.2013.01.012.

[59] F. Arduini, J.Q. Calvo, G. Palleschi, D. Moscone, A. Amine, Bismuth-modified electrodes for lead detection, TrAC - Trends Anal. Chem. 29 (2010) 1295–1304. doi:10.1016/j.trac.2010.08.003.

[60] C. Kokkinos, A. Economou, I. Raptis, C.E. Efstathiou, T. Speliotis, Novel disposable bismuth-sputtered electrodes for the determination of trace metals by stripping voltammetry, Electrochem. Commun. 9 (2007) 2795–2800. doi:10.1016/j.elecom.2007.09.022.

[61] B. Pérez-López, A. Merkoçi, Nanoparticles for the development of improved (bio)sensing systems, Anal. Bioanal. Chem. 399 (2011) 1577–1590. doi:10.1007/s00216-010-4566-y.

[62] N. Baig, M. Sajid, T.A. Saleh, Recent trends in nanomaterial-modified electrodes for electroanalytical applications, TrAC - Trends Anal. Chem. 111 (2019) 47–61. doi:10.1016/j.trac.2018.11.044.

[63] M. Sillanpää, M. Sillanpää, L. Rassaei, F. Marken, C.M. Cirtiu, M. Amiri, Nanoparticles in electrochemical sensors for environmental monitoring, TrAC Trends Anal. Chem. 30 (2011) 1704–1715. doi:10.1016/j.trac.2011.05.009.

[64] A. Waheed, M. Mansha, N. Ullah, Nanomaterials-based electrochemical detection of heavy metals in water: Current status, challenges and future direction, TrAC - Trends Anal. Chem. 105 (2018) 37–51. doi:10.1016/j.trac.2018.04.012.

[65] R.W. Kelsall, I.W. Hamley, M. Geoghegan, Nanoscale science and technology, John Wiley & Son, New Jersey, 2005. doi:10.1002/0470020873.

[66] J. García-Barrasa, J.M. López-de-Luzuriaga, M. Monge, Silver nanoparticles: Synthesis through chemical methods in solution and biomedical applications, Cent. Eur. J. Chem. 9 (2011) 7–19. doi:10.2478/s11532-010-0124-x.

[67] V. Georgakilas, J.A. Perman, J. Tucek, R. Zboril, Broad family of carbon nanoallotropes: Classification, chemistry, and applications of fullerenes, carbon dots, nanotubes, graphene, nanodiamonds, and combined superstructures, Chem. Rev. 115 (2015) 4744–4822. doi:10.1021/cr500304f.

[68] X. Li, J. Ping, Y. Ying, Recent developments in carbon nanomaterial-enabled electrochemical sensors for nitrite detection, TrAC - Trends Anal. Chem. 113 (2019) 1–12. doi:10.1016/j.trac.2019.01.008.

[69] A.C. Power, B. Gorey, S. Chandra, J. Chapman, Carbon nanomaterials and their application to electrochemical sensors: A review, Nanotechnol. Rev. 7 (2018) 19–41. doi:10.1515/ntrev-2017-0160.

[70] S.K. Pandey, P. Singh, J. Singh, S. Sachan, S. Srivastava, S.K. Singh, Nanocarbon-based electrochemical detection of heavy metals, Electroanalysis. 28 (2016) 2472–2488. doi:10.1002/elan.201600173.

[71] A. Uhlir Jr., Electrolytic shaping of germanium and silicon, Bell Syst. Tech. J. 35 (1956) 333–347. doi:10.1002/j.1538-7305.1956.tb02385.x.

[72] L.T. Canham, Silicon quantum wire array fabrication by electrochemical and chemical dissolution of wafers, Appl. Phys. Lett. 57 (1990) 1046–1048. doi:10.1063/1.103561.

[73] V. Lehmann, U. Gösele, Porous silicon formation: A quantum wire effect, Appl. Phys. Lett. 58 (1991) 856–858. doi:10.1063/1.104512.

[74] L. Canham, Handbook of porous silicon, 2nd ed., Springer, Birmingham, UK, 2017. doi:10.1007/978-3-319-04508-5.

[75] A. Santos, T. Kumeria, Electrochemical etching methods for producing porous silicon, in: Electrochemically engineered nanoporous materials, vol. 220, Springer International Publishing, Switzerland, 2015. doi:10.1007/978-3-319-20346-1.

[76] M.J. Sailor, Porous silicon in practice: preparation, characterization and applications, Wiley-VCH Verlag GmbH & Co. KGaA, Weinheim, Germany, 2012. doi:10.1002/9783527641901.

[77] J. Salonen, M. Kaasalainen, O.-P. Rauhala, L. Lassila, M. Hakamies, T. Jalkanen, R. Hahn, P. Schmuki, E. Mäkilä, Thermal carbonization of porous silicon: the current status and recent applications, ECS Trans. 69 (2015) 167–176. doi:10.1149/06902.0167ecst.

[78] J. Salonen, E. Mäkilä, Thermally carbonized porous silicon and its recent applications, Adv. Mater. 30 (2018) 1703819–1703837. doi:10.1002/adma.201703819.

[79] K. Guo, A. Sharma, R.J. Toh, E. Alvárez de Eulate, T.R. Gengenbach, X. Cetó, N.H. Voelcker, B. Prieto-Simón, Porous silicon nanostructures as effective faradaic electrochemical sensing platforms, Adv. Funct. Mater. 29 (2019) 1809206–1809217. doi:10.1002/adfm.201809206.

[80] X. Cetó, N.H. Voelcker, B. Prieto-Simón, Bioelectronic tongues: New trends and applications in water and food analysis, Biosens. Bioelectron. 79 (2016) 608–626. doi:10.1016/j.bios.2015.12.075.

[81] J.M. Díaz-Cruz, C. Pérez-Ràfols, X. Cetó, N. Serrano, C. Ariño, M. Esteban, Voltammetric electronic tongues, in: Recent advances in analytical techniques, vol. 4, Bentham Science, Sharjah, UAE, 2019.

[82] Y. Vlasov, A. Legin, A. Rudnitskaya, C. Di Natale, A. D'Amico, Nonspecific sensor arrays ("electronic tongue") for chemical analysis of liquids, Pure Appl. Chem. 77 (2005) 1965–1983. doi:10.1351/pac200577111965.

[83] M. del Valle, Sensor arrays and electronic tongue systems, Int. J. Electrochem. 2012 (2012) 1–12. doi:10.1155/2012/986025.

[84] M. del Valle, Electronic tongues employing electrochemical sensors, Electroanalysis. 22 (2010) 1539–1555. doi:10.1002/elan.201000013.

[85] X. Cetó, F. Céspedes, M. del Valle, Comparison of methods for the processing of voltammetric electronic tongues data, Microchim. Acta. 180 (2013) 319–330. doi:10.1007/s00604-012-0938-7.

[86] F. Winquist, Voltammetric electronic tongues - Basic principles and applications, Microchim. Acta. 163 (2008) 3–10. doi:10.1007/s00604-007-0929-2.

[87] K.J. Siebert, Using chemometrics to classify samples and detect misrepresentations, in: Progress in authentication of food and wine, American Chemical Society, Washington DC, 2011. doi:10.1021/bk-2011-1081.ch004.

[88] L.A. Stone, R. Kennard, Computer aided design of experiments, Technometrics. 11 (1969) 137–148. doi:10.1080/00401706.1969.10490666.

[89] J. Wang, Analytical electrochemistry, John Wiley & Sons, Hoboken, NJ, 2006. doi:10.1002/0471790303.

[90] J.M. Pingarrón, P. Sánchez, Química electroanalítica: Fundamentos y aplicaciones, Editorial Sintesis, Madrid, Spain, 2003.

[91] Y. Leng, Materials characterization: Introduction to microscopic and spectroscopic methods, J. Wiley, Hoboken, NJ, 2008. doi:10.1002/9780470823002.

[92] R.G. Brereton, Applied chemometrics for scientists, John Wiley & Son, Chichester, UK, 2007. doi:10.1002/9780470057780.ch1.

[93] T. Naes, T. Isaksson, T. Fearn, T. Davies, A user-friendly guide to multivariate calibration and classification, NIR Publications, Chichester, UK, 2002. doi:10.1002/cem.815.

[94] S. Wold, H. Antti, F. Lindgren, J. Öhman, Orthogonal signal correction of near-infrared spectra, Chemom. Intell. Lab. Syst. 44 (1998) 175–185. doi:10.1016/S0169-7439(98)00109-9.

[95] S. Wold, J. Trygg, A. Berglund, H. Antti, Some recent developments in PLS modeling, Chemom. Intell. Lab. Syst. 51 (2001) 131–150. doi:10.1016/S0169-7439(01)00156-3.

[96] B.E. Saxberg, B.R. Kowalski, Generalized standard addition method, Anal. Chem. 51 (1979) 1031–1038. doi:10.1021/ac50043a059.

[97] I.E. Frank, J.H. Kalivas, B.R. Kowalski, Partial least squares solutions for multicomponent analysis, Anal. Chem. 55 (1983) 1800–1804. doi:10.1021/ac00261a035.

[98] K. Martínez, C. Ariño, J.M. Díaz-Cruz, N. Serrano, M. Esteban, Multivariate standard addition for the analysis of overlapping voltammetric signals in the presence of matrix effects: application to the simultaneous determination of hydroquinone and catechol, Chemom. Intell. Lab. Syst. 178 (2018) 32–38. doi:10.1016/j.chemolab.2018.05.002.

[99] M. Delamar, G. Désarmot, O. Fagebaume, R. Hitmi, J. Pinson, J. Savéant, Modification of carbon fiber surfaces by electrochemical reduction of aryl diazonium salts: Application to carbon epoxy composites, Carbon. 35 (1997) 801–807. doi:10.1016/S0008-6223(97)00010-9.

[100] W. Richard, D. Evrard, P. Gros, New insight into 4-nitrobenzene diazonium reduction process: Evidence for a grafting step distinct from NO_2 electrochemical reactivity, J. Electroanal. Chem. 685 (2012) 109–115. doi:10.1016/j.jelechem.2012.09.014.

[101] W. Richard, D. Evrard, B. Busson, C. Humbert, L. Dalstein, A. Tadjeddine, P. Gros, The reduction of 4-nitrobenzene diazonium electrografted layer: An electrochemical study coupled to in situ sum-frequency generation spectroscopy, Electrochim. Acta. 283 (2018) 1640–1648. doi:10.1016/j.electacta.2018.07.073.

[102] B. Sciacca, S.D. Alvarez, F. Geobaldo, M.J. Sailor, Bioconjugate functionalization of thermally carbonized porous silicon using a radical coupling reaction, Dalt. Trans. 39 (2010) 10847–10853. doi:10.1039/c0dt00936a.